



HAL
open science

Role of the ciliopathy gene *Ftm/Rpgrip1l* and primary cilia in forebrain patterning and morphogenesis

Abraham Andreu Cervera

► **To cite this version:**

Abraham Andreu Cervera. Role of the ciliopathy gene *Ftm/Rpgrip1l* and primary cilia in forebrain patterning and morphogenesis. *Biochemistry [q-bio.BM]*. Sorbonne Université, 2018. English. NNT : 2018SORUS223 . tel-02483157v2

HAL Id: tel-02483157

<https://theses.hal.science/tel-02483157v2>

Submitted on 18 Feb 2020

HAL is a multi-disciplinary open access archive for the deposit and dissemination of scientific research documents, whether they are published or not. The documents may come from teaching and research institutions in France or abroad, or from public or private research centers.

L'archive ouverte pluridisciplinaire **HAL**, est destinée au dépôt et à la diffusion de documents scientifiques de niveau recherche, publiés ou non, émanant des établissements d'enseignement et de recherche français ou étrangers, des laboratoires publics ou privés.

Sorbonne Université

Ecole doctorale Complexité du Vivant

Laboratoire de Biologie du Développement

**Role of the ciliopathy gene *Ftm/Rpgrip1l* and
primary cilia in forebrain patterning and
morphogenesis**

Présenté par

Abraham ANDREU CERVERA

Thèse de doctorat de Biologie du Développement

Dirigée par Sylvie SCHNEIDER-MAUNOURY

Présentée et soutenue publiquement le 25 septembre 2018

Devant un jury composé de:

Dr. Sylvie SCHNEIDER-MAUNOURY

Directrice de Recherche

Directrice de Thèse

Dr. Isabelle CAILLÉ

Maître de Conférences

Examineur, Président du jury

Dr. Fiona FRANCIS

Directrice de Recherche

Examineur

Dr. Anne CAMUS

Chargée de Recherche

Examineur

Dr. Bénédicte DURAND

Professeur

Rapporteur

Dr. Sandra BLAESS

Professeur

Rapporteur



Except where otherwise noted, this work is licensed under
<http://creativecommons.org/licenses/by-nc-nd/3.0/>

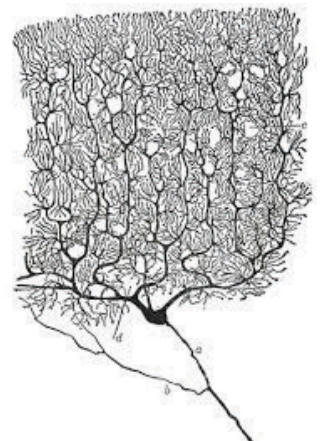
A mi madre Margarita

*“Es preciso sacudir enérgicamente el **bosque** de las neuronas cerebrales adormecidas; es menester hacerlas vibrar con la emoción de lo nuevo e infundirles nobles y elevadas inquietudes.”*

«Il est nécessaire d'agiter vigoureusement la forêt des neurones des cerveaux endormis; il faut les faire vibrer avec l'émotion du nouveau et susciter des intérêts nobles et élevés »

“It is necessary to shake vigorously the forest of the sleepy brain neurons; it is necessary to make them vibrate with the emotion of the new and arouse them noble and high interests.”

<<Santiago Ramón y Cajal>>



Rôle du gène de ciliopathie *Ftm/Rpgrip1l* et des cils primaires dans la régionalisation et la morphogenèse du cerveau antérieur

Résumé

Les cils primaires sont essentiels au développement du système nerveux central. Chez la souris, ils jouent un rôle essentiel dans l'organisation de la moelle épinière et du télencéphale via la régulation de la signalisation Hedgehog/Gli. Cependant, malgré la perturbation fréquente de cette voie de signalisation dans les malformations du cerveau antérieur chez l'homme, le rôle des cils primaires dans la morphogenèse du cerveau antérieur a été peu étudié en dehors du télencéphale. Pendant mon doctorat, j'ai étudié le développement du diencephale, de l'hypothalamus et des yeux chez des souris mutantes pour le gène de ciliopathie *Ftm/Rpgrip1l*. En fin de gestation, les fœtus *Ftm*^{-/-} présentent une anophtalmie, une réduction de l'hypothalamus ventral et une désorganisation du diencephale. Chez les embryons *Ftm*^{-/-}, l'expression de *Sonic hedgehog (Shh)* est perdue dans le cerveau antérieur ventral, mais maintenue dans la zona limitans intrathalamica (ZLI), l'organisateur diencephalique. Dans le diencephale, l'activité de Gli est atténuée dans les régions adjacentes à la ZLI, mais montre un niveau de base plus élevé dans les autres régions. Nos données révèlent un rôle complexe des cils dans le développement du diencephale, de l'hypothalamus et des yeux via le contrôle régional du ratio entre les formes activatrices et répressives des facteurs de transcription Gli. Ils sont en faveur d'un examen plus approfondi des anomalies du cerveau antérieur dans les ciliopathies sévères et de la recherche de gènes de ciliopathie comme modificateurs dans d'autres maladies humaines présentant des anomalies du cerveau antérieur.

Role of the ciliopathy gene *Ftm/Rpgrip1l* and primary cilia in forebrain patterning and morphogenesis

ABSTRACT

Primary cilia are essential for central nervous system development. In the mouse, they play a critical role in patterning the spinal cord and telencephalon via the regulation of Hedgehog/Gli signaling. However, despite the frequent disruption of this signaling pathway in human forebrain malformations, the role of primary cilia in forebrain morphogenesis has been little investigated outside the telencephalon. Here we studied development of the diencephalon, hypothalamus and eyes in mutant mice in which the *Ftm/Rgrip1l* ciliopathy gene is disrupted. At the end of gestation, *Ftm*^{-/-} fetuses displayed anophthalmia, a reduction of the ventral hypothalamus and a disorganization of diencephalic nuclei and axonal tracts. In *Ftm*^{-/-} embryos, we found that the ventral forebrain structures and the rostral thalamus were missing. Optic vesicles formed but lacked the optic cups. We analyzed the molecular causes of these defects. In *Ftm*^{-/-} embryos, *Sonic hedgehog* (*Shh*) expression was lost in the ventral forebrain but maintained in the zona limitans intrathalamica (ZLI), the mid-diencephalic organizer. In the diencephalon, Gli activity was dampened in regions adjacent to the *Shh*-expressing ZLI but displayed a higher Hh-independent ground level in the other regions. Our data uncover a complex role of cilia in development of the diencephalon, hypothalamus and eyes via the region-specific control of the ratio of activator and repressor forms of the Gli transcription factors. They call for a closer examination of forebrain defects in severe ciliopathies and for a search for ciliopathy genes as modifiers in other human conditions with forebrain defects.

TABLE OF CONTENTS

INTRODUCTION	9
<u>I. Formation and patterning of the Central Nervous System</u>	10
1. Formation and closure of the neural tube: neurulation	10
2. Patterning of the Central nervous system	14
2.1. The brain vesicles and their derivatives	14
2.2. Brain patterning: a diversity of processes	15
2.3. Dorso-ventral (DV) patterning of the neural tube	17
2.4. The Hedgehog (Hh) pathway and its role in spinal cord and DV patterning	18
<u>II. Forebrain development in mouse</u>	24
1. Specification of the telencephalon	24
2. Hypothalamus formation	26
3. Formation of the eyes	29
4. Diencephalic specification	31
5. Defects in Shh pathway: the holoprosencephaly.	35
<u>III. The primary cilia</u>	38
1. Structure and ciliogenesis	39
1.1. Structure of primary cilia	39
1.2. Primary cilia assembly and disassembly	42
1.3. Intraflagellar transport (IFT) complexes and cilia trafficking	45
2. Role of primary cilia in Hedgehog (HH) signalling pathway	48
3. Developmental processes that require primary cilia	51
3.1. Primary cilia in patterning of the neural tube	52
4. Dysfunction of primary cilia in humans: the ciliopathies	55
<u>IV. The <i>Ftm/Rpgrip1l</i> ciliopathy gene</u>	57
1. Structure and functions	57
1.1. Identification of the gene and the structure of the protein	57
1.2. Localisation of Rpgrip1l	58
1.3 Cellular functions of Rpgrip1l	59
1.4. Function of Ftm/Rpgrip1l in vertebrate development	62
2. <i>Ftm/Rpgrip1l</i> and ciliopathies	64
<u>V. Aims of the thesis project</u>	66

RESULTS	67
Title, Abstract and Keywords	68
Introduction.....	69
Results.....	72
• <i>Ftm</i> ^{-/-} fetuses at the end of gestation display microphthalmia and profound perturbations of the diencephalon and hypothalamus.	72
• Patterning of the diencephalon and hypothalamus is affected in <i>Ftm</i> ^{-/-} embryos.	72
• The rostral thalamus is absent in <i>Ftm</i> ^{-/-} embryos	74
• Optic vesicles form in <i>Ftm</i> ^{-/-} embryos and display patterning defects	75
• Hh expression and pathway activity are impaired in the forebrain of <i>Ftm</i> ^{-/-} embryos	76
• <i>Shh</i> expression and Hh/Gli pathway activity show different perturbations in distinct domains of the E12.5 diencephalon	77
• Reintroduction of Gli3R into the <i>Ftm</i> background rescues aspects of the forebrain phenotype	78
• Cilia are severely reduced in number in forebrain neural progenitors	79
Discussion.....	81
• Patterning defects in the diencephalon and hypothalamus of <i>Ftm</i> mutants reflect the loss of primary cilia on neural progenitors	81
• Region-specific defects in Hh/Gli signalling in the forebrain of <i>Ftm</i> mutants.	82
• ZLI formation is independent of primary cilia.	83
• A double role of cilia in eye development	83
• Primary cilia in the forebrain: a balance of GliA and GliR activity	84
• Clinical relevance of our study for human ciliopathies and holoprosencephaly	84
Material and methods	86
References	90
Figure legends	99
Supplementary figure legends.....	104
Figures	107
Supplementary Figures.....	115

DISCUSSION	120
• Loss of primary cilia in neural progenitors of <i>Ftm</i> mutants leads to patterning defects in the diencephalon and hypothalamus	122
• Region-specific defects in Hh/Gli signalling in the forebrain of <i>Ftm</i> mutants	123
• Zona limitans intrathalamica formation does not require primary cilia	125
• Role of primary cilia in eye development	126
• A balance of GliA and GliR is essential for forebrain and eye specification	127
• A <i>Ptch1</i> prepatterning in the diencephalon of <i>Ftm</i>^{-/-} embryos	129
• Are other pathways affected apart from Hh signalling in <i>Ftm</i> mutant?	130
• Links between ciliopathies, holoprosencephaly and other human forebrain malformations linked to defects in Hh signalling	132
CONCLUSION	138
BIBLIOGRAPHY	140



INTRODUCTION

I. Forebrain development in mouse

In vertebrates, the central nervous system is composed by two main structures: the spinal cord and the brain. These structures arise from a sheet of epithelial cells, the neural plate, which forms during and after gastrulation. Later on, the neural plate folds to form the neural tube, a process called neurulation. The most anterior portion of the neural tube will form the three different parts of the brain: the hindbrain or rhombencephalon, located in the caudal part, followed by the midbrain or mesencephalon and rostrally the forebrain or prosencephalon (Fig. 1).

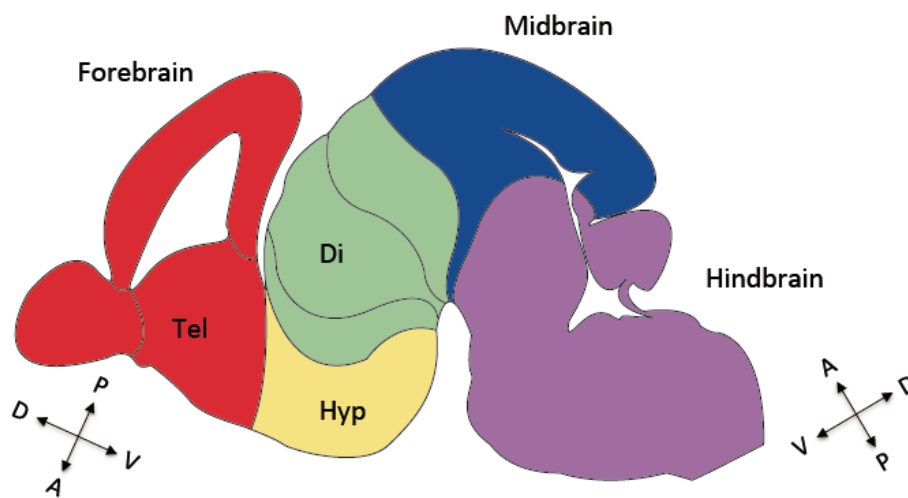


Figure 1. Representation of the different regions of the brain in a mouse foetus at 18.5 days of gestation (E18.5). Anterior to posterior we can observe the forebrain (comprising the telencephalon, hypothalamus and diencephalon), the midbrain and the hindbrain. Di, diencephalon; Hyp, hypothalamus; Tel, telencephalon.

1. Formation and closure of the neural tube: neurulation

Neurulation is the process by which the neuroepithelium, derived from the ectoderm, will form the neural tube. Neurulation involves two distinct processes, primary and secondary neurulation, which occur sequentially and in different regions of the CNS (Copp et al., 2003; Nikolopoulou et al., 2017). During primary neurulation, which starts at E8.5 in the mouse, the borders of the neural plate fold upwards, forming the neural folds, and fuse in the dorsal midline to form the neural tube (Fig. 2A). In the

mouse, closure is initiated in the caudal hindbrain, and proceeds like a zipper in both directions, toward the future brain and spinal cord. A second closure point starts at the forebrain-midbrain limit and a third is initiated at the rostral end of the forebrain. Primary neurulation ends with the closure of the three neuropores: the anterior neuropore, the hindbrain neuropore and the posterior neuropore (Fig. 2C-F). Secondary neurulation is a process by which the most caudal part of the spinal cord (sacral and coccygeal regions) is formed. This process involves the condensation of tail bud cells to form the secondary neural tube and notochord (Fig 2B).

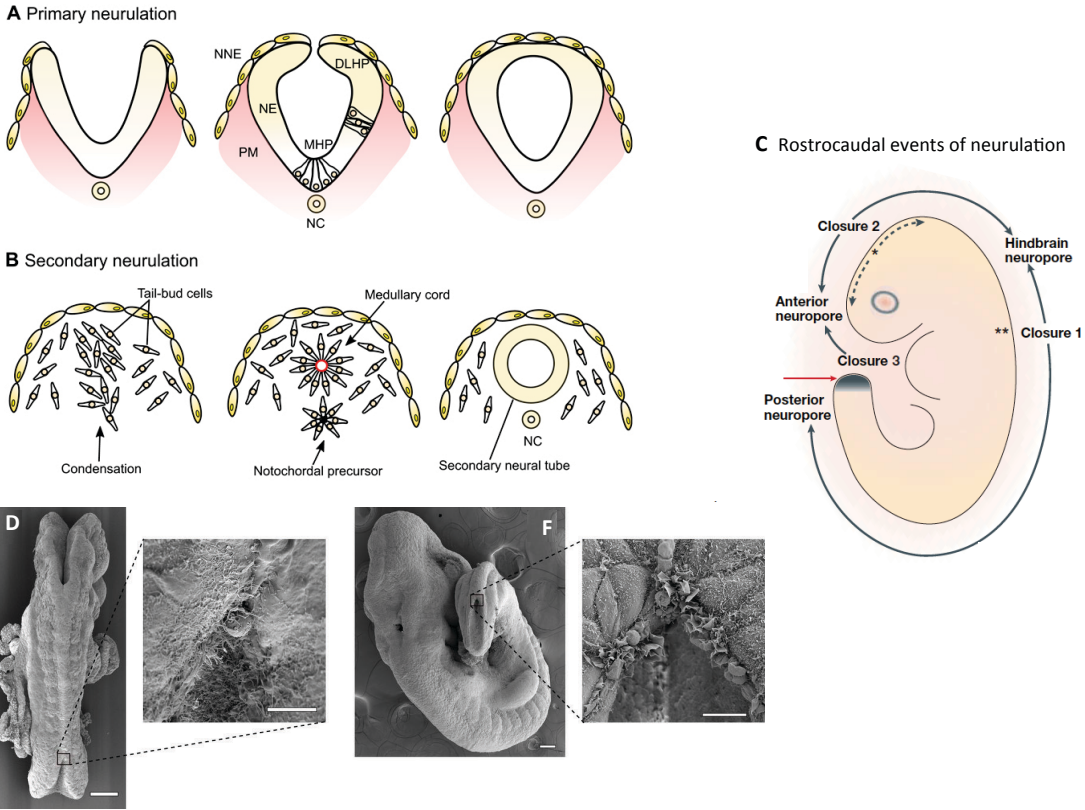


Figure 2. **A.** Representation of the primary neurulation, including the elevation of the neural folds and bending and fusion of the neural tube. **B.** Secondary neurulation. Cells from the tail bud condense and form the medullary cord and notochordal precursor in the midline, generating the secondary neural tube and notochord. **C.** Illustration of the sequence of events of neural tube closure during primary neurulation in mouse embryos. Closure starts at the hindbrain/cervical boundary at E8.5 (Closure 1). A second de novo closure event occurs at the forebrain/midbrain boundary (Closure 2) and a third one occurs at the rostral extremity of the forebrain (Closure 3). The closure of the neural tube finishes at the end of anterior neural tube (posterior neuropore) where the secondary neurulation begins (red arrow). **D-F.** Scanning electron microscopy of the closing neural tube at two different stages, 10 somites (**D**) and 25 somites (**E**). Scale bars: 10 μ m in D and E, 10 μ m in insets. Adapted from Nikolopoulou et al., 2017 and Copp et al., 2003.

Neurulation varies between vertebrate species, with regard to the number and position of the closure points, the dynamics of closure, and the neurulation movements. However, all vertebrates analysed have both primary and secondary neurulation (Copp et al., 2003; Nikolopoulou et al., 2017).

The closure of the neural tube is a complex process involving different cellular mechanisms such as convergence-extension, bending and elevation of the neural folds, neural fold adhesion and tissue fusion. These processes are controlled by molecular pathways such as the Wnt/PCP (planar cell polarity), the Hedgehog (Hh) and the Bone Morphogenetic Protein (BMP) signalling pathways (Nikolopoulou et al., 2017). Convergence-extension of the neural plate requires mediolateral convergence and anterior-posterior extension of axial tissues. In mouse, the neural plate is formed by a single-layer, pseudostratified epithelium called the neuroepithelium. Neuroepithelial cells display apicobasal polarity and interkinetic nuclear migration (IKNM), by which their nucleus migrates apicobasally during the cell cycle, with mitosis occurring at the apical (ventricular) surface. (Spear and Erickson, 2012). The neural plate cells are organized in rosette-like structures, which drive the formation of new medio-lateral junctions leading tissue extension. Convergence-extension is driven by the Wnt/PCP pathway. For instance, mutations of the genes encoding Vangl2 and Ptk7, two members of the PCP pathway, result in defective convergence-extension (Williams et al., 2014).

During convergence-extension, the lateral regions of the neural plate start to fold upwards forming the neural folds. In the mouse neural tube, two types of neural folds are found. In the midbrain, the neural folds first have a biconvex shape and then when they bow dorsally the folds become biconcave (Morriss-Kay, 1981). In contrast, in the spinal cord the neural folds remain straight, except for the midline and dorsolateral bending (Shum and Copp, 1996). As mentioned before, the neuroepithelium is pseudostratified, and the local bending of the median hinge (at the midline) is due to IKNM (McShane et al., 2015). In contrast, the dorsolateral hinges do not depend on IKNM, but on actomyosin dynamics (Sawyer et al., 2010). The bending of the neural plate is driven by ventral induction from the notochord (Shh pathway) and from the non-neural ectoderm in the dorsal regions that secretes BMPs. The formation of the medial hinge point depends on Shh secretion by the notochord (Smith and Schoenwolf,

1989). The dorsal non-neural ectoderm controls the formation of dorsolateral hinges in the neuroectoderm. In anterior regions, ectodermal cells secrete BMP2, preventing the formation of dorsolateral hinges. In posterior regions, the BMP antagonist Noggin is expressed and represses BMP signalling, leading dorsolateral hinge formation (Ybot-Gonzalez et al., 2007).

After neural fold formation, completion of neural tube closure involves the fusion of the dorsal region of the neural folds. During this fusion, two new epithelia are shaped, the internal neural tube and the external non-neural ectoderm that will form the epidermis (Copp et al., 2003). Neural fold fusion includes the formation of cellular protrusions required for the attachment of the distal folds to form the dorsal midline (Mak, 1978; Waterman, 1976). These protrusions, filopodia or lamellipodia, are rich in actin structures. The first contact of the neural folds in midbrain, hindbrain and spinal cord is made by non-neural ectodermal cells. In contrast, in the forebrain the first contact is made by neuroectodermal cells (Nikolopoulou et al., 2017).

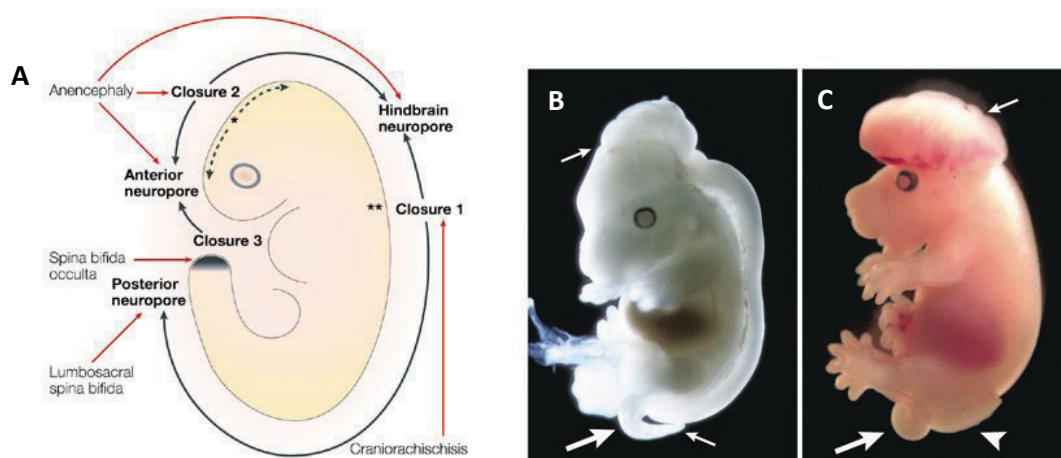


Figure 3. Mouse foetuses with neural tube closure defects. **A.** Schematic representation of neural tube closure defects. Defects in the first closure cause craniorachischisis, a totally open neural tube. Problems in the anterior neuropore, the hindbrain neuropore, the second and the third closure produce anencephaly. Defects in the posterior neuropore lead to the formation of lumbosacral spina bifida and spina bifida occulta. **B.** Mouse foetus mutant for *Celsr1* (a binding partner of Frizzled, the receptor of Wnt ligands) at E15.5, showing craniorachischisis. **C.** The mouse curly tail (*ct*) mutant foetus at E15.5 showing exencephaly and open spina bifida. Adapted from Copp et al. 2003.

More than 300 genes have been implicated in neural tube closure defects in mice (Wilde et al., 2014), and 82 genes in humans (Pangilinan et al., 2012). Defects in fusion of the cranial neural folds lead to exencephaly progressing to anencephaly due to degeneration of the neural tissues. In mice, *Par1*^{-/-}/*Par2*^{-/-} or *Celsr1*^{-/-} fetuses display exencephaly (Fig. 3; Camerer et al., 2010; Robinson et al., 2012). Failure of spinal cord closure leads to spina bifida (also known as myelomeningocele). Mutations of *Zic2* (encoding a member of Zic family of zinc-finger protein) or the paired box transcription factor *Pax3* result in spina bifida and exencephaly in mice (Epstein et al., 1991, Elms et al., 2003). A milder defects in secondary neurulation leads to occult spina bifida, in which the spinal cord does not separate from the surrounding tissues (Fig. 3; Copp et al., 2003).

2. Patterning of the central nervous system

2.1. The brain vesicles and their derivatives.

During neurulation, the anterior part of the neural tube undergoes drastic changes, generating, by differential proliferation, the three rostro-caudal primary vesicles of the brain. In the most posterior region, the hindbrain (rhombencephalon) will give rise to the cerebellum (coordination of complex muscular movements), the pons (connexion between the cerebellum and the cortex) and the medulla oblongata (sensorymotor control of the face and neck through cranial nerves, regulation of reflexes and involuntary movements and of vegetative functions). Anterior to the hindbrain, the midbrain (mesencephalon) will give rise to the tectum and the brain peduncles (temperature regulation, motor control and visual processing). Finally, in the most anterior part of the neural tube, the forebrain (prosencephalon) will give rise to the diencephalon (implicated in relaying sensory signals to the cortex), the hypothalamus (important for the regulation of sleep and temperature), the eyes and the telencephalon (involved in smell, memory storage and learning; Fig. 4; Darnell and Gilbert, 2017).

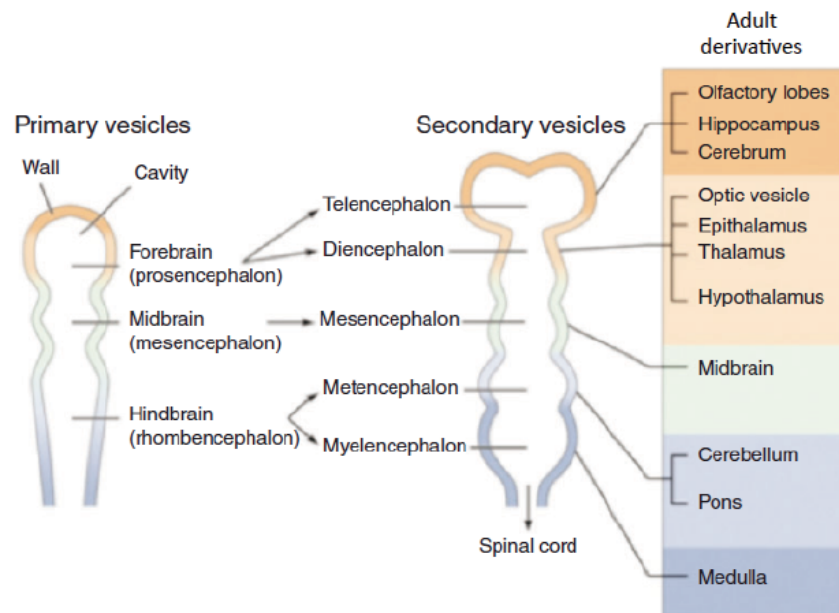


Figure 4. Formation of the brain vesicles. The three primary vesicles forebrain, midbrain and hindbrain will give rise to the different structures of the adult brain. Adapted from Darnell and Gilbert, 2017.

2.2. Brain patterning: a diversity of processes

Beyond the morphological transformation, distinct developmental processes are involved in spinal cord and brain patterning. The hindbrain becomes subdivided along its anteroposterior (AP) axis into 7-8 transiently reiterated units called rhombomeres. Rhombomeres (a condensation from rhombencephalon and metameres) are considered as true segments and they are units of gene expression, cellular differentiation and lineage restriction (Schneider-Maunoury et al., 1998). Rhombomere formation involves a regulatory network including *Krox20/Egr2*, *MafB* and *HNF1b*, as well as several *Hox* genes, while acquisition of rhombomere identity and fate (up to r2) is controlled by *Hox* genes (for review, Schneider-Maunoury 1998). While no true metameres have been identified anterior to the hindbrain, many studies have led to the definition of “prosomeres” and “mesomeres” (see below). This is embedded in a theory of brain development and patterning called the “prosomeric model”, developed principally by Pr. L. Puelles and Pr. John L. R. Rubenstein, which is constantly evolving and refining. The prosomeric model will be presented below in Chapter II.

Patterning of the brain relies on a series of signalling centres, which form at boundaries between different brain domains. These signalling centres are called secondary organizers, to distinguish them from the primary organizer or Spemann's organizer, which induces the embryonic axes. They secrete diverse signalling molecules or morphogens that act at a distance and in a concentration-dependent manner to organize cell fate and cell proliferation in adjacent territories. The main organizing centres along the AP axis of the brain are the anterior neural ridge (ANR) at the rostral end of the anterior neural tube; the zona limitans intrathalamica (ZLI) or mid-diencephalic organizer (MDO) within the diencephalon, and the isthmus organizer (IsO) at the midbrain-hindbrain boundary (Fig.5; Vieira et al., 2010).

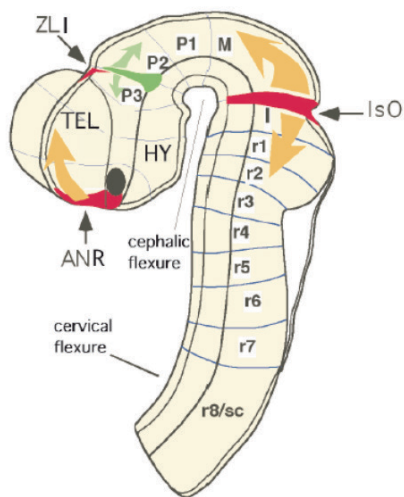


Figure 5. Representation of the secondary organizers in the E10.5 mouse embryo neural tube. The main secondary organizers active in the brain are the ANR in the rostral forebrain, the ZLI in the mid-diencephalon and the IsO at the midbrain-hindbrain boundary. ANR, anterior neural ridge; IsO, isthmus organizer; ZLI, zona limitans intrathalamica. Adapted from Vieira et al., 2010.

The anterior organizer, the ANR, is a source of Fibroblast growth factors (Fgf), principally Fgf8. The ANR is essential for the regionalization of the telencephalon (Shimamura and Rubenstein, 1997; Ye et al., 1998). The specification and cell fate of diencephalic structures is mediated by the morphogen Sonic hedgehog (Shh) secreted by the ZLI. This morphogenetic activity of Shh controls the compartmentalization of the different prosomeres through the control of gene expression (see below; Kobayashi et al., 2002; Vieira et al., 2005). Moreover, in the dorsal part of the MDO, Fgf8 and a member of wingless family, Wnt1, are expressed and regulate cell fate specification during diencephalic development (McMahon and Bradley, 1990; Crossley and Martin, 1995). Finally, the IsO controls the formation of the midbrain and of the anterior hindbrain via the secretion of the morphogens Fgf8 and Wnt1 (McMahon and Bradley, 1990; Garda et al., 2001).

2.3. Dorso-ventral (DV) patterning of the neural tube

Dorso-ventral (DV) patterning of the neural tube also results from the activity of signalling centres. In the spinal cord, there are two main organizing centres along the DV axis, a ventral one composed of the notochord and floor plate (FP), and a dorsal one, the roof plate (Ulloa and Martí, 2010). Lateral signals derived from somites are also involved in DV patterning of the spinal cord. The secreted signalling molecules and pathways involved have been extensively studied. These molecules are Sonic hedgehog (Shh), Wnt family ligands, Bmps, Fgfs and Retinoic acid (RA). The morphogen Shh is initially expressed in the notochord, located ventral to the neural tube, and induces its own expression in the ventral midline to form the FP. Secreted Shh forms a gradient and is involved in ventral fate specification in a concentration- and time-dependent manner. Another signalling centre located dorsally, the roof plate, secretes BMP and Wnt signalling molecules to control cell fate in the dorsal spinal cord (Fig. 6). These DV signalling centres are conserved in the brain. The prechordal plate, which is the most anterior portion of the axial endo-mesoderm anterior to the notochord, expresses *Shh*. *Shh* induces its own expression in the ventral midline of the hypothalamus and diencephalon (see below in Chapter II; Blaess et al., 2015).

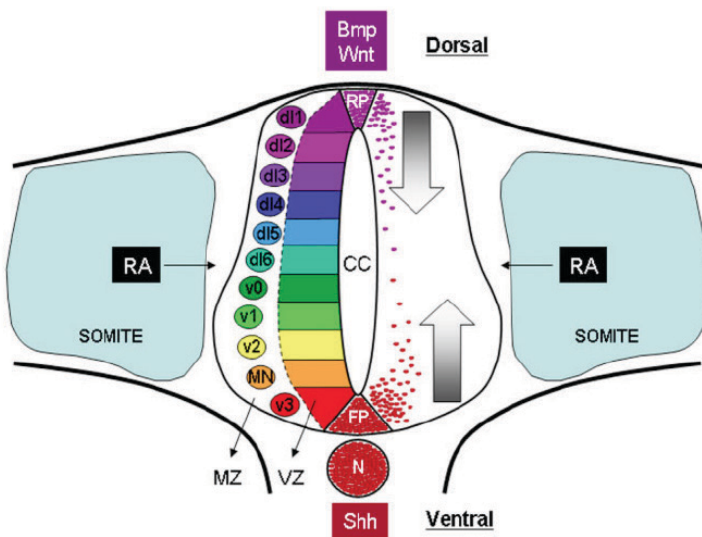


Figure 6. Scheme of the developing spinal cord. The neural tube contains progenitor cells located in the ventricular zone (VZ) close to the central canal (CC). These progenitors will differentiate into postmitotic neurons, which will form the mantle zone (MZ). Patterning of the ventral spinal cord is due to the secretion of Shh from the floor plate (FP) and notochord, and Wnts and BMPs form the roof plate (RP). These signalling molecules and their downstream pathways regulate a number of

transcription factor genes, which together specify cell fate along the DV axis of the spinal cord. Other signals involved in DV patterning derive from the somites, such as retinoic acid (RA). Adapted from Ulloa and Martí, 2010.

2.4. The Hedgehog (Hh) pathway and its role in spinal cord DV patterning

In 1988 Mohler and colleagues identified Hedgehog (Hh) as a segment polarity gene in *Drosophila melanogaster*. Its name comes from the phenotype of the mutant larvae, which present spines resembling that of a hedgehog (Mohler, 1988). The Hh ligand is initially formed as a 46 kDa precursor (Lee et al., 1997). An autocatalytic cleavage occurring in the endoplasmic reticulum produces a N-terminal domain of 19 kDa (Hh-N) and a C-terminal domain of 25 kDa (Hh-C) (Chen et al., 2011). The C-terminal domain acts as a cholesterol transferase, attaching covalently a cholesterol molecule in the carboxy-terminal end of Hh-N followed by addition of a palmitoyl group (Porter et al., 1996). The resulting hydrophobic molecule Hh-Np is transported to the cell membrane (Ramsbottom and Pownall, 2016). Hh-Np is released from the plasma membrane in multimeric complexes with the help of heparin sulphate proteoglycans (HSPGs). HSPGs facilitate the oligomerization and liberation of the Hh ligand (Goetz et al., 2006). In vertebrates there are several Hh ligands. The three Hh ligands in mammals are Shh, Indian Hedgehog (Ihh) and Desert Hedgehog (Dhh). Shh is the major ligand involved in neural patterning (Lee et al., 2011).

In the receiving cell, the Hh pathway comprises its membrane receptor Patched (Ptch) of which Ptch1 is the main member in vertebrates, and another transmembrane protein, the G protein coupled receptor (GPCR) family protein Smoothed (Smo), that initiates intracellular signalling. The effectors of Hh signalling are a family of zinc finger proteins, the Gli transcription factors. In the absence of ligand, Ptch1 inhibits the activity of Smo. In the presence of Shh ligand, Shh binds to Ptch1 which relieves Ptch1 inhibition of Smo, which induces the activation of the pathway (Fig. 7). In *Drosophila*, there is only one Gli factor called Cubitus Interruptus, which can be either a transcriptional activator in its full length form, or a transcriptional repressor after cleavage by the proteasome. In the presence of Hh ligand, Ci is under its activator form, while in the absence of Hh ligand, Ci is under its repressor form. In vertebrates, there are at least three Gli transcription factors downstream of Smo: Gli1, Gli2 and Gli3. In the absence of Hh ligand, Gli2 and Gli3 proteins are subject to a cascade of post-translational modifications initiated by phosphorylation by PKA, which leads to their targeting to the proteasome,

where they are cleaved into a transcriptional repressor form that inhibits the expression of Hh target genes. The Gli transcription factors are differentially controlled by the Hh pathway. In the absence of Shh, Gli2 is mainly degraded by the proteasome, while Gli3 is transformed into a strong transcriptional repressor (Gli3R) by proteasomal activity. In the presence of Hh ligand, Gli2 is transformed through several post-translational modifications into a strong transcriptional activator (Gli2A), which activates the expression of target genes, among which are two genes encoding members of the pathway, *Ptch1* and *Gli1* (Fig. 7). Gli1 is not cleaved in the absence of ligand, and thus is a constitutive activator, whose expression is enhanced by the Hh pathway (Lee et al., 2011). Another essential actor in Hh signalling in vertebrates is the primary cilium. Many Hh signalling events occur within the cilium or at its base and require the integrity of primary cilia (Ribes and Briscoe, 2016). The role of the cilium and ciliary proteins in Hh signalling will be presented in greater detail in Part III.

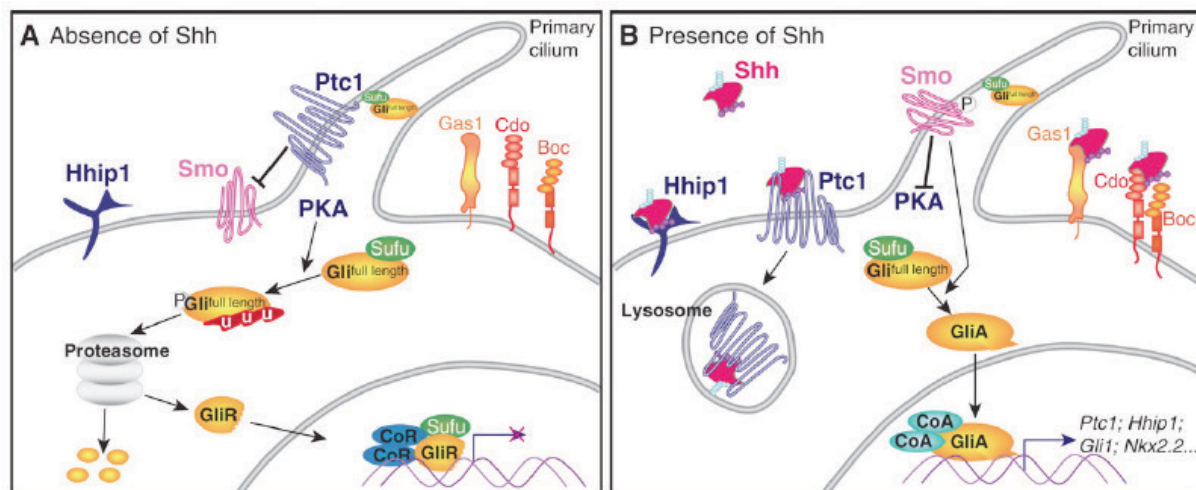


Figure 7. Shh signal transduction. **A.** In the absence of Shh, its receptor Ptch1 represses the transmembrane protein Smo, in part by preventing it from entering the cilium. Then Gli transcription factors are processed by the proteasome into repressor forms (GliR) that translocate to the nucleus to repress the target genes. **B.** In the presence of Shh ligand, Shh binds Ptch1, which allows Smo to translocate into the cilium. The activation of Smo inhibits the proteolytic processing of Gli and their activated form GliA translocates to the nucleus and activates target gene expression. Adapted from Ribes and Briscoe, 2016.

In the mouse neural tube, Hh signalling regulates the activity of Gli transcription factors, such that Gli2A concentration is high ventrally and decreases ventral to dorsal,

while *Gli3R* presents an opposite gradient. Likewise, the target genes *Ptch1* and *Gli1* are expressed in a ventral to dorsal decreasing gradient (Ribes and Briscoe, 2016).

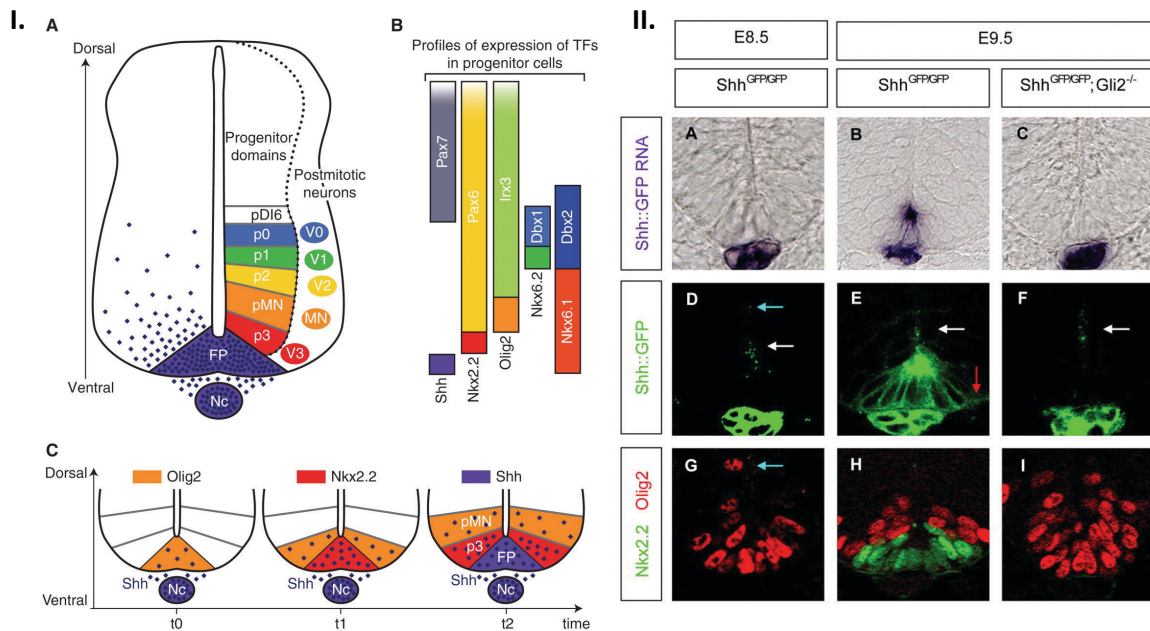


Figure 8. Linear progression and temporal gene induction in the ventral neural tube. **I.A.** Ventro-dorsally there are six progenitor domain, FP, p3, pMN, p2, p1 and p0 that will give rise to the neuronal subtypes V0 to V3 and MN. The ventral pattern is established by the secretion of Shh by the FP and notochord (Nc). **I.B.** The specific expression of *Nkx2.2*, *Olig2*, *Nkx6.1*, *Nkx6.2*, *Dbx1*, *Dbx2*, *Irx3*, *Pax6*, and *Pax7* transcription factors in each type of progenitor cells are regulated by the gradient of secreted Shh. **I.C.** *Olig2*, *Nkx2.2* and *Shh* expression specifies the three most ventral progenitor domains pMN, p3 and FP, respectively. The expression of each transcription factor is initiated at a different time-point in the ventral midline and then extends to more dorsal positions with the appearance of the next marker at the midline. **II.A-II.C.** *Shh::GFP* expression visualized by RNA in situ hybridization. **II.D-II.F.** *Shh::GFP* protein distribution visualized by confocal microscopy. *Shh::GFP* concentrated in an apical region of ventral midline cells overlying the notochord (white arrows in **II.D-II.F**) and basolateral region (red arrow, **II.E**). **II.G-II.I.** Immunostaining showing *Shh*-dependent neural progenitor domains p3 (*Nkx2.2*) and pMN (*Olig2*). Note that the most dorsally positioned *Shh::GFP* ligand signal in **II.D** is punctate and is adjacent to the most dorsally positioned pMN cell in **II.G** (blue arrows). Adapted from Chamberlain et al., 2008 & Ribes and Briscoe, 2009.

In the mouse, the role of Shh as a morphogen to specify cell fate has been extensively studied in the spinal cord. Shh is first secreted by the underlying notochord. Then, a second source of the protein is the cells of the FP in the neural tube (Marti et al., 1995; Roelink et al., 1995). This second source of Shh is established after the expression

of six molecular markers in the ventral progenitors of the spinal cord, *Nkx2.2* (P3) *Olig2* (pMN), *Nkx6.1* (p3-pMN-p2), *Nkx6.2* (p2), *Dbx1* (p0) and *Dbx2* (p1-p0), suggesting that ventral patterning is first due to the secretion of Shh from the notochord (Chamberlain et al., 2008). The majority of the ventral progenitors are exposed to Shh and inhibiting the Hh pathway represses ventral marker gene expression and blocks cell differentiation (Ribes and Briscoe, 2016). In the ventral spinal cord there are five neural cell types and one non-neural class, called V0, V1, V2, MN, V3 and FP, from dorsal to ventral (Ericson et al., 1997; Matisse and Joyner, 1997). V0-V3 are interneurons subtypes, MN stands for motoneurons and FP cells. The neural subtypes are generated in the ventricular zone from specific neural progenitors expressing distinct transcription factors (named p0, p1, p2, pMN and p3) (Briscoe et al., 2000). All these progenitors are not produced at the same time, there is a temporal sequence of gene activation where the early progenitor markers induced are positioned more dorsal as soon as the later progenitor maker genes are induced in the ventral part. *Nkx6.2* and *Nkx6.1* genes are expressed early defining the p1 and p2 domains, followed by the expression of *Olig2* (pMN), *Nkx2.2* (p3) and *FoxA2* (FP) (Matisse, 2013). Furthermore, p0 progenitors express *Dbx1*, in the most dorsal region of the ventral spinal cord (Fig. 8; Dessaud et al., 2008).

In the ventral spinal cord there is a spatial gradient of Shh that decreases ventro-dorsally (Chamberlain et al., 2008). The most ventral progenitor domains, FP and p3 are exposed to the highest levels of Shh. The level of Shh then decreases in the pMN domain and is lowest in the p2 domain. During development of the neural tube there is an increase of Shh levels, resulting in a temporal gradient. As a result, cells near to the ventral midline are exposed to higher levels of Shh ligand over a longer period of time than more dorsal cells (Jeong and McMahon, 2005; Chamberlain et al., 2008). Accordingly, Hh target gene expression shows spatio-temporal switches. As example, the transcription factor *Olig2*, required for MN formation, is initially localized in ventral midline cells exposed to low levels of Shh (produced by the notochord) for a short period of time. Later, *Olig2* expression expands more dorsally. Followed by this, the level of Shh protein increases in the ventral midline, producing a change of the fate of the ventral cells to *Nkx2.2*-positive identity. *Nkx2.2* requires not only higher levels of SHh but also longer exposure times. (Figure 8C; Jeong and McMahon, 2005; Dessaud et al., 2007; Chamberlain et al., 2008).

The final progenitor fate is also dependent on cross-repressive interactions between the transcription factors activated by the Gli gradient. For instance, Pax6, Nkx2.2 and Olig2 are involved in these cross-regulations. Combined with the temporal and spatial gradient of Shh expression and the corresponding Gli activity gradient, this leads to the establishment of distinct, sharp domains of gene expression driving progenitor fate specification (Balaskas et al., 2012; Figure 8).

In the absence of Shh, Gli3R is produced and Gli2 is degraded. In the neural tube, Gli3R is present in the dorsal regions where there is no Shh ligand. Mouse embryos mutant for *Gli3* show a dorsal expansion of the ventral neural tube, showing an increase of Nkx6.2, Dbx1 and Dbx2 progenitor domains (Wang et al., 2000; Persson et al., 2002). Reintroducing Gli3R constitutively in these *Gli3*^{-/-} mouse embryos restores the formation of the dorsal progenitor domains, demonstrating the essential role of Gli3R in dorsal neural tube formation (Persson et al., 2002). In cells responding to Shh, the processing of Gli3 is inhibited, resulting in the reduction of Gli3R levels. The response to high levels of the ligand also requires an activation of Gli2 into Gli2A. This is required for the formation of the ventral progenitor domains. Mutations in *Gli2* gene lead to the loss of FP and p3 cells in mouse embryos (Matisse et al., 1998; Persson et al., 2002; Pan et al., 2006). These studies suggest the different levels of Gli activity facilitate the graded response of cells to Shh.

In conclusion, the logics of the response to Hh signaling in the spinal cord can be summarized as follows:

1. The Shh ligand forms a spatial gradient, highest in the most ventral part of the spinal cord and decreasing dorsally.
2. The Shh ligand also forms a temporal gradient, inducing the expression of different ventral transcription factors in a different time-points.
3. The Shh gradient is transformed into a GliA-GliR gradient, which determines the activation of Hh target genes encoding transcription factors.
4. The final progenitor domains are established through cross-repressive interactions between the transcription factors, which control cell fate.

It should be noted that in the FP, this logic is modified: FP cell fate specification requires an initial high level of Hh signaling, followed by a decrease in Hh responsiveness. The forkhead transcription factor *Foxa2* is expressed in the FP in response to Shh and then induces FP fate independently of Hh (Ribes et al., 2010). Thus, the most ventral region of the neural tube has a distinct mode of response to Hh signaling.

II. Morphogenesis of the forebrain

During development, each region of the neural tube expresses a specific combination of genes encoding transcription factors and members of signalling pathways. This gene expression pattern characterizes the different subdivisions of the brain and leads to the region-specific control of essential processes such as proliferation, cell fate acquisition, differentiation, migration, etc. In the mouse forebrain, all of these processes will give rise to a variety of different structures along the AP and DV axes of the three main regions, the telencephalon, the hypothalamus and the diencephalon (Fig. 9). Concerning the molecular mechanisms, we will focus on the role of the Hh pathway.

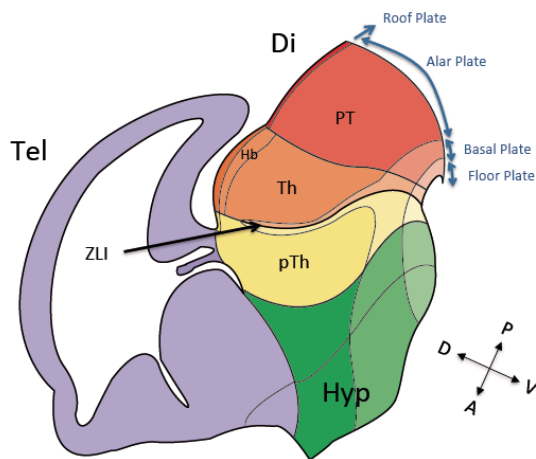


Figure 9. Representation of E13.5 parasagittal forebrain section showing the different AP structures: the telencephalon (Tel), the hypothalamus (hyp) and the diencephalon (Di). Hb, habenula; PT, pretectum; pTh, prethalamus; Th, thalamus; ZLI; zona limitans intrathalamica. Along the DV axis, the brain is divided into four main regions: the floor plate, the basal plate, the alar plate and the roof plate.

1. Specification of the telencephalon

The dorso-anterior part of the forebrain, the telencephalon, is an important region of the brain implicated in memory, learning, sensory integration, etc. It can be divided in two main regions, the pallium, located in the most dorsal part, separated by the pallio-subpallial boundary from the subpallium. The subpallium is located dorsal to the hypothalamus. The pallial region is subdivided in medial pallium that will give rise the hippocampus (important for learning and memory), the dorsal pallium that will form the neocortex (implicated in cognition, awareness, language, attention and memory), and the lateral and ventral pallium that will differentiate into the olfactory bulbs, amygdala (involved in olfaction and perception of the emotions and storage of memory events respectively) and other structures. The subpallium contains the medial,

lateral and caudal ganglionic eminences. These structures will give rise to the striatum and globus pallidus (implicated in voluntary movements) and are a source of GABAergic interneurons that will migrate tangentially into the neocortex (Fig. 10; Puelles et al., 2013; Puelles, 2016).

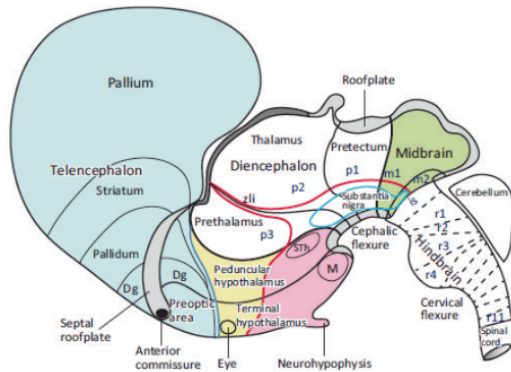


Figure 10. Lateral view of an embryonic brain. The telencephalon is divided into pallium and subpallium (striatum, pallidum or globus pallidus and preoptic area). Adapted from Puelles et al., 2013.

The anterior neural ridge (ANR) is a secondary organizer that regulates gene expression in the telencephalon. At early stages of development, *Fgf8* is expressed in the ANR. *Fgf8* is required for *FoxG1* expression, important for cell proliferation in the telencephalon (Shimamura and Rubenstein, 1997; Xuan et al., 1995; Ye et al., 1998). Another signal secreted in the telencephalon, in close proximity to the ANR, is *Shh*, which is required for the specification of the ventral telencephalon, mainly through the inhibition of the formation of *Gli3R* (Rallu et al., 2002; Vieira et al., 2010). A third essential signalling centre in the telencephalon is the dorsal midline (including the roof plate and the cortical hem) which expresses *Wnts* and *BMPS* and is essential for patterning the medial pallium and the cortex. All these signalling centres interact with one another to set up cell proliferation, neurogenesis and cell fate in the telencephalon (Fig. 11; Hebert and Fishell, 2008).

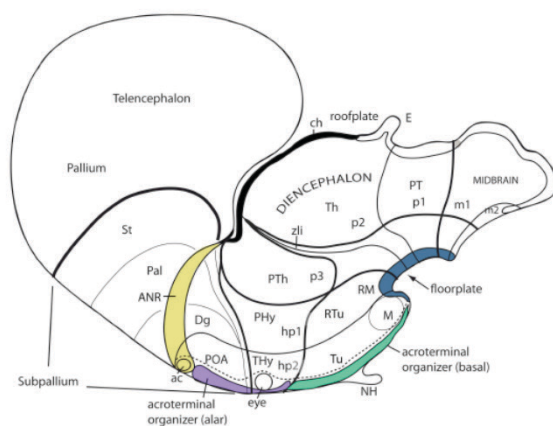


Figure 11. Illustration showing different sources of diffusible molecules that have effects in telencephalon and hypothalamus patterning. The anterior neural ridge, ANR, is a source of *Fgf8*; the mammillary and retromammillary floor plate secrete *Shh* at early stages and later *Shh* expression is displaced laterally, at the tuberal – alar limit of the hypothalamus. The acroterminal regions (basal and alar) are other sources of *Fgf8*, *Fgf10* and *Fgf18*. Adapted from Puelles and Rubenstein, 2015.

2. Hypothalamus formation

The hypothalamus is a complex structure important for endocrine and metabolic regulation. Rostral to the diencephalon, it represents the most anterior part of the neural tube. Theories on the AP and DV subdivisions of the hypothalamus have varied a lot and are still not totally fixed. This is due in part to the difficulty in defining the position of the rostral extremity of the AP axis. We use the subdivisions from Puelles and Rubenstein, 2015. According to this model, the anterior extremity of the of the brain (i.e. of the alar-basal boundary, Figure 11) is located within the hypothalamus, between the tuberal and alar domains. The hypothalamus has both AP and DV subdivisions. Along the AP axis, the posterior part of the hypothalamus that abuts the prethalamus is the peduncular hypothalamus (PHy or hypothalamic prosomere 1, hp1) and the anterior part is the terminal hypothalamus (THy or hypothalamic prosomere 2, hp2) (Puelles and Rubenstein, 2015). Along the DV axis, the subdivisions, summarized in Figure 10, will give rise to multiple nuclei essential for the secretion of numerous neuropeptides. In addition, several regions of the hypothalamus are important for eye development. The terminal paraventricular hypothalamus (TPa) contains the eye vesicle, the optic stalk and the optic chiasma, and the terminal subparaventricular hypothalamus (TSPa) contains the optic tract. Finally, the preoptic area (POA), localized dorsal to the TPa (included in hp2) has been long considered as hypothalamic for its function in adult, but embryologically it has telencephalic origin (Fig. 10 and 12; Puelles et al., 2013; Diaz et al., 2015; Puelles and Rubenstein, 2015; Puelles 2016).

To simplify the terminology of the hypothalamic regions, in the next parts of description, results and discussion, mammillary and tuberal areas will be termed “ventral hypothalamus”, as opposed to the alar (formerly called anterior) hypothalamus. Moreover, the forebrain midline will be called “ventral midline” even in the alar hypothalamus, to acknowledge that, like in the tuberal and mammillary regions, the midline receives Hh signals from the underlying mesoderm (i.e. from the prechordal plate).

The Hh pathway is essential for hypothalamus formation and patterning. During development, at E8.5 the prechordal plate expresses Shh and induces the expression of

Shh in the ventral midline of the future hypothalamus. Thus, according to the Puelles, model, part of the “ventral” hypothalamus, which receives high Hh signalling from the prechordal plate, is in fact in the alar domain of the forebrain. Later on, at E9.5-E10.5 Shh expression is downregulated in the FP and is activated laterally (Figure 13; Blaess et al., 2015). The hypothalamus has a different mode of Hh signalling than the more caudal regions. In the hindbrain as in the spinal cord, Shh acts as a morphogen and it is non-neurogenic: it is never expressed in neuronal progenitors. In contrast, in the hypothalamus, genetic fate-mapping has shown that most of the mammillary and tuberal regions are derived from Shh-expressing cells. However, Shh may also act as a morphogen to specify structures in the alar hypothalamus, where it is not expressed (Figure 12; Alvarez-Bolado et al., 2012, Blaess et al., 2015; Zhang & Alvarez-Bolado, 2016).

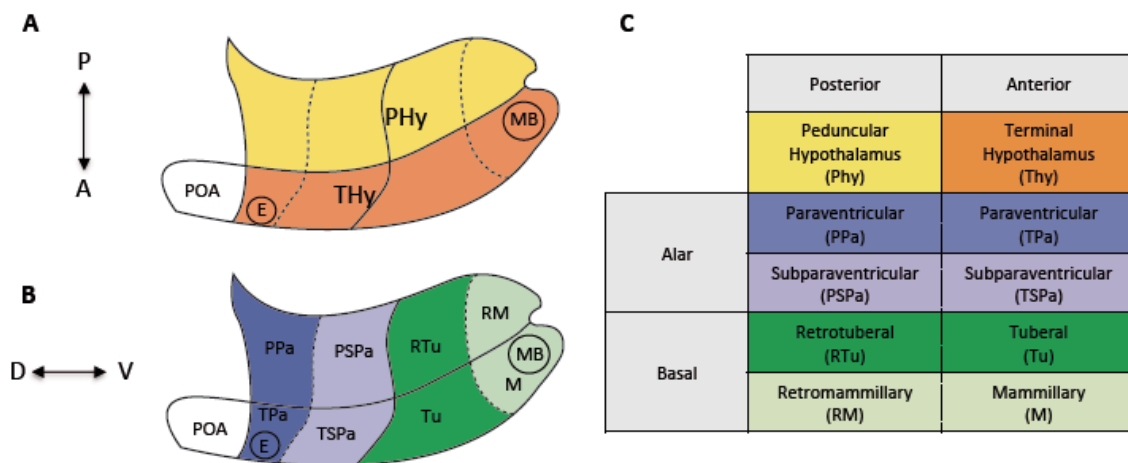


Figure 12. Scheme of a lateral view of the hypothalamic regions. **A.** Representation of the AP regions. The most anterior region is the terminal hypothalamus (THy, in orange) followed by the peduncular hypothalamus (PHy, in yellow) that abuts the prethalamus. **B.** DV structures of the hypothalamus. The alar regions of the hypothalamus are (in dark and light violet) the paraventricular and subparaventricular areas (dorsal to ventral). The ventral regions (in dark and light green) correspond to the tuberal and mammillary areas. **C.** Summary and names of each region of the hypothalamus. E, eye; MB, mammillary body; POA, preoptic area.

The first sign of Shh activity is the induction of the *Nkx2.1* and *Nkx2.2* transcription factors. This expression expands during development and leads to the subdivisions of the hypothalamic vesicle into mammillary, tuberal and alar

hypothalamus (Figure 12). Around E10, the expression of *Nkx2.1* expands to the basal telencephalon and the POA (Fig. 13; Shimamura et al., 1995; Crossley et al., 2001; Ware et al., 2014).

Studies of null and conditional *Shh* mutant mice have shown that prechordal plate-derived *Shh* is essential to maintain the prechordal plate and to induce the hypothalamic midline (Aoto et al., 2009), while neural plate-derived *Shh* is required for the formation of the mammillary and tuberal hypothalamus, and for the specification of lateral hypothalamic neurons (Szabo et al., 2009; Shimogori et al., 2010; Zhao et al., 2012). *Gli1* and *Gli2* are together required for the formation of the hypothalamic ventral midline (Park et al., 2000). Hypothalamic defects in *Gli3* mutant mice are not reported (Haddad-Tóvolli et al., 2015).

Other signalling molecules are involved in the development of the hypothalamus, such as Wnt antagonists, NODAL and BMPs (Kiecker and Nihers, 2001; Mathieu et al., 2002; Manning et al., 2006). Their role will not be discussed here.

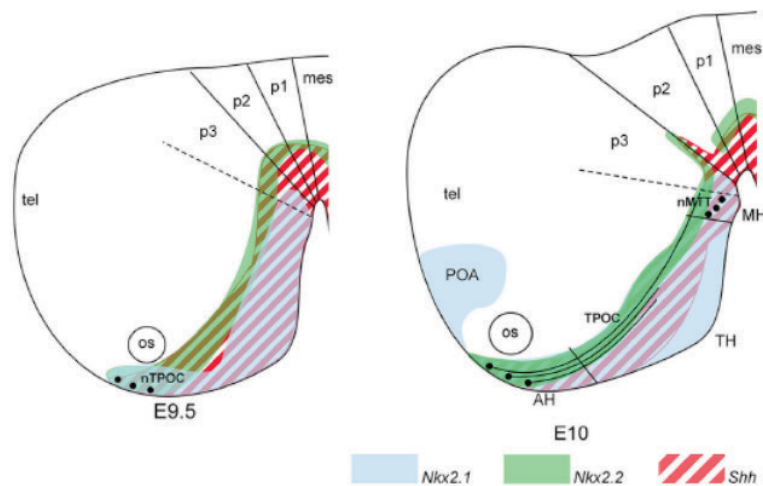


Figure 13. Schematic representation of the hypothalamic vesicle in the mouse brain. The three subdivisions of the hypothalamus are based on *Shh* expression and on the expression of the target genes *Nkx2.1* and *Nkx2.2*. AH, alar hypothalamus; MH, mammillary hypothalamus; TH, tuberal hypothalamus. Adapted from Ware et al., 2014.

3. Formation of the eyes

The development of the vertebrate eyes results from the coordinated interaction between the extraocular mesenchyme, the neuroepithelium and the surface of the ectoderm. The neuroepithelium of the alar hypothalamus evaginates to form the bilateral optic vesicles. Later on, the vesicles grow towards the surface of the ectoderm to form the lens placode and then invaginate to create the optic cups. The interaction between the lens placode and the distal part of the optic vesicle leads to invagination of the lens. The inner layer of the optic cup will develop into the neural retina (where retinal ganglionic cells, RGC, differentiate) while the outer layer becomes the retinal pigmented epithelium or RPE. Furthermore, the proximal optic cup will give rise to the optic stalk (neuroectoderm-derived), which connects to the brain (Fig. 14; Wallace, 2008; Fuhrmann, 2010; Graw, 2010).

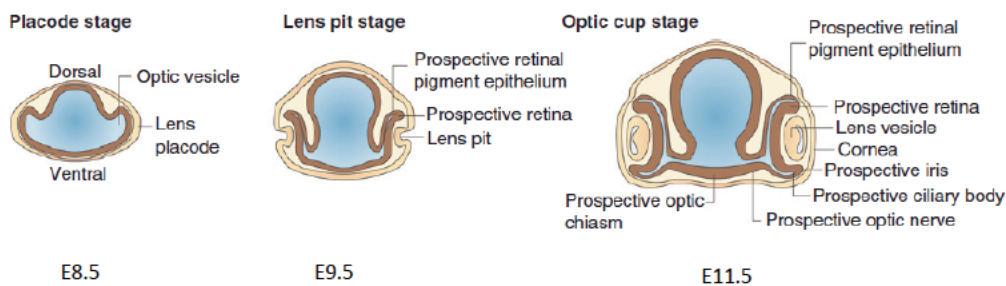


Figure 14. Schematic view of a developing vertebrate eye. Adapted from Graw, 2010.

During development of the eye, genes encoding molecules of Hh signalling pathway, *Shh*, *Ptch1* and the three *Gli*, are expressed in specific domains (Furimsky and Wallace, 2006). Eye morphogenesis is induced at E8.0 by Shh secreted from the prechordal plate and then by the ventral forebrain (FP) (Marti et al., 1995). This separates the eye fields and forms the bilateral optic vesicles (Chiang et al., 1996). Hh signalling contributes to both DV and proximo-distal (PD) patterning of the eye. It regulates the expression of paired box (*Pax*) genes to repress distal and promote proximal fates of the optic vesicles. *Pax2*, expressed in the optic stalk, represses *Pax6*, a marker of the neural retina, thus separating these two regions. Later, BMP4 secreted from the dorsal optic vesicle and Shh from the ventral midline play opposite roles in optic vesicle patterning. Target genes of the Hh (*Vax2*) and BMP (*Tbx5*) pathways

expressed in the ventral and dorsal neural retina, respectively, repress each other to establish the D-V axis of the optic vesicles (Fig. 15.A-B).

The effectors of the pathway, Gli1, Gli2 and Gli3, play an important role in the formation of the eyes and the optic stalks. Shh represses the formation of Gli3R in the midline to promote bilateral eye development (Furimsky and Wallace, 2006). Mutations in Gli3 produce several defects in the eyes, such as anophthalmia, microphthalmia and coloboma; whereas the optic stalk is well defined (Hui and Joyner, 1993; Furimsky and Wallace, 2006). Gli3R is required for the formation of the retina and optic nerve territories. Gli2A and Gli1 play a role complementary to Gli3R, inducing the formation of optic stalks. Gli2 null mutants present defects in the ventral neural tube, but the eyes and optic stalk are still formed (Ding et al., 1998; Matise et al., 1998; Furimsky and Wallace, 2006) whereas double mutants of Gli2 and Gli1 show a strong reduction of the optic stalk (Furimsky and Wallace, 2006). All of these data reveal the essential functions of Gli3 in eye formation and of Gli1 and Gli2 in optic stalk specification (Figure 15.C).

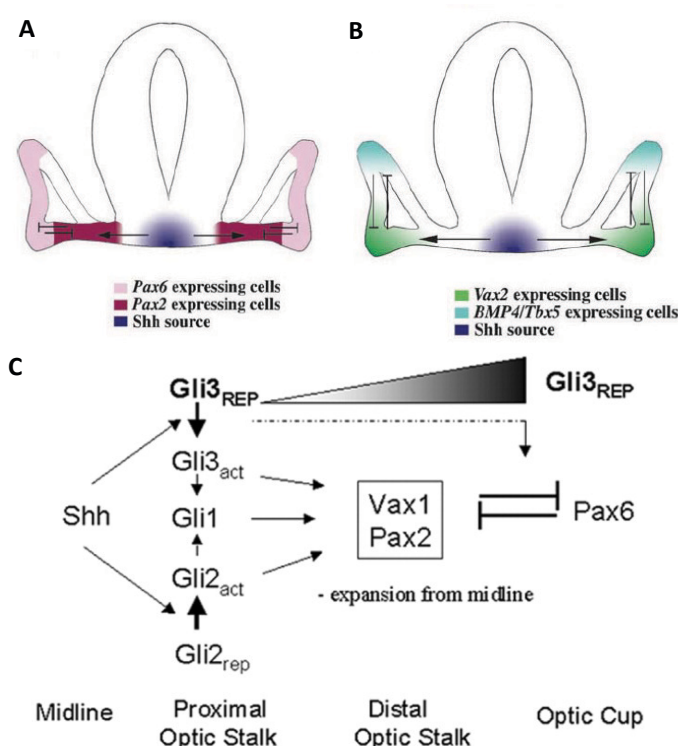


Figure 15. A-C. Hh signalling in eye vesicle patterning. Shh is involved in PD and DV specification of the optic vesicles. **C.** Model of complementary Gli function during early development of the eyes. Adapted from Amato et al., 2004 and Furimsky and Wallace, 2006.

4. Diencephalic specification

The diencephalon is a sophisticated structure located between the secondary prosencephalon (telencephalon and hypothalamus) and the midbrain. The prosomeric model proposed by Rubenstein and Puelles (Rubenstein et al., 1994) defines several landmarks that subdivide the diencephalon. This model, now broadly accepted, defines the AP and alar-basal (DV) territories of the forebrain. According to the prosomeric model, the diencephalon is subdivided along the AP axis into three prosomeres (from caudal to rostral): the pretectum or prosomere 1 (p1), the thalamus or prosomere 2 (p2) and the prethalamus or prosomere 3 (p3) (Fig. 9). Note that the pretectum, thalamus and prethalamus correspond to the alar parts of p1, p2 and p3, respectively.

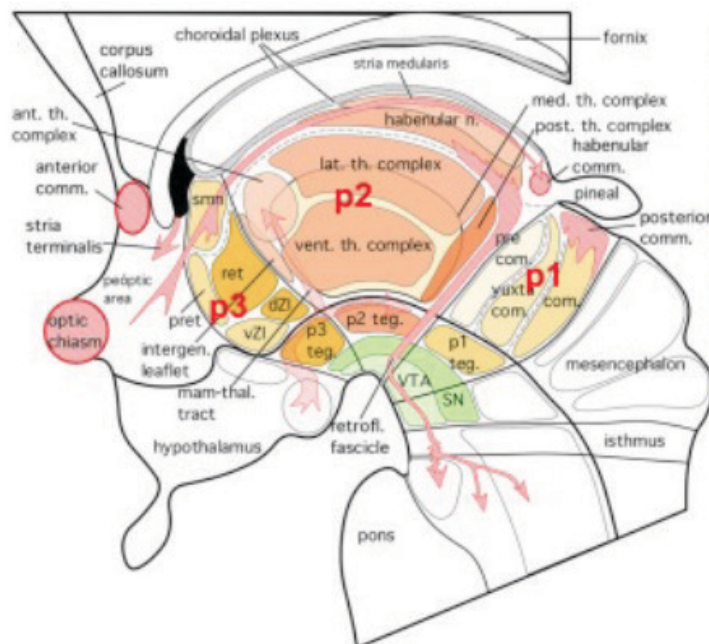


Figure 16. Illustration of the different nuclei and structures of mouse diencephalon. Representation of alar-basal and rostro-caudal subdivisions and axonal tracts. Adapted from Martinez-Ferre and Martinez, 2012.

Prosomere 1, the pretectum, presents two main alar structures at postnatal stages, the caudal part called the commissural pretectum (associated with the posterior commissure) and the rostral part called the pre-commissural pretectum. The border between p1 and p2 corresponds to the retroflex tract (an axonal tract with habenular

origin). Pretectal structures are important for the correct regulation of visual inputs and visual reflexes. P1 ventral structures, the ventral tegmental area (VTA) and the substantia nigra, are involved in the control of reward behaviour and voluntary movements, respectively (Fig. 16).

Prosomere 2 alar derivatives are the thalamus and epithalamus. The alar p2 develops the thalamic nuclear system. In addition, it is divided in two sub-regions: the rostral thalamus (Th-R) and the caudal thalamus (Th-C). Th-C comprises a large number of thalamic nuclei with several functions, such as the regulation of alertness, learning and memory, as well as motor and sensory functions. The caudal thalamus is connected with the cortex by the cortico-thalamic (CTA) and thalamo-cortical (TCA) axonal tracts. The Th-R is a small region that does not project axons to the cortex and is composed mostly of GABAergic inhibitory neurons. These neurons, at E13.5, migrate to form the subcortical visual shell, a group of interconnected nuclei involved in entrainment of the circadian rhythm (Delogu et al., 2012). The epithalamus, situated in the dorsal part of the thalamus, is composed of the habenula, the stria medullaris tract and the pineal gland (epiphysis). The habenula is implicated in motor and cognitive functions. From the habenula emerges a tract called fasciculus retroflexus that projects to the interpenduncular nucleus in the hindbrain. The epiphysis secretes melatonin for the control of circadian rhythms. The basal plate of p2 is composed by the interstitial rostral nucleus, implicated in visual reflexes, the VTA and the substantia nigra (Fig. 16).

Prosomere 3, the prethalamus, is composed of different nuclei. These alar nuclei connect with the epithalamus controlling afferent and efferent information, and receive inputs from the retina, essential for the circadian regulation. The most dorsal part of the prethalamus is composed of the choroid plexus, important for the secretion of different molecules in the ventricle, and of the prethalamic eminence. Additionally, the prethalamus has a role in navigation of the TCA and CTA tracts between the cortex and the thalamus (Fig. 16).

The topological distribution of the AP and alar-basal structures of the diencephalon begins at 9.5 days of gestation and at is completed by E12.5. The specification of the different regions of the diencephalon requires, as in other regions of

the brain, the involvement of signalling molecules produced by organizing centres and transcription factors in responding tissues. As in other more caudal regions, *Shh* is produced by the notochord underlying the diencephalon and then by the ventral diencephalon, where it organizes DV patterning. The principal AP organizing centre of the diencephalic morphogenesis is the mid-diencephalic organizer (MDO) or zona limitans intrathalamica (ZLI), an alar region located between the thalamus and prethalamus. Although other signals such as FGFs and Wnts are secreted in this region (Zeltser et al., 2001; Kiecker and Lumsden, 2004; Scholpp et al., 2006), the predominant morphogen expressed in the ZLI is *Shh*, whose expression progressively expands from ventral to dorsal between E9.5 and E11.5 (Fig. 17; Shimamura et al., 1995).

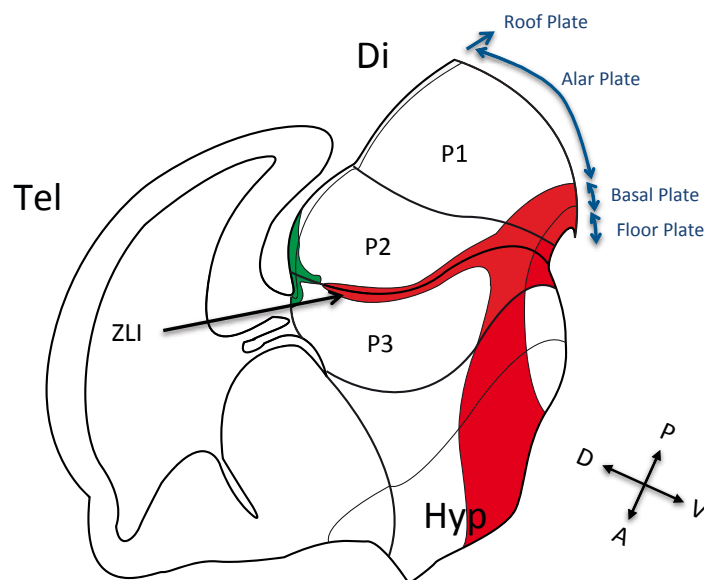


Figure 17. Schematic representation of *Shh* source (in red) and Wnts/FGFs sources (in green) in the diencephalon. *Shh* is expressed in the ZLI, basal plate and floor plate of the diencephalon. Wnts and FGFs are expressed dorsal to the ZLI and in the roof plate. Di: diencephalon; Hyp: hypothalamus; P1: pretectum; P2: thalamus; P3: prethalamus; Tel: telencephalon; ZLI: zona limitans intrathalamica.

The ZLI forms at the junction between thalamus and prethalamus in an *Otx*-positive region and is positioned by the repressive function of *Fez* (prethalamus) and *Irx* (thalamus) transcription factors (Scholpp and Lumsden, 2010). The formation of the ZLI is thought to involve an inductive process requiring Hh signaling from the ventral diencephalon (Kiecker and Lumsden, 2004; Zeltser, 2005; Vieira and Martinez, 2006).

Shh is secreted first by FP cells underlying the future ZLI and is then activated within the ZLI with a ventro-dorsal progression. Experiments in chicken embryos have shown that Shh from the basal plate is required for *Shh* expression in the ZLI (Kiecker and Lumsden, 2004; Zeltser, 2005; Vieira and Martinez, 2006). The ZLI itself is considered as part of the alar plate since it is not formed by the migration of basal plate cells (Zeltser, 2005). This requirement for basal Shh is not conserved in the zebrafish, and studies in mouse mutants have led to contradictory conclusions. Nevertheless, a conditional mouse mutant in which Shh is absent from the basal forebrain clearly shows that basal Shh is required for ZLI formation and for the correct segregation of ZLI cells from the thalamus (Szabo et al., 2009b; Vieira and Martinez, 2006; Epstein 2012).

Three different Shh-dependent steps can be distinguished during regionalisation of thalamus and prethalamus primordia (Scholpp and Lumsden, 2010) in the ZLI:

1. The prethalamus and thalamus acquire distinct identities depending on their response to Shh exposure. This distinct competence to respond to Hh signalling is due in part to the previous expression of Iroquois homeobox factors (*Irx* genes) in thalamic primordium. Overexpression of *Irx3* in the prethalamus leads to the Shh-dependent expression of thalamic genes, *Sox14* (in Th-R) and *Gbx2* (in Th-C) (Kiecker and Lumsden, 2004). *Fez* genes would play a similar function in the prethalamus (Hirata et al., 2006).
2. Shh signalling from the ZLI induces the proneural genes *Neurogenin1* (*Ngn1*) and *Neurogenin2* (*Ngn2*) in the Th-C and *Mash1* (or *Ascl1*) in the Th-R and prethalamus (Vue et al., 2007). This differential expression of the proneural genes leads to the specification of glutamatergic neurons (*Ngn1* and *Ngn2* expressing cells) in the Th-C and of inhibitory GABAergic neurons (*Mash1* expressing cells) in Th-R and prethalamus. Studies in mouse have shown that blocking the Shh pathway leads to an absence of the Th-R and to a strong reduction of the Th-C (Vue et al., 2009).
3. The last step involves the expression of different transcription factors that depend on the concentration of Shh. High levels of Shh activity induce the expression of *Nkx2.2*, *Olig2*, *Sox14*, *Tal1* and *Gad1* in Th-R. In contrast, only low levels of Shh are required for *Gbx2*, *Dbx1*, *Olig3* and *Lhx2* in Th-C (Barth and Wilson, 1995; Hashimoto-Torii et al., 2003; Kiecker and Lumsden, 2004; Szabo et al., 2009; Vue et al., 2009).

al, 2009). Consequently, the reduction of Shh signalling from the ZLI leads to an absence of rostral thalamic nuclei such as lateral and medial geniculate nucleus at later stages of the development (Szabo et al., 2009b). Thus, Shh from the ZLI acts as a morphogen to regulate AP patterning of the diencephalon as it does for DV patterning in the spinal cord (Scholpp and Lumsden, 2010).

Other signalling pathways, such as the Wnt and Fgf pathways, are active in the vertebrate diencephalon. Wnt ligands are present in the diencephalic roof plate and in the ZLI where they overlap with Shh. Fgf ligands are in the dorsal diencephalon and in the prethalamus. Wnt signalling has a role in survival of the ZLI in zebrafish and promotes thalamic fate at the expense of prethalamic fate. It also plays later roles in compartmentation and neurogenesis within the thalamus. Fgf activity downstream of Shh is important for the development of GABAergic neurons in the Th-R and prethalamus (Hagemann and Scholpp, 2012). Many studies have addressed the function of these signalling pathways, but I will not detail them further.

5. Defects in the Shh pathway in humans : holoprosencephaly.

Holoprosencephaly is a complex and very severe malformation affecting the most rostral region of the neural tube. It is characterized by a lack or a partial defect of cleavage of the prosencephalon, concerning mainly the telencephalon but also the diencephalon. Such a cleavage is provided by the ventral midline but also by the dorsal one. These two midlines differ from the developmental origin as from the molecular regulations that ensure their formation. Several neuropathological forms have been described according to the severity of this malformation. Classically recognized forms are as follows: alobar holoprosencephaly (in which the telencephalon is a totally uncleaved holosphere), semi-lobar forms (with a presence of an incomplete inter-hemispheric fissure which is present at the posterior pole but absent at the frontal pole), and lobar forms (cerebral hemispheres are then completely separated but a bridge of cerebral cortex connecting the two sides and passing over the corpus callosum is present). Other forms have been isolated more recently: the septo-preoptic forms in which cleavage is perturbed in the septal or preoptic regions (Hahn et al., 2010), the middle hemispheric variants in which the defect of cleavage involves only the posterior

frontal and anterior parietal cortex (Fig. 18; Barkovich and Quint, 1993; Lewis et al., 2002; Simon et al., 2002).

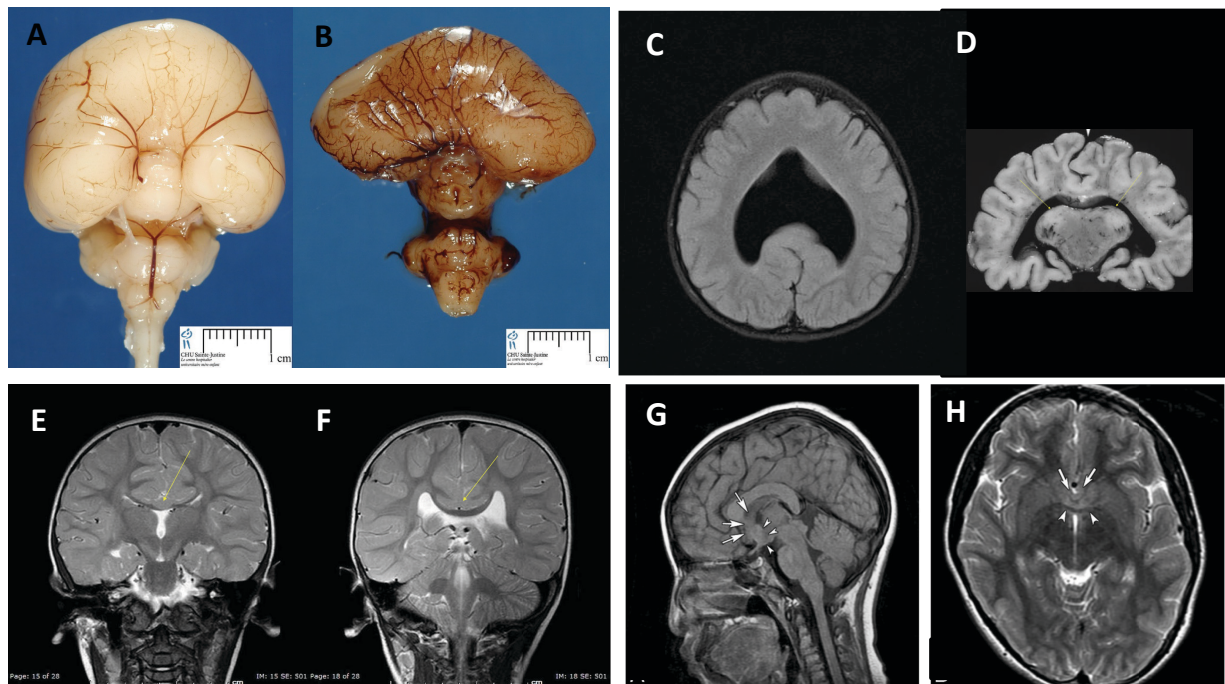


Figure 18. Illustrative cases of holoprosencephaly. **A-B.** Two cases of alobar holoprosencephaly (ventral view). The two prosencephalic hemispheres are totally fused. **C-D.** Two cases of semilobar holoprosencephaly. In the axial view of **C**, the frontal poles are fused whereas an interhemispheric fissure is evidenced at the occipital regions. In the coronal view of the case **D** the thalami are fused. **E-F.** Rostral and caudal views of coronal sections in a case with lobar holoprosencephaly. The cortex extends and covers the midline. **G-H.** Sagittal and axial view of a case with middle interhemispheric variant of holoprosencephaly that presents defects in the septo-preoptic cortex. Sources Hahn et al., 2010; humpath.com; radiopaedia.org.

Holoprosencephaly is in a proportion of the cases associated with chromosomal abnormalities (Mercier et al., 2011). Heterozygous mutations in 14 genes have been identified as causing holoprosencephaly, four of which are considered as major causal genes: SHH, ZIC2, SIX3 and TGIF, which in total amount to 25-30% of the known holoprosencephaly cases. SHH mutations are the most frequent (10% of the cases in a European cohort, Mercier et al., 2011). Other members of the Hh pathway are also mutated in holoprosencephaly cases: GLI2, PTCH1 (probably dominant active mutations), DISP1 (regulation of Hh ligand secretion and internalization), GAS1 and CDON (membrane proteins that act with Ptch1 and positively regulate Hh signaling). Mouse models have been very informative in the mechanisms of HPE. They point to a

prime involvement of defects in *Shh* expression and signaling in the forebrain. According to these studies, the pathogenicity of the mutations in the three major holoprosencephaly genes, outside *Shh*, are explained by the role of these genes in *Shh* expression or pathway activity in the forebrain. *Zic2* is essential for the formation of the prechordal plate (Warr et al., 2008); *Six3* directly regulates *Shh* expression in the forebrain (Jeong 2008, Geng 2008); *Tgif1* has an indirect action on *Shh* signaling by regulating *Gli3* and *Nodal* independently (Taniguchi 2012, 2017). Thus, the study of HPE shows that the importance of Hh signaling in forebrain morphogenesis is conserved in human.

III. The primary cilium

The cilium is a slim microtubule-based organelle that projects from the cell surface of many cell types. Cilia are typically classified in primary cilia (or non-motile cilia) and motile cilia (called in some cases flagella). Motile cilia are present in several cell types, either individually (in the vertebrate laterality organ for instance, or in the zebrafish FP) or in large numbers (in the murine trachea and ependyma). Motile cilia are involved in generating or maintaining fluid flow, for instance for the cerebrospinal fluid (CSF) in the brain ventricular cavities or for the mucus in respiratory airways or in the *Xenopus* skin, and have been proposed to help transport determinants within these fluids (Lun et al. 2015; Chang et al. 2016). Motile cilia and flagella are also essential for locomotion in many simple organisms and embryos (such as the unicellular alga *Chlamydomonas*, paramecia, cnidarian embryos and planarians) or in specialized cell types (spermatozoa; Fig. 19).

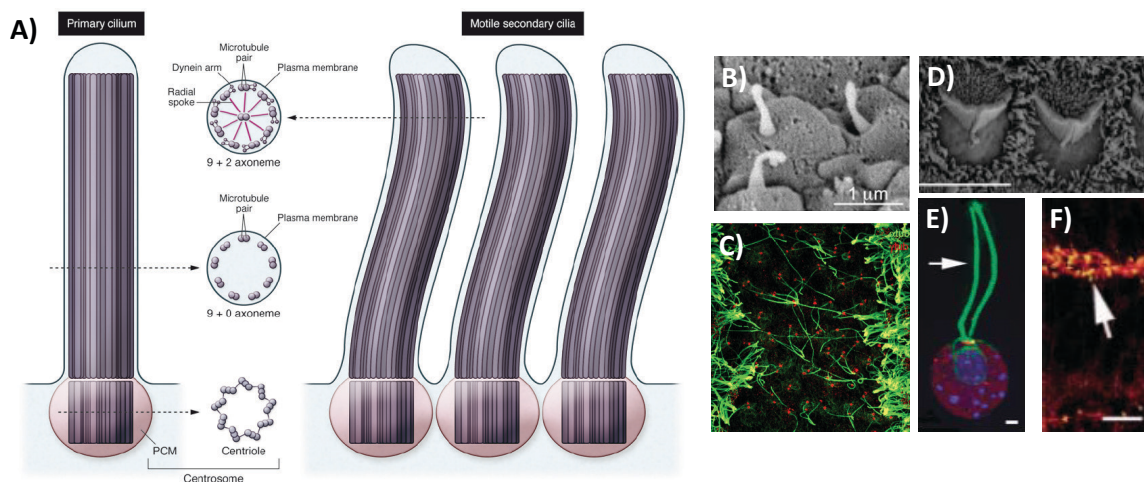


Figure 19. A. Representation of motile and non-motile cilia. B. Primary cilia (non-motile cilia) in the ventricle of the mouse neural tube C. Motile cilia in multiciliated ependymal cells. Adapted from Liu and Zeitlin, 2011. D) Kinocilia in mechanosensory cells of the mouse inner ear. E. Flagella of the green alga *Chlamydomonas*. F. Motile cilia of floor plate in the neural tube of zebrafish. Pictures from Singla and Reiter, 2006; Besse et al., 2011; Mahuzier et al., 2012; Mirzadeh et al., 2017.

Primary cilia are present in nearly all vertebrate cells and they have been proposed as receptors of several signals from the cell environment, such as chemical compounds, small proteins, light (in photoreceptors) and mechanical forces (for instance to fluid flow in the kidney tubules). Primary cilia have been implicated in the

transduction of several signalling pathways. In humans, a variety of inherited diseases with diverse manifestations and severities have been linked to primary cilia dysfunctions and called ciliopathies. Defects found in ciliopathies include kidney cysts, retinal degeneration, intellectual disability, obesity, polydactyly, skeletal abnormalities and brain malformations (Reiter and Leroux, 2017).

1. Structure and ciliogenesis

1.1. Structure of primary cilia

Primary cilia consist of a specialized plasma membrane supported by a specific microtubule network, the axoneme, anchored to a centriolar structure, the basal body. In between the axoneme and the basal body lies a distinct structure called the transition zone. The axoneme consists of nine outer doublet microtubules that elongate from the basal body. Each doublet comprises one complete microtubule (the A-tubule) connected to an incomplete microtubule (the B-tubule). In addition to this basic structure, motile cilia have two complete microtubules in the centre of the axoneme called the central pair, which is attached to the outer doublets by radial spokes and dynein arms (Fig. 20; Nicastro et al., 2006; Singla and Reiter; 2006; Sui and Downing, 2006; Ishikawa and Marshall, 2011). The tubulin of the outer doublets is exposed to different post-translational modifications to regulate cilia assembly and motility such as glycylation, glutamylation and acetylation (Thazhath et al., 2004; Ikegami et al., 2010).

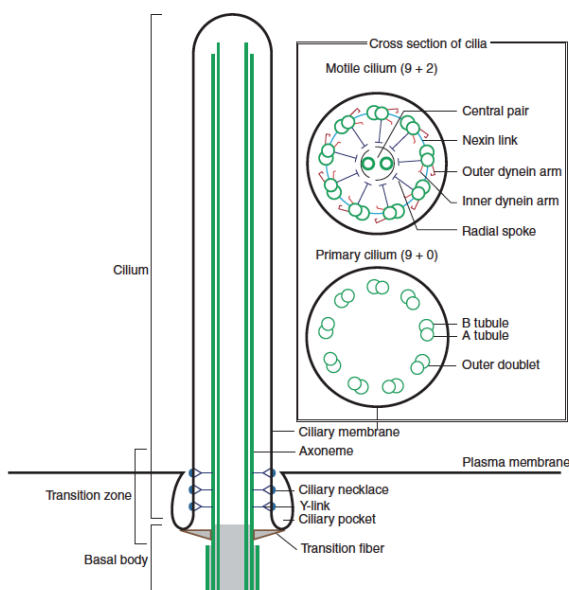


Figure 20. Architecture of cilia. Longitudinal section of primary cilia structure. The square shows transversal sections of motile and non-motile cilia. Modified from Ishikawa and Marshall, 2018.

The basal body is important to nucleate the cilium and it is formed after mitosis by maturation of the oldest centriole, known as the “mother centriole”, of the cell. The centrioles are microtubule-based structures with several functions in mammals such as cell proliferation, cell polarity, signalling and motility (Loncarek and Bettencourt-Dias, 2017). They are composed by 9 outer triplet microtubules with a complete microtubule (A tubule) and two incompletes microtubules (B and C tubules; Carvalho-Santos et al., 2011). Surrounding the centrioles, the pericentriolar material (PCM) is important for microtubule nucleation. The PCM is a defined supramolecular material composed of many proteins that extend radially, such as pericentrin, PLK, CEP and CDK proteins (Lawo et al., 2012; Mennella et al., 2012; Conduit et al., 2015). In primary cilia, the basal body remains close to the daughter centriole, which is not the case in multiciliated cells (Fig. 21).

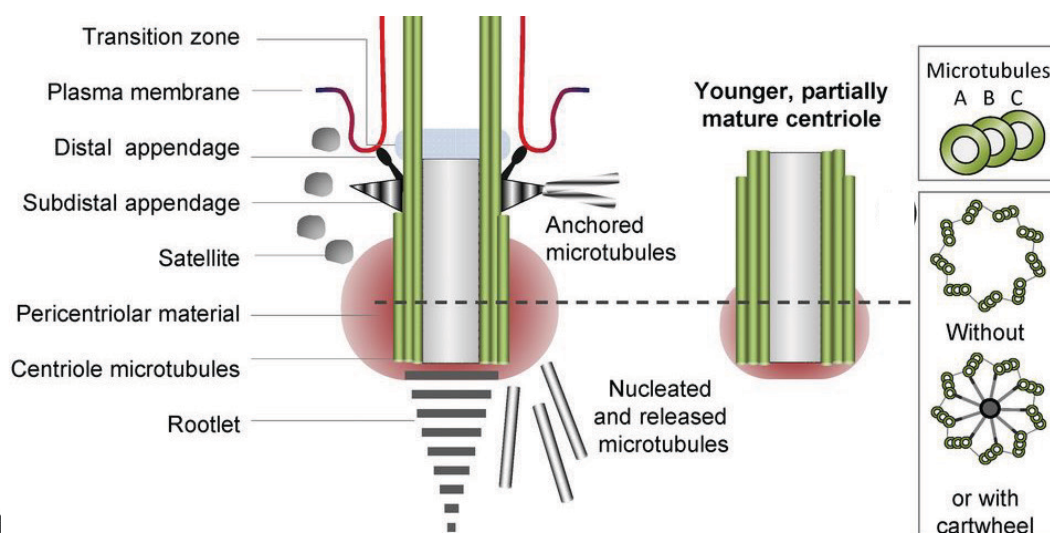


Figure 21. Basal body structure. Longitudinal sections of two centrioles. Both centrioles are composed by nine microtubule triplets in radial symmetry. The centriole is decorated by distal and subdistal appendages and by the rootlet. In many vertebrates, satellites surround the centriole and its proximal end its embedded in the pericentriolar material. Adapted from Loncarek and Bettencourt-Dias, 2017.

The basal body is characterized by the presence of appendages. At the most distal part of the mother centriole, close to the transition zone, a variable number (depending on the cell type in mammals) of distal appendages appear, such as the transition fibers, which connect the basal body to the membrane. These distal appendages are involved in ciliogenesis by interacting with the vesicle that caps the future cilium and in which the

axoneme grows (Tanos et al., 2013). Subdistal appendages harbour proteins such as Odf2, Cep128 and Ninein and are involved in cilium planar polarity, centriole cohesion and in maintaining cilia submerged within deep membrane invaginations (Galati et al., 2016). Some cilia possess a basal foot instead of subdistal appendages. At the proximal part, the centrioles sometimes display a rootlet. The rootlet is a fibrous appendage-like striated structure that provides structural support to ciliated cells and is associated with actin filaments (Yang et al., 2005; Yang and Li, 2006; Loncarek and Bettencourt-Dias, 2017). It contains Rootletin, which is also involved together with c-Nap1 in centrosome cohesion. Subdistal appendages, basal foot and the rootlet, as well as centrosome cohesion, are all dispensable for ciliogenesis.

The transition zone is located distal to the centriole, where the triplet microtubules of the basal body make the transition with the doublets of the axoneme. This region is characterized by Y-shaped links that bind the microtubules of the axoneme with the ciliary plasma membrane. Between the transition zone membrane and the plasma membrane, an invagination of the plasma membrane called ciliary pocket is often observed. The ciliary pocket is important for endocytosis of ciliary components. The transition zone is required for making the cilium a true cell compartment, despite the fact that it is not completely separated from the cytosol by membranes. An essential function of the transition zone is indeed to control the entry and exit of different ciliary components in and out of the cilium (Garcia-Gonzalo et al., 2011; Reiter et al.; 2012). This includes both membrane proteins and cytoplasmic proteins. In mammals, three different protein complexes compose the transition zone: the MKS, NPHP and CEP290 complexes. The MKS complex, whose inactivation is associated with a severe ciliopathy in humans, Meckel Syndrome, is an important module of multiple proteins for cilia formation in some tissues (Garcia-Gonzalo et al., 2011). The NPHP (for nephronophthisis disorder) complex has interactions with MKS proteins. Together they are involved in transition zone assembly and in cilia building, regulating the entry of several proteins (Yee et al., 2015). Moreover, the centrosomal proteins CEP290 and NPHP5 (CEP290 complex) interact with MKS and NPHP complexes for their recruitment and for construction of the transition zone (Schouteden et al., 2015; Li et al., 2016). These complexes interact with other ciliary proteins implicated in cilia formation, ciliary trafficking and signalling, such as RPGRIP1L, IFT (intraflagellar

transport) proteins and BBSome components (Fig. 22; see below; Yee et al., 2015; Avidor-Reiss et al., 2017; Gonçalves and Pelletier, 2017; Garcia et al., 2018). RPGRIP1L is the main protein I have focused on during my PhD and it will be presented in greater detail in Chapter IV.

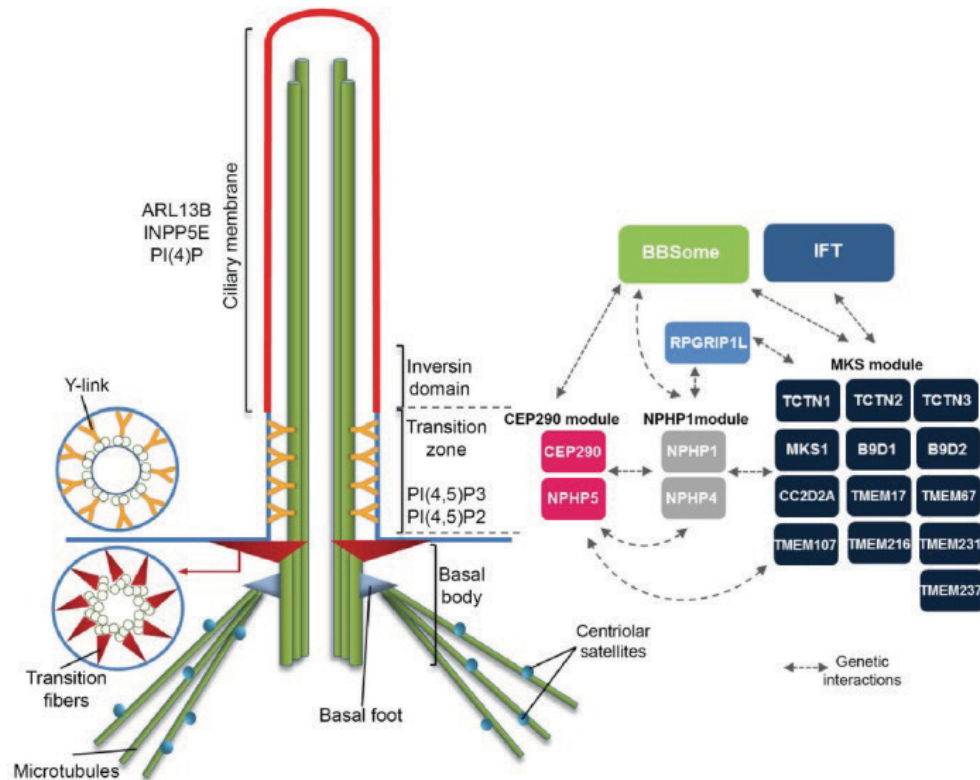


Figure 22. transition zone structure. The transition zone lies proximal to the axoneme. Distal to the transition zone, there is an inversin domain which lacks Y-links and displays protein composition different from that of the transition zone. The right scheme shows the modules of the transition zone (CEP290, NPHP1 and MKS) and the genetic interactions between components of the BBSome and IFT. Adapted from Gonçalves & Pelletier, 2017.

1.2. Primary cilia assembly and disassembly

Ciliogenesis starts in interphase when the cells exit the cell cycle (G0) in response to differentiation signals (Wheatley et al., 1996; Stinchcombe et al., 2015). In G0, cytoplasmic vesicles produced in the Golgi, called distal appendage vesicles (DAVs), accumulate and dock to the distal appendages of the mother centriole (Schmidt et al., 2012). DAV fusion makes a ciliary vesicle at the distal part of the centriole. At the distal tip, the centriolar microtubules extend below the ciliary vesicle, enclosing its shape in a

double membrane. The newly born cilium docks and fuses to the plasma membrane of the cell, creating a continuity of the compartments (Fig. 23.A; Sánchez and Dynlacht, 2016).

It has been reported that small Rab GTPases have an important role in ciliary vesicle formation and extension. Rab8a is involved in ciliary membrane assembly (Yoshimura et al., 2007; Westlake et al., 2011) and is localized in *trans*-face of Golgi and cytoplasmic vesicles. Once DAVs are formed, the Ehd1 protein is recruited and promotes an enlargement of these vesicles and a merging with Rab8-positive vesicles to produce the primary cilium membrane. The endosomes positives for Rab11 transport the GEF (guanine nucleotide exchange factors), Rabin8 (an activator for Rab8) and TrappII (membrane-tethering complex) to the location of Rab8 to activate Rab8-ciliogenic signal. Rab8 is activated with the fusion of Rab11- and Rab8-positive vesicles leading the activation of the ciliary assembly program (Fig. 23.B; Westlake et al., 2011).

Several components of the basal body are subjected to numerous changes during the initial steps of cilium assembly. One of the proteins involved is CP110, essential for centriole duplication and size regulation. CP110 interactions with Cep97 and its asymmetric abolition in the mother centriole may be important for the initiation of the ciliogenesis (Spektor et al., 2007). The elongation of the axoneme occurs after the docking of the basal body to the plasma membrane through distal appendages. The association of distal appendages to the mother centriole involves the accumulation of five proteins (Cep83, Cep89, Cep164, SCLT1 and FBF1) (Tanos et al., 2013). As an example, Cep164, a distal appendage protein, helps dock vesicles through interaction with Rabin8 and Rab8 (Sánchez and Dynlacht, 2016).

During cell cycle progression, the disassembly of the cilia occurs in G1/M phase. Recent studies identified numerous regulators of cilium disassembly, such as HEF1 (a scaffolding protein) and Aurora A (a calcium-calmodulin activated kinase which phosphorylates and activates the histone deacetylase HDAC6). HDAC6 promotes the deacetylation of the stable tubulins in the axoneme, promoting cilia disassembly (Plotnikova et al., 2012). Another function of Aurora A is to activate the phosphatase INPP5E, which supports high levels of the phosphatidylinositol PtdIns(4)P and

suppresses ciliogenesis (Xu et al, 2016). Furthermore, there are two activators of Aurora A at the basal body, trichoplein and Pitchfork (Pifo), both playing a role in cilia disassembly (Fig. 23.C; Kinzel et al., 2010; Plotnikova et al., 2012).

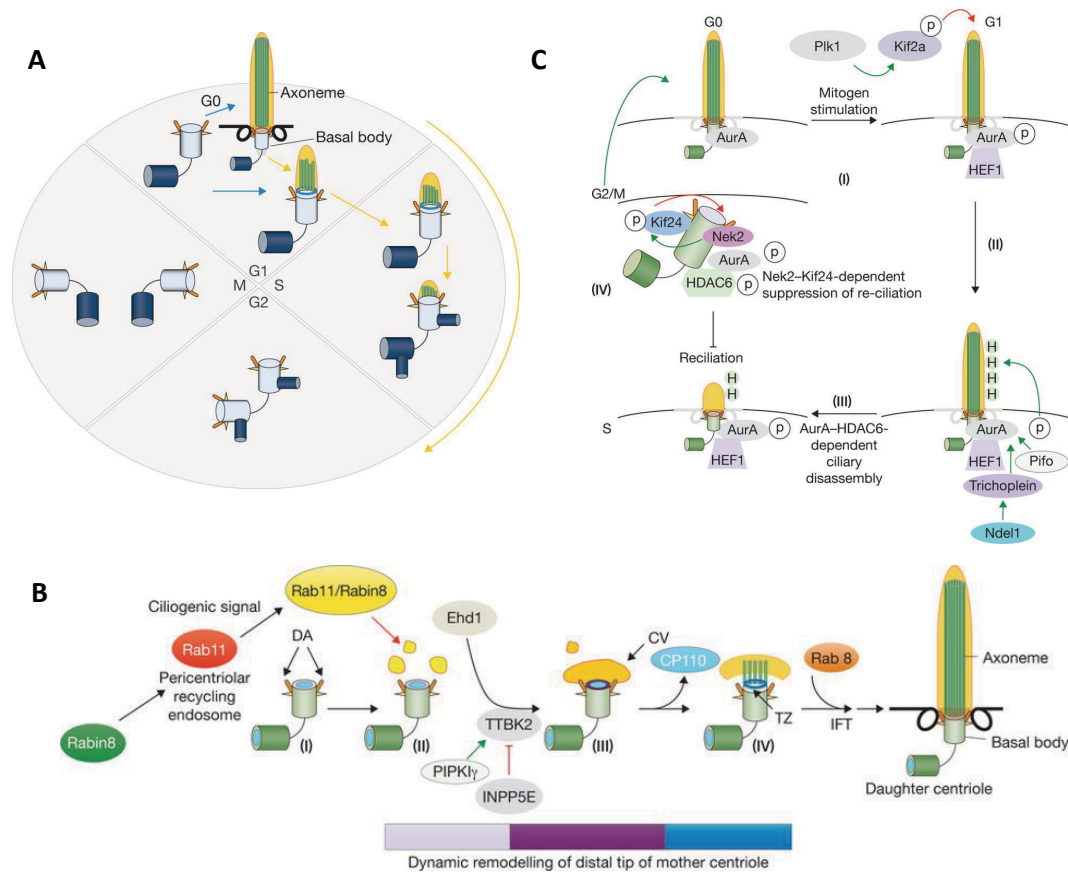


Figure 23. Cilia assembly and disassembly. **A.** Links between the ciliogenesis cycle and the cell cycle. **B.** Principal components of cilia assembly. **C.** Cilium disassembly and principal molecules implicated. Adapted from Sanchez and Dynlacht, 2016.

Two de-polymerizing kinesins, members of the Kinesin13 family, Kif2a and Kif24, are involved in cilia disassembly (Sánchez and Dynlacht, 2016). Kif2a localizes in the appendages of the mother centriole and it is activated by phosphorylation produced by the G2/M kinase Plk1. Its activation stimulates the de-polymerization of the axoneme microtubules, producing cilia disassembly and initiating a proliferative signal (Miyamoto et al., 2015). Kif24, associated with CP110, localizes at the distal centrioles. This kinesin has de-polymerizing activity and it is regulated by its phosphorylation by Nek2. Nek2 is expressed in S/G2 phase, activating Kif24 in cells that lack cilia (Kim et al., 2015). In this manner, Kif2a and Kif24 are activated by kinases expressed in S/G2

(Nek2) or G2/M (Plk1) phase, additionally linking cell cycle progression with the maintenance of disassembly required for mitosis (Fig. 23.C; Sánchez and Dynlacht, 2016).

As presented above, the assembly and disassembly of primary cilia are tightly linked to the cell cycle. Cilium disassembly is required for proper cell cycle in proliferating cells. The central point of this relation between cell division and primary cilia is the common use of the same centrioles in cilia assembly and in the mitotic spindle. As shown previously, ciliogenesis starts during the G1/G0 phase, however the retraction of the cilium is initiated at S/G2 to enter again in the cell cycle (Elliott and Brugmann, 2018). Numerous proteins have been involved in the repression or activation of these two cellular events. The IFT proteins play an important role in the cell cycle. The partial knockdown of Ift27 produces defects in cytokinesis. Furthermore, the inactivation of Ift88 accelerates S/G2/M progression and upregulation of Ift88 represses G1/S advance, leading to apoptosis (Qin et al., 2007; Robert et al., 2007). Two other proteins implicated in cell division, Trichlopin and Aurora A, are required for cilia resorption (Pan et al., 2004; Inoko et al., 2012). Trichlopin localizes in mother and daughter centrioles during cell division, but is lost in G0. Overexpression of Trichlopin represses ciliogenesis, in contrast, depletion induces cilia assembly. Aurora A is important for cilium resorption, and its inactivation induces ciliogenesis and cell cycle arrest (Inoko et al., 2012). Thus, cilia have a direct role on the control of the cell cycle. It should be remembered that cilia may also control proliferation and cell cycle length through their modulation of signalling pathways such as Wnt and Hh, both of which control these processes.

1.3. Intraflagellar transport (IFT) complexes and cilia trafficking

The building of the axoneme needs a selective import and transport of ciliary proteins by intraflagellar transport (IFT). When cilia assembly is finished, the cilium will develop its function as a receptor antenna to transduce several signalling pathways (see below). IFT is a bidirectional protein transport system inside the cilia that brings ciliary components from the cell body to the tip of cilia (anterograde transport) and sends back the products to the cell body from cilia (retrograde transport) (Ishikawa and Marshall,

2011 and 2017). The IFT bidirectional transport is mediated by IFT complexes called IFT trains (Kozminsky, 1993).

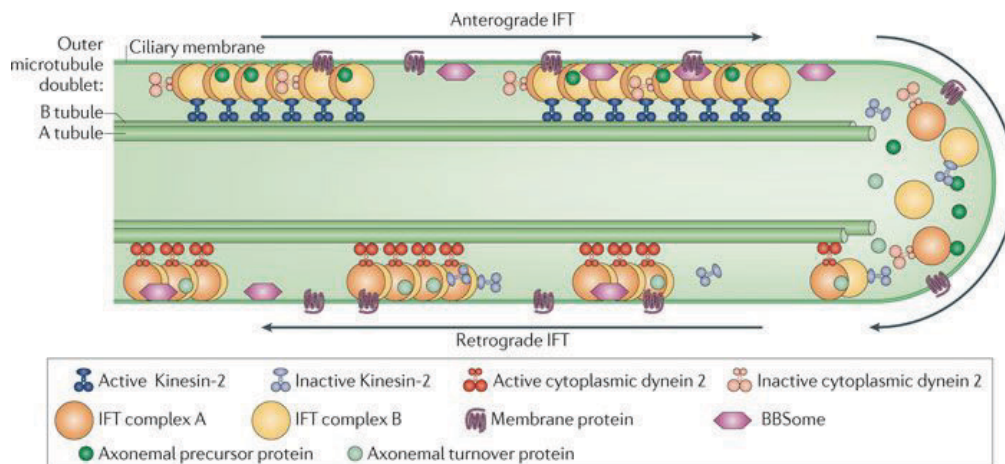


Figure 24. Intraciliary transport machinery. The anterograde IFT motor, kinesin-2, transports IFT complexes A and B, and the inactive dynein 2. At the ciliary tip, anterograde IFT trains release the axonemal proteins. Thus, the retrograde IFT machinery is rearranged and dynein 2 is activated to transport the complexes back to the cell body. Adapted from Ishikawa and Marshal, 2011.

Two different types of microtubule motors drive IFT: kinesin-2 for anterograde transport and cytoplasmic dynein 2 for retrograde transport. There are two different kinesin-2 motors (heterotrimeric and homodimeric). The most common anterograde IFT motor is the heterotrimeric kinesin-2 composed by two heterodimeric kinesin-2 motor subunits and an accessory subunit, the kinesin-associated protein (KAP). Heterotrimeric kinesin-2 is required for the assembly and maintenance of cilia in most ciliated cells (Nonaka, 1998). Homodimeric kinesin-2 is involved the assembly of specific types of cilia such as the connecting cilium of photoreceptors in the vertebrate retina (Snow et al., 2014; Insinna et al., 2009). The IFT motor cytoplasmic dynein 2 is a multiprotein complex comprising 4 different subunits: a heavy chain, a light intermediate chain, an intermediate chain and a light chain (Ishikawa and Marshall, 2017). The cytoplasmic dynein 2 is required for the assembly of cilia and is not essential for cilia maintenance (Fig. 24; Engel et al., 2012).

The IFT trains consist in two large complexes, called IFT complex A and complex B (Piperno and Mead, 1997 ; Cole et al., 1998). IFT complexes A and B are associated and move together within the cilium. IFT complex A contains six known proteins and complex B contains 16 known proteins. IFT complex A is involved in retrograde transport, returning the proteins to the cytoplasm, and is not required for cilia assembly (Iomini et al., 2009; Tsao and Gorovsky, 2008). In contrast, IFT complex B, required for anterograde transport, is essential for cilia assembly and maintenance (Fig. 24; Pazour et al., 2000; Follit et al., 2006).

The Bardet-Biedl Syndrome (BBS) proteins are required for the transport of several membrane proteins to cilia (Jin et al., 2010). Eight core BBS proteins (BBS1, BBS2, BBS4, BBS5, BBS7, BBS8, BBS9 and BBIP10) form a complex called the BBSome. The BBSome recognizes ciliary targeting sequences in proteins important for their transport, such as the N-terminal RVxP and the C-terminal VxPx sequences. Rabin8 binds BBS1 together with Rab11 and regulates Rab8 activity. The BBSome-Rab8/Rab11 interaction mediates ciliary transport of selected cargos from the Golgi to ciliary membrane (Malicki and Avidor-Reiss, 2014; Malicki and Johnson, 2017). Several studies have shown that the BBSome is involved in the ciliary localization of opsin, somatostatin receptor 3 (SSTR3), melanin concentrating hormone receptor (MCHR1), neuropeptide Y receptor (NPYR2) and G protein-coupled receptors (GPCRs) (Malicki and Avidor-Reiss, 2014). The BBSome is not a direct component of cilium formation but the lack of BBS proteins lead to cilia-related defects in cell signaling and embryogenesis.

The proteins not associated to the plasma membrane are transported into the cilium through the transition zone by an active or by a passive mechanism. Small soluble proteins can enter the cilium by passive diffusion across the filter-like transition zone. It has been found that proteins with less than 9 nm can diffuse and enter the cilia, but the size limit depends on the cell type (Breslow et al., 2013). Nevertheless, bigger soluble proteins need active mechanisms to pass the transition zone filter. As an example of active transport, the radial spokes (composed by 22 polypeptides and required for the mechanical movement of the motile axoneme) are transported to the ciliary tip by IFT proteins. The IFT anterograde machinery is authorized to cross the transition zone by crucial interactions with transition zone proteins (Malicki and Avidor-Reiss, 2014).

These direct interactions are essential for the transport into the cilium. Other proteins require extra cargo-specific adapters (such as Inversins and MKS proteins) to be transported (Zhao and Malicki, 2011).

2. Role of primary cilia in the Hedgehog (Hh) signalling pathway

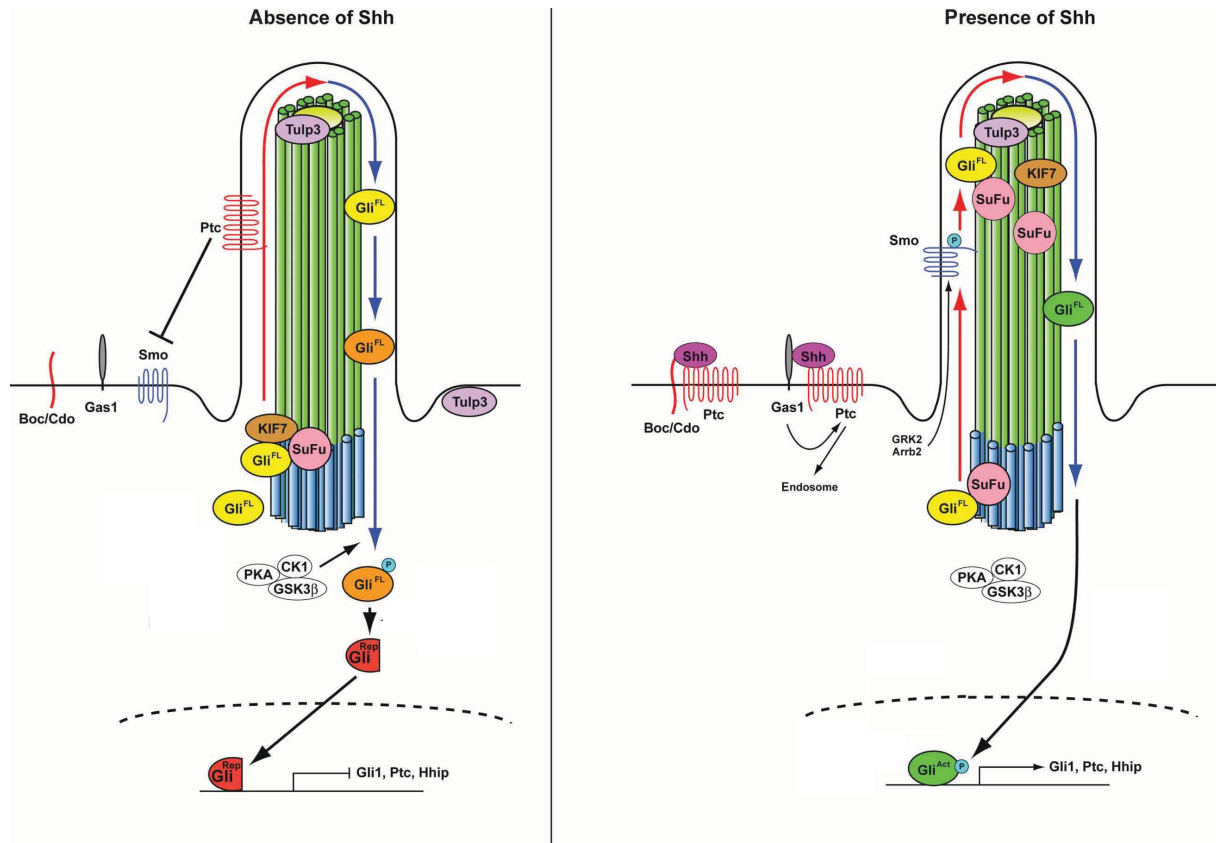


Figure 25. Hedgehog signaling pathway and primary cilia. In the absence of Hh ligand, the receptor Ptc localizes to cilia and inhibits Smo from entering the cilia. Full-length Gli (yellow Gli^{FL}) bind to SuFu and Kif7. Gli^{FL} is phosphorylated by PKA-Gsk3β-Ck1 at the cilia base (orange Gli^{FL}). Then Gli^{FL} is processed by the E3-proteasome system to form the truncated form of Gli (red Gli^{Rep}). Gli^{Rep} dissociates from SuFu and moves to the nucleus to repress the target genes. In the presence of HH ligand, Ptc leaves the ciliary membrane allowing the activation and the entry of Smo to the cilium. The Gli^{FL} - SuFu complex dissociates in the cilium, and Gli^{FL} is transformed into an activator form (green Gli^{Act}). Gli^{Act} then translocates into the nucleus to activate the expression of HH target genes. Adapted from Sasai and Briscoe, 2012.

Cilia have been involved in the reception, transduction and modulation of several signalling pathways. The Hh pathway is the best studied and will be presented in detail

below. Cilia have also been involved in the balance of the Wnt pathways by downregulating the canonical, Wnt- β -catenin pathway and promoting the Wnt-PCP (planar cell polarity) pathway (Gerdes and Katsanis, 2008; Wallinford and Mitchell, 2011). In addition, cilia have been involved in the PDGF α (Schneider et al., 2005), Notch (Ezratty et al., 2011), Hippo (Habbig et al., 2011) and mTOR (Boehlke et al., 2010) pathways.

During the last 15 years, genetic studies in mouse have uncovered an essential role for cilia in the transduction of the Hedgehog (Hh) signalling pathway. The signalling starts with the binding of Hh ligand to the receptor Ptch, which occurs in or around the cilium. This binding relieves the Ptch-mediated repression of the Smo receptor (Stome et al., 1996) allowing Smo entry into the ciliary membrane. Smo activates signal transduction in the cilium by the activation of Gli transcription factors, which accumulate at the tip of cilia upon pathway activation. Then Gli factors translocate to the nucleus and activate the expression of target genes of Hh such as *Ptch* and *Gli1*. In the absence of ligand, Gli2 and Gli3 are cleaved into Gli repressor forms (Gli2R and Gli3R) in a cilium-dependent manner (Fig. 25; Bai et al., 2004; Sasaki et al., 1999).

Other important positive or negative regulators of Hh signalling are present in the cilium. SuFu is essential for vertebrate embryogenesis and localizes at primary cilia (Haycraft et al., 2005). In the absence of Hh ligands, SuFu binds Gli transcription factors and this binding is essential for GliR production (Humke et al., 2010). Smo activates the pathway by releasing Gli proteins from their binding to SuFu (Ocbina and Anderson, 2008). However, recent data have complicated the picture, by showing that SuFu suppresses the Hh pathway by restricting the nuclear translocation of the Gli transcription factors (Elliott and Brugmann, 2018). Moreover, upon Hh binding to Ptch, SuFu acts as a chaperone to transport GliA into the nucleus and GliR out of the nucleus, thereby being required for high levels of pathway activation (Zhang et al., 2016). Kif7 is an atypical kinesin that binds Gli transcription factors and favours their transport to the cilium in the Hh-dependent manner. (Corbit et al., 2005; Liem et al., 2009; Endoh-Yamagami et al., 2009). GPR161, a G-protein coupled receptor, is a negative regulator of the Hh pathway which binds IFTA and Tulp3, increases ciliary cAMP levels required for PKA activation, and favours Gli targeting to the proteasome. Hh binding to Ptch1

removes GPR161 from the cilium and this is necessary for pathway activation (Fig. 25; Mukhopadhyay et al., 2013).

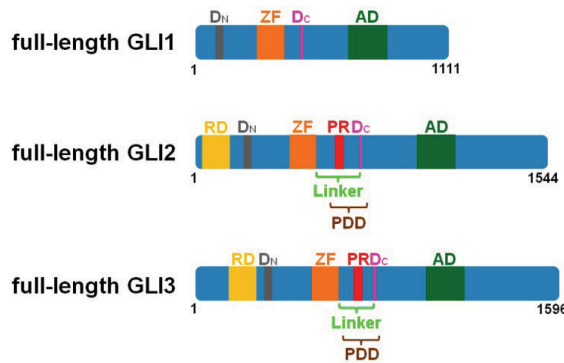


Figure 26. Scheme of the different domains of Gli1, Gli2 and Gli3. Adapted from Gerhardt et al., 2016. Gli1, Gli2 and Gli3 bind to the DNA by zinc-finger domains (ZF). The three proteins have activation domain (AD) whereas only Gli2 and Gli3 repressor domain (RD), a processing determinant domain (PDD) and a processing region (PR). The N-terminal degron (DN) is important for the degradation of all the Gli proteins. The degron of C-terminal is a signal for Gli1 degradation and is a processing signal in Gli1 and Gli2.

In the absence of Hh, Ptch remains in the ciliary membrane and inhibits the entry of Smo. The Sufu-Gli complex is at the basal body where Gli is processed into its truncated form GliR. Then GliR enters the nucleus where it recruits a co-repressor complex to repress the transcription of Hh target genes (Fig. 25; Cheng and Bishop, 2002; Pan and Wang, 2007). Several studies have analysed in greater detail the processing of Gli transcription factors. As mentioned above, *Gli1* is a target gene of Gli2A and Gli3A, and only acts as a constitutive activator (Hynes et al., 1997). The proteolytic processing of Gli2 and Gli3 full-length proteins into the truncated repressor forms (Gli2R and Gli3R) is executed by the ubiquitin-proteasome system. This system is composed by three ubiquitin enzymes (E1, E2 and E3) and the proteasome (Coux et al., 1996; Gerhardt et al., 2016). Gli1 gets degraded by the proteasome while Gli2 and Gli3 are proteolytically processed (Kaesler et al., 2000). Before and essential to the partial proteolysis of Gli2 and Gli3, full-length forms are phosphorylated by Protein Kinase A (PKA) at the basal body (Tuson et al., 2011). This triggers their phosphorylation by other kinases, Casein kinase 1 (Ck1) and Glycogen synthase kinase 3 β (Gsk3 β). The phosphorylation of Gli2 and Gli3 is recognized by an E3 ubiquitin ligase. Gli2 and Gli3 are then ubiquitinated at the cilia base and targeted to the proteasome where they are processed into their repressor forms, Gli2R and Gli3R (Fig. 25; Sasai and Briscoe, 2012; Wang et al., 2014; Elliott and Brugmann, 2018). Several studies have shown that Gli2 is less efficiently processed than Gli3, acting mostly as Gli2A. The processing efficiency is controlled by three sites in Gli proteins. The first processing site is the zinc-finger (ZF)

domain of Gli3. The second is located between the ZF domain and the degron sequence (lysine sites). The third is the degron protein sequence (Fig. 26; Pan et al., 2007; Schrader et al., 2011; Gerhardt et al., 2016).

In conclusion, cilia are essential for two aspects of Hh/Gli signalling that normally occur at very different levels of pathway activity. They are required for the formation of activator forms of Gli transcription factors, GliA (Gli2A and Gli3A) normally achieved in the presence of high levels of Shh ligand. They are also required for the proteasomal processing of Gli into a repressor form, GliR (in particular Gli3R), which is normally present in the absence of Hh ligand. This dual and opposite roles of primary cilia in Hh/Gli signal transduction are key to understand the phenotype of mouse ciliary mutants (see below).

3. Developmental processes that require primary cilia

Obtaining mouse mutants for ciliary genes has allowed to dissect the multiple functions of primary cilia in development. The first defects described in ciliary mutants are kidney cysts, polydactyly and neural tube patterning defects.

Kidney cysts have been studied in detail and are caused by dilatation of the nephric tubules. Cilia are present at the apical surface of kidney epithelial cells where they respond to mechanical stress cause by fluid flow within the tubule. The potential cellular mechanisms identified for kidney cyst formation are increased proliferation, altered orientation of cell divisions and increased tubule cell size. The signalling pathways affected are the Wnt pathways, since the balance between canonical Wnt and Wnt-PCP regulates proliferation and oriented cell divisions, and the mTOR pathway, which regulates cell size (Patel et al., 2008; Lancaster et al., 2010; Boehlke et al., 2010).

Polydactyly and neural tube patterning defects are both related to the modulation of Hh/Gli signalling. The role of cilia in neural tube patterning will be presented in detail below. Polydactyly is caused by a defect in limb anteroposterior (AP) patterning. Limb AP patterning relies on the Hh pathway; a posterior region of the limb bud called the Zone of Polarizing Activity (ZPA) is the source of Shh for limb AP

patterning. Downregulation of the Hh pathway leads to a reduction in digit numbers, while an increase in Gli activity leads to polydactyly (augmentation in the number of digits). Gli3 is central to limb formation and Gli3 mutants display polydactyly, showing that Gli3 acts mainly as a repressor. Thus, polydactyly in ciliary mutants is interpreted as a defect in the production of Gli3R (Liu et al., 2005; May et al., 2005).

Brain morphogenesis defects have also been observed in mouse ciliary mutants, such as exencephaly (Huangfu and Anderson, 2005; Besse et al., 2011), hydrocephaly and ventriculomegaly (Baas et al., 2006; Foerster et al., 2017), agenesis of the olfactory bulbs and corpus callosum (Besse et al., 2011; Benadiba et al., 2012; Laclef et al., 2015), and cerebellar hypoplasia (Lancaster et al., 2011). I will present these defects in Part IV in context with the role of the *Ftm/Rpgrip1l* gene in development. In addition, the cilium has been shown to be involved in a number of cellular processes. I will present below data about cell division and cell migration.

3.1. Primary cilia in patterning of the neural tube

The role of primary cilia in Hh signalling has been discovered thanks to a large-scale genetic screen for mouse mutants with defects in neural tube patterning performed in Kathryn Anderson's laboratory (Huangfu et al., 2003). Many mutants identified were found to have mutations in IFT genes, and showed a reduction in number or an absence of ventral progenitor types, as well as reduced expression levels of Hh target genes, which rapidly led to the proposal that primary cilia were involved in Hh signalling.

As mentioned above, Shh is produced in the notochord and FP and forms a ventro-dorsal decreasing gradient. The response of neuroepithelial cells depends on the level of Hh signals they receive and on the time of exposure (Stamatakis et al., 2005). High levels of Shh signal transduction induce the expression of *Nkx2.2*, a marker of p3 progenitors, while lower levels are sufficient to induce the expression of *Olig2*, a marker of pMN. Low levels of Shh also repress the expression of *Pax7*, which is restricted to the dorsal progenitor domain (Dessaud et al., 2010; Sasai and Briscoe, 2012).

In the absence of Shh or Smo, the ventral markers of the spinal cord are not expressed and the dorsal marker *Pax7* is extended ventrally. In contrast, in the absence of functional *Ptch1*, the pathway is constitutively activated (i.e. independently of the ligand), which leads to a dorsal extension of the expression of FP and P3 markers (Fig. 27; Jeong et al., 2005).

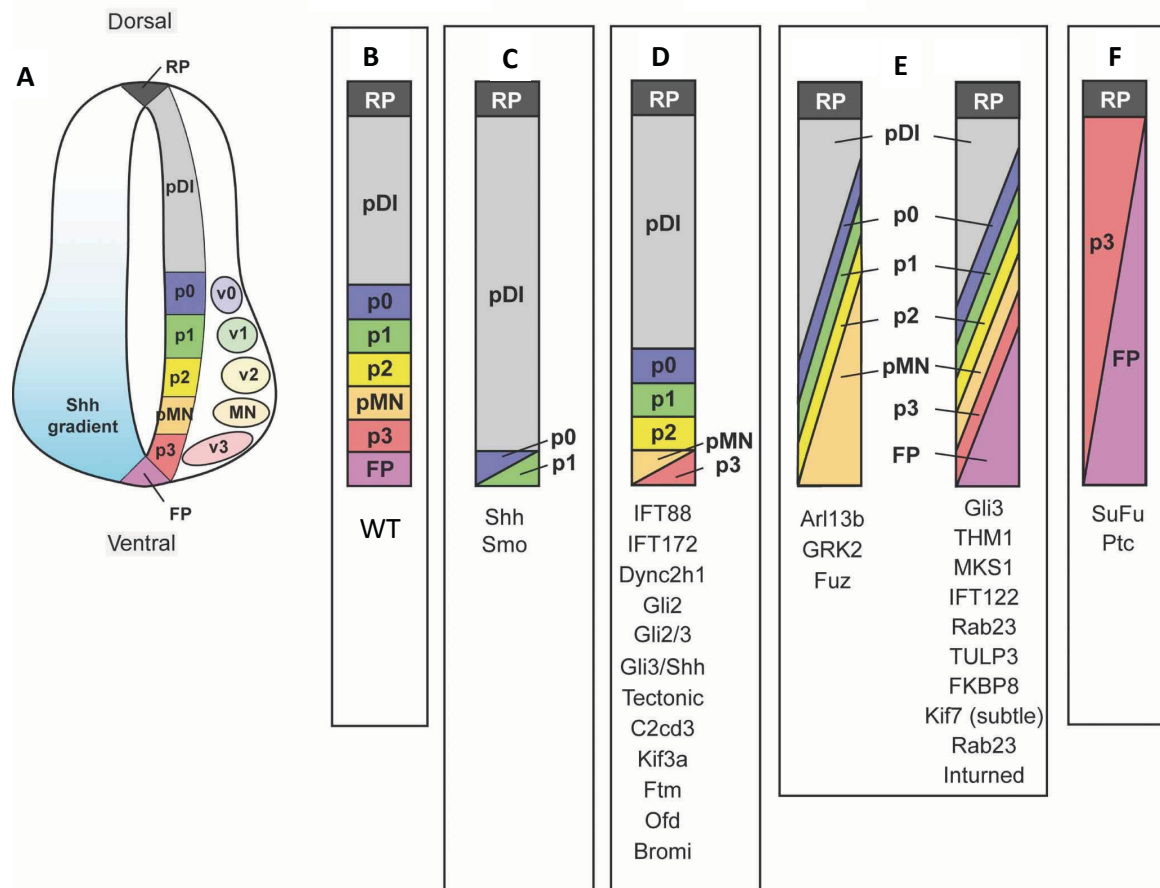


Figure 27. Classification of neural tube phenotypes in mutant mice lacking Shh-related ciliary factors. **A.** Illustration of dorso-ventral patterning of the neural tube. Each interneurons subtypes (v0-v3) and motor neurons (MNs) differentiate to their progenitor domains (p0-p3, pMN) located in specific dorso-ventral position. **B-F.** Classification of different patterning defects observed in progenitor domains of the neural tube, indicating the mutated genes that produce these phenotypes. Adapted from Sasai and Briscoe, 2012.

Several mutants involved in IFT, such as *Kif3a*, *Ift172* and *Ift88*, show defects of intermediate severity. Markers that require high levels of Gli activity, such as *Nkx2.2* (p3), are lost. However, genes that require intermediate levels of Hh signalling such as *Olig2* (pMN) are still expressed in a region more ventral than in controls and the dorsal marker *Pax7* is not expanded ventrally (Bai et al., 2004). The phenotype of these IFT mutants is very similar to that of embryos lacking both the repressor and activator

forms of Gli transcription factors, such as compound Gli2 x Gli3 mutants. The IFT mutants mentioned above present a total lack of the ciliogenesis. A similar but sometimes less severe phenotype is found in mutants for genes encoding components of the basal body or transition zone (such as *Talpid 3* and *Ftm/Rpgrip11*, respectively). In these embryos, the genes requiring high levels of Shh activity are repressed, whereas the expression of *Olig2* and *Pax7* is still present (Fig. 27; Davey et al., 2006; Vierkotten et al., 2007; Corbit et al., 2008).

In contrast, ciliary mutants with abnormal morphology of primary cilia present a partial activation of Shh signal transduction. For example, mouse mutants for the gene encoding the GTPase *Arl13b* produce malformed primary cilia with a shorter axoneme. These mutants lack progenitors that require high levels of Shh activity, but they show a dorsal expansion of the genes that require low levels of Shh, suggesting that there is a basal production of GliA in these mutants (Fig. 27; Caspary et al., 2007; Sasai and Briscoe, 2012).

All these observations indicate that the ventro-dorsal gradient of GliA/GliR ratio present in the spinal cord is disrupted in ciliary mutants, with distinct severities depending on the extent of cilia defects. The study of double mutants for IFT genes suggests that these genes act on Hh signaling mainly via their role in cilia structure (Ocbina et al., 2011). The role of cilia in patterning of ventral neural structures may be conserved in the brain as shown in the midbrain, where cilia are required for the formation of ventral dopaminergic neurons via Hh signalling (Gazea et al., 2016).

If cilia are essential for Hh activity, cilium length may have a negative impact on Hh signalling, and this may explain the decreased responsiveness of FP cells to Hh signals in the ventral neural tube. The transcription factor *Foxj1* is expressed in the FP in response to Shh. *Foxj1* is a master gene of motile ciliogenesis and its overexpression increases ciliary length in the spinal cord. These *Foxj1*-induced longer cilia have reduced Hh signalling (Cruz et al., 2010). This difference in ciliary structure and length may explain in part the reduced sensitivity to Shh of FP cells.

4. Dysfunction of primary cilia in humans: the ciliopathies

The importance of cilia has been studied in recent years because of its important role in human development and diseases. Ciliopathies are complex human disorders of cilia (motile and non-motile) including defects in the kidney, brain, eyes, lungs and limbs. Motile cilia are present in lung epithelial cells, oviduct cells, ependymal cells (in brain ventricles) and on the node (responsible for right-left axis establishment in early development). Defects in motile cilia produce a motile ciliopathy called primary cilia dyskinesia (PCD). PCD is characterized by sinusitis, chronic bronchitis, atelectasis, situs inversus (left-right axis inverted) and male infertility. In some cases, the ciliopathies are associated with hydrocephaly and defects in female infertility (Fig. 28; Horany et al., 2016).

As discussed previously, primary cilia control several signalling pathways and defects in these pathways affect the function of different organs such as the heart, the kidney, the brain and the skeleton. An example is HH pathway (Reiter and Leroux, 2017). HH components comprise several proteins that localize into the cilium such as PTCH1, SMO and GLI proteins. Defects reminiscent of Hh pathway dysfunction are observed in ciliopathies, for example polydactyly in BBS and in Meckel syndrome (MKS) (Zhang et al., 2012). Several ciliopathies are associated with impairment of different structures of the primary cilia such as the formation of basal body, transition zone formation and ciliary trafficking. Disruption of the distal appendages components, CEP164 or CEP83, triggers cystic kidney disease, nephronophthisis (NPHP), and defects in SCLT1 produces orofacioidigital syndrome (OFD), with polydactyly and craniofacial abnormalities (Failler et al., 2014; Adly et al., 2014). Mutations in components of the distal region of the basal body, such as HYL1, produce hydrocephaly and brain defects (hydroletharus syndrome) or Joubert syndrome (JBTS) (Mee et al., 2005; Oka et al., 2016).

Defects in transition zone proteins are widely implicated in ciliopathies. The NPHP and MKS complex are linked with NPHP and MKS ciliopathies (that give name to these protein complexes). Impairment of MKS proteins lead in to defects in the transport of membrane associated proteins, such as ARL13B, INPP5E, ADCY3 and SMO, associated

with ciliopathy developmental defects (Reiter and Leroux, 2017). Moreover, mutations in RPGRIP1L, a NPHP component, produce MKS, JBTS and COACH (cerebellar vermis hypo/aplasia, oligophrenia, ataxia, ocular coloboma and hepatic fibrosis) (Delous et al., 2007). Mutations in other transition zone proteins, including polycystin 1 or 2 (PKD1 and PKD2), generate the polycystic kidney disease (ADPKD) and MKS (Huang et al., 2014).

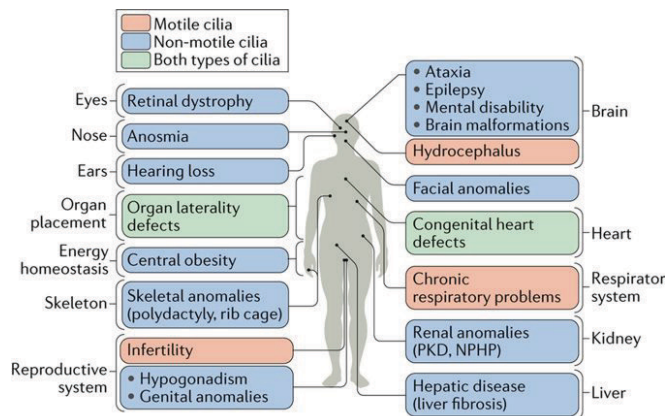


Figure 28. Dysfunctions in motile and non-motile cilia cause defects in many human organ system. The Scheme shows the different organs that are affected in diverse ciliopathies. In orange, motile ciliopathy defects; in blue, non-motile ciliopathy defects and in green common motile and non motile defects in human organs. Adapted from Reiter and Leroux, 2017.

Apart from the structural defects in primary cilia, impairment of IFT trafficking and BBSome components are involved in ciliopathies. IFT mutations lead to skeletal defects in humans. Mutations in genes of IFT retrograde transport (DYNC2H1, DYNC2L1 or TCTEX1D2) and IFT-A complex (IFT43, IFT121 OR IFT122) are related with Jeune asphyxiating thoracic dystrophy (JATD), cranioectodermal dysplasia (CED) and short-rib polydactyly syndrome (Reiter and Leroux, 2017). The defects of BBSome arise from mutations in genes encoding the eight BBS proteins. The BBS-related ciliopathies induce retinal degradation, obesity, cystic kidneys and polydactyly (Zhang et al., 2012).

IV. The *Ftm/Rpgrip1l* ciliopathy gene

1. Structure and functions

1.1. Identification of the gene and structure of the protein

The *Ftm/Rpgrip1l* gene has been identified as one of the deleted genes in *Fused toes* (*Ft*) mouse mutants. *Ft* mutants, obtained in Ulrich Rüter's lab in Düsseldorf (Germany) result from a deletion of 1.6 Mb in the chromosome 8, including the Iroquois B cluster (*Irx3*, *Irx5* and *Irx6*) and three genes called *Ftm*, *Fto* and *Fts* (Fig. 29; Peters et al., 2002). *Ft* mutant embryos present malformations in craniofacial structures, defects in right-left asymmetry, polydactyly, and defects in forebrain and ventral spinal cord (Götz et al., 2005; Anselme et al., 2007). These defects suggested an impairment of the Hh pathway indicating that one of the six genes deleted in *Ft* are implicated in this pathway. Further studies from U. Rüter's lab have shown that *Ftm* null mutant embryos reproduce the majority of the defects of *Ft* mutants (Vierkotten et al., 2007), especially in left-right asymmetry and neural tube patterning.

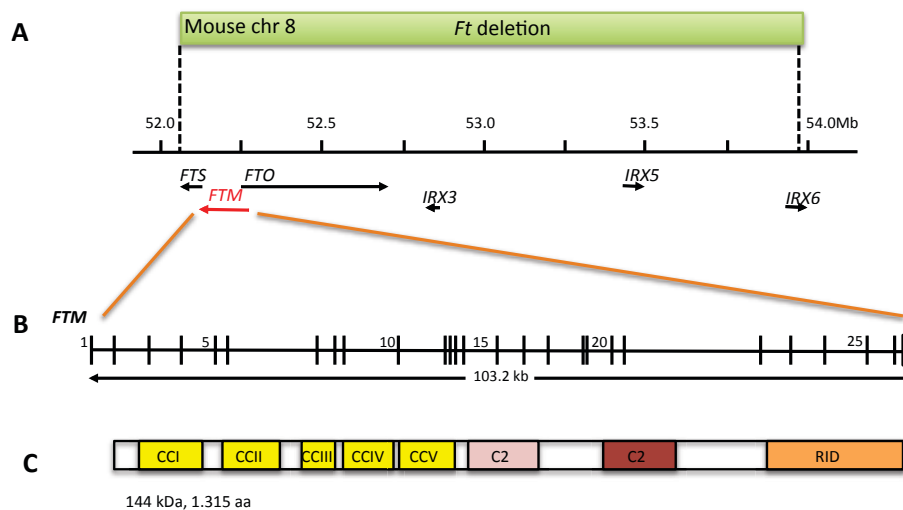


Figure 29. Chromosomal deletion in the *Fused toes* (*Ft*) mutant and structure of the *Ftm* gene. **A.** The green bar indicates the region deleted in the *Ft* mouse, comprising the *Irx3*, *Irx5*, *Irx6*, *Fto*, *Fts* and *Ftm* genes. **B.** Exon-intron representation of the *Ftm* gene composed by 27 exons (vertical hatches) and extending over 103.2 kb. **C.** Representation of the domain structure of the *Ftm* protein. CC, coil-coiled domain; C2, protein kinase C (PKC) conserved region 2 motif; RID, domain with homology to the RPGR-interacting domain of RPGRIP1. Adapted from Delous et al., 2007.

Ftm encodes a protein of 1264 amino acids, which encompasses three distinct regions with protein-protein interaction domains (Vierkotten et al., 2007). It contains five coiled-coil domains involved in the formation of homo-polymers, two C2 domains (protein kinase C-conserved region 2) and a RID domain (RPGR-Interacting Domain, where RPGR stands for Retinitis Pigmentosa GTPase regulator; Fig. 29). *Ftm* is the paralog of another gene called *Rpgrip1* (which stands for RPGR-interacting protein 1), with a very similar structure. The RID domain was characterized before in *Rpgrip1* (retinitis pigmentosa GTPase regulator interacting protein 1). *Rpgrip1* has been identified in connecting cilia of the photoreceptors and has a high homology with *Ftm*, thus also known as *Rpgrip1l* (*Rpgri1*-like). The *Ftm* mouse protein presents 82% homology with the human protein RPGRIP1L, with the same functional domains (Arts et al., 2007; Delous et al., 2007). *RPGRIP1L* gene is localized in the human chromosome 16 and the protein presents 1315 amino acids (Arts et al., 2007; Delous et al., 2007).

1.2. Localisation of Rpgrip1l

The *Ftm/Rpgrip1l* gene is widely expressed during embryogenesis in mouse, zebrafish and humans. In mouse and humans, its expression has been reported in the retina, brain, kidney and liver (Arts et al., 2007; Delous et al., 2007; Vierkotten et al., 2007; Mahuzier et al., 2012). The subcellular localization of *Rpgrip1l* has been analysed in vitro and in vivo by transfection of fusion proteins constructs and using specific antibodies. In different cell lines, the *Rpgrip1l* protein is observed in the transition zone of the cilium where it co-localizes with the NPHP4 and CEP290 ciliopathy proteins (Gerhardt et al., 2015; Yang et al., 2015; Shi et al., 2017; Wiegering et al., 2018). In vivo, *Rpgrip1l* is localized in the transition zone of the connecting cilia in retinal photoreceptors, and in the transition zone of the cilia in brain, in neural progenitor cells, ependymal cells and in the choroid plexus (Fig. 30; Arts et al., 2007; Delous et al., 2007; Vierkotten et al., 2007). *Rpgrip1l* has also been found outside of cilia, in centrosomes during cell division (Gerhardt et al., 2015) and at cell junctions together with *Nphp1* and *Nphp4* (Delous et al., 2009 and personal communication from M. Delous and S. Saunier).

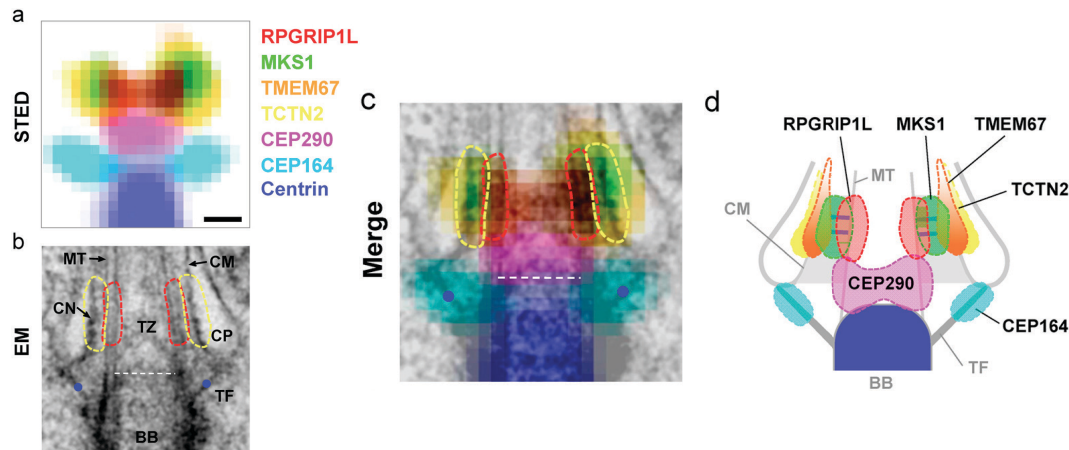


Figure 30. Molecular architecture at the base of the primary cilium obtained by overlapping coordinate-defined super-resolution images of transition zone proteins. **A.** A 7-color super-resolution image obtained by merging multiple single-color STED images illustrating the relative locations of important transition zone (transition zone) proteins. **B.** Transmission electron microscopy (TEM) image of a primary cilium in an RPE-1 cell, where transition fibres (TF) are marked as blue dots, areas of microtubule doublets (MT) circled with red dashed lines, areas of the ciliary membrane (CM) covering the ciliary neck (CN) circled with yellow dashed lines, and the distal end of the basal body (BB) marked by a white dashed line. CP, ciliary pocket. **C.** A merged image of **A-B** obtained by aligning the TFs in TEM and CEP164 in STED. RPGRIP1L is close to the microtubule doublets; TMEM67 and TCTN2 are localized mostly toward the transition zone membrane, while MKS1 is localized midway between the membrane and microtubules. CEP290, right above the BB, is localized at a different axial level from the other transition zone proteins. **D.** A localization model of transition zone proteins at the ciliary base pinpointing the positions of these proteins relative to each other and to known structural elements. Scale bar, 200 nm. Adapted from Yang et al., 2015.

1.3. Cellular functions of Rpgrip11

1. Cilium integrity and construction of the transition zone

Rpgrip11 is a component of the transition zone and its role in transition zone construction has been studied in several species. In *C. elegans* sensory neurons, *Rgrip11* (often called *MKS5* in this species) mutants have no overt ciliary defect (Williams et al., 2011), Compound [*Rgrip11*; *Nphp4*] mutants or compound mutants with *MKS* genes have abnormal dye filling and osmotic avoidance, two defects characteristic of ciliary dysfunction. Cilia are shorter and abnormally oriented and the transition zone is disconnected from the ciliary membrane and presents abnormal ultrastructure,

including the loss of Y links. Rpgrip1l localizes to the transition zone independently of other transition zone proteins and is essential for the transition zone localization of all other known transition zone proteins, in particular those of the NPHP and MKS modules. IFT is not affected in these mutants, but Rpgrip1l is required for the “ciliary gate” function of the transition zone, preventing proteins to enter the cilium. Rpgrip1l also excludes other ciliary proteins such as GPCRs from the transition zone (Williams et al., 2011; Jensen et al., 2015). Thus, the *C. elegans* data suggest that Rpgrip1l is a central player in transition zone construction and function as a ciliary gate.

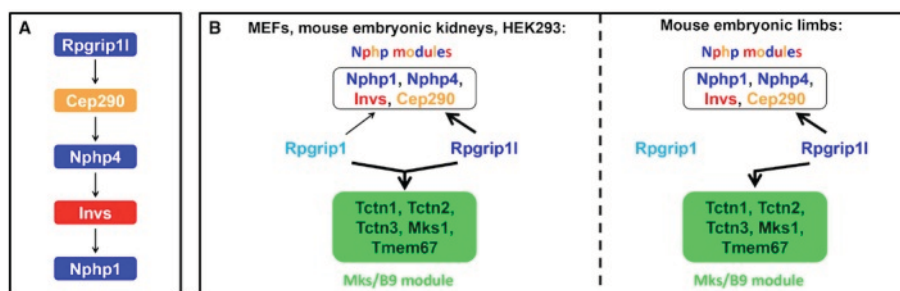


Figure 31. Schematic illustration of the transition zone assembly organisation in vertebrates. **A.** Proposed model of the organisation of the Rpgrip1l-Cep290-Nphp4-Invs-Nphp1 axis. The arrows indicate the quantitative dependency between the transition zone proteins. Rpgrip1l regulates the amount of Cep290 at the vertebrate transition zone. In turn, Cep290 controls the transition zone amount of Nphp4 which ensures the proper amount of Invs at the transition zone. Finally, Invs governs the transition zone amount of Nphp1. **B.** Two schemes that depict the cell type-specific roles of Rpgrip1l and Rpgrip1 in the vertebrate transition zone assembly hierarchy. Adapted from Wiegeling et al., 2018.

In vertebrate cells, Rpgrip1l has a cell type-specific role in transition zone construction. In mouse embryonic fibroblasts (MEFs), it is required for ensuring a correct amount at the transition zone of proteins of the NPHP complex (Nphp4, Nphp1, Nphp2/Inv, Nphp6/Cep290), but not of proteins of the MKS complex (Mks1, Tmem67/Mks3, Tctn1, Tctn2 and Tctn3). Interestingly, in vivo, a similar result is obtained in embryonic kidneys, while in limb buds, proteins of both complexes are affected by the inactivation of Rpgrip1l (Wiegeling et al., 2018). Cilia form and are longer than in controls, but their ultrastructure is perturbed, and some microtubules are present as singlets in the axoneme. Interestingly, the cognate protein Rpgrip1 is present in higher amount at the basal body in *Rpgrip1l*^{-/-} MEFs than in controls and the compound [*Rpgrip1l*; *Rpgrip1*] mutant presents a strong reduction of both NPHP and

MKS complex protein at the transition zone, indicating a compensation of the Rpgrip11 deficiency by Rpgrip1 (Wiegering et al., 2018). Thus, the cell-type specificity of Rpgrip11 function in vertebrates can be, at least in part, explained by partial functional redundancy with Rpgrip1 (Fig. 31).

As in *C. elegans*, Rpgrip11 also acts as a gatekeeper in mice, since the amount of Arl13b is severely reduced in *Rpgrip11*^{-/-} MEFs. However, Smo amount in cilia is not perturbed, while it is reduced in Rpgrip11 mutant tracheal cells in culture, here again indicating a cell-type -specific function of Rpgrip11 in cilium construction (Gerhard et al., 2015; Shi et al., 2017).

In vivo, the perturbations in cilia structure are also cell-type specific. In mouse *Ftm*^{-/-} embryos, many embryonic cells display longer and thinner cilia. However, cilia are either absent or very short and bloated in neural progenitor cells and in the node, and are shorter in the heart (Vierkotten et al., 2007; Besse et al., 2011; Gerhardt et al., 2015).

1. Function of Rpgrip11 in proteasomal activity and autophagy

Gli3 processing is reduced in *Ftm*^{-/-} mice (Vierkotten et al., 2007; Besse et al., 2011), While this can be explained by an upstream defect in post-tranlational modification or ciliary trafficking of Gli3, Gerhardt et al. tested the idea of a defect in

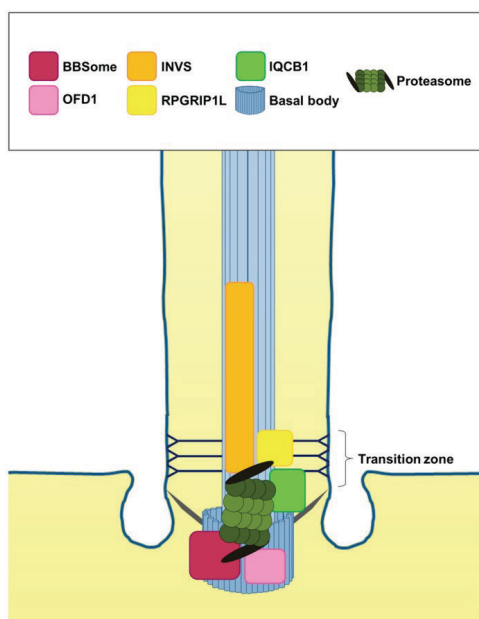


Figure 32. Interactions between ciliary proteins and the cilia-regulated proteasome. INVS is located in the Inversin compartment and in the transition zone and interacts with components of the 19S proteasomal subunit (black lid of the proteasome). The TRANSITION ZONE protein RPGRIP1L interacts with components of the 19S proteasomal subunit. IQCB1 is present at the TRANSITION ZONE and the basal body and interacts with components of the 20S proteasomal subunit. OFD1 localises to the basal body and interacts with components of the 19S proteasomal subunit. Components of the BBSome are located at the basal body and interact with components of the 19S and 20S proteasomal subunit. Adapted from Gerhardt et al., 2016.

general proteasomal activity (Gerhardt et al., 2015). Strikingly, they found that in *Rpgrip11*^{-/-} MEFs, proteasomal activity is specifically reduced around the cilium base. Investigating the molecular cause of this defect, they found that Rpgrip11 interacts with the proteasomal subunit Psmd2. Thus, Rpgrip11 has a specific function in proteasomal activity at the cilium base (Fig. 32; Gerhardt et al., 2015).

Interestingly, pharmacological restoration of proteasomal activity in *Rpgrip11*^{-/-} mutant cells does not rescue longer cilia, suggesting additional mechanisms of control of the ciliary length. Recently, Struchtrup et al. (2018) showed that Rpgrip11 also regulates autophagy by downregulating the mTOR pathway. Application of the mTOR inhibitor rapamycin rescued autophagic activity and cilia length but not proteasomal activity in *Rpgrip11*^{-/-} MEFs. This suggests that Rpgrip11 regulates autophagy and proteasomal activity independently from each other (Struchtrup et al., 2018).

1.4. Function of Ftm/Rpgrip11 in vertebrate development

Ulrich R  ther's laboratory has generated a knock-out mouse line for *Ftm/Rpgrip11*, called the *Ftm* mutant. *Ftm*^{+/-} animals are viable and fertile and do not present any obvious defect. *Ftm*^{-/-} fetuses die at or before birth. The phenotype of mouse *Ftm* mutant embryos is similar to that of several ciliary gene mutants described in the literature: exencephaly, hydrocephaly, polydactyly, dorsalized neural tube, laterality defects. However, IFT mutants which resemble the *Ftm* mutant are usually hypomorphs, and null IFTB mutants such as IFT172 die around E12.5 (Willaredt et al., 2008; Gorivodsky et al., 2009). In addition, *Ftm*^{-/-} fetuses display dilatation of kidney tubules, cerebellar hypoplasia (Delous et al., 2007), defects in heart septation (Gerhardt et al., 2013) and in hair follicle development (Chen et al., 2015). Moreover, they display abnormal planar cell polarity in the cochlea and PCP defects (affecting the planar polarization of cilia). These defects are also found in zebrafish *Rpgrip11* morphants (Mahuzier et al., 2012).

In the neural tube, *Ftm*^{-/-} embryos show a loss of the FP and of p3 progenitors, a strong reduction in motoneuron progenitors, and a ventral expansion of intermediate and dorsal progenitors. This phenotype is partially rescued in compound [*Ftm*^{-/-};

$Gli3^{Xt/Xt}$ embryos ($Gli3^{Xt}$ is a null allele of $Gli3$). $Gli3$ processing is impaired in the mutant (Fig. 33.I). Moreover, $Ftm^{-/-}$ MEFs isolated from mutant embryos have reduced $Gli1$ and $Ptch1$ response to Hh stimulation (Vierkotten et al., 2007).

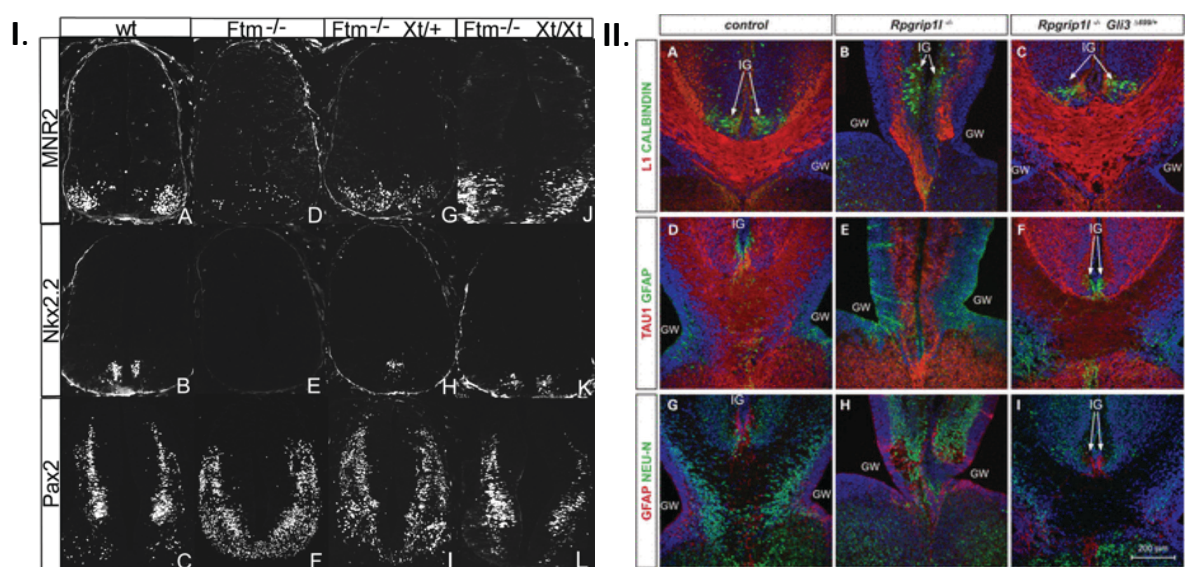


Figure 33. I. Rescue of neural tube patterning in $Ftm^{-/-}$ embryos by abrogating $Gli3$ function. A-C. In wild-type embryos, MNR2 (A) is expressed lateral to Nkx2.2 (B), which is expressed adjacent to the floor plate. Furthermore, Pax2 is expressed in the dorsal region of the neural tube (C). D-F. By contrast, $Ftm^{-/-}$ embryos show a strong reduction of MNR2-positive cells (D) and Nkx2.2-expressing cells (E). Expression of Pax2 is expanded into the most ventral part of the neural tube (F). G-I. In $Ftm^{-/-}$; Xt/+ embryos, the number of MNR2-positive (G) and Nkx2.2-positive (H) cells is increased, but these cells still cross the midline. Pax2-expressing cells are expanded into more ventral parts within the neural tube, but there are fewer cells crossing the midline (I). J-L. In $Ftm^{-/-}$; Xt/Xt embryos, MNR2-expressing (J) and Nkx2.2-expressing (K) cells are absent from the midline and located in two lateral distinct domains. Pax2-expressing cells (L) seem to be completely restored. **II.** Rescue of corpus callosum (CC) formation by expressing GLI3R in $Rpgrip11^{-/-}$ mice. A-F. L1 and TAU1 label the callosal axons and show that, in contrast to $Rpgrip11^{-/-}$ fetuses (B and E), in $Rpgrip11^{-/-}$; $Gli3^{\Delta699/+}$ double mutant (C and F), the callosal axon cross the midline and form a CC very similar to the control (A and D). Immunohistochemistry for CALBINDIN (A-C) labelled the guidepost neurons in the indusium griseum (IG) and showed that IG positioning is rescued in $Rpgrip11^{-/-}$; $Gli3^{\Delta699/+}$ double mutant (C) and appeared very similar to control IG (A), in contrast to the loose and asymmetric IG found in $Rpgrip11^{-/-}$ mutants (B). Immunohistochemistry for GFAP (D-I) and NEU-N (G-I) labelled the glial guidepost cells and subcallosal sling (SCS) neurons, respectively, and showed a significant rescue of glial and SCS cell organization in $Rpgrip11^{-/-}$; $Gli3^{\Delta699/+}$ double mutant (F and I) compared with $Rpgrip11^{-/-}$ fetuses (E and H). Adapted from Vierkotten et al., 2017 and Laclef et al., 2015.

My laboratory has used the *Ftm* mutant line as a model to study the role of cilia in brain patterning and morphogenesis. Indeed, contrary to many other tissues, the neuroepithelium has almost no cilia in the mutants (the remaining are very short and do not contain an axoneme) (Besse et al., 2011). At the end of gestation, *Ftm* mutants display agenesis of the olfactory bulbs (OB) and of the corpus callosum (CC), a major axon tract joining the left and right cortices. *Ftm*^{-/-} embryos show a dorsal expansion of the subpallium (ventral telencephalon) at the expense of the pallium (dorsal telencephalon), which is a likely cause of the OB and CC agenesis. Indeed, my laboratory could show that reintroducing GliR into the *Ftm* mutant background (in [*Ftm*^{-/-}, *Gli3*^{Δ699}] mutants) rescues telencephalic DV patterning and OB and CC agenesis (Besse et al., 2011; Laclef et al., 2015). The *Gli3*^{Δ699} allele corresponds to a knock-in of a truncated Gli3 form into the *Gli3* locus, leading to the constitutive production of Gli3R (Böse et al., 2002). These data demonstrate that, in the telencephalon, *Ftm* is required for DV patterning through controlling Gli3R production (Fig. 33.II). CC agenesis and defective DV telencephalic patterning have also been found in mice mutant for *Rfx3*, a transcription factor of the *Rfx* family involved in ciliogenesis (Benadiba et al., 2012).

In collaboration with N. Spassky and A. Alvarez-Buylla, our lab has also shown that *Ftm* is required for the Hh-dependent proliferation of granule progenitors in the cerebellum and dentate gyrus. This phenotype is also found in conditional mutants for *Ift88* and *Kif3A*, demonstrating that it corresponds to a ciliary function (Spassky et al., 2008; Han et al., 2009).

Altogether these data demonstrate an essential role of *Ftm/Rpgrip1l* in Hh signalling in the brain and spinal cord, for both repressor and activator activity of Gli transcription factors.

2. *Ftm/Rpgrip1l* and ciliopathies

The phenotype of the *Ftm* mouse mutant is reminiscent of severe ciliopathies. Therefore, my laboratory undertook a collaboration with human geneticists in Necker hospital in order to look for mutations in the human *RPGIRP1L* gene in two severe recessive ciliopathies with brain abnormalities: Meckel-Grüber syndrome (MIM

611561) and Joubert type B (CORS) syndrome (MIM 213300). Meckel syndrome, the most severe ciliopathy, is lethal at or before birth and is mainly characterized by central nervous system malformations, occipital encephalocele, polydactyly and a very severe cystic kidney disease. Joubert syndrome is usually less severe and is characterized by central nervous system malformations, mainly midbrain-hindbrain malformations identified on MRI as the “molar tooth sign”. Joubert type B syndrome is characterized, in addition, by either nephronophtosis (a kidney disease with interstitial fibrosis and cysts) or retinal dystrophy. Mutations on both alleles of the *RPGRIP1L* gene were found in these ciliopathies, with a good genotype -phenotype correlation: truncating mutations in MKS and missense mutations in JBTS type B. other studies also reported Rpgrip1l mutations in Joubert syndrome (Arts et al., 2007; Brancati et al., 2008) and as a modifier gene in retinal degeneration (Khanna et al., 2009).

V. Aims of the thesis project

In the last years, studies of the ciliopathy gene *Rpgrip1l* have uncovered its functions in several cellular processes as well as its role during development in different tissues. Specifically, in the neural tube, *Rpgrip1l* and primary cilia are required for the correct formation of the ventral spinal cord and are essential for the genesis of the olfactory bulb and corpus callosum. During my PhD, I studied the role of the *Rpgrip1l* gene and of primary cilia in forebrain patterning and morphogenesis, focusing on three specific regions: the diencephalon, the hypothalamus and the eyes. The aims of my thesis project are:

1. To describe the defects in morphogenesis and neural progenitor fate in the diencephalon, hypothalamus and eyes of *Ftm/Rpgrip1l* mouse mutants.
2. To uncover the cellular and molecular mechanisms which cause these defects, with particular interest in the Hh/Gli pathway.



RESULTS

THE CILIOPATHY GENE *Ftm/Rpgrip1l* CONTROLS MOUSE FOREBRAIN PATTERNING VIA REGION-SPECIFIC MODULATION OF Hedgehog/Gli SIGNALLING.

Abraham Andreu-Cervera, Isabelle Anselme, Alice Karam, Martin Catala and Sylvie Schneider-Maunoury*

Sorbonne Université, Centre National de la Recherche Scientifique (CNRS) UMR7622, Institut national pour la Santé et la Recherche Médicale (Inserm) U1156, Institut de Biologie Paris Seine – Laboratoire de Biologie du Développement (IBPS-LBD), 9 Quai Saint Bernard, 75005 Paris, France.

* corresponding author: sylvie.schneider-maunoury@upmc.fr

ABSTRACT

Primary cilia are essential for brain development. In the mouse, they play a critical role in patterning the telencephalon via the regulation of Hedgehog/Gli signalling. However, despite the frequent disruption of this signalling pathway in forebrain malformations, the role of primary cilia in morphogenesis of other forebrain regions has been little investigated. Here we studied development of the diencephalon, hypothalamus and eyes in mutant mice in which the *Ftm/Rgrip1l* ciliopathy gene is disrupted. We found that ventral forebrain structures were strongly reduced in *Ftm*^{-/-} embryos. The ventral structures of the diencephalon and hypothalamus were missing and dorsal diencephalic structures were expanded ventrally. The rostral thalamus was absent, and eyes were severely reduced in size. We analysed Hedgehog/Gli activity pathway using different readouts. *Sonic hedgehog* expression was lost in the ventral forebrain but maintained in the zona limitans intrathalamica. In the diencephalon, Gli activity was dampened in regions adjacent to *Shh*-expressing domains but displayed a higher Hh-independent ground level in the other regions. Our data uncover a complex role of cilia in development of the diencephalon, hypothalamus and eyes. They call for a closer examination of forebrain defects in severe ciliopathies and for a search for ciliopathy genes as modifiers in other human conditions with forebrain defects.

Keywords: forebrain, diencephalon, hypothalamus, primary cilia, ciliopathy, holoprosencephaly, Hedgehog, Gli, Gli3.

INTRODUCTION

The Hedgehog (Hh) pathway plays an essential role in forebrain patterning. This is illustrated in humans by holoprosencephaly, a phenotypically and genetically heterogeneous condition defined as a defect in the formation of midline structures of the forebrain and face (Muenke & Beachy, 2001). The most severe forms of holoprosencephaly are associated with cyclopia and formation of a proboscis. Among the causal genes of holoprosencephaly are several members of the Hh pathway, among which the gene encoding the Sonic Hedgehog (Shh) secreted protein and, less frequently, the gene encoding the Gli2 transcription factor, an effector of the pathway (Fernandes & Hébert, 2008). In mice, many studies have addressed the role of the Hh pathway in ventral forebrain formation and patterning. Null mouse mutants for *Shh* display growth retardation as well as a “holoprosencephaly” phenotype, including cyclopia and proboscis (Chiang et al., 1996). A series of studies involving gene inactivation in mouse (including conditional and compound mutants), lineage tracing and loss- and gain-of-function approaches in chick identified the multiple, successive functions of the Hh pathway in the diencephalon, hypothalamus and eyes (Vue et al., 2009; Jeong et al., 2011; Alvarez-Bolado et al., 2012; Furimsky & Wallace, 2006; Haddad-Tovolli et al., 2012, 2015; reviewed in Blaess et al. 2015; Zhang & Alvarez-Bolado 2016).

In vertebrates, transduction of Hh/Gli signalling depends on primary cilia (Goetz & Anderson, 2010). Primary cilia are sensory, antenna-like structures pointing out of many vertebrate cells. They are made of an axoneme composed of nine doublets of microtubules, surrounded by a specialized plasma membrane enriched in receptors of signalling pathways. The cilium builds on a basal body derived from the mother centriole of the cell, and on a transition zone (TZ) located between the basal body (BB) and the axoneme. The TZ is considered as the “ciliary gate” because it controls the entry and exit of proteins in and out of the cilium and is essential for cilium construction and function (Reiter et al., 2012). In the developing central nervous system, primary cilia are essential for proper dorso-ventral (DV) patterning of the spinal cord via modulating Hh signalling. Shh binds to its receptor Ptch1, which removes Ptch1 from the cilium and relieves the inhibition of the G-protein coupled receptor (GPCR) Smoothened (Smo) by Ptch1. Hh signalling at the cilium leads to the translocation of the Gli transcription factors into the nucleus and their activation into Gli activator form (GliA). In the absence of ligand, Gli2 and Gli3 are targeted to the proteasome in a cilium-dependent manner. Proteasomal cleavage of Gli2 and Gli3 gives rise to short forms with transcriptional repressor activity, among which Gli3R is a particularly strong repressor. Thus, the primary cilium is essential for the

production of both GliR and GliA forms (Goetz & Anderson., 2010). In the forebrain, functional primary cilia are required for correct DV patterning of the telencephalon (Besse et al., 2011, Laclef et al., 2015, Willaredt et al. 2008, Stottmann et al., 2009; Benadiba et al., 2012; Willaredt et al. 2013) and for the proliferation of granule cell precursors in the cerebellum (Spassky et al., 2008) and dentate gyrus (Han et al., 2008). Surprisingly, despite the essential function of Hh signalling in the forebrain, the role of primary cilia outside the telencephalon has been little explored (Willaredt et al., 2013).

In this paper we study the function of the *Ftm/Rpgrip1l* ciliopathy gene in the forebrain. *RPGRIP1L* is a causal gene in severe human ciliopathies with brain abnormalities, Meckel-Grüber syndrome (MKS5 OMIM # 611561) and Joubert syndrome type B (also called CORS syndrome, JBTS7 OMIM # 611560) (Delous et al. 2007, Arts et al 2007). The Rpgrip1l protein is enriched at the TZ in many embryonic cell types (Vierkotten et al 2007; Mahuzier et al., 2012), including neural progenitors in the brain (Besse et al., 2011). Rpgrip1l is essential for the TZ localization of many other ciliopathy proteins of the NPHP and MKS complexes (Reiter et al., 2012; Shi et al., 2017, Wiegering et al., 2018). In addition to its role in TZ construction, Rpgrip1l is required for proteasome activity at the cilium base through its interaction with the Psm2 regulatory subunit of the proteasome (Gerhardt et al., 2015), and for autophagy via downregulation of mTOR signalling (Struchtrup et al., 2018).

Ftm homozygous mouse mutants display laterality defects, polydactyly, a reduction in ventral spinal cord cell types, and renal cysts (Vierkotten et al., 2007, Delous et al., 2007). They show an almost total loss of cilia in the developing telencephalon. However, unlike several null IFT mutants (Goridovsky et al., 2009), *Ftm*^{-/-} fetuses can be recovered until birth. Thus, *Ftm* mutant mice are an excellent model to study the role of primary cilia in brain patterning and morphogenesis and to help understand the developmental origin of brain abnormalities found in severe ciliopathies. Using this mutant, our lab has previously shown that primary cilia are required for DV patterning of the telencephalon by controlling the production of the repressor form of Gli3. In *Ftm*^{-/-} embryos, the olfactory bulbs (OB) and corpus callosum (CC), two dorsal telencephalic structures, are missing (Besse et al., 2011; Laclef et al., 2016). This is linked to an expansion of ventral telencephalic structures at the expense of dorsal ones. The phenotype is rescued by introduction, into the *Ftm* mutant background, of one allele of *Gli3*^{Δ699} (Besse et al., 2011; Laclef et al., 2015), which produces only and constitutively a short, repressor form of *Gli3* (Böse et al., 2002). These studies show that the main role of cilia in telencephalic patterning is to permit Gli3R formation.

Is this also the case in other forebrain regions? We showed here that *Ftm*^{-/-} fetuses at the end of gestation displayed a severely disorganized hypothalamus and diencephalon and lacked eyes. Using molecular markers of the different diencephalic and hypothalamic subdivisions in *Ftm* embryos, we observed that the dorsal structures were enlarged and ventrally fused and the ventral structures were missing. Analysing eye development, we found that the retina was strongly reduced in size and malformed, and that the lens was missing. To further understand the origin of these defects, we investigated the molecular mechanisms involved in patterning of the affected structures, with particular interest for Hh/Gli signalling. We found that *Shh* expression itself was differentially affected in different forebrain regions. In order to quantify Gli transcriptional activity in the forebrain, we made use of the transgenic reporter Tg[GBS::GFP] mouse line in which GFP expression is driven by eight concatamerized Gli binding sites. Our results showed that Hh/Gli signalling was strongly downregulated in the *Ftm*^{-/-} embryonic forebrain in regions of high Hh signalling. We also identified a ground, Hh-independent level of Gli activity in the diencephalon of *Ftm* mutant embryos, likely caused by the reduction in Gli3R. To confirm this hypothesis and identify the respective roles of the reduction of Gli1A and of GliR levels in the observed phenotype, we analysed the forebrain phenotype of compound [*Ftm*, *Gli3*^{Δ699}] embryos. Ground level Gli activity was lost in these mutants, and some defects such as optic cup formation were totally rescued. Our results uncover essential and diverse functions for *Ftm*/*Rpgrip1l* and cilia in Gli activity in patterning the ventral forebrain and eyes and call for further examination of the role of ciliopathy genes in holoprosencephaly, a human condition linked to defects in Hh signalling.

RESULTS

***Ftm*^{-/-} fetuses at the end of gestation display microphthalmia and profound perturbations of the diencephalon and hypothalamus.**

Histological analysis combined with dye labelling of axonal tracts showed profound defects in the diencephalon and hypothalamus of *Ftm*^{-/-} fetuses at the end of gestation (E18.5; Fig. 1). The ventral regions of the diencephalon and hypothalamus were particularly affected, with a highly thickened ventral part and a perturbed position and shape of the 3rd ventricle (Fig. 1A-D). In wild type fetuses, habenular and thalamic nuclei were clearly visible in the dorsal region (Fig. 1A and C). In *Ftm*^{-/-} fetuses, these nuclei were also present even if their organization was mildly perturbed (Fig. 1B and D). In contrast, the ventral brain appeared highly disorganized in *Ftm*^{-/-} fetuses (Fig. 1A-D). The ventral midline, normally thin in wild type, was enlarged in *Ftm*^{-/-}, likely due to the absence of the most ventral region and secondary fusion of the lateral parts. The most medial hypothalamic nuclei (such as the anteroventral nuclei) were indistinguishable. The dorsal diencephalon and hypothalamus were present although malformed. In both regions, the axonal tracts (internal capsule (IC) and retroflexus tract (RT)) were defasciculated in *Ftm*^{-/-} brains (arrowheads in Fig. 1B, D). Defects in cortico-thalamic (CTA) and thalamo-cortical (TCA) axonal tracts were confirmed with carbocyanine dye labelling (Fig. 1E-H). In wild type brains, both CTA (red) and TCA (green) axons were visualized and colocalized in the IC (Fig. 1E and G). In *Ftm*^{-/-} brains, neither CTA nor TCA grew sufficiently to reach the IC (Fig. 1F and H). The eyes were absent in *Ftm*^{-/-} foetuses (Fig. 1I-L), only remnants of the retinal pigmented epithelium were observed under the brain (arrowhead in Fig. 1L). We next focused on the developmental origin of these defects.

Patterning of the diencephalon and hypothalamus is affected in *Ftm*^{-/-} embryos.

The developing diencephalon is subdivided along the DV axis in roof, alar, basal and floor plates, and along the caudo-rostral axis in three regions or prosomeres, p1, p2 and p3. The alar plates of p1, p2 and p3 give rise to the pretectum (PT), thalamus (TH) and prethalamus (PTH), respectively (Fig. 2A). The zona limitans intrathalamica (ZLI) is located at the junction between the TH and PTH. The ZLI acts as an organizer for the TH and PTH, regulating proliferation and cell fate in these two regions (Epstein, 2012; Hagemann & Scholpp, 2012; Zhang & Alvarez-Bolado, 2016).

To investigate diencephalon patterning in *Ftm* mutants, we performed *in situ* hybridization (ISH) for genes expressed in these different regions, on coronal and sagittal sections of E13.5 embryos. We first used the alar plate-expressed genes *Pax6* (PTH), *Gbx2* (TH) and *Gad67* (PTH and PT) (Fig. 2) encoding, respectively, two transcription factors involved at multiple steps of brain patterning and neurogenesis and a subunit of the glutamate decarboxylase involved in the synthesis of GABA (Stoykova and Gruss, 1994; Stoykova et al, 1996, Miyashita-Lin et al, 1999; Katarova et al., 2000; Hevner et al, 2002). We found that the expression domains of these genes were expanded along the DV axis in *Ftm*^{-/-} embryos (Fig. 2). In control embryos, robust *Pax6* expression was detected in both the ventricular and subventricular zones (VZ and SVZ) of the PTH as well as in differentiating neuronal populations (Fig. 2B, D, F and H). *Pax6* was also more faintly expressed in the VZ of the adjacent regions. In *Ftm*^{-/-} embryos, we observed a ventral expansion of the *Pax6* expression domain, which now reached the ventral midline (green arrowheads in Fig. 2C, E, G and I). In addition, in anterior coronal sections, the hypothalamic, *Pax6*-negative region was absent from the sections shown (Fig. 2E). *Gbx2* expression in control embryos was observed in differentiating neurons of the TH but not in the tegmental areas (TA) of the diencephalon (Fig. 2J, L, N and P). In *Ftm*^{-/-} embryos, *Gbx2* expression expanded ventrally (Fig. 2K, M, O and Q). *Gad67* expression in the control diencephalon was widespread in neurons of the PT and PTH and absent from diencephalic TA (Fig. 2R, T and X). In *Ftm*^{-/-} embryos, the PT and PTH expression domains expanded ventrally (Fig. 2S, U and Y). The ventral expansion of the diencephalic alar plate and the reduction of the basal plate in *Ftm*^{-/-} embryos were confirmed using additional marker genes, *Lhx2* for TH (Nakagawa and O'Leary, 2001; Puelles et al, 2006) (Supplementary Fig. 1), *Ebf1* for PT and *Six3* for PTH (Garel et al., 1997; Kobayashi et al, 2002) (Supplementary Fig. 1).

The hypothalamus can be subdivided into three main regions, the mammillary area (MAM), the tuberal hypothalamus (TUB) and the anterior hypothalamus (ANT). According to the revised prosomeric model (Puelles et al., 2012; Zhang & Alvarez-Bolado 2016), the MAM and TUB are in the basal plate of the hypothalamus while the ANT (also called alar hypothalamus) is in the alar plate (Fig. 3A). The preoptic area (POA), formerly considered as a hypothalamic region, is actually part of the telencephalon. *Nkx2.1* is expressed in the HYP in response to Hh signals from the underlying mesendoderm (Dale et al., 1997, Zhao et al., 2012, Blaess et al., 2015). *Nkx2.1* is also expressed in the POA and medial ganglionic eminence (MGE) (Fig. 3B, D, F). In *Ftm*^{-/-} embryos, the *Nkx2.1* expression domain was preserved in the telencephalon (Fig. 3B, C, F and G) but strongly reduced in the hypothalamus (Fig. 3D-G). *Dbx1* expression in progenitors of the TUB (Fig. 3H, I, L and M) and MAM

(Fig. 3J-M) regions was severely reduced as well, whereas it was maintained and even expanded in the thalamus (Fig. 3H-M). Analysis of *Wnt8b* and *Pitx2* expression confirmed the reduction in the surface of the MAM (Supplementary Fig. 2). *Ebf1* expression in the ANT was still present but fused at the midline (Fig. 2N-Q).

These data strongly suggest a strong reduction or loss of the basal plate and ventral midline of the forebrain in *Ftm*^{-/-} embryos. Conversely, the alar plate of the diencephalon appears expanded ventrally at all anteroposterior levels.

The rostral thalamus is absent in *Ftm*^{-/-} embryos

We took advantage of the expression of two proneural genes, *Ngn2* and *Mash1/Ascl1*, expressed in distinct and complementary progenitor domains (Fode et al., 2000), to analyse diencephalic subdivisions with greater precision. *Ngn2* is expressed in progenitors of most of the TH, in the ZLI and in the tegmental areas (TA) of the diencephalon, in a domain in the POA and in the dorsal telencephalon (Fode et al., 2000; Vue et al., 2007) (Fig. 4B, D, F and H). *Mash1* is expressed in progenitors of the PTH, in the prospective rostral thalamus (TH-R, see below) and in different hypothalamic subdivisions (McNay et al. 2006; Vue et al., 2007; Kim et al., 2008) (Fig. 4J-P). In *Ftm*^{-/-} embryos, *Ngn2* expression was lost in the TA and activated ectopically in a salt-and-pepper manner in regions adjacent to the telencephalon (Fig. 4C and I, white arrowheads), suggesting a perturbation of the telencephalic-diencephalic boundary (Fig. 4C and E, black arrowheads). *Mash1* was still expressed in the PTH and HYP, but very reduced caudally (MAM, black arrowheads in Q). The analysis of *Ngn2* and *Mash1* expression also revealed a thickening of the progenitor domains in the TH and PTH at E12.5-E13.5 (Fig. 4F-I, N and O). This was confirmed using other progenitor markers and we showed that this increase in progenitor number, particularly striking in the thalamus, correlated with a delay in neurogenesis (Supplementary Fig. 3). Progenitors were labelled Sox2 and Pax6, which label neural progenitors in the PTH and in the whole diencephalon, respectively. (Supplementary Fig. 3A-D) and with Ki67, a general marker of cycling cells (Supplementary Fig. 3G-J). Neurons were labelled with Tuj1 (Supplementary Fig. 3A-D and G-J) in all regions and with Calbindin and Pax6 in the TH (Supplementary Fig. 3E-F). At the beginning of neurogenesis in the ventricular zone of the thalamus, at E11.5, controls and *Ftm* mutants did not present differences in this proliferative layer (Supplementary Fig. 3A, B and K). In contrast, later at E12.5 and E13.5, in *Ftm*^{-/-} embryos the ventricular zone was thicker than in controls, suggesting an increase of the number of proliferative cells (Supplementary Fig. 3C-D). To confirm the increase of neural progenitors, we quantified the density of their

apical endfeet in the thalamus by en face immunostaining of the ventricular surface. *Ftm*^{-/-} embryos presented elevated density of endfeet (Supplementary Fig. 3L-N). Furthermore, *Ftm*^{-/-} embryos presented a reduction of the neuronal populations observed with Tuj1, Calbindin and Pax6 (Supplementary Fig. 3A-F and G-K). These increased of the neuronal progenitors and decrease of the neurons, strongly suggest a delay in neurogenesis in the diencephalon of *Ftm* mutants.

The nested domains of *Ngn2* and *Mash1* expression in the diencephalon preFig. the intrinsic subdivision of the thalamus into antero-ventral (TH-R) and postero-dorsal (TH-C) territories (Vue et al., 2007). *Ngn2* and *Mash1* domains in the TH and PTH, respectively, were continuous in *Ftm*^{-/-} embryos, suggesting a perturbation of thalamic subdivisions (Fig. 4C and K, asterisks). This was confirmed by a closer examination of *Ngn2* and *Mash1* nested expression domains (Fig. 4R-AA). We performed combined Shh/*Mash1*, Shh/*Ngn2* and *Ngn2*/*Mash1* fluorescence ISH and immunostaining to analyse the relationship of the different diencephalic domains with respect to the ZLI. In *Ftm*^{-/-} embryos, the domain of *Mash1* expression posterior to the Shh-positive ZLI was lost (white asterisks in Fig. 4Y). The *Ngn2*-positive TH-C and *Mash1*-positive PTH domains abutted at the level of the ZLI (Fig. 4Z and AA).

The TH-R contributes to GABAergic nuclei that participate in the subcortical visual shell, involved in the entrainment of the circadian rhythm (Delogu et al. 2012). Thus, neurons of the TH-R express *Gad67* like those of the PTH, while neurons of the TH-C do not (Fig. 2V). In *Ftm*^{-/-} embryos, the stripe of *Gad67* expression in the thalamus was absent, confirming the loss of the TH-R (Fig 2W).

In conclusion, the TH-R is lost in *Ftm*^{-/-} embryos and the TH-C now abuts the ZLI.

Optic vesicles form in *Ftm*^{-/-} embryos and display patterning defects

Since eyes were severely reduced or absent in *Ftm*^{-/-} fetuses at the end of gestation (Fig. 1), we investigated eye formation and patterning at E11.5. Eye development begins with the formation of the eye field in the alar hypothalamus and its separation into two bilaterally symmetrical optic vesicles. The expanding optic vesicles induce the surface ectoderm to form the lens placodes. The optic vesicle separates into the optic stalk proximally and the optic cup distally. Then the optic cup invaginates with the lens placode, forming two layers, the outer layer differentiates into the retinal pigmented epithelium (RPE) and the inner layer into the neural retina (Furimsky & Wallace 2006).

We analyzed the expression patterns of the *Pax2*, *Vax2*, *Pax6* and *Chx10* transcription factor genes, which define distinct eye territories (Furimsky and Wallace

2006). At this stage, *Pax6* and *Pax2* are expressed in the optic cup and optic stalk, respectively (Fig. 5F and K), where they repress each other. *Pax6* is required for optic cup formation, whereas *Pax2* null mice display increased optic cups at the expense of optic stalk (Schwarz et al., 2000). *Chx10* is also expressed in the optic cup (Fig. 5P). *Vax2* is expressed in the ventral domain of the optic cup (Fig. 5A), where it promotes ventral optic fates. In *Ftm*^{-/-} embryos, the neural retina was absent as assessed by the absence of *Chx10* and *Vax2* expression (Fig. 5B and Q). Only a tiny region of the RPE could be detected thanks to cell pigmentation (empty arrowheads in Fig. 5B, G, L and Q). *Pax2* was expressed, indicating the presence of the optic stalk (Fig. 5G), which suggests correct eye field separation. Consistently, optic vesicles formed in E9 *Ftm*^{-/-} embryos as in controls (Fig. 6S, U and V).

In conclusion, in *Ftm*^{-/-} embryos, eye field separation occurs correctly but proximo-distal patterning of the optic vesicle is incorrect, leading to an absence of the optic cup and of lens induction.

Hh expression and pathway activity are impaired in the forebrain of *Ftm*^{-/-} embryos

The reduction of the ventral forebrain in *Ftm* mutants suggests defects in the Hh pathway. To test this hypothesis, we analysed Hh signalling activity in the forebrain by ISH with probes for *Shh* itself and for the Hh target genes *Ptch1* and *Gli1*. In addition, in order to obtain a context-independent assay of Hh transcriptional activity through Gli transcription factors binding to their DNA targets, we introduced into the *Ftm* mutant background the Tg[GBS::GFP] reporter transgenic line in which GFP expression is driven by a concatemer of Gli-binding sites (Balaskas et al., 2012).

In mouse embryos, *Shh* is initially expressed from E7.5 in axial tissues underlying the neural plate (notochord posteriorly and prechordal plate anteriorly), where it signals to the overlying neural plate to induce ventral structures. Hh signalling induces *Shh* expression in the ventral forebrain from E8.0 onwards (Dale et al., 1997). While *Shh* expression in the axial mesoderm was unperturbed in E7.5 *Ftm*^{-/-} embryos as compared to controls (asterisks in Fig. 6A and B), *Ptch1* expression in the ventral neural plate (black arrowheads in Fig. 6C) was lost in *Ftm*^{-/-} (empty arrowheads in Fig. 6D). In E8.5 control embryos, *Shh* is still expressed in the mesendoderm underlying the brain (asterisks in Fig. 6E and I). In addition, it is activated in the ventral neural tube, including the ventral forebrain (Dale et al., 1997; Alvarez-Bolado et al., 2012) (Fig. 6E, I, black arrowhead in Fig. 6E). In E8.5 *Ftm*^{-/-} embryos, *Shh* expression persisted in the notochord and prechordal plate (Fig. 6F, J, black arrowhead in Fig. 6F) but was not detected in the ventral neural tube and brain (Fig.

6F, J, empty arrowheads in Fig. 6F). *Ptch1* expression in two stripes surrounding the *Shh* expression domain in the ventral neural tube and brain of control embryos (black arrowheads in Fig.6G) was not found in *Ftm*^{-/-} (empty arrowheads in Fig. 6H), consistent with the loss of *Shh* expression. *Foxa2*, a target of Hh signalling expressed in the ventral floor plate and in the ventral forebrain (Hallonet et al., 2002; Ribes et al., 2010) (Fig. 6K), was faintly expressed in the neural plate of *Ftm*^{-/-} embryos, confirming the very low Hh activity (Fig. 6L).

At E9.0-E9.5, *Shh* expression is down-regulated in the most ventral hypothalamus and is activated in two lateral stripes in the basal plate (Szabo et al., 2009; Alvarez-Bolado et al., 2012, Blaess et al., 2015) (Fig. 6Q, S and U). *Shh* expression was lost in the whole ventral forebrain of *Ftm*^{-/-} embryos, except in a tiny spot in the diencephalic ventral midline located roughly at the antero-posterior (AP) level of the future ZLI (Fig.6P, R, T). Gli activity as assessed by Tg[GBS::GFP] was observed lateral to *Shh* expression domain in all forebrain regions of control embryos (Fig. 6Q, S and U), whereas in *Ftm*^{-/-} embryos, Gli activity could not be detected (Fig. 6R, T and V).

Overall our results show that Hh signalling activity is drastically reduced in the ventral forebrain of *Ftm*^{-/-} embryos as early as E8.5.

***Shh* expression and Hh/Gli pathway activity show different perturbations in distinct domains of the E12.5 diencephalon**

We next investigated Hh/Gli pathway activity at E12.5, when the ZLI is fully formed and secretes *Shh* to organize cell fate in the thalamus and prethalamus (Epstein, 2012; Zhang and Alvarez-Bolado, 2016). The ZLI was formed in both control and *Ftm*^{-/-} embryos, and its DV extent was increased in *Ftm*^{-/-} compared to control embryos (Fig. 7A and B). In contrast, *Shh* expression was absent from the ventral forebrain of *Ftm*^{-/-} embryos (empty arrowheads in Fig. 7B). In order to test whether Hh signaling was active at the ZLI, we analyzed *Ptch1* and *Gli1* expression as well as Gli transcriptional activity with Tg[GBS::GFP]. Surprisingly, *Gli1* and *Ptch1* were differently affected in *Ftm*^{-/-} embryos (Fig. 7C-F). *Gli1* expression was dampened in the regions close to the *Shh* expression domains (Fig 7C and D). In contrast, *Ptch1* expression was totally downregulated in the thalamus and upregulated in the prethalamus and pretectum (Fig. 7E and F). Using FISH on sections and signal quantification, we confirmed the differential expression of *Ptch1* on both sides of the ZLI in *Ftm*^{-/-} embryos and found that this upregulation was more striking at a distance from the ventricular surface (Fig. 7M-N', R and S). To test whether this reflected differential Gli activity on both sides of the ZLI, we observed GFP expression in

Tg[GBS::GFP] embryos. At this stage, GFP-positive blood cells were present within the neural tube in all genotypes examined (green arrowheads in Fig. 7G-I point to examples of these GFP-positive blood cells). We found that Gli activity was downregulated in the diencephalon and hypothalamus of *Ftm*^{-/-} embryos as compared to controls, in the ventral regions (Fig. 7G and H) as well as on both sides of the ZLI (Fig. 7J-K''). However, Gli activity was not totally absent on both sides of the ZLI (Fig. 7K-K''). Moreover, in *Ftm*^{-/-} embryos, the Shh-positive ZLI appeared larger along the AP axis. Quantification of Shh and GFP immunofluorescence intensity confirmed the reduction of Gli activity and the increased width of the ZLI. In addition, it uncovered the presence in *Ftm* mutants of a ground level of Gli transcriptional activity along the whole AP extent of the TH and PTH, higher than in control embryos (Fig. 7P and Q).

In conclusion, in the *Ftm*^{-/-} embryos, *Shh* expression is strongly reduced in the ventral forebrain but maintained and even expanded in the ZLI. Gli activity is dampened in regions adjacent to Shh-expressing domains and displays a ground level higher than in control embryos in other regions. The loss of *Ftm* also uncovered a differential prepattern of *Ptch1* and *Gli1* expression in different diencephalic prosomeres.

Reintroduction of Gli3R into the *Ftm* background rescues aspects of the forebrain phenotype

The increased ground level of Gli activity in *Ftm*^{-/-} embryos is likely caused by the impaired production of Gli3R (Vierkotten et al., 2007, Besse et al., 2011). We thus tested how Gli activity in the diencephalon was modified in compound [*Ftm*^{-/-}; *Gli3*^{Δ/+}] embryos, by performing quantification of *GFP* and *Shh* expression in [*Ftm*^{-/-}; *Gli3*^{Δ699/+}] mutant embryos harbouring Tg[GBS::GFP]. The *Gli3*^{Δ699} allele produces constitutively a short form of Gli3 with partial repressor activity (Hill et al., 2007; Cao et al., 2013). We found that both the ground level of Gli activity and the Shh-dependent Gli activity adjacent to the ZLI were reduced in these compound mutants (Fig. 7I, L-L'', P and Q). *Ptch1* expression in the prethalamus was also downregulated (Fig. 7O, O', R and S). Moreover, the increased width of *Shh* expression in the ZLI was rescued in double mutants (Fig. 7J-O).

We then tested the consequences of Gli3R reintroduction on forebrain patterning and eye formation. ISH for *Shh*, *Ngn2*, *Gbx2*, *Pax6* and *Gad67* indicated that the reduction of the ventral forebrain was still observed and even worsened in [*Ftm*^{-/-}; *Gli3*^{Δ/+}] (Supplementary Fig. 4B-P). As in *Ftm*^{-/-} embryos, the alar plate of the diencephalon was expanded ventrally (Supplementary Fig. 4E-P), and *Shh* expression was absent from the ventral forebrain but present in the ZLI

(Supplementary Fig. 4C and D). In contrast, optic cup formation was totally restored in compound mutants, and the optic cup showed correct DV patterning (Fig. 5C, D, H, I, M, N, R and S). However, the eyes were internalized and brought together in [*Ftm*^{-/-}; *Gli3*^{Δ699/+}] embryos, and even more [*Ftm*^{-/-}; *Gli3*^{Δ699/Δ699}] embryos, and this was associated with a very reduced optic stalk (Fig. 5C, D, H, I, M, N, R and S). We also analysed [*Ftm*^{+/+}; *Gli3*^{Δ699/Δ699}] embryos, which looked similar to controls (Fig. 5E, J, O and T) as found in another study (Christoph Gerhardt, personal communication), indicating that only GliR is required for optic cup formation.

In conclusion, reintroducing Gli3R into the *Ftm* background rescues some of the defects of *Ftm*^{-/-} embryos, such as retinal agenesis and ZLI enlargement but worsens others such as the reduction in size of the ventral diencephalon and hypothalamus and of the optic stalk.

Cilia are severely reduced in number in forebrain neural progenitors

In the telencephalon of *Ftm*^{-/-} embryos, neural progenitors are devoid of primary cilia (Besse et al., 2007). Since our data indicate that Hh activity is not totally lost in the diencephalon and hypothalamus of *Ftm*^{-/-} embryos, we tested the status of cilia in this region. We first analyzed Rpgrip11 expression in E12.5 controls and found that it was present at the ciliary transition zone in different diencephalic domains including the ZLI (Fig. 8A-C'''). We then compared cilia in the control and *Ftm* mutant brain at different stages by immunofluorescence for Arl13b. Cilia were present in the forebrain of E8.5 control embryos (Fig. 8D-F) but were not detected in *Ftm*^{-/-} embryos (Fig. 8G-I). In the E12.5 diencephalon, cilia were present in the TH, PTH and ZLI in control embryos (Fig. 8J-L) and severely reduced in number in *Ftm*^{-/-} embryos (Fig. 8M-O and P). Arl13b staining was less intense in the remaining cilia (Fig. 8M-O). To analyze cilia shape in greater detail we performed scanning electron microscopy (SEM) of the ventricular surface of E13.5 control and *Ftm*^{-/-} brains, at different AP levels: in the TH, ZLI, PTH and HYP (Fig. 8Q-X and Supplementary Fig. 5). In control embryos, cilia of about 1 μm in length were found in the TH, PTH and ZLI (arrows in Fig. 8Q, S and U), while in the HYP cilia were frequently up to 3 μm long (arrows in Fig. 8W). Cilia were more difficult to recognize in the ZLI since the ventricular surface of the cells was rich in protrusions and vesicles (Fig. 8S). In the diencephalon and hypothalamus of the *Ftm*^{-/-} forebrain, cilia were in majority reduced to button-like structures (arrowheads in Fig. 8R, T, V and X), with a few very long cilia often abnormal in shape (arrows in Fig. 8R, T, V and X). These remaining cilia were present in all regions, but more frequently in the ZLI (Fig. 8T).

In conclusion, cilia were absent from the forebrain of *Ftm*^{-/-} embryos as early as E8.5. At E12.5 they were reduced in number in the diencephalon and hypothalamus, and the remaining cilia were longer than in controls and often presented an abnormal shape.

DISCUSSION

The role of cilia in the forebrain has been little studied outside of the telencephalon. In this paper we have studied the role of the *Ftm/Rpgrip1l* ciliopathy gene in forebrain patterning and morphogenesis, focusing on the diencephalon, hypothalamus and eyes. At the end of gestation, *Ftm*^{-/-} foetuses displayed a reduction of the ventral hypothalamus and a disorganization of diencephalic nuclei and of the internal capsule, a bidirectional axonal tract joining the cerebral cortex and the subcortical regions. Eyes were almost totally absent. We examined the developmental defects underlying this phenotype. Investigating the Hh pathway, we identified region-specific perturbations of Gli target gene expression and of Gli activity. Combined with our previous studies, our data lead to a global understanding of the role of primary cilia in forebrain patterning and morphogenesis of their relationship with Hh signalling.

Patterning defects in the diencephalon and hypothalamus of *Ftm* mutants reflect the loss of primary cilia on neural progenitors

Examination of forebrain markers during development showed a strong reduction of ventral forebrain structures: the tegmental areas of the diencephalon, the mammillary and tuberal areas of the hypothalamus, and the ventral part of the anterior hypothalamus. This was accompanied by a dorsoventral expansion of alar diencephalic domains, thalamus, prethalamus and pretectum. This phenotype is consistent with that observed in the spinal cord of *Ftm* mutants, where the most ventral cell types (FP, V3 interneurons and motoneurons) are absent or considerably reduced, and intermediate neuronal types are expanded ventrally (Vierkotten et al., 2007). In contrast, in the telencephalon, ventral structures are expanded at the expense of dorsal ones, leading to agenesis of the olfactory bulbs and corpus callosum, two dorsal telencephalic structures (Besse et al. 2011; Laclef et al., 2015).

Do the observed defects correspond to a ciliary phenotype? While the disorganization of the diencephalic-telencephalic boundary had already been noticed in ciliary mutants (Willaredt et al., 2008; reviewed in Willaredt et al., 2013), the other defects observed in this study have not been reported in other ciliary mutants. Interestingly, a reduction of the midbrain floor plate and derived dopaminergic neurons was reported in conditional *IFT88* mutants (Gazea et al., 2016). It was thus important to study the integrity of cilia in different forebrain regions in *Ftm* mutants. We have previously reported that cilia are absent from telencephalic progenitors in E12.5 *Ftm*^{-/-} embryos (Besse et al., 2011). Here we analysed the status of primary cilia in the diencephalon and hypothalamus of *Ftm*^{-/-} embryos at different stages. We

found a near-total loss of cilia in the progenitors of the forebrain of *Ftm*^{-/-} embryos at E8.5. At E12.5, cilia were severely reduced in number, and their shape (MEB) and content (Arl13b immunofluorescence) were abnormal. This, combined with our previous studies, strongly suggests that the forebrain defects observed in *Ftm* mutants are due to the ciliary defects in progenitors.

Region-specific defects in Hh/Gli signalling in the forebrain of *Ftm* mutants.

The reduction in ventral forebrain areas and the loss of the TH-R in *Ftm* mutants suggested an impaired response to Hh/Gli signalling. Indeed, tegmental areas of the diencephalon and hypothalamus depend on Hh signalling from the notochord and prechordal plate, which induces *Shh* expression in the forebrain midline (Dale et al., 1997). Neural Shh is in turn required for correct formation of the basal diencephalon and hypothalamus (Szabo et al., 2009; Shimogori et al., 2010; Zhao et al., 2012). The strategies of Hh signalling are different in the basal diencephalon and hypothalamus. In the diencephalon, as in the spinal cord, the Shh-expressing cells are non-neurogenic. In contrast, genetic fate-mapping has shown that most of the mammillary and tuberal regions are derived from Shh-expressing progenitors (Alvarez-Bolado et al., 2012, Blaess et al., 2015; Zhang & Alvarez-Bolado, 2016). Despite these differences, the loss of primary cilia in *Ftm* mutants has similar consequences in the basal plate of the hypothalamus and diencephalon, i.e. a severe reduction of these domains.

High Hh activity is also required for the formation of the TH-R, which gives rise to thalamic GABAergic neurons, while formation of the TH-C requires lower Hh activity (Hashimoto-Torii et al., 2003). Loss of *Shh* expression from E10.5 onwards in the ventro-caudal diencephalon by deletion of the SBE1 intronic enhancer results in a loss of the TH-R, showing that Shh signals from the ZLI are not sufficient to form this region (Jeong et al., 2011). Thus, our observation of the loss of the TH-R and the expansion of the TH-C in *Ftm*^{-/-} embryos is consistent with the strong reduction of Gli activity and the near-total absence of *Shh* expression in the ventral diencephalon.

For the ZLI, the situation is different. *Shh* is expressed in the ZLI of *Ftm*^{-/-} embryos and appears to be able to signal, although with lower efficiency than in controls. This may explain why the thalamus and prethalamus are of normal size, unlike in *Shh* mutants (Ishibashi and McMahon 2002; Szabo et al., 2009). Only the TH-R, which requires high Gli activity, is lost. Thus, the Hh/Gli signalling pathway is still active in *Ftm* mutants. Moreover, a basal, low level of Gli activity appears to be present throughout the diencephalon, likely caused by the reduction in Gli3R levels (Besse et al., 2011).

ZLI formation is independent of primary cilia.

The ZLI has been proposed, initially in chick, to form through an inductive process requiring Hh signaling from the diencephalic basal plate (Kiecker and Lumsden, 2004; Zeltser, 2005, for review Epstein, 2012). In mouse mutants in which expression of a functional Shh ligand is absent from the ventral diencephalon, the ZLI does not form (Szabo et al., 2009). However, impaired production of functional Shh protein in the forebrain from E10.5 onwards does not affect *Shh* expression in the ZLI, suggesting that Hh signaling is required for the initiation, but not for the maintenance, of ZLI formation (Vue et al., 2009). Surprisingly, the ZLI forms in *Ftm*^{-/-} embryos and it is even wider along the AP axis than in controls. This widening is accounted for by the reduction in Gli3R levels, since it is rescued in compound [*Ftm*^{-/-}, *Gli3*^{Δ699/+}] embryos. Consistent with this data, Gli3 repression by Wnt signals is required for controlling the width of the ZLI in chicken embryos (Martinez-Ferre et al., 2013).

If ZLI formation requires Hh signals from the basal plate, how can it occur in *Ftm* mutants, which display no *Shh* expression in the basal diencephalon? In E9.5 *Ftm*^{-/-} embryos, a discrete patch of *Shh* expression remained in the basal plate at the level of the future ZLI. We propose that this patch of *Shh* expression is sufficient for the initiation of ZLI formation in *Ftm* mutants. Because this patch of Shh does not give rise to high Gli activity, we can speculate that here Shh might signal through Gli-independent, non-canonical pathway (Carballo et al., 2018). This independence of Gli activity of ZLI formation is consistent with the presence of a *Shh*-expressing ZLI in [*Gli2*^{-/-}, *Gli3*^{-/-}] compound mutants (Bai et al., 2004). Indeed Gli1 is a target of Hh signaling and cannot activate the pathway on its own in mice (Bai et al., 2002).

A double role of cilia in eye development

Separation of the eye fields requires Shh from the prechordal plate (Chiang et al 1996), and later proximo-distal patterning of the optic vesicle involves Hh/Gli activity (Furimsky & Wallace 2006). Our data show that cilia are essential for eye formation. In *Ftm*^{-/-} embryos, the optic cup and lens are totally absent. However, optic vesicles form, indicating that eye field separation occurred, and the optic stalk is present. This phenotype is consistent with a strong reduction in Gli3R, known to be required for optic cup formation. Accordingly, optic cups with correct DV patterning were observed in compound [*Ftm*^{-/-}, *Gli3*^{Δ699/+}] and [*Ftm*^{-/-}, *Gli3*^{Δ699/Δ699}] embryos, showing that the repressor form of Gli3 is crucial for optic cup formation, and that cilia function in this structure is totally mediated by Gli3R. This sole requirement for Gli3R in the retina was confirmed by the analysis of [*Ftm*^{+/+}, *Gli3*^{Δ699/Δ699}] siblings, which displayed normally formed and patterned retina. In compound [*Ftm*^{-/-}, *Gli3*^{Δ699/+}] and [*Ftm*^{-/-},

Gli3^{Δ699/Δ699}] embryos, the eyes were closer to each other under the ventral forebrain and even partially fused in some cases, and the optic stalk was almost totally absent, consistent with a requirement for GliA activity in the formation of the optic stalk. However, this requirement is less conspicuous in *Ftm*^{-/-} embryos, probably because the reduction in GliA levels is counterbalanced by the reduction in GliR levels.

The *Ftm* mutant phenotype does not show cyclopia, even when two copies of Gli3R are reintroduced. This suggests that a low level of Hh activity from the underlying prechordal mesendoderm is produced and is sufficient to separate the eye fields. The absence of Gli2R in the *Ftm*^{-/-} brain may contribute to this residual Hh activity.

Primary cilia in the forebrain: a balance of GliA and GliR activity

The phenotype of the *Ftm* mutant in the forebrain is very different from that of a *Shh* mutant. Early on, there is enough Hh/Gli activity for proper growth and survival of diencephalic progenitors. This is not the case in *Shh* mutants, where proliferation and survival of diencephalic precursors is reduced as soon as the E8.5 stage, and thus the whole diencephalon is extremely reduced in size (Ishibashi & McMahon 2002). Cell proliferation is decreased throughout the diencephalon and correlates with downregulation of CyclinD1 expression (Ishibashi & McMahon 2002).

More generally, our results show that, in *Ftm* mutants, forebrain structures requiring high GliA activity, such as the rostral thalamus and tegmental areas of the diencephalon and hypothalamus, do not form. Similarly, structures that require high GliR activity, such as the optic cup, are also absent. In contrast, structures that require low or intermediate Hh activity, such as TH-C or the optic stalk, are present and sometimes expanded. This is to be attributed to the dual role of primary cilia in Hedgehog signalling: in the production of fully activator forms of Gli transcription factors, and in the cleavage of full-length Gli2 and Gli3 proteins to form transcriptional repressors (Götz & Anderson, 2010). Of note, Rpgrip1l plays a direct role in proteasomal activity at the cilium base via binding of the Psmd2 proteasomal subunit (Wiegering et al., 2017). Thus, Gli3R formation may be particularly sensitive to the loss of Rpgrip1l.

Clinical relevance of our study for human ciliopathies and holoprosencephaly

Hypothalamic and diencephalic malformations are rarely reported in ciliopathies. This may be partly explained by the fact that a precise analysis of the forebrain is rarely possible in fetuses with either anencephaly or large occipital encephalocele, which is often the case for Meckel syndrome due to mutation of *RPGRIP1L*. Benign tumours

called diencephalic hamartomas have been observed in cases of Meckel (Roume et al., 1998) or Finnish hydrolethalus syndrome (Paetau et al., 2008) and other ciliopathies (Poretti et al. 2011; Del Giudice et al., 2014; Poretti et al., 2017). Interestingly, diencephalic hamartomas are a near-constant feature of Pallister-Hall syndrome, characterized by a dominant mutation in *GLI3* leading to the constitutive production of Gli3R (Shin et al., 1999). Furthermore, somatic mutations affecting genes acting on SHH signaling have been described in 37% of the cases of sporadic hypothalamic hamartomas (Hildebrand MS et al., 2016). This strongly suggests that hypothalamic hamartomas observed in cases of ciliopathies are caused by defects in SHH signaling.

Holoprosencephaly, a defect of the forebrain midline often associated with mutations in *SHH*, is rarely described in ciliopathies, and only in the most severe form, Meckel syndrome (Paetau et al., 1985, Ahdab-Barmada & Claassen, 1990). This may be surprising, given the essential role of cilia in vertebrate Hh signalling. Our study of the forebrain of *Ftm* mutants provides a potential explanation, as we find clear phenotypic differences between the *Ftm* mutants and Hh pathway mutants. Nevertheless, ciliopathy genes could act as modifier genes for HPE. HPE shows high phenotypic variability in single families, which has led to the proposal that a combination of mutations in HPE genes could account for the variability in severity of the phenotype (the multi-hit hypothesis). In favour of this hypothesis, digenic inheritance has been identified in several HPE families (Mouden et al., 2016 and ref therein). Interestingly, homozygous mutations in the *STIL* gene encoding a pericentriolar and centrosomal protein have been found in patients with HPE and microcephaly (Mouden et al., 2015, Kakar et al., 2015). Mouse *Stil* homozygous mutant embryos display severe forebrain midline defects and die at E10.5 (Israeli et al., 1999). Ciliogenesis and centriole duplication, as well as Hh signaling, are defective in the absence of *STIL* (Mouden et al., 2015). Whole genome sequencing in heterogenous HPE families will allow testing the involvement of ciliopathy gene variants in this disease.

More generally, our study of the ciliopathy gene mutant *Rpgrip11/Ftm* calls for further examination of ciliary and ciliopathy genes in human neurodevelopmental diseases associated with SHH pathway defects.

MATERIALS & METHODS

Mice

All experimental procedures involving mice were made in agreement with the European Directive 2010/63/EU on the protection of animals used for scientific purposes, and the French application decree 2013-118. Mice were raised and maintained in the IBPS mouse facility, approved by the French Service for Animal Protection and Health, with the approval numbers C-75-05-24. The project itself has been approved by the local ethical committee "Comité d'éthique Charles Darwin", under the authorization number 2015052909185846. *Gli3*^{Δ699} and *Ftm*-deficient mice were produced and genotyped as described previously (Böse et al., 2002; Besse et al., 2011). Mutant lines were maintained as heterozygous (*Ftm*^{+/-} or *Gli3*^{Δ699/+}) and double heterozygous (*Ftm*^{+/-}; *Gli3*^{Δ699/+}) animals in the C57Bl6/J background. Note that the eye phenotype of the *Ftm*^{-/-} animals was totally penetrant in the C57Bl6/J background used here, unlike in C3H or mixed backgrounds (Delous et al., 2007 and C. Gerhardt, personal communication). The transgenic line Tg[GBS::GFP] was maintained in the C57Bl6/J background and genotyped as described (Balaskas et al., 2012). In analyses of *Ftm* mutant phenotypes, heterozygous and wild-type (wt) embryos did not show qualitative differences, and both were used as 'control' embryos. The sex of the embryos and fetuses was not analyzed. Embryonic day (E) 0.5 was defined as noon on the day of vaginal plug detection.

Histology, In situ hybridization (ISH) and immunofluorescence (IF)

For whole-mount ISH, embryos were dissected in cold phosphate buffered saline (PBS) and fixed in 4% paraformaldehyde (PFA) in PBS for a time depending on the embryonic age and then processed as described in (Anselme et al., 2007). For histology and ISH on sections, embryos were dissected in cold PBS and fixed overnight in 60% ethanol, 30% formaldehyde and 10% acetic acid. Embryos were embedded in paraffin and sectioned (7 μm). Cresyl thionin staining and ISH were performed on serial sections, as described previously (Anselme et al., 2007, Besse et al., 2011, Laclef et al., 2015). For fluorescence ISH (FISH), immunodetection of the probe was done overnight at 4°C with anti-digoxigenin peroxidase-conjugated antibody (Roche), diluted 1/50 in maleate buffer supplemented with 2% Boehringer Blocking Reagent (Roche). Peroxidase activity was detected with FITC-coupled tyramide (1/50).

For IF, embryos were fixed overnight in 4% paraformaldehyde (PFA). E18.5 fetuses were perfused with 4% PFA. Immunofluorescence staining was performed on 14 μ m serial cryostat sections, as described previously (Anselme et al., 2007; Laclef et al., 2015), with antibodies against Shh (Cell signaling 2207, 1:200 and R&D Systems AF445, 1:200), Arl13b (Neuromab 75-287; 1:1500), Calb (Swant CB-38, 1:500), FoxA2 (Abcam ab23630; 1:200), GFP (Aves GFP-1020; 1:200), Mash1 (BD Pharmigen 556604; 1:200), Ki67 (Millipore AB9260, 1:500), Pax6 (DSHB PAX6, 1:100), Pericentrin (Covance-Genetech PRB-432C, 1:500), Rpgrip1l (Besse et al., 2011; 1:800), Sox2 (Millipore MAB4343, 1:300), Tuj1 (Sigma T8578, 1:500), ZO1 (Zymed-Invitrogen 33-9100, 1:500). Secondary antibodies were Alexa-Fluor conjugates from Molecular Probes (1:1000). Nuclei were stained with DAPI (1:500).

Dil/DiA labelling

Brains of E18.5 fetuses were dissected in PBS 1x and fixed overnight in 4% PFA. After three washes in PBS, were labelled by 1,1'-dioctadecyl-3,3',3'-tetramethylindocarbocyanine perchlorate (Dil; Invitrogen D383) or 4-Di-16 ASP (4-(4-(Dihexadecylaminostyryl)-N-Methylpyridinium iodide (DiA, Invitrogen D3883) crystals, in the cortex or in the diencephalon of control and *Ftm*^{-/-} brains, as indicated in Fig. 1. Samples were kept for at least two weeks in PFA 4% at 37°C for the lipophilic dye to diffuse along the fixed cell membranes. Then, the brains were embedded in 4% agarose in PBS, and thick coronal vibratome (LeicaVT1000S) sections were made.

Image acquisition and quantification of fluorescence intensity

ISH images were acquired with a bright-field Leica MZ16 stereomicroscope. IF, FISH and axonal tract dye labelling images were observed with a fluorescent binocular (LeicaM165FC) and acquired with a confocal microscope (Leica TCS SP5 AOBS).

Fluorescence intensity was measured using the ImageJ software. For Shh-GFP immunofluorescence, adjacent squares of 50 μ m side were drawn in the diencephalon, all along the ventricular surface from posterior to anterior. Total fluorescence intensity was measured in each square on three distinct optical sections. For each optical section, the background intensity was measured by taking three squares in the 3rd ventricle, and the mean background intensity was subtracted from all the measurements of the same image. Images from three controls, three *Ftm*^{-/-} and two [*Ftm*^{-/-}, *Gli3* ^{Δ 699/+}] embryos were used for quantification. For comparison, the measurements were aligned using as a reference the square corresponding to the AP level of the ZLI (point 6 of the abscissa on the diagrams in

Fig. 7P and Q). The diagrams in Fig. 8K indicate the mean intensity for each position of each genotype.

For quantification of *Ptch1* FISH, adjacent squares of 20 μm side were drawn in the diencephalon, from posterior to anterior, at two apico-basal levels: along the ventricular surface and about 40 μm away from the ventricular surface. Total fluorescence intensity was measured in each square on three distinct optical sections. Images from 4 controls, 4 *Ftm*^{-/-} and 3 [*Ftm*^{-/-}, *Gli3* ^{Δ 699/+}] embryos were used for quantification. For comparison, the measurements were aligned using as a reference the square corresponding to the AP level of the ZLI (point 17 of the abscissa on the diagrams in Fig. 7R and S).

Scanning electron microscopy

Embryos were dissected in 0.1 M sodium cacodylate (pH 7.4), and fixed overnight with 2% glutaraldehyde in 0.1 M sodium cacodylate (pH 7.4) at 4°C. Heads were then sectioned to separate the dorsal and ventral parts of the telencephalon, exposing their ventricular surfaces. Head samples were washed several times in 1.22 X PBS and post-fixed for 15 minutes in 1.22 X PBS containing 1% OsO₄. Fixed samples were washed several times in ultrapure water, dehydrated with a graded series of ethanol and critical point dried (CPD 300, Leica) at 79 bar and 38 °C with liquid CO₂ as the transition fluid and then depressurized slowly (0,025 bar/s). They were then mounted on aluminum mounts with conductive silver cement. Samples surfaces were coated with a 5 nm platinum layer using a sputtering device (ACE 600, Leica). Samples were observed under high vacuum conditions using a Field Emission Scanning Electron Microscope (Gemini 500, Zeiss) operating at 3 kV, with a 20 μm objective aperture diameter and a working distance around 3 mm. Secondary electrons were collected with an in-lens detector. Scan speed and line compensation integrations were adjusted during observation.

Experimental design and statistical analysis

In all experiments, the number of embryos or fetuses analyzed was ≥ 3 for each genotype, unless otherwise stated. For the comparison of the number of cilia in the different diencephalic regions of control and *Ftm*^{-/-} embryos (Fig. 8P), quantification was made in 4 control and 4 mutant embryos. For the comparison of the thickness of Tuj1 and Ki67 positive tissue was made in 3 control and 3 mutant embryos (Supplementary Fig. 3K). For the comparison of the density of endfeet was made in 3

control and 3 mutant embryos (Supplementary Fig. 3N). For statistical analysis, unpaired t-test was performed using the Prism software.

REFERENCES

- Ahdab-Barmada M, Claassen D (1990) A distinctive triad of malformations of the central nervous system in the Meckel-Gruber syndrome. *J Neuropathol Exp Neurol* 49:610-620.
- Alvarez-Bolado G, Paul FA, Blaess S (2012) Sonic hedgehog lineage in the mouse hypothalamus: from progenitor domains to hypothalamic regions. *Neural Dev* 7(4):2-18.
- Arts HH, Doherty D, van Beersum SEC, Parisi MA, Letteboer SJF, Gordien NT, Peters TA, Märker T, Voeselek K, Kartono A, Ozyurek H, Knoers NVAM, Roepman R (2007) Mutations in the gene encoding the basal body protein RPGRIP1L, a nephrocystin-4 interactor, cause Joubert syndrome.
- Bai CB, Auerbach W, Lee JS, Stephen D, Joyner AL. Gli2, but not Gli1, is required for initial Shh signaling and ectopic activation of the Shh pathway. *Development*. 2002 Oct;129(20):4753-61.
- Bai CB, Stephen D, Joyner AL. All mouse ventral spinal cord patterning by hedgehog is Gli dependent and involves an activator function of Gli3. *Dev Cell*. 2004 Jan;6(1):103-15.
- Balaskas N, Ribeiro A, Panovska J, Dessaud E, Sasai N, Page KM, Briscoe J, Ribes V (2012) Gene Regulatory Logic for Reading the Sonic Hedgehog Signaling Gradient in the Vertebrate Neural Tube. *Cell* 148, 273–284.
- Benadiba C, Magnani D, Niquille M, Morlé L, Valloton D, Nawabi H, Ait-Lounis A, Reith W, Theil T, Horning JP, Lebrand C, Durand B (2012) The ciliogenic transcription factor RFX3 regulates early midline distribution of guidepost neurons required for corpus callosum development. *PLoS Genet* 8:3 e1002606.
- Besse L, Neti M, Anselme I, Gerhardt C, Rüther U, Laclef C, Schneider-Maunoury S (2011) Primary cilia control telencephalic patterning and morphogenesis via Gli3 proteolytic processing. *Development* 138:2079-88.
- Blaess S, Szabó N, Haddad Tóvölli R, Zhou X, Álvarez-Bolado G (2015) Sonic hedgehog signaling in the development of the mouse hypothalamus. *Front Neuroanat* 8:1-6.
- Böse J, Grotewold L, Rüther U (2002) Pallister–Hall syndrome phenotype in mice mutant for Gli3. *Hum Mol Genet* 11:1129–1135.
- Carballo GB, Honorato JR, de Lopes GPF, Spohr TCLSE (2018) A highlight on Sonic hedgehog pathway. *Cell Commun Signal* 16 (11): 1-15.

Chiang C, Litingtung Y, Lee E, Young KE, Corden JL, Westphal H, Beachy PA (1996) Cyclopia and defective axial patterning in mice lacking *Sonic hedgehog* gene function. *Nature* 383:407-413.

Dale JK, Vesque C, Lints TJ, Smapath TK, Furley A, Dodd J, Placzek M (1997). Cooperation and BMP7 and SHH in the induction of forebrain ventral midline cells by prochordal mesoderm. *Cell* 90:257-269.

David A, Liu F, Tibelius A, Vulprecht J, Wald D, Rothermel U, Ohana R, Seitel A, Metzger J, Ashery-Padan R, Meinzer HP, Gröne HJ, Izraeli S, Krämer A (2014) Lack of centrioles and primary cilia in STIL(-/-) mouse embryos. *Cell Cycle* 13:2859-68.

Del Giudice E, Macca M, Imperati F, D'Amico A, Parent P, Pasquier L, Layet V, Lyonnet S, Stamboul-Darmency V, Thauvin-Robinet C, Franco B, Oral-Facial-Digital Type I (OFD1) collaborative group (2014) CNS involvement in OFD1 syndrome: a clinical, molecular, and neuroimaging study. *Orphanet J Rare Dis* 10;09:74.

Delogu A, Sellers K, Zagoraiou L, Bocianowska-Zbrog A, Mandal S, Guimera J, Rubenstein JLR, Sugden D, Jessell T, Lumsden A (2012) Subdortical visual shell nuclei targeted by ipRGCs develop from a Sox14+-GABAergic progenitor and require Sox14 to regulate daily activity rhythms. *Neuron* 75:648-662.

Delous M et al. (2007) The ciliary gene *RPGRIP1L* is mutated in cerebello-oculorenal syndrome (Joubert syndrome type B) and Meckel syndrome. *Nat Genet* 39:875-881.

Epstein D (2012) Regulation of thalamic development by Sonic hedgehog. *Front Neurosci* 6: article 57.

Fernandes M, Hébert JM (2008) The ups and downs of holoprosencephaly: dorsal versus ventral patterning forces. *Clin Genet* 73:413-423.

Fode C, Ma Q, Casarosa S, Ang SL, Anderson DJ, Guillemot F (2000) A role for neural determination genes in specifying the dorsoventral identity of telencephalic neurons. *Genes Dev* 14:67-80.

Furimsky M, Wallace VA (2006) Complementary Gli activity mediates early patterning of the mouse visual system. *Dev Dyn* 235: 594-605.

Garel S, Marin F, Mattei MG, Vesque C, Vincent A, Charnay P (1997) Family of Ebf/Olf-1-related genes potentially involved in neuronal differentiation and regional specification in the central nervous system. *Dev Dyn* 210:191-205.

Gazea M, Tasouri E, Tolve M, Bosch V, Kabanova A, Gojak C, Kurtulmus B, Novikov O, Spatz J, Pereira G, Hübner W, Brodski C, Tucker K, Blaess S (2016) Primary cilia

are critical for Sonic hedgehog dopaminergic neurogenesis in the embryonic midbrain. *Dev Biol* 409:55-71.

Gerhardt C, Lier JM, Burmühl S, Struchtrup A, Deutschmann K, Vetter M, Leu T, Reeg S, Grune T, Rütger U (2015) The transition zone protein Rpgrip11 regulates proteasomal activity at the primary cilium. *J Cell Biol* 210:115-133.

Goetz SC, Anderson KV (2010) The primary cilium: a signaling centre during vertebrate development. *Nat Rev Genet* 11:331-344.

Gorodovskiy M, Mukhopadhyay M, Wilsch-Braeuninger M, Phillips M, Teufel A, Kim C, Malik N, Huttenr W, Westphal H. Intraflagellar transport protein 172 is essential for primary cilia formation and plays a vital role in patterning the mammalian brain. *Dev Biol* 325:24-32.

Haddad-Tovoli R, Heide M, Zhou X, Blaess S, Alvarez-Bolado G (2012) Mouse thalamic differentiation: Gli-dependent and Gli-independent prepattern. *Front Neurosci* 6 article 27.

Haddad-Tovoli R, Paul FA, Zhang Y, Zhou X, Theil T, Puelles L, Blaess S, Alvarez-Bolado G (2015) Differential requirements for Gli2 and Gli3 in the regional specification of the mouse hypothalamus. *Front Neurosci* 9 article 34.

Hagemann AIH, Scholpp S (2012) The tale of the three brothers – Shh, Wnt, and Fgf during development of the thalamus. *Front Neurosci* 6: article 76.

Hallonet M, Kaestner KH, Martin-Parras L, Sasaki H, Betz UAK, Ang SL (2002) Maintenance of the specification of the anterior definitive endoderm and forebrain depends on the axial mesendoderm: a study using HNF3 β /Foxa2 conditional mutants. *Dev Biol* 243:20-33.

Han YG, Spassky N, Romaguera-Ros M, Garcia-Verdugo JM, Aguilar A, Schneider-Maunoury S, Alvarez-Buylla A (2008) Hedgehog signaling and primary cilia are required for the formation of adult neural stem cells. *Nat Neurosci*. 11:277-84.

Hashimoto-Torii K, Motoyama J, Hui CC, Kuroiwa A, Nakafuku M, Shimamura K (2003) Differential activities of Sonic hedgehog mediated by Gli transcription factors define distinct neuronal subtypes in the dorsal thalamus. *Mech Dev* 120: 1097–1111.

Hevner RF, Miyashita-Lin E, Rubenstein JL (2002) Cortical and thalamic axon pathfinding defects in Tbr1, Gbx2, and Pax6 mutant mice: evidence that cortical and thalamic axons interact and guide each other. *J Comp Neurol* 447:8-17.

Hildebrand MS, Griffin NG, Damiano JA, Cops EJ, Burgess R, Ozturk E, Jones NC, Leventer RJ, Freeman JL, Harvey AS, Sadleir LG, Scheffer IE, Major H, Darbro BW, Allen AS, Goldstein DB, Kerrigan JF, Berkovic SF, Heinzen EL (2016) Mutations of

the Sonic hedgehog pathway underlie hypothalamic hamartoma with gelastic epilepsy. *Am J Hum Genet.* 99:423-9.

Ishibashi M, McMahon AP (2002) A sonic hedgehog-dependent signaling relay regulates growth of diencephalic and mesencephalic primordia in the early mouse embryo. *Development* 129:4807-4819.

Izraeli S, Lowe LA, Bertness VL, Good DJ, Dorward DW, Kirsch IR, Kuehn MR (1999) The *SIL* gene is required for mouse embryonic axial development and left-right specification. *Nature* 399:691-694.

Jeong Y, Dolson DK, Waclaw RR, Matise MP, Sussel L, Campbell K, Kaestner KH, Epstein DJ (2011). Spatial and temporal requirements for Sonic hedgehog in the regulation of thalamic interneuron identity. *Development* 138:531-541.

Kakar N, Ahmad J, Morris-Rosendahl DJ, Altmüller J, Friedrich K, Barbi G, Nürnberg P, Kubisch C, Dobyns WB, Borck G (2015) *STIL* mutation causes autosomal recessive microcephalic lobar holoprosencephaly. *Hum Genet.* 134:45-51.

Katarova Z, Sekerkova G, Prodan S, Mugnaini E, Szabo G (2000) Domain-restricted expression of two glutamic acid decarboxylase genes in midgestation mouse embryos. *J Comp Neurol* 424:607-627.

Kiecker C, Lumsden A (2004) Hedgehog signaling from the ZLI regulates diencephalic regional identity. *Nat Neurosci* 7:1242-1249.

Kim EJ, Battiste J, Nakagawa Y, Johnson JE (2008) *Ascl1* (*Mash1*) lineage cells contribute to discrete cell populations in CNS architecture. *Mol Cell Neurosci* 38:595-606.

Kobayashi D, Kobayashi M, Matsumoto K, Ogura T, Nakafuku M, Shimamura K (2002) Early subdivisions in the neural plate define distinct competence for inductive signals. *Development* 129:83-93.

Laclef C, Anselme I, Besse L, Catala M, Palmyre A, Baas D, Paschaki M, Pedraza M, Métin C, Durand B, Schneider-Maunoury S (2016) The role of primary cilia in corpus callosum formation is mediated by production of the *GLI3* transcriptional repressor. *Hum Mol Genet* 24: 4997-5014.

Mahuzier A, Gaudé HM, Grampa V, Anselme I, Silbermann F, Leroux-Berger M, Delacour D, Ezan J, Montcouquiol M, Saunier S, Schneider-Maunoury S, Vesque C (2012) Dishevelled stabilization by the ciliopathy protein *Rpgrip1l* is essential for planar cell polarity. *The J Cell Biol*, 198: 927-940.

Martinez-Ferre A, Navarro-Garberi M, Bueno C, Martinez S (2013) Wnt Signal Specifies the Intrathalamic Limit and Its Organizer Properties by Regulating Shh Induction in the Alar Plate. *J Neurosci* 33:3967–3980.

McNay DEG, Pelling M, Claxton S, Guillemot F, Ang SL (2006) *Mash1* is required for generic and subtype differentiation of hypothalamic neuroendocrine cells. *Mol Endocrinol* 20:1623-1632.

Miyashita-Lin EM, Hevner R, Wassarman KM, Martinez S, Rubenstein JL (1999) Early neocortical regionalization in the absence of thalamic innervation. *Science* 285:906-9.

Mouden C, de Tayrac M, Dubourg C, Rose S, Carré W, Hamdi-Rozé H, Babron MC, Akloul L, Héron-Longe B, Odent S, Dupé V, Giet R, David V (2015) Homozygous STIL mutation causes holoprosencephaly and microcephaly in two siblings. *PLoS One* 10:e0117418.

Mouden C, Dubourg C, Carré W, Rose S, Quelin C, Akloul L, Hamdi-Rozé H, Viot G, Salhi H, Darnault P, Odent S, Dupé V, David V (2016) Complex mode of inheritance in holoprosencephaly revealed by whole exome sequencing. *Clin Genet* 89:659-68.

Muenke M, Beachy PA (2001) Holoprosencephaly. In: Scriver CR et al, eds. *The metabolic and molecular bases of inherited disease*, 8th edn. New York, NY: McGraw-Hill: 6203-6230.

Nakagawa Y, O'Leary DD (2001) Combinatorial expression patterns of LIM-homeodomain and other regulatory genes parcellate developing thalamus. *J Neurosci* 21:2711-25.

Paetau A, Salonen R, Haltia M (1985) Brain pathology in the Meckel syndrome: a study of 59 cases. *Clin Neuropathol* 4:56-62.

Paetau A, Honkala H, Salonen R, Ignatius J, Kestilä M, Herva R (2008) Hydroletharus syndrome: neuropathology of 21 cases confirmed by HYL1 gene mutation analysis. *J Neuropathol Exp Neurol* 67:750-762.

Poretti A, Huisman TA, Scheer I, Boltshauser E (2011) Joubert syndrome and related disorders: spectrum of neuroimaging findings in 75 patients. *AJNR Am J Neuroradiol* 32:1459-1463.

Poretti A, Snow J, Summers AC, Tekes A, Huisman TAGM, Aygun N, Carson KA, Doherty D, Parisi MA, Toro C, Yildirimli D, Vemulapalli M, Mullikin JC, NISC Comparative Sequencing Program, Cullinane AR, Vilboux T, Gahl WA, Gunay-Aygun M (2017) *J Med Genet* 54:521-529.

- Puelles E, Acampora D, Gogoi R, Tuorto F, Papalia A, Guillemot F, Ang SL, Simeone A (2006) Otx2 controls identity and fate of glutamatergic progenitors of the thalamus by repressing GABAergic differentiation. *J Neurosci* 26:5955-64.
- Puelles L, Martinez de la Torre M, Bardet S, Rubenstein JLR (2012) Hypothalamus, Chapter 8 in *The Mouse nervous system*, eds C Watson, G Paxinos, L Puelles (London, San Diego, CA : Academic Press/Elsevier, 221-312.
- Reiter JF, Blacque OE, Leroux M (2012) The base of the cilium: roles for transition fibres and the transition zone in ciliary formation, maintenance and compartmentalization. *EMBO Rep* 13:608-618.
- Ribes V, Balaskas N, Sasai N, Cruz C, Dessaud E, Cayuso J, Tozer S, Yang LL, Novitsch B, Marti E, Briscoe J (2010) Distinct Sonic Hedgehog signaling dynamics specify floor plate and ventral neuronal progenitors in the vertebrate neural tube. *Genes Dev* 24:1186-1200.
- Roume J, Genin E, Cormier-Daire V, Ma HW, Mehaye B, Attie T, Razavi-Encha F, Falet-Bianco C, Buerner A, Clerget-Darpoux F, Munnich A, Le Merrer M (1998) A gene for Meckel syndrome maps to chromosome 11q13. *Am J Hum Genet* 63:1095-1101.
- Schwarz M, Cecconi F, Bernier G, Andrejewski N, Kammandel B, Wagner M, Gruss P (2000) Spatial specification of mammalian eye territories by reciprocal transcriptional repression of Pax2 and Pax6. *Development* 127:4325-4334.
- Shi X, Garcia III G, Van DeWeghe JC, McGorty R, Pazour GJ, Doherty D, Huang B, Reiter JF (2017) Super-resolution microscopy reveals that disruption of ciliary transition-zone architecture causes Joubert syndrome. *Nature Cell Biol* 19:1178-1191.
- Shimogori T, Lee DA, Miranda-Angulo A, Yang Y, Wang H, Jiang L, Yoshida AC, Kataoka A, Mashiko H, Avetisyan M, Qi L, Qian J, Blackshaw S (2010) A genomic atlas of mouse hypothalamic development. *Nat Neurosci* 13: 767-775.
- Shin SH, Kogerman P, Lindström E, Toftgard R, Biesecker LG (1999) *Proc Natl Acad Sci USA* 16:2880-2884.
- Spassky N, Han YG, Aguilar A, Strehl L, Besse L, Laclef C, Romaguera Ros M, Garcia-Verdugo JM, Alvarez-Buylla A (2008) Primary cilia are required for cerebellar development and Shh-dependent expansion of progenitor pool. *Dev Biol* 317:246-259.
- Stoykova A, Fritsch R, Walther C, Gruss P (1996) Forebrain patterning defects in Small eye mutant mice. *Development* 122:3453-65.

Stoykova A, Gruss P (1994) Roles of Pax-genes in developing and adult brain as suggested by expression patterns. *J Neurosci* 14:1395-412.

Stottmann RW, Tran PV, Turbe-Doan A, Beier DR (2009) Ttc21b is required to restrict sonic hedgehog activity in the developing mouse forebrain. *Dev Biol* 335:166-178.

Struchtrup A, Wiegering A, Stork B, Rütther U, Gerhardt C (2018) The ciliary protein RPGRIP1L governs autophagy independently of its proteasome-regulating function at the ciliary base in mouse embryonic fibroblasts. *Autophagy* 14:567-583.

Szabo NE, Zhao T, Cankaya M, Theil T, Zhou X, Alvarez-Bolado G (2009a) Role of neuroepithelial Sonic hedgehog in hypothalamic patterning. *J Neurosci* 29:6989-7002.

Szabo NE, Zhao T, Zhou X, Alvarez-Bolado G (2009b) The role of Sonic hedgehog of neural origin in thalamic differentiation in the mouse. *J Neurosci* 29:2453-2466.

Vierkotten J, Dildrop R, Peters T, Wang B, Rütther U (2007) Ftm is a novel basal body protein of cilia involved in Shh signaling. *Development* 134:2569-2577.

Vue TY, Aaker J, Taniguchi A, Kazemzadeh C, Skidmore JM, Martin DM, Martin JF, Treier M, Nakagawa Y (2007) Characterization of progenitor domains in the developing mouse thalamus. *J Comp Neurol* 505:73-91.

Vue TY, Bluske K, Alishashi A, Yang LL, Koyano-Nakagawa N, Novitsch B, Nakagawa Y (2009) Sonic Hedgehog signaling controls thalamic progenitor identity and nuclei specification in mice. *J Neurosci* 29:4484-4497.

Wiegering A, Dildrop R, Kalfhues L, Spychala A, Kuschel S, Lier JM, Zobel T, Dahmen S, Leu T, Struchtrup A, Legendre F, Vesque C, Schneider-Maunoury S, Saunier S, Rütther U, Gerhardt C (2018) Cell type-specific regulation of ciliary transition zone assembly in vertebrates. *EMBO J* e97791 DOI 10.15252/emj.201797791.

Willaredt MA, Hasenpusch-Theil K, Gardner AR, Kitanovic I, Hirschfeld-Warneken VC, Gojak CP, Gorgas K, Bradford CL, Spatz J, Wölfl S, Theil T, Tucker KL (2008) A crucial role for primary cilia in cortical morphogenesis. *J Neurosci* 28:12887-12900.

Willaredt MA, Tasouri E, Tucker KL (2013) Primary cilia and forebrain development. *Mech Dev* 130:373-380.

Zeltser LM (2005) Shh-dependent formation of the ZLI is opposed by signals from the dorsal diencephalon. *Development* 132:2023-2033.

Zhang Y, Alvarez-Bolado G (2016) Differential developmental strategies by Sonic hedgehog in thalamus and hypothalamus. *J Chem Neuroanat* 75:20-27.

Zhao L, Zevallos SE, Rizzoti K, Jeong Y, Lovell-Badge R, Epstein DJ (2012) Disruption of SoxB1 dependent Sonic hedgehog expression in the hypothalamus causes septo-optic dysplasia. *Dev Cell* 22:585-596.

ACKNOWLEDGEMENTS

We are grateful to the animal and imaging facilities of the IBPS (Institut de Biologie Paris-Seine FR3631, Sorbonne Université, CNRS, Paris, France) for their technical assistance. We thank Michaël Trichet (electron microscopy facility, IBPS) for electron microscopy analysis. We are grateful to Christine Vesque and Marie Breau (IBPS-Developmental Biology laboratory, Paris, France) and Christoph Gerhardt (Institute for Animal Developmental and Molecular Biology, Heinrich Heine University Düsseldorf, Germany) for critical reading of the manuscript. We thank James Briscoe (Crick Institute, London, UK) for the kind gift of the Tg[GBS::GFP] transgenic line. This work was supported by funding from the Agence Nationale pour la Recherche (ANR, project CILIAINTHEBRAIN to SSM), the Fondation pour la Recherche Médicale (Equipe FRM DEQ20140329544 funding to SSM) and the Fondation ARC pour la Recherche sur le Cancer (Project ARC PJA 20171206591 to SSM).

FIGURE LEGENDS

Figure 1. Histology and dye labelling of axon tracts in the brain of E18.5 fetuses.

A-D) Nissl staining on coronal sections of the brain at two distinct antero-posterior levels of thalamic and hypothalamic regions in E18.5 wild type (A, C) and *Ftm*^{-/-} (B, D) fetuses. C, D are more posterior sections than A, B. Both levels of sections correspond to the ventral hypothalamus and the alar thalamus. Black arrowheads in B-D point to axon fascicles of the IC and Rt. Double black arrows in B, D point to the dysmorphic hypothalamus in *Ftm* mutants. **E-H)** Carbocyanine dye staining of corticothalamic (DiI, magenta) and thalamocortical (DiA, green) axons in E18.5 wild type (E, G) and *Ftm*^{-/-} (F, H) brains. G and H are higher magnification of the boxed regions in E and F, respectively. **I-L)** Nissl staining on coronal sections at the level of the eyes of the head of E18.5 wild type (I, K) and *Ftm*^{-/-} (J, L) fetuses. K and L are higher magnification of the boxed regions in I and J, respectively. The arrowhead in L points to remnants of the RPE. AN: anteroventral nucleus, CX: cortex; HB: Habenula; HYP: hypothalamus; IC: internal capsule; NR: neural retina; RPE: retinal pigmented epithelium; RT: retroflexus tract; TH: thalamus; V3: 3rd ventricle. Scale bars: 1 mm in A-D (shown in A) and in I and J (shown in I); 0.5 mm in E and F (shown in E); 0.1 mm in G and H (shown in G); 0.2 mm in K and L (shown in K).

Figure 2. Diencephalon patterning at E13.5

A) Schematic drawings of the E13.5 forebrain in sagittal (left) and coronal (right) views. The position of the coronal (B-E, J-M, R-W) and sagittal (F-I, N-Q, X, Y) sections shown below is indicated with dashed lines. Note that in the left diagram, antero-posterior and dorso-ventral axes are indicated at the level of the ZLI. **B-Y)** In situ hybridisation with probes for *Pax6* (B-I), *Gbx2* (J-Q) and *Gad67* (R-Y) in coronal sections at two distinct antero-posterior levels (B-E, J-M, R-W) and in sagittal sections at lateral (F, G, N, O, X, Y) and medial (H, I, P, Q) levels. The genotype (*control* or *Ftm*^{-/-}) is indicated on the left of the figure, where control stands for *Ftm*^{+/+} or *Ftm*^{+/-}. In sagittal sections, the brain is outlined with dotted lines. Black and green arrowheads point to neuronal progenitors and neurons, respectively. Ant: anterior; AP: alar plate; BP: basal plate; FP: floor plate; HYP: hypothalamus; RP: roof plate; Post: posterior; PT: pretectum; PTH: prethalamus; TA: tegmental areas; TEL: telencephalon; TH: thalamus; TH-R: rostral thalamus; ZLI: zona limitans intrathalamica; 3V: third ventricle. Scale bars: 0.5 mm in all pictures (shown in B for coronal sections and in F for sagittal sections) except in V and W where scale bar is

100 μ m (shown in V).

Figure 3. Hypothalamus patterning at E13.5

A) Schematic drawings of the E13.5 forebrain in sagittal (left) and coronal (right) views. The position of the coronal (B-E, H-K, N-O) and sagittal (F, G, L, M, P, Q) sections shown below is indicated with dashed lines. Note that in the left diagram, antero-posterior and dorso-ventral axes are indicated at the level of the hypothalamus. **B-Q)** In situ hybridisation with probes for *Nkx2.1* (B-G), *Dbx1* (H-M) and *Ebf1* (B-E) in coronal sections at different antero-posterior levels and in sagittal sections. The genotype (*control* or *Ftm*^{-/-}) is indicated on the left of the figure. Black arrowheads point to neuronal progenitors. In sagittal sections the brain is outlined with dotted lines. Ant: anterior; ANT: anterior hypothalamus; AP: alar plate; BP: basal plate; FP: floor plate; HYP: hypothalamus; MAM: mammillary area; MGE: medial ganglionic eminence; POA: preoptic area; Post: posterior; RP: roof plate; PT: pretectum; PTH: prethalamus; TA: tegmental areas; TEL: telencephalon; TH: thalamus; TUB: tuberal hypothalamus; ZLI: zona limitans intrathalamica. Scale bars: 0.5 mm in all pictures (shown in B for coronal sections and in F for sagittal sections).

Figure 4. Progenitor domains at E12.5-E13.5

A) Schematic drawings of the E13.5 forebrain in sagittal view. The position of the coronal sections (D-I, L-Q) shown below is indicated with dashed lines. **B-U)** In situ hybridisation with probes for *Ngn2* (B-I, R, S) and *Mash1* (J-Q, T, U) in whole mount hybridization on sagittally-bisected brains viewed from the ventricular side (B, C, J, K) or on coronal sections at different antero-posterior levels (D-I, L-Q, R-U). The genotype is indicated on the left of the figure. **V, W)** Shh immunofluorescence (magenta) combined with *Ngn2* fluorescence in situ hybridization (green). **X, Y)** Double immunofluorescence for Shh (magenta) and *Mash1* (green). **Z, AA)** *Mash1* immunofluorescence (magenta) combined with *Ngn2* fluorescence in situ hybridization (green). In C, black arrowheads point to patchy *Ngn2* expression in the prethalamus and white arrowheads point to missing *Ngn2* expression domain in the ventral forebrain. In P, black arrowheads point to remnants of the MAM. Asterisks in C, K, S and Y point to the absence of the *Ngn2*-negative, *Mash1*-positive TH-R in *Ftm*^{-/-} embryos. Ant: anterior; ANT: anterior hypothalamus; AP: alar plate; BP: basal plate; FP: floor plate; HYP: hypothalamus; MAM: mammillary area; POA: preoptic

area; RP: roof plate; Post: posterior; PT: pretectum; PTH: prethalamus; TA: tegmental areas; TEL: telencephalon; TH: thalamus; TH-C: caudal thalamus; TH-R: rostral thalamus; TUB: tuberal hypothalamus; ZLI: zona limitans intrathalamica. Scale bars: 0.5 mm in B-Q (shown in B for whole mount ISH and in D for coronal sections); 100 μ m in R-U (shown in R); 50 μ m in V-Z and AA (shown in V).

Figure 5. Eye morphogenesis in E11.5 embryos

A-T) ISH on coronal sections in the region of the eye of E11.5 *Ftm*^{+/+} (A, E, I, M), *Ftm*^{-/-} (B, F, J, N), *Ftm*^{-/-}, *Gli3*^{Δ/+} (C, G, K, O), *Ftm*^{-/-}, *Gli3*^{Δ/Δ} (D, H, L, P) and *Ftm*^{+/+}, *Gli3*^{Δ/Δ} (E, J, O, T) with probes for *Vax2* (A-E), *Pax2* (F-J), *Pax6* (K-O) and *Chx10* (P-T). Empty arrowheads in B, G, L and Q point to the missing optic cup; empty arrowhead in I points to the reduced optic stalk; black arrowhead in N points to partially fused optic cups. doc: dorsal optic cup; dos: dorsal optic stalk; l: lens; voc: ventral optic cup; vos: ventral optic stalk. Scale bars: 100 μ m (shown in A).

Figure 6. Hh expression and Hh/Gli signaling in the E7.5-E9.5 embryo forebrain

A-H) Whole-mount ISH on E7.5 (A-D) and E8.5 (E-H) embryos with probes for *Shh* (A, B, E, F) or *Ptch1* (C, D, G, H). Black arrowheads indicate *Shh* and *Ptch1* expression sites in the neural plate; black asterisks indicate *Shh* expression in the mesoderm underlying the neural plate. Empty arrowheads in D, F and H indicate absence of *Shh* and *Ptch1* expression in the neural plate of *Ftm*^{-/-} embryos. **I-P)** IF for Shh (I, J, M-P) and FoxA2 (K, L) on coronal sections of E8.5 (I-L) and sagittal sections of E9.5 (M-P) embryos. The white arrowhead in P points to the small dot of Shh expression in the basal plate of *Ftm*^{-/-} embryos. **Q-V)** Double IF for Shh and GFP in Tg[GBS::GFP] transgenic embryos. Green arrowheads point to GFP-positive blood cells. The genotypes are indicated on the left of the figure. Control stands for *Ftm*^{+/+} or *Ftm*^{-/-}. **W, X)** Schematics indicating the approximate levels of sections in Q-V. Note that the sections are tilted, so they do not look bilaterally symmetric. Ov: optic vesicle. Scale bars: 50 μ m in A-H (shown in A for A-D and in E for E-H); 20 μ m in I-L (shown in I); 500 μ m in M, N (shown in M); 100 μ m in O, P (shown in O) and in Q-V (shown in Q).

Figure 7. Hh expression and Hh/Gli signaling in the E12.5 embryo forebrain.

A-F) Whole-mount ISH on E12.5 control (A, C, E) or *Ftm*^{-/-} (B, D, F) half-brains viewed from the ventricular surface, with probes for *Shh* (A, B), *Gli1* (C, D) or *Ptch1* (E, F). **G-L'')** IF on coronal sections of control (G, J, J', J''), *Ftm*^{-/-} (H, K, K', K'') or [*Ftm*, *Gli3*^{Δ699/+}] (I, L, L', L'') Tg[GBS::GFP] embryos. IFs were performed with antibodies for Shh and GFP. In J', J'', K', K'', L', L'', fire versions of Shh and GFP are shown (fire scale in J'). Empty arrowheads in B point to the missing Shh expression domain in the ventral forebrain. **M-O')** Combined fluorescence ISH *Ptch1* and IF for Shh on coronal sections for of the diencephalon of E12.5 control (M, M'), *Ftm*^{-/-} (N, N') and compound [*Ftm*^{-/-}, *Gli3*^{Δ699/+}] (O, O') embryos. M'-O' show fire versions of *Ptch1* FISH. Green arrowheads in M, N and O point to GFP-positive blood cells. **P-S)** Diagrams showing the quantification of the intensity of Shh (P) or GFP (Q) IF and *Ptch1* FISH (R, S) along the diencephalon. *Ptch1* FISH intensity was quantified next to the ventricular surface (R) or 40 μm away from the ventricular surface (S). Numbers on the abscissa relate to the position of the squares of quantification. Fluorescence intensity in ordinate is given in arbitrary units (AUF). HYP: hypothalamus; PT: pretectum; PTH: prethalamus; TH: thalamus; ZLI: zona limitans intrathalamica. Scale bars: 0.5 mm in A-F (shown in A); 100 μm in G-O' (shown in G).

Figure 8. Cilia in the forebrain of *Ftm* mutants

A-C''') Immunofluorescence on coronal sections of E12.5 control embryos with antibodies for Shh (green), Arl13b (magenta) and Rpgrip1l (white). Nuclei are stained with DAPI. In B''' and C''', only Rpgrip1l is shown. **D-I)** Immunofluorescence on coronal sections of E8.5 control (D-F) and *Ftm*^{-/-} (G-I) embryos with antibodies for Shh (red) and Arl13b (white). Nuclei are stained with DAPI. White squares in D and G indicate the regions magnified in E, F and in H, I, respectively. **J-O)** Immunofluorescence on coronal sections of E12.5 control (J-L) and *Ftm*^{-/-} (M-O) embryos with antibodies for Shh (green) and Arl13b (magenta). In J and M, nuclei are stained with DAPI. White rectangles in J and M indicate the regions magnified in K, L and in N, O, respectively. **P)** Graph comparing the number of cilia in the diencephalon of control and *Ftm*^{-/-} embryos. * indicates that the statistical unpaired T-test is significant, with P value = 0.0223 for TH, 0.0263 for ZLI and 0.0421 for PTH. **Q-X)** SEM of the ventricular surface in different regions of control (Q, S, U, W) and *Ftm*^{-/-} (R, T, V, X) hemisected brains. White arrows point to the base of cilia, white arrowheads point to button-like structures surrounded by a ciliary pocket, similar to

those found in the cortex of *Ftm*^{-/-} embryos (Besse et al., 2011). HYP: hypothalamus; PTH: prethalamus; TH: thalamus; ZLI: zona limitans intrathalamica. Scale bars: 50 μm in A, J and M (shown in A and J); 20 μm in D, G (shown in D); 5 μm in B, C (shown in B) and in E, F, H and I (shown in E); 2 μm in B' and C' (shown in B') and in K, L, N, O (shown in K); 1 μm in B'', B''', C'', C''' (shown in B'') and in Q-X (shown in Q).

SUPPLEMENTARY FIGURE LEGENDS

Supplementary Figure 1. Additional markers of diencephalon patterning

A) Schematic drawings of the E13.5 forebrain in sagittal (left) and coronal (right) views. The position of the coronal (B-E, J-M) and sagittal (F-I, N-Q) sections shown below is indicated with dashed lines. **B-Q)** In situ hybridisation with probes for *Lhx2* (B-I), *Six3* (J-M) and *Ebf1* (N-Q) in coronal sections at two distinct antero-posterior levels (B-E, J-M) and in sagittal sections at lateral (F, G, N, O) and medial (H, I, P, Q) levels. In sagittal sections, the brain is outlined with dotted lines. Black and green arrowheads point to neuronal progenitors and neurons, respectively. *Lhx2* displays widespread expression in the thalamus, and no expression in tegmental areas, of control embryos (B, D, F H). In *Ftm*^{-/-} embryos, *Lhx2* expression is still restricted to the thalamus along the anteroposterior axis (C, G), but is expanded ventrally (E, G, I). *Six3* expression in the PTH (J, L) also shows a ventral expansion in *Ftm*^{-/-} embryos, with an apparent loss of *Six3*-negative, hypothalamic structures (K, M). *Ebf1* expression confirms the ventral expansion of PTH and TH in *Ftm*^{-/-} embryos as compared to controls (N-Q). Ant: anterior; AP: alar plate; BP: basal plate; FP: floor plate; HYP: hypothalamus; RP, roof plate; Post: posterior; PT, pretegmentum; PTH, prethalamus; TA, tegmental areas; TEL: telencephalon; TH: thalamus; ZLI: zona limitans intrathalamica. Scale bars: 0.5 mm in all pictures (shown in B for coronal sections and in F for sagittal sections).

Supplementary Figure 2. Additional markers of hypothalamus patterning

A) Schematic drawings of the E13.5 forebrain in sagittal view. The position of the coronal sections (B, C, F, G) shown below is indicated with dashed lines. **B-I)** In situ hybridisation with probes for *Pitx2* (B-E) and *Wnt8b* (F-I) on coronal sections (B, C, F, G) or in whole mount ISH on sagittally-bisected brains (viewed from the ventricular side) (D, E, H, I). The genotype of the embryo is indicated on the left of the figure. Ant: anterior; ANT: anterior hypothalamus; AP: alar plate; BP: basal plate; FP: floor plate; HYP: hypothalamus; MAM: mammillary area; MGE: medial ganglionic eminence; POA: preoptic area; Post: posterior; RP: roof plate; PT: pretegmentum; PTH: prethalamus; TA: tegmental areas; TEL: telencephalon; TH: thalamus; TUB: tuberal hypothalamus; ZLI: zona limitans intrathalamica. Scale bars: 0.5 mm in all pictures (shown in B for coronal sections and in D for whole mount ISH).

Supplementary Figure 2. Additional markers of hypothalamus patterning

A) Schematic drawings of the E13.5 forebrain in sagittal view. The position of the coronal sections (B, C, F, G) shown below is indicated with dashed lines. **B-I)** In situ hybridisation with probes for *Pitx2* (B-E) and *Wnt8b* (F-I) on coronal sections (B, C, F, G) or in whole mount ISH on sagittally-bisected brains (viewed from the ventricular side) (D, E, H, I). The genotype of the embryo is indicated on the left of the figure. MBO: mammillary body; PT: pretectum; MAM: Mammillary area. Scale bars: 0.5 mm in all pictures (shown in B for coronal sections and in D for whole mount ISH).

Supplementary Figure 3. Neurogenesis is delayed in the thalamus of *Ftm*^{-/-} embryos.

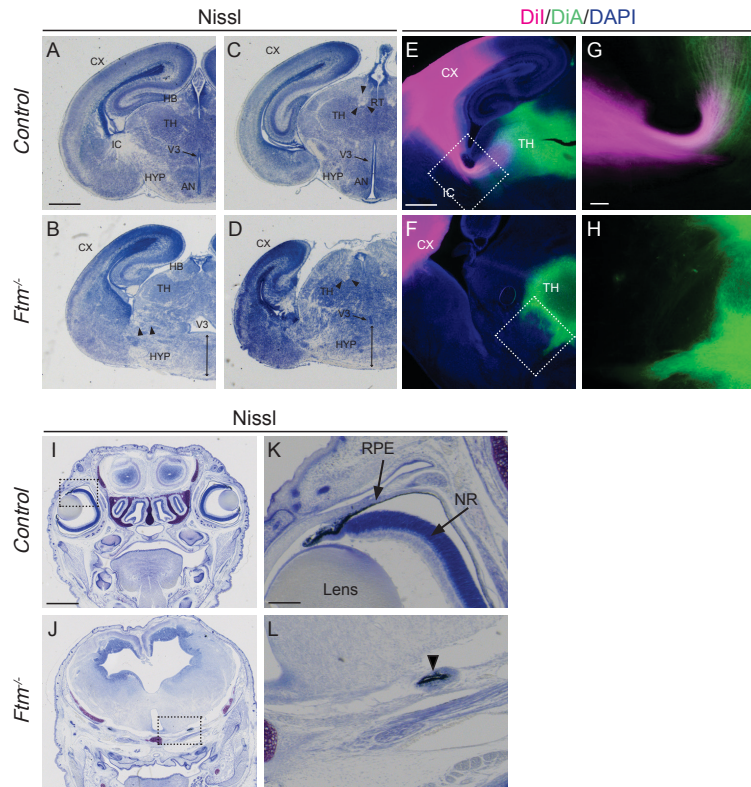
A-F) Immunofluorescence for antibodies to Pax6, Sox2, Tuj1 and Calbindin (Calb) (as colour coded on the figure) on coronal sections of the diencephalon of E13.5 control (A, C, E) and *Ftm*^{-/-} (B, D, F) embryos. The ventricular zone (high Pax6 and Sox2 labelling in A-D) is thicker in *Ftm*^{-/-} than in controls, while the neuronal layer (Tuj1+ in C, D, Calbindin+ in E, F) is thinner in *Ftm*^{-/-}. **G-J)** Immunofluorescence for antibodies to Ki67 and Tuj1 (as colour coded on the figure) on coronal sections of the diencephalon of E11.5 (G, H) and E12.5 (I, J) control (G, I) and *Ftm*^{-/-} (H, J) embryos. Neurogenesis is just starting at E11.5, and there is no obvious difference between control and *Ftm*^{-/-} embryos. However, at E12.5, the progenitor layer is thicker and the neuronal layer is thinner in the *Ftm*^{-/-} than in the control thalamus. **K)** Diagrams showing the thickness of the neuronal (Tuj1+) layer and of the cycling progenitor (Ki67+) layer. The thickness of the neuronal layer increases faster in control than in *Ftm*^{-/-} embryos. The Ki67+ cell layer increases in size in *Ftm*^{-/-} while it does not in controls. ns indicates that the statistical unpaired T-test is not significant, at E11.5 for Tuj1 and Ki67, with P=0.1579 and P=0.2532 values respectively. *** indicates that the statistical unpaired T-test is significant, at E12.5 for Tuj1 and Ki67, with P=0.0006 and P<0.0001 values respectively. **L, M)** En-face views of the ventricular surface in the thalamus of control and *Ftm*^{-/-} embryos stained with ZO1 to label apical junctions and Pericentrin to label the centrosome/basal body. **N)** Quantification of the density of end-feet, showing a higher density in the *Ftm*^{-/-} thalamus as compared with control. The higher density of ventricular end-feet strongly suggests an increase in the density of progenitors. * indicates that the statistical unpaired T-test is significant, with P value = 0.0251 for endfeet density. PTH: prethalamus; TH: thalamus. Scale bars: 100 µm in A-D (shown in A) and F-K (shown in F); 10 µm and 1 µm in L, M (shown in L).

Supplementary Figure 4. Diencephalon and hypothalamus patterning in compound [*Ftm*^{-/-}, *Gli3*^{Δ699}] mutants.

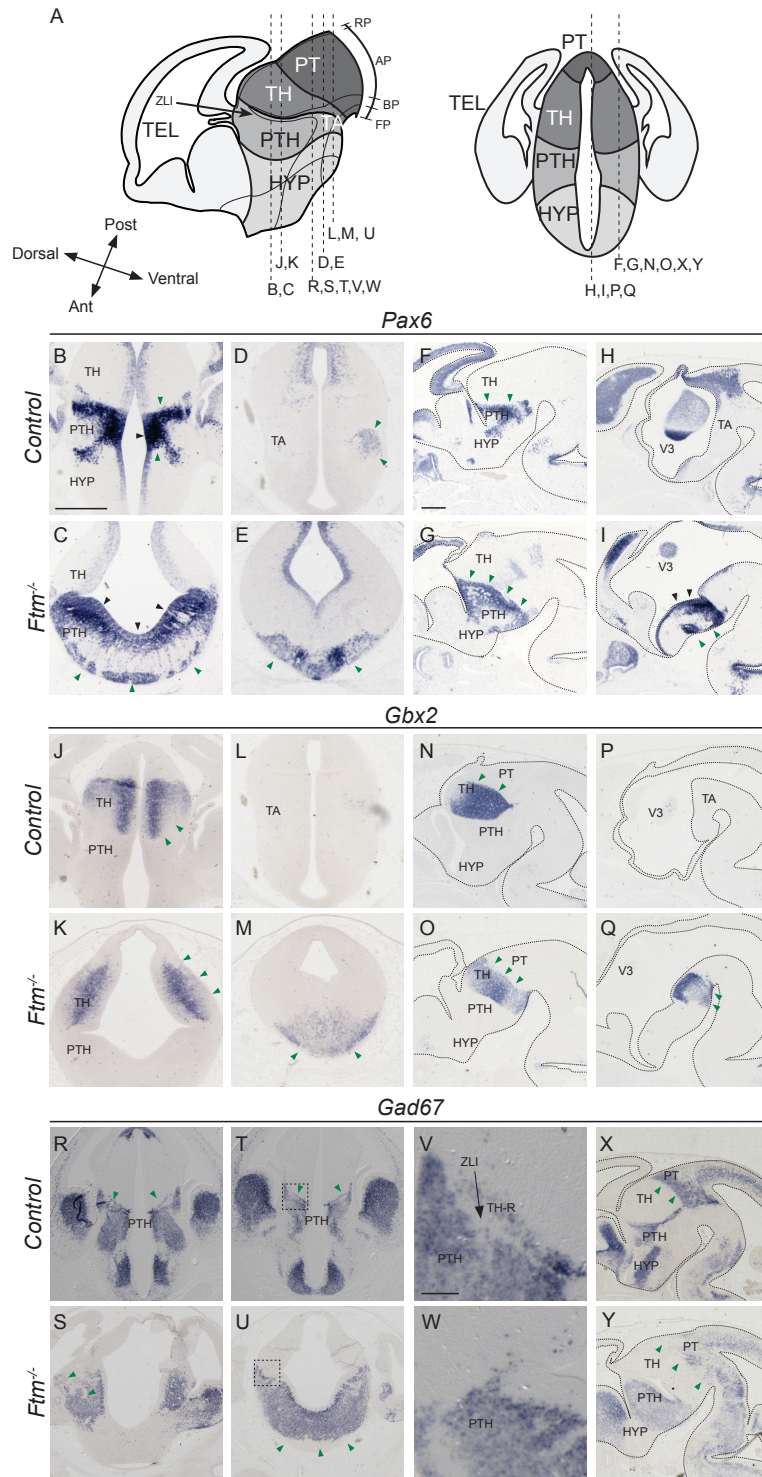
A) Schematic drawings of the E13.5 forebrain in sagittal view. The position of the coronal sections (H-P) shown below is indicated with dashed lines. **B-G)** Whole mount ISH with probes for *Shh* (B-D) or *Ngn2* (E-G) on sagittally-bisected brains viewed from the ventricular side. Black asterisks in C, D, F and G point to the absence of ventral forebrain. **H-P)** ISH on coronal sections with probe for *Gbx2* (H-J), *Pax6* (K-M) or *Gad67* (N-P). The genotype of the embryo is indicated on the top of the figure. Ant: anterior; AP: alar plate; BP: basal plate; FP: floor plate; HYP: hypothalamus; RP, roof plate; POA: preoptic area; Post: posterior; PT, pretectum; PTH, prethalamus; TA, tegmental areas; TEL: telencephalon; TH: thalamus; ZLI: zona limitans intrathalamica. Scale bars: 0.5 mm in all pictures (shown in B for whole mount ISH and in H for coronal sections).

Supplementary Figure 5. Scanning electron microscopy (SEM) of the brain ventricular surface in at E13.5 shows ciliary defects in different forebrain regions of *Ftm*^{-/-} embryos.

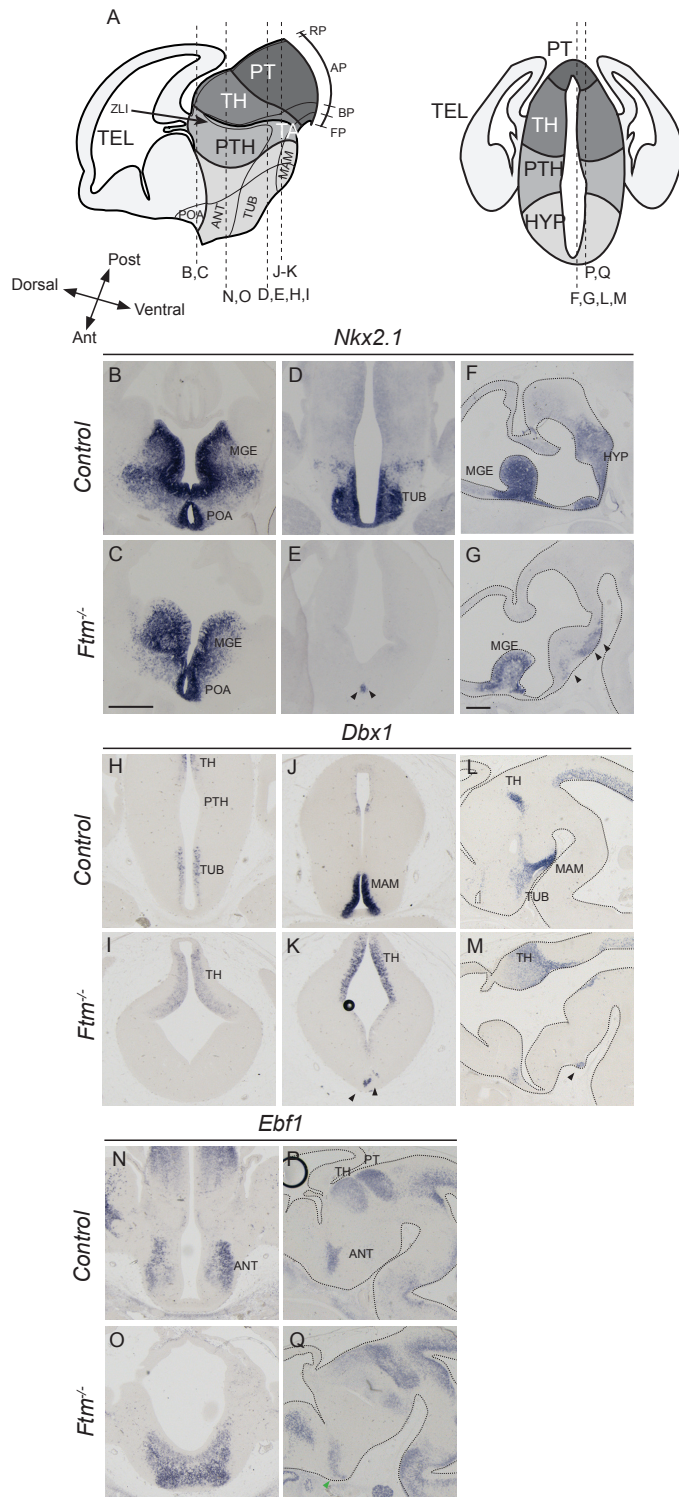
A, B) View of a control (A) and a *Ftm*^{-/-} hemisected brain used for SEM, indicating the regions observed at higher magnification (dotted squares). **C-N)** SEM of different regions of the surface. White arrows point to the base of cilia, white arrowheads point to button-like structures surrounded by a ciliary pocket, similar to those found in the cortex (Besse et al., 2011). C, F, I and L show images of control brains. In TH and PTH, cilia are 1 μm long and easily recognized. In the ZLI, cilia are also 1 μm length and are more difficult to see due to the presence of many protrusions and vesicles on the cell surface. In the HYP, much longer cilia (up to 3 μm) were found. D, E, G, H, J, K, M and N show images of *Ftm*^{-/-} brains. In TH, PTH and HYP, few cilia were present and usually longer than in controls, and many button-like structures were found (D, E, J, K, M, N). In the ZLI, many very long cilia were found, often malformed (G, H, see the club-shaped cilium in H). Overall, in the diencephalon and hypothalamus of the *Ftm*^{-/-} forebrain, cilia were in majority reduced to button-like structures, with a few very long cilia often abnormal in shape. These remaining cilia were present in all regions, but more frequently in the ZLI. HYP: hypothalamus; PTH: prethalamus; TH: thalamus; ZLI: zona limitans intrathalamica. Scale bars: 200 μm in A, B (shown in A); 1 μm in C-N (shown in C).



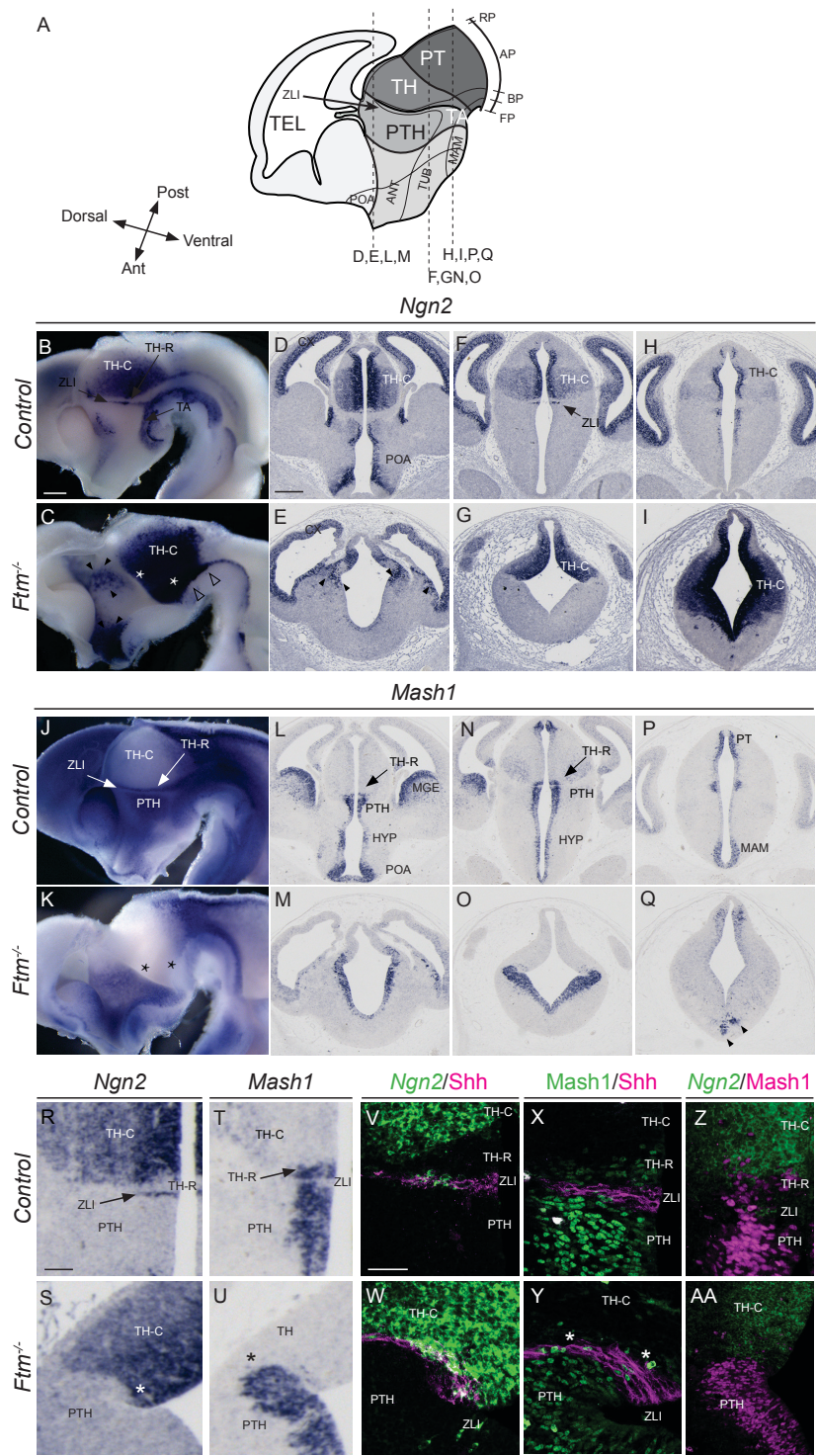
Andreu-Cervera et al., Figure 1



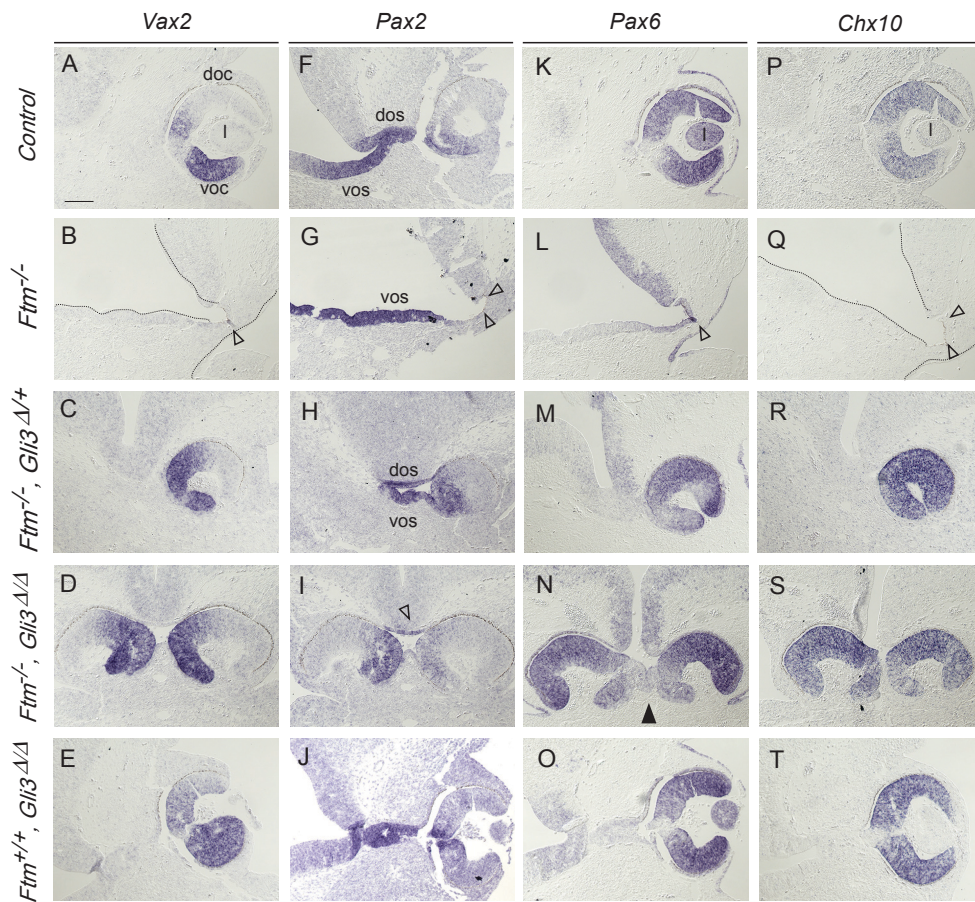
Andreu-Cervera et al., Figure 2



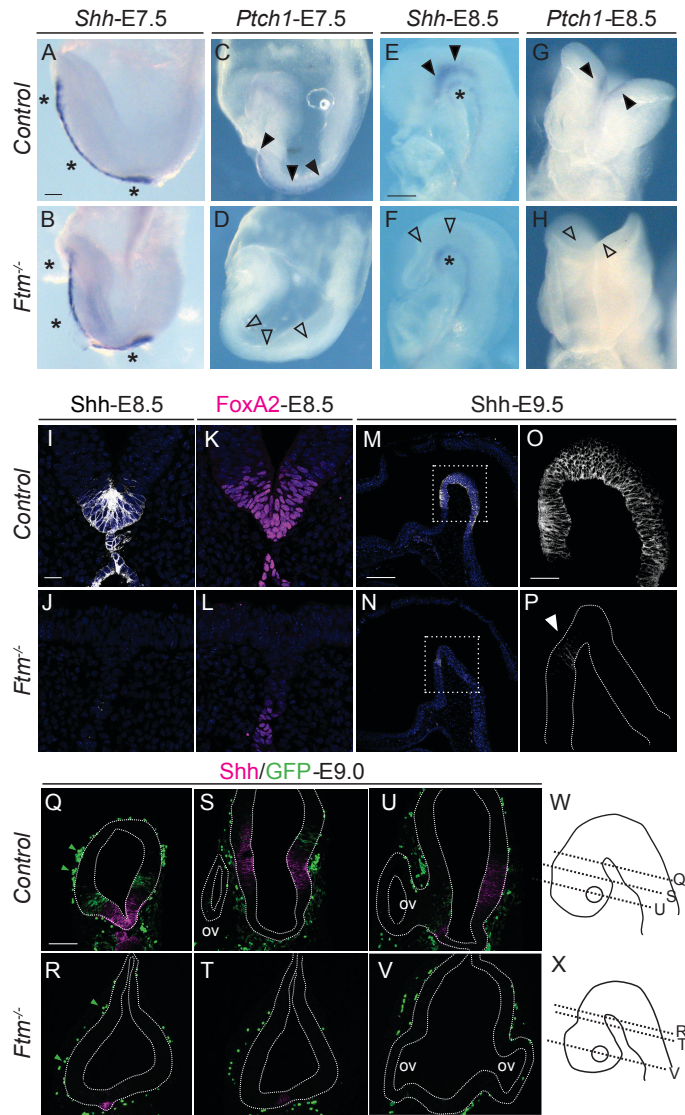
Andreu-Cervera et al., Figure 3



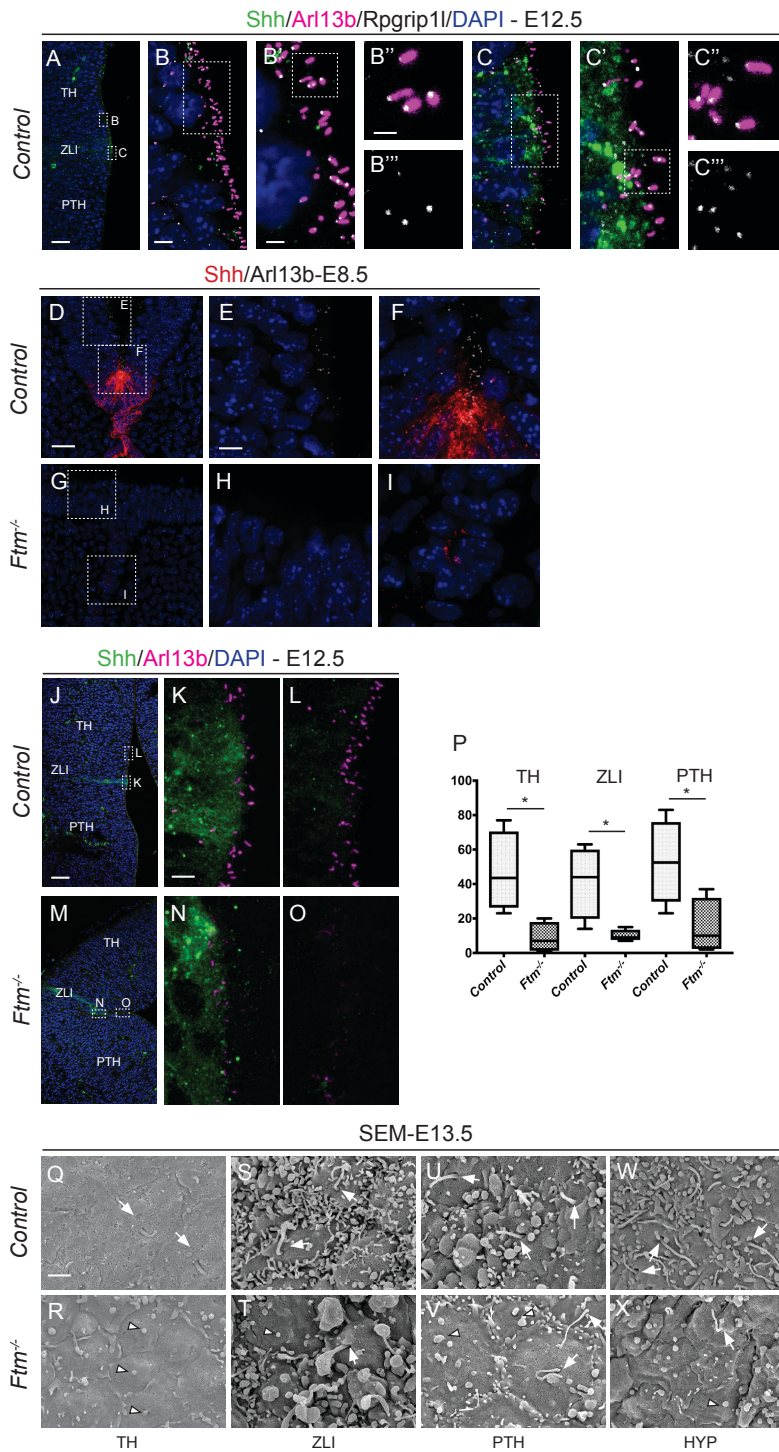
Andreu-Cervera et al., Figure 4



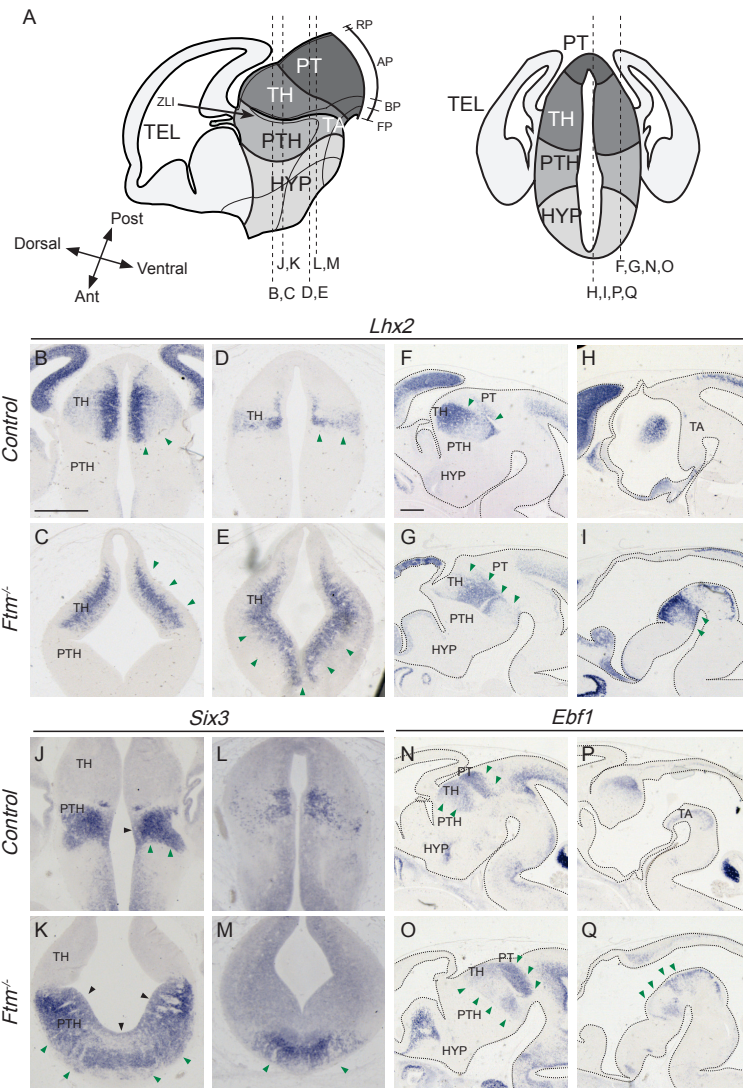
Andreu-Cervera et al., Figure 5



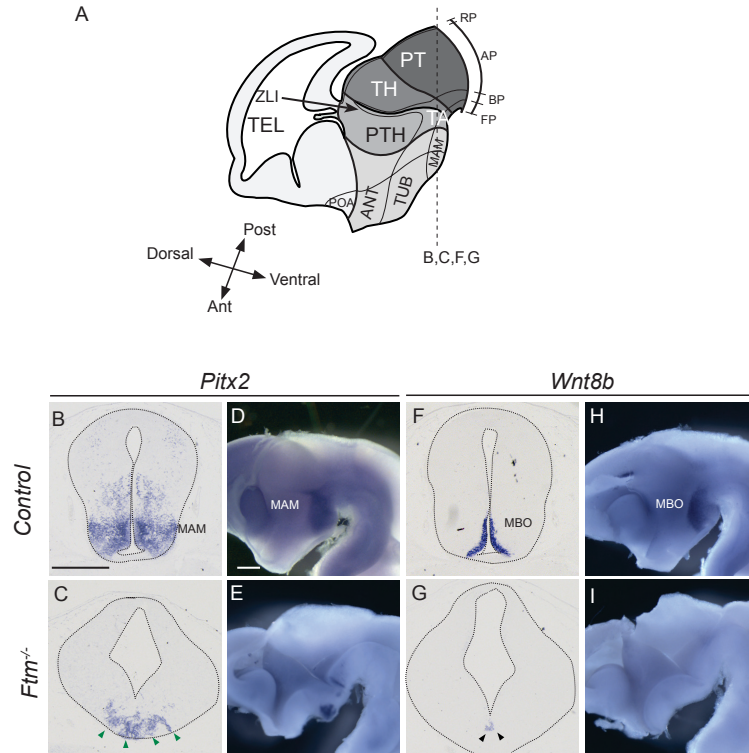
Andreu-Cervera et al., Figure 6



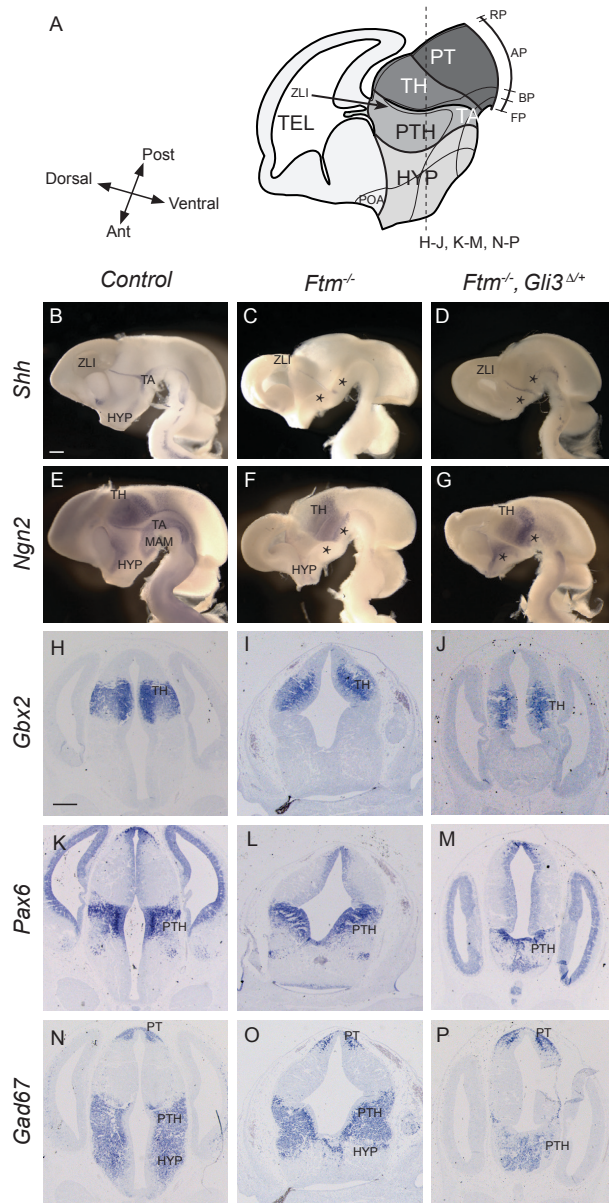
Andreu-Cervera et al., Figure 8



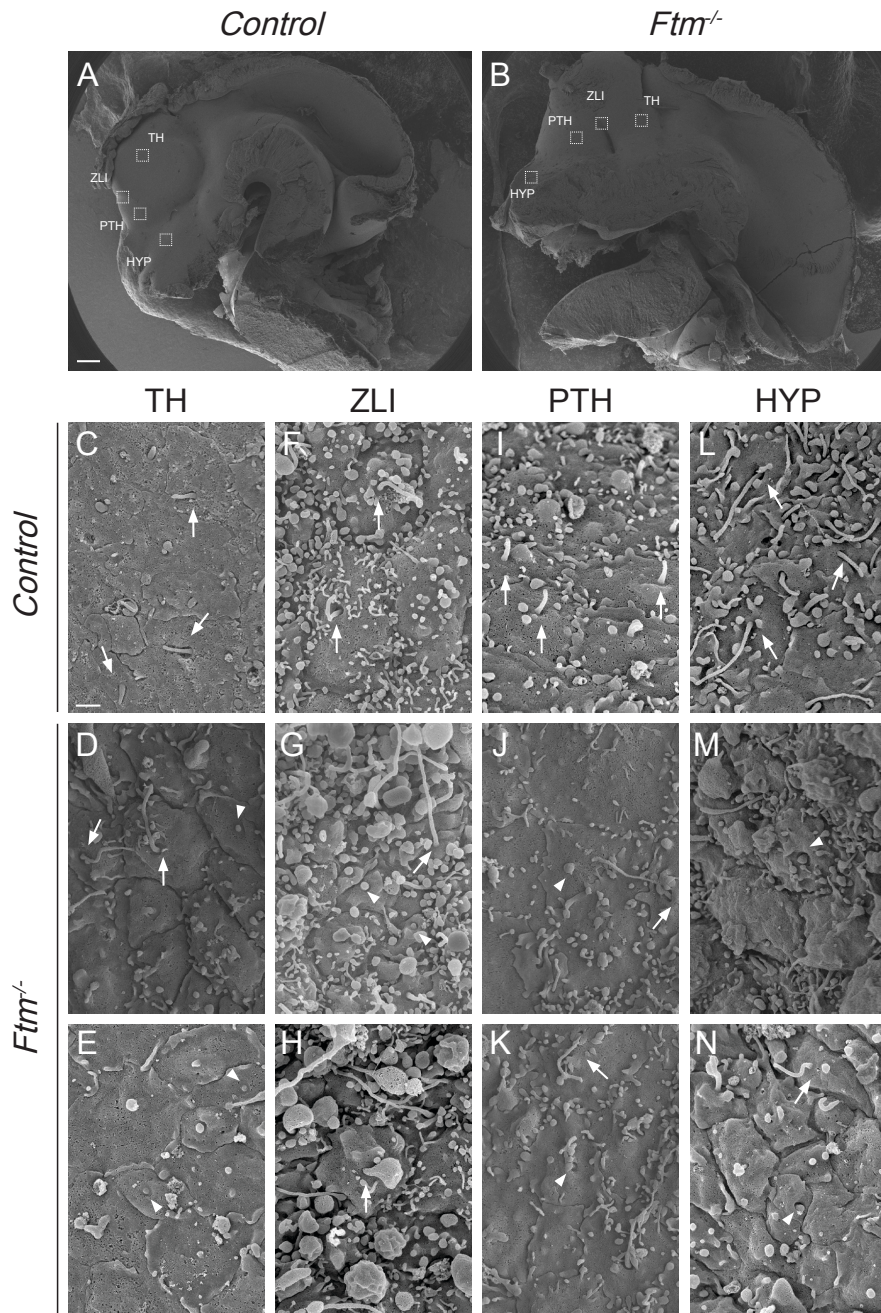
Andreu-Cervera et al. Supplementary Figure 1



Andreu-Cervera et al., Supplementary Figure 2



Andreu-Cervera et al., Supplementary Figure 4



Andreu-Cervera et al., Supplementary Figure 5



DISCUSSION

DISCUSSION

Primary cilia are present in neural progenitors in the mouse neural tube. Several studies have identified their functions in neural tube development and progenitor fate through the transduction of different signalling pathways. In the last 15 years, researchers demonstrated that primary cilia are essential for the transduction of the Hh signalling pathway, implicated in the specification and formation of ventral neural tube and other structures (Marti et al., 1995; Roelink et al., 1995). These studies have been mainly performed in the spinal cord and the telencephalon, and very little is known about the role of primary cilia diencephalon and hypothalamus.

My thesis project was to study the role of the ciliopathy gene *Ftm/Rpgrip1l* and of primary cilia in forebrain patterning and morphogenesis, with particular attention to the diencephalon, hypothalamus and eyes. *Ftm* encodes a ciliary protein, located in the transition zone, that is involved in primary cilium formation as well as other functions such as proteasomal activity at the cilium base and autophagy (Gerhardt et al., 2015; Struchtrup et al., 2018). The *Ftm* protein and primary cilia have been implicated in progenitor specification in the ventral spinal cord and in the formation of olfactory bulbs and corpus callosum in the forebrain (Vierkotten et al., 2007; Besse et al., 2011; Laclef et al., 2015). Mutations in the human *RPGRIP1L* gene lead to two autosomal recessive ciliopathies, Meckel and Joubert syndromes, characterized by brain malformations. Thus, the *Ftm* mouse model is a good tool to study the physiopathology of these human conditions.

Ftm^{-/-} foetuses at the end of gestation present several defects in the diencephalon, hypothalamus and eyes. The ventral hypothalamus is drastically reduced; in the diencephalon, the tegmental areas are reduced in size. The diencephalon also presents a severe disorganization of the nuclei and of the internal capsule (containing cortico-thalamic and thalamo-cortical tracts that connect the cortex and the thalamus); the eyes are almost totally absent. We studied the molecular defects causing these perturbations. We paid particular attention to the Hh pathway. Using genetic tools, we discovered region-specific perturbations of Gli target genes and Gli activity. All these data helped us

to understand the role of primary cilia and of *Ftm* in forebrain patterning and morphogenesis and its relationship with Hh signalling.

Loss of primary cilia in neural progenitors of *Ftm* mutants leads to patterning defects in the diencephalon and hypothalamus

Using genetic markers of the forebrain during development, we observed a severe reduction in the ventral structures of the forebrain. The ventral tegmental areas in the diencephalon and the mammillary and tuberal hypothalamus were reduced drastically. The alar diencephalic domains (the pretectum, thalamus and prethalamus) were ventrally expanded. Furthermore, these different domains and the alar hypothalamus were fused ventrally showing a one continuous hemisphere. These defects are consistent with the observation of the ventral spinal cord of *Ftm* mutant embryos. Using molecular markers, such as MNR2, Nkx2.2 and FoxA2 that label the pMN, V3 progenitors and FP respectively, Vierkotten et al. (2007) have shown that these progenitors were absent in *Ftm*^{-/-} embryos. The alar markers Pax6 and Pax2 were expanded ventrally, suggesting a strong reduction of the ventral region of the spinal cord in *Ftm* knockout embryos. In contrast, studies in the lab have shown that, in the telencephalon, two dorsal domains, the olfactory bulb and the corpus callosum, are absent, due to an expansion of the subpallium (ventral telencephalon) at the expense of the pallium (dorsal telencephalon) (Besse et al., 2011; Laclef et al., 2015).

Are the defects observed in *Ftm*^{-/-} embryos caused by a dysfunction of primary cilia? Defects in the forebrain have been reported in some ciliary mutants. For instance, the *Cobblestone* hypomorphic *Ift88* mutant presents malformations of the hippocampus, choroid plexus and cortical hem, and perturbed pallial-subpallial and telencephalon-diencephalon boundaries (Willaredt et al., 2008). *Ift139* (*alien*) knockout mutant embryos present a ventralization of the forebrain and a disorganized cortex (Stottmann et al., 2009). Despite these studies showing defects in the forebrain, the diencephalon and hypothalamus have not been analysed in detail. Therefore, it is important to study these regions of the forebrain. My PhD lab has previously shown that primary cilia (more precisely the axoneme) are not formed in the progenitor domains of the pallium and subpallium in E12.5 *Ftm*^{-/-} embryos suggesting an important function of Rpgrip11 in

cilia formation (Besse et al., 2011). In this study, we analysed the presence of primary cilia in *Ftm* mutant embryos at different stages in the hypothalamus and diencephalon. We observed that, at E8.5 the cilia were almost totally lost in the ventral forebrain (corresponding to the ventral hypothalamus and diencephalon). At E12.5 in the alar diencephalic and hypothalamic structures, primary cilia were severely reduced in number and the remaining cilia were malformed. These results suggest that the hypothalamic and diencephalic defects observed in *Ftm* mutant embryos are due to the loss of cilia in progenitor domains. To support this hypothesis, other studies have shown ventral defects in the spinal cord in ciliary mutants in which the primary cilia are absent or malformed in ventricular progenitor domains. As examples, mutants of genes encoding IFT proteins, such as *Ift172*, *Ift88* or *Ift57* (Hippi; Huangfu et al., 2003; Liu and Wang, 2005; Houde et al., 2006) and mutants of the basal body proteins, such as, *Stil/SIL*, *Tectonic*, *Tectonic2* or *Tectonic3* (Izraeli et al., 2001; Reiter and Skarnes, 2006; Sang et al., 2011; Wang et al., 2018), show a loss of the ventral midline and a strong reduction of the ventral progenitor cells, pMN and pV3.

Region-specific defects in Hh/Gli signalling in the forebrain of *Ftm* mutants

In addition to the ventral defects in hypothalamus, we found that in *Ftm* mutant embryos the Th-R was missing. The absence of the ventral structures and of the Th-R indicate defects in Hh/Gli signalling pathway.

During development, *Shh* is expressed in the prechordal plate and notochord from E7.5 onwards. Shh secretion from the axial mesoderm is required for the induction of *Shh* expression in the floor and basal plates of the diencephalon and hypothalamus, starting at E8.5. This latter source of Shh in the ventral midline of the forebrain is essential for its correct formation (Szabo et al., 2009a, 2009b; Jeong et al., 2011). In the ventral diencephalon and hypothalamus, Shh acts as a morphogen to control the formation of the ventral structures (the diencephalic tegmental areas and the hypothalamic tuberal and mammillary areas). Moreover, in the hypothalamus, the tuberal and mammillary areas are derived from Shh-expressing cells. Genetic lineage tracing experiments using the *Shh^{CreER}* and *Rosa26^{LoxP}* mouse lines have identified three different

time-windows important for the production of neural population in the hypothalamus. Before E9.5, Shh-positive cells derived from the mammillary and tuberal hypothalamus (cells) give rise to neurons, astrocytes and midline tanicytes. After E9.5, neurons and astrocytes are generated from the tuberal hypothalamus. Finally, after E12.5, all the Shh-positive cells give rise to hypothalamic astrocytes (Alvarez-Bolado et al., 2012). In *Ftm*, mutants we found that *Shh* expression was not induced in the ventral diencephalon and hypothalamus, causing an extreme reduction of the tegmental, tuberal and mammillary areas.

Another source of Shh in the diencephalon is in the zona limitans intrathalamica (ZLI), also called the mid-diencephalic organizer (MDO). Shh expression in the ZLI is required for the correct specification of the antero-posterior structures of the diencephalon. This specification depends on the level of Hh/Gli activity on both sides of the ZLI. Diencephalic explant culture experiments have shown that low levels of Hh/Gli activity are enough to induce the prethalamus and the Th-C, whereas a high level of Hh activity is required for the formation of Th-R (Hashimoto-Torii et al., 2003). Treatment with *SmoM2* mutants, which cause an over-activation of Shh pathway, independent of the ligands and receptor, leads to an increase in the territory of the Th-R and Th-C (Vue et al., 2009). In contrast, conditional knockouts of *Smo* and *Shh* in the thalamus show a loss of Th-R and a reduction of Th-C region (Vue et al., 2009). However, Hh activity from the ZLI is not the only source of Hh required for Th-R induction. A conditional knockout of Shh in the ventro-caudal region of the diencephalon by deletion of the SBE1 intronic *Shh* enhancer results in a strong reduction of the Th-R, indicating that ventral activity is also required for the formation of this territory (Jeong et al., 2011). In *Ftm* mutant embryos, we observed that the Th-R was not formed, which suggests a strong reduction of Gli activity in the ventral diencephalon and ZLI.

Interestingly, in *Ftm* mutant embryos, *Shh* is expressed in the ZLI and seems to induce Gli activity in neighbouring cells, albeit at a lower level than in wild types. Indeed we studied Gli activity using a reporter mouse line *Tg(GBS-GFP)* (a construct in which concatemerized Gli binding sites drive GFP expression). Previous studies using this transgenic line have shown a spatio-temporal requirement for Shh in the ventral spinal cord, where high levels of Gli activity and long exposure to Shh are required for the

formation of ventral progenitors (pV3) and FP in ventral spinal cord, while lower levels and shorter exposure are required for the formation of pMN (Ribes et al., 2009; Balaskas et al., 2012). This is consistent with our observation of *Ftm*^{-/-}*tg(GBS-GFP)* in which there is a strong reduction of Gli activity in the ventral forebrain, leading to a strong reduction of the diencephalic tegmental areas and of the basal hypothalamus. In wild type embryos we observed a strong Gli activity caudal to the ZLI, consistent with the requirement of high Gli activity for Th-R formation. In contrast, in *Ftm*^{-/-}*tg(GBS-GFP)* this activity was strongly reduced, logically leading to the absence of Th-R in *Ftm* mutant embryos. However, our quantification of Gli activity suggest that ground levels of Gli activity are present throughout the diencephalon, probably allowing the formation of the prethalamus and Th-C, two regions that required lower levels of Hh/Gli activity.

Zona limitans intrathalamica formation does not require primary cilia

The ZLI emerges from the ventral midline at the thalamic/prethalamic boundary, coinciding with the prechordal/notochordal limit, at the 25 somite stage in mouse embryos (Vieira et al., 2005) and extends towards the dorsal neural tube. The induction of the ZLI requires *Shh* expression in the ventral diencephalon. In *Shh* conditional knockout embryos for the ventral forebrain, the ZLI is not formed (Szabo et al., 2009). However, inactivation of the *Shh* pathway using a conditional knockout of *Smo* in the MDO showed that *Shh* expression was still present in the ZLI. These results suggest that the maintenance, but not the initiation, of *Shh* expression in the ZLI is independent of *Shh* signalling (Vue et al., 2009). Surprisingly, in *Ftm* mutants the ZLI forms and is more extended along the DV axis and larger along the AP axis than in wild type embryos. The greater extension of the ZLI in *Ftm*^{-/-} embryos is likely due to the reduction of the Gli3R levels, since it is rescued by reintroducing Gli3R in *Ftm* mutants (*Ftm*^{-/-}*Gli3^{A/+}*). To support this hypothesis, it has been shown that Wnt signalling in the alar diencephalon stops the dorsal progression of *Shh* expression in the ZLI by the inhibition of *Gli3* expression (Martinez-Ferre et al., 2013).

Primary cilia are present in neural progenitor cells projecting in the ventricle of the neural tube. As mentioned above, in *Ftm* mutants we observed a strong reduction of the number of cilia early on, at E9.5, in the ventral forebrain. Later on, when the ZLI is

formed, we also observed a strong reduction in the number of cilia in the hypothalamus, prethalamus, thalamus and in the ZLI. Since in *Ftm*^{-/-} the ZLI is formed, these observations suggest that the ZLI formation is independent of primary cilia. Nevertheless, the role of primary cilia in ZLI formation has not been studied in other ciliary mutants. In the *cobblestone* mutant, a hypomorphic mutant in IFT88, the ZLI is also formed. However, mutants have cilia, so they are not the right model to study the role of cilia in ZLI formation (Willaredt et al., 2008). How is possible that the ZLI is formed in *Ftm* knockout embryos having a lack of Shh expression in the ventral diencephalon? We observed at E9.5 a small region of Shh expression in *Ftm* mutants at the level of ZLI. We proposed that this region is sufficient for the induction of the ZLI in *Ftm*^{-/-}. Interestingly, [Gli2, Gli3] double mutants have a ZLI while lacking ventral SHh signalling (Bai et al., 2004). Moreover, in the mouse Gli1 acts as a target of Hh signalling and cannot activate the pathway on its own in the neural tube (Bai et al., 2002). This, together with our results, suggests that high Gli activity in the ventral diencephalon is not required for ZLI formation. It is thus possible than Shh does not signal through Gli to induce its own expression in the ZLI. Such non-canonical Shh pathway has been shown to be active in neuronal migration for instance (Hashimoto-Torii et al., 2003).

Role of primary cilia in eye development

Early on during development, the secretion of Shh from the prechordal plate is essential for the separation of the eye fields. In *Shh* mutant embryos, the separation of the eye fields does not occur, causing the fusion of the two optic vesicles (cyclopia; Chiang et al., 1996). Later, a balance of Hh/Gli activity regulates the proximo-distal patterning of the optic vesicles. *Gli1* and *Gli2* (GliA) are essential for the expansion of the proximal optic vesicle which gives rise to the optic stalk. *Gli2* mutants showed normal optic stalk formation but reduced eye separation. However, double mutants for *Gli1* and *Gli2* showed a strong reduction of the optic stalk (Furimsky and Wallace, 2006) indicating an essential role of GliA in optic stalk specification. In contrast, *Gli3* (GliR) is important for the optic cup and lens vesicle formation that will give rise to the neural retina, retinal pigment epithelium and the lens. *Gli3*^{Xt/Xt} mutant embryos present an agenesis of the eyes in most of the cases (Furimsky and Wallace, 2006). Our results show that primary cilia are required for eye formation. Although the optic vesicles were

formed, *Ftm* mutant embryos showed an agenesis of the neural retina and the lens, whereas the optic stalk was still present. These results indicate that the separation of the eye fields occurred, suggesting that there is a ground level of Hh/Gli activity allowing this split. Conversely, there is a strong reduction of Gli3R, known to be required for neural retina and lens formation. In double *Ftm*^{-/-}*Gli3*^{Δ/Δ} or *Ftm*^{-/-}*Gli3*^{Δ/+} mutants, the retina and the lens were rescued, indicating an essential role of the repressor form of *Gli3* for their genesis.

All these results obtained in *Ftm* mutant embryos indicate the distinct requirements of GliA and GliR for eye formation. *Ftm*^{-/-} embryos do not present cyclopia, even when reintroducing two copies of Gli3R, suggesting that there is a basal Gli activity in the early hypothalamic primordium sufficient to separate the eye fields. However, we have not been able to detect this basal activity so far in the *Ftm* mutant.

A balance of GliA and GliR is essential for forebrain and eye specification

The formation of specific regions of the forebrain and the eyes required a specific balance of GliA and GliR. In *Ftm* mutants, the tegmental areas of the diencephalon, the tuberal and mammillary hypothalamic areas and the Th-R were not formed. This is consistent with high levels of GliA being required for the formation of these structures (Hashimoto-Torii et al., 2003; Vue et al., 2009). In the *Tg(GBS-GFP)* reporter line in the *Ftm*^{-/-} background, a strong reduction of Gli activity in the ventral regions and in the Th-R is observed, leading to the absence of formation of these structures (Fig. 34.I-II). We confirmed this result using ventral markers of each region of the diencephalon and hypothalamus (*Shh*, *FoxA2*, *Pitx2*, *Wnt8b*, and *Dbx1*) and markers for Th-R, such as *Mash1/Ascl1* or *Gad67*. On the other hand, *Ftm*^{-/-} embryos show an agenesis of the neural retina and of the lens, likely due to the reduction in GliR levels, *Gli3* being required for their formation (Furimsky and Wallace, 2006). To support this hypothesis, we reintroduced the repressor form of Gli3 in *Ftm* mutants. Surprisingly, the neural retina was totally rescued in double [*Ftm*^{-/-} *Gli3* Δ699] mutant and the specific genes *Vax2*, *Pax6* and *Chx10*, were correctly expressed, demonstrating the high requirement of GliR for retina formation (Fig. 34.III).

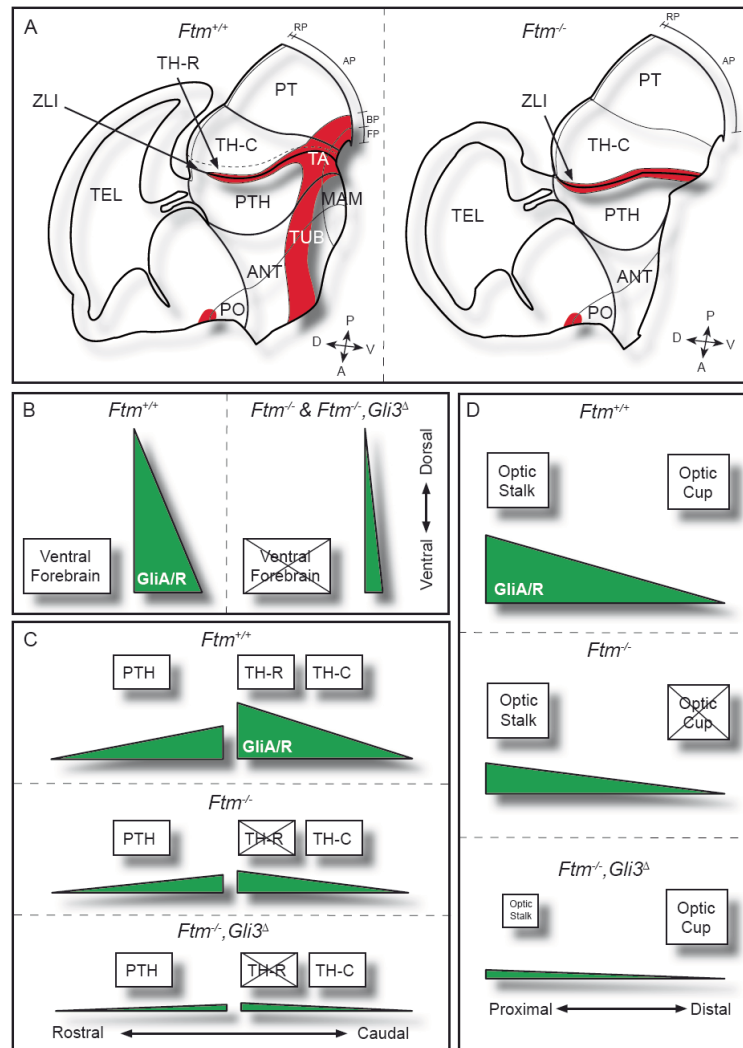


Figure 34. Schematics of forebrain patterning defects in *Ftm* embryos and their link to perturbations of Gli activity. **A.** Schematic drawings of the forebrain of E13.5 control (left) and *Ftm*^{-/-} (right) embryos. Shh expression domains are in red. **B-D.** Interpretive schematics of the GliA/GliR ratios (green) during ventral forebrain formation (B), alar diencephalon patterning (C) and optic vesicle patterning into optic stalk and optic cup (D) in control, *Ftm*^{-/-} and [*Ftm*^{-/-}, *Gli3*^Δ] embryos. **B.** A high GliA/GliR ratio is required for the formation of the ventral forebrain. In *Ftm*^{-/-} as well as in compound [*Ftm*^{-/-}, *Gli3*^Δ] embryos, the reduction of this ratio causes a strong reduction of the ventral forebrain. **C.** In the alar diencephalon, a high GliA/GliR ratio is required for TH-R formation, while a lower ratio is sufficient for PTH and TH-C formation. In *Ftm*^{-/-} embryos the TH-R is lost but the ratio is sufficient for PTH and TH-C formation. **D.** Optic stalk formation requires a high GliA/GliR ratio, while the optic cup requires that only GliR is present. Low levels of GliA are sufficient for optic stalk formation in *Ftm*^{-/-} embryos. In contrast, the optic cup is not formed due to the reduction of GliR levels. In compound [*Ftm*^{-/-}, *Gli3*^Δ] embryos, the optic cup is rescued and the optic stalk is reduced (the eyes are closer to one another) due to the reintroduction of Gli3R. A : anterior; ANT : anterior hypothalamus; AP : alar plate; BP : basal plate; D : dorsal; FP : floor plate; MAM : mammillary hypothalamus; P : posterior; PT : preteectum; PTH : prethalamus; PO : preoptic area; RP : roof plate; TA : tegmental areas; TEL : telencephalon; TH-C : caudal thalamus; TH-R : rostral thalamus; TUB : tuberal hypothalamus; V : ventral; ZLI : zona limitans intrathalamica.

In contrast to the high requirements of GliA or GliR, other structures of the forebrain and the eyes need low levels of Gli signalling. In the diencephalon, the prethalamus and the caudal thalamus (Th-C) require low levels of GliA to be formed. In *Ftm*^{-/-} embryos, these structures are formed, indicating that there is sufficient Hh/Gli activity for growth and survival of the diencephalic structures (Fig. 34.II). In the case of the eyes, the optic stalk also requires low levels of GliA to form. In *Ftm* mutants, the optic stalks are present indicating that there is still a basal level of GliA leading to its formation (Fig. 34.III). To support this observations, we found that in *Ftm* mutants the eye fields were well separated sustaining that there is a ground levels of GliA.

A *Ptch1* prepattern in the diencephalon of *Ftm*^{-/-} embryos

At the end of the Hh/Gli transduction cascade, several generic and tissue-specific target genes are expressed. Two generic target genes of the Hh pathway are *Ptch1* (encoding the Shh receptor) and *Gli1* (encoding a transcriptional effector of the pathway). In the ventral forebrain of E7.5 mouse embryos, non-neural *Shh* expression in the prechordal plate and notochord induces the expression of *Ptch1* and *Gli1* in a ventro-dorsal decreasing gradient. Later, at E8.5, *Shh* is expressed in the ventral forebrain and the expression of *Ptch1* and *Gli1* is restricted to the lateral domains (Haddad-Tovolli et al., 2015). In *Ftm* mutant embryos, *Ptch1* was not expressed in the forebrain at E8.5, indicating that the *Shh* pathway is down-regulated. Later, the expression of *Ptch1* and *Gli1* is also activated around another source of *Shh* in the diencephalon, the ZLI. The ZLI is the only AP organizing center expressing *Shh* (Hagemann and Scholpp, 2012; Epstein, 2012; Zhang and Alvarez-Bolado, 2016). In the ZLI, *Ptch1* and *Gli1* are both expressed in a gradient, high in contact to the ZLI and decreasing toward anterior in the prethalamus and toward posterior in the thalamus. Surprisingly, the expression of *Ptch1* and *Gli1* was differently affected in *Ftm* mutants. *Ptch1* expression was drastically reduced in the thalamus and strongly upregulated in the prethalamus. In contrast, *Gli1* was reduced on both sides of the ZLI. Thus, the loss of primary cilia in the *Ftm* mutant uncovers a prepattern of *Ptc1* expression in the diencephalon, indicating that other mechanisms regulate this target gene outside the Hh pathway. However, these genes remain responsive to Gli activity, since the re-introduction of Gli3R (in [*Ftm*^{-/-}; *Gli3*^{Δ/+}] embryos) abolishes *Ptch1* overexpression in the prethalamus. The consequences of *Ptch1* over-

expression in the PTH are not known. *Ptch1* overexpression usually inhibits Hh signalling by preventing Smo from entering the cilium. However, in the *Ftm* mutant, there are no or few cilia in the prethalamus, and Smo activity is strongly downregulated anyway. *Ptch1* also acts as a dependence receptor, triggering apoptosis when it is expressed in the absence of ligand, in particular in the nervous system (Thibert et al., 2003). Therefore it would be very interesting to test whether apoptosis is increased in the PTH of *Ftm* mutants.

Are other pathways affected apart from Hh signalling in *Ftm* mutant?

Other signalling pathways such as the Fgf and Wnt pathways are known to be essential for proliferation and cell fate in the diencephalon (Zeltser et al., 2001; Kiecker et al., 2004; Scholpp et al., 2006). Are these other signalling pathways affected in *Ftm*^{-/-} embryos? The *Wnt* pathway is essential for the regulation of the progression of the ZLI (through the inhibition of Gli3) and controls neuroepithelial cell proliferation (Bluske et al., 2012; Martinez-Ferre et al., 2013). Several *Wnt* proteins are expressed in dorsal diencephalon and ZLI, such as *Wnt1* and *Wnt3a*. In *Ftm* mutant these genes were still expressed in the diencephalon and one of the Wnt target genes, *Axin2*, was normally induced (Fig. 35.A-F). These results suggest that *Wnt* signalling is not affected in *Ftm* mutants.

The Fgf pathway is implicated in neurogenesis and in cell specification in the thalamus (Kataoka and Shimogori, 2008; Martinez-Ferre et al., 2016). In *in utero* electroporation assays in the mouse thalamus, overexpression of Fgf8 or repression of the pathway by blocking its receptors, showed an increase or a reduction of the Th-R, respectively (Kataoka and Shimogori, 2008). In addition, in *Fgf15* mutant embryos, neurogenesis is reduced in the Th-C, and the Th-R is absent (Martinez-Ferre et al., 2016). *Fgf15* is important for proper neurogenesis in the thalamus (Martinez-Ferre et al., 2016). We thus wondered whether the Fgf pathway was affected in *Ftm* knock-out mouse embryos.

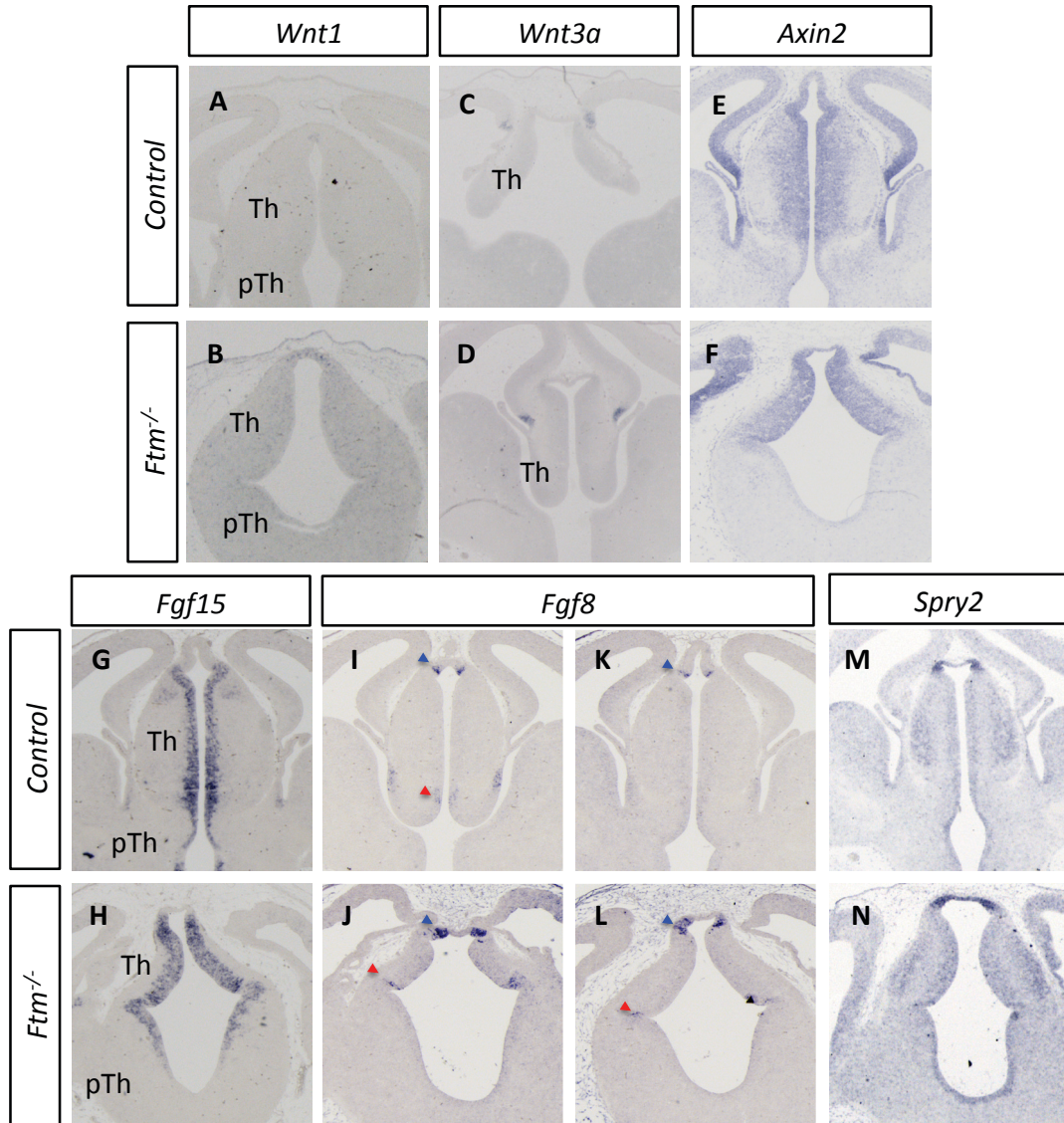


Figure 35. Analysis of *Wnt* and *Fgf* pathways. **A-F.** *In situ* hybridisation of *Wnt1*, *Wnt3a* and *Axin2* in controls and *Ftm*^{-/-}. **G-N.** *In situ* hybridisation of *Fgf15*, *Fgf8*, and *Spry2*. The arrowheads indicate the dorsal diencephalic expression (in blue) and ZLI expression (in red). Th: thalamus; pTh: prethalamus

Fgf8 is expressed in the dorsal ZLI and in the thalamic roof plate. In *Ftm*^{-/-} embryos, *Fgf8* expression was slightly expanded ventrally (Fig. 35.I-L). This may be due to the reduction in *Gli3R*. Indeed, previous studies have shown that *Gli3* regulates the expression of *Fgf8* in the diencephalon: in *Gli3* knockout embryos, the expression of *Fgf8* is upregulated (Aoto et al., 2002). *Fgf15*, is expressed in neural progenitors of the diencephalon. In *Ftm*^{-/-} embryos, *Fgf15* expression was normal (Fig.35.G-H). One of the target genes of the *Fgf* pathway is *Sprouty2* (*Spry2*), expressed in neural progenitors and

newly born neurons in the thalamus. In *Ftm* mutants, *Spry2* was correctly expressed (Fig. 35.M-N). Thus, we have no clear indication of defects in the Fgf pathway in *Ftm* mutants. This could be further tested, since defects in the Fgf pathway could contribute to the defects in neurogenesis and Th-R formation observed in the *Ftm* mutant.

Links between ciliopathies, holoprosencephaly and other human forebrain malformations linked to defects in Hh signalling

Ciliopathies and diencephalic:hypothalamic hamartomas

Hamartomas are malformations that contain tissues and cells normally present in this location. They resemble benign neoplasms even if they display radically different behavior. Hypothalamic or diencephalic hamartomas have been described in human ciliopathies: some cases of Meckel (Roume et al, 1998) or Finnish hydrolethalus syndrome (Paetau et al., 2008) and rarely in both Joubert syndromes (Poretti et al., 2017), OFD1 (Del Giudice et al., 2014) and Bardet-Biedl syndrome (Diaz et al., 1991). Furthermore they are frequent in oral-facial-digital syndrome type VI (Poretti et al., 2011).

What is the pathological substratum of hamartomas in human ciliopathies? Only neuroradiological features are available for hypothalamic hamartoma in case of Bardet-Biedl syndrome (Diaz et al. 1991), Joubert syndrome (Poretti et al. 2017), OFD 1 (Del Giudice et al. 2014), OFD VI (Poretti et al. 2011). Unfortunately, no histological description of the hypothalamic hamartoma is available in case of Meckel syndrome (Roume et al. 1998). In the Finnish hydrolethalus syndrome, neurons grouped in nodules have been described by Paetau et al. (2008). More descriptions of these lesions in human ciliopathies are needed for classification of these lesions into different subgroups.

Ciliopathies, obesity and hypothalamic defects

Obesity is a common trait observed in human ciliopathies. It is constant in Bardet-Biedl syndrome (OMIM # 209900), Alström syndrome (OMIM # 203800) and MORM syndrome (OMIM # 610156). It has also been reported in some cases of Joubert

syndromes (JBTS8 in Thomas et al., 2015; Martin Catala unpublished observation). Obesity has been particularly studied in human Bardet-Biedl syndrome or in its animal models. Patients or mice are resistant to leptin (Eichers et al., 2006, Rhomouni et al., 2008, Feuillan et al., 2011), such a resistance could be explained by the requirement of certain proteins involved in Bardet-Biedl syndrome for the correct trafficking of leptin receptor and therefore for its signaling pathway (Seo et al., 2009).

However, a longitudinal analysis over time of a conditional murine mutant for *Ift88* shows that the mice become obese even before being resistant to leptin (Berbari et al., 2013). Thus, this resistance may be a secondary consequence and not the primary cause of obesity in ciliopathies. An alternative explanation accounting for this obesity could be the population of uni- and biciliated ependymal cells present on the floor of the third ventricle (Mirzadeh et al., 2017). These cells are also known as tanycytes and are derived from a Sonic Hedgehog-expressing domain (Mirzadeh et al., 2017). These cells play a role in regulating hypothalamic functions, including in the regulation of food intake (Prévot et al., 2018). Thus, a dysfunction of these cells could explain the development of obesity. We have shown that the positive SHH region of the hypothalamus depends on cilia. We believe that the population of the tanycytes of the floor of the third ventricle could be one of the factors explaining the obesity observed in some human ciliopathies.

Ciliopathies and Holoprosencephaly

Holoprosencephaly (OMIM 236100) is defined as an incomplete separation of forebrain hemispheres and of left and right facial components, due to defects in the formation of midline structures. It is the most frequent developmental forebrain defect in humans: 1/ 10000 live births, and 1 in 250 cases of spontaneous abortions. HPE is a highly heterogeneous condition, which involves both genetic and environmental factors. The mode of inheritance is in majority autosomal dominant, with incomplete penetrance and high intra- and inter-familial phenotypic variability (Fernandes & Hébert 2008).

There are two major classes of holoprosencephaly: classic holoprosencephaly in which the ventral forebrain is most affected, and midline interhemispheric

holoprosencephaly (also called syntelencephaly) in which the dorsal midline of the forebrain is most affected. Classic holoprosencephaly encompasses three severity classes: alobar (no separation of the ventral forebrain, often associated with cyclopia and proboscis), semilobar (anterior hemispheres fail to separate) and lobar (milder separation defects). Lobar holoprosencephaly is often associated with hypoplastic or missing olfactory bulbs and corpus callosum and dysmorphic third ventricle. holoprosencephaly is sometimes associated with multiple malformation syndromes such as CHARGE.

The neuropathological study of cases of holoprosencephaly in humans has been largely carried out but it mainly concerned fetuses or infants. Cases analyzed during embryogenesis are rare (Müller and O'Rahilly 1989, Yamada et al., 2004). In the Kyoto collection, 221 cases of holoprosencephaly were observed among 44,000 specimens (Yamada et al., 2004). Only 43 of them could be analyzed histologically because the preservation of others was not compatible with such an examination. Their age ranges from 32 days embryonic (E32 or Carnegie Stage CS 13) to E48 (CS21). In the Carnegie Institute collection, 4 embryos were analyzed (Müller and O'Rahilly, 1989), three at E38 (CS16) and one at E45 (CS19-20). The salient feature observed in these cases is a frank hypoplasia of prosencephalon. The inter-hemispheric fissure is either absent (in case of cyclopia or synophthalmia) or considerably reduced (in case of hypotelorism). The diencephalon is considered as normal but no markers have been used to precisely delineate subdivisions of this region. The hypothalamus is poorly described. In conclusion, the description of these cases is limited and is based on simple stains without labelling to highlight the different early territories of the neural tube at these ages. Nevertheless, these results are important and must be taken into account for the interpretation of later stages.

The neuropathology of late-observed cases has often focused on cortical damage to the detriment of a more precise description of diencephalic and hypothalamic disorders (see Marcorelles and Laquerrière 2010 for an example). Most often, it is specified that the two thalamus merge on the midline obliterating the third ventricle. The late-observed thalamic defect is to be correlated with the absence of gross anomaly observed in cases seen early. It is interesting to note that the diencephalic ventricle is

present in these early cases and that the fusion of the thalamus is therefore a secondary phenomenon. The presence of ependymal remains within the fused thalamic mass is an argument to favour this hypothesis of secondary deformation.

However, an interesting observation is worth mentioning: Case HCP-16-54 reported by Paul Yakovlev (1959). This is the case of a newborn girl who died at 15 hours of age and who presents an alobar form of holoprosencephaly. The hypothalamus is described as grossly malformed whereas the thalamus displays some normal nuclei and others which are absent. This discrepancy between a highly involved hypothalamus and a more preserved thalamus is reminiscent of our results on *Ftm*^{-/-}. The significant hypothalamic impairment described by Yakovlev is related to the high incidence of diabetes insipidus (70%) observed in cases of holoprosencephaly, especially in severe forms (Hahn et al., 2005). In addition, Yakovlev (page 50) describes an antero-posterior gradient of telencephalic impairment, the anterior pole is always more affected than the posterior pole. This is reminiscent of the gradient of patterning defect observed in the mutant mouse.

In human ciliopathies, thalamic nuclei and subthalamic region have been poorly analyzed. In Meckel syndromes, thalami are commonly described as fused giving rise to hypoplastic third ventricle (Ahdab-Barmada and Claassen 1990, Roume et al. 1998). This thalamic fusion is also the case for the Finnish hydroletharus syndrome due to mutation of *HYLS1* (Paetau et al. 2008). The thalamus is considered as sparsely cellular in term of neurons whereas the germinal matrix (namely the progenitor domain) is prominent. This pathological feature is reminiscent of our observation of delayed of neurogenesis with expansion of progenitors in *Ftm* mutant. In Joubert syndrome, only a few observations have described the thalamic region. The thalamus is reported as normal in some cases (Friede and Boltshauser 1978, cases 1, 2 and 5 from Juric-Sekhar et al. 2012). Other cases of Joubert syndrome display thalamic abnormalities: fragmentation of the posterior thalamus with absence of some subthalamic nuclei (Yachnis and Rorke 1999), disorganization of the thalamus (case 3 due to mutation of *OFD1* in Juric-Sekhar et al. 2012), reduced cellularity (case 4 due to mutation of *TCTN2* in Juric-Sekhar et al. 2012). These results suggest that the thalamus is involved in human ciliopathies but has been ill described in the literature.

Holoprosencephaly has been reported in two series of patients with Meckel syndrome (Paetau et al., 1985, Ahdab-Barmada and Claassen 1990). Paetau et al. report ten neuropathologically studies fetuses with the Finnish form of Meckel syndrome (MKS1). Their case 3 is described as holoprosencephalic, however, the authors add that the lateral ventricles are absent, such a feature contradicts the diagnosis of alobar holoprosencephaly since in this pathology a single ventricle is one of the elements of the syndrome. Ahdab-Barmada and Claassen (1985) report a series of 7 cases analyzed in Pittsburgh (PA). Two cases (1 and 4) are described as holoprosencephalic. Nevertheless, Figure 1A illustrating case 1 does not show holoprosencephaly but a ventricle with septal agenesis. Joubert syndrome (JBTS) is a highly heterogeneous condition in which at least 33 different genes have been associated with. No case of holoprosencephaly has been described in association with such a genetic condition (Poretti et al., 2011; Poretti et al., 2017). Oral-facial-digital syndromes (OFD) are heterogeneous. Genes are known only for three OFD syndrome (OFD1, OFD4 and OFD6). These three genes (*OFD1*, *TCTN3* and *CPLANE1*) are also responsible for Joubert syndrome. A case of holoprosencephaly has not been reported in OFD syndromes related to a known mutation.

Thus, holoprosencephaly does not appear to be frequently associated with ciliopathies. The cases described in the literature are not convincing to link such a condition with Meckel syndrome. This may be surprising, given the essential role of cilia in vertebrate Hh signalling. Our study of the forebrain of *Ftm* mutants provides a potential explanation, as we find clear phenotypic differences between the *Ftm* mutants and Hh pathway mutants.

Nevertheless, ciliopathy genes could act as modifier genes for HPE. HPE shows high phenotypic variability in single families, which has led to the proposal that a combination of mutations in HPE genes could account for the variability in severity of the phenotype (the multi-hit hypothesis). In favour of this hypothesis, digenic inheritance has been identified in several HPE families (Mouden et al., 2016 and ref therein). Interestingly, homozygous mutations in the *STIL* gene encoding a pericentriolar and centrosomal protein have been found in patients with HPE and microcephaly (Mouden et al., 2015, Kakar et al., 2015). Mouse *Stil* homozygous mutant

embryos display severe forebrain midline defects and die at E10.5 (Izraeli et al., 1999). Ciliogenesis and centriole duplication, as well as Hh signaling, are defective in the absence of STIL (Mouden et al., 2015). Whole genome sequencing in heterogenous HPE families will allow testing the involvement of ciliopathy gene variants in this disease.

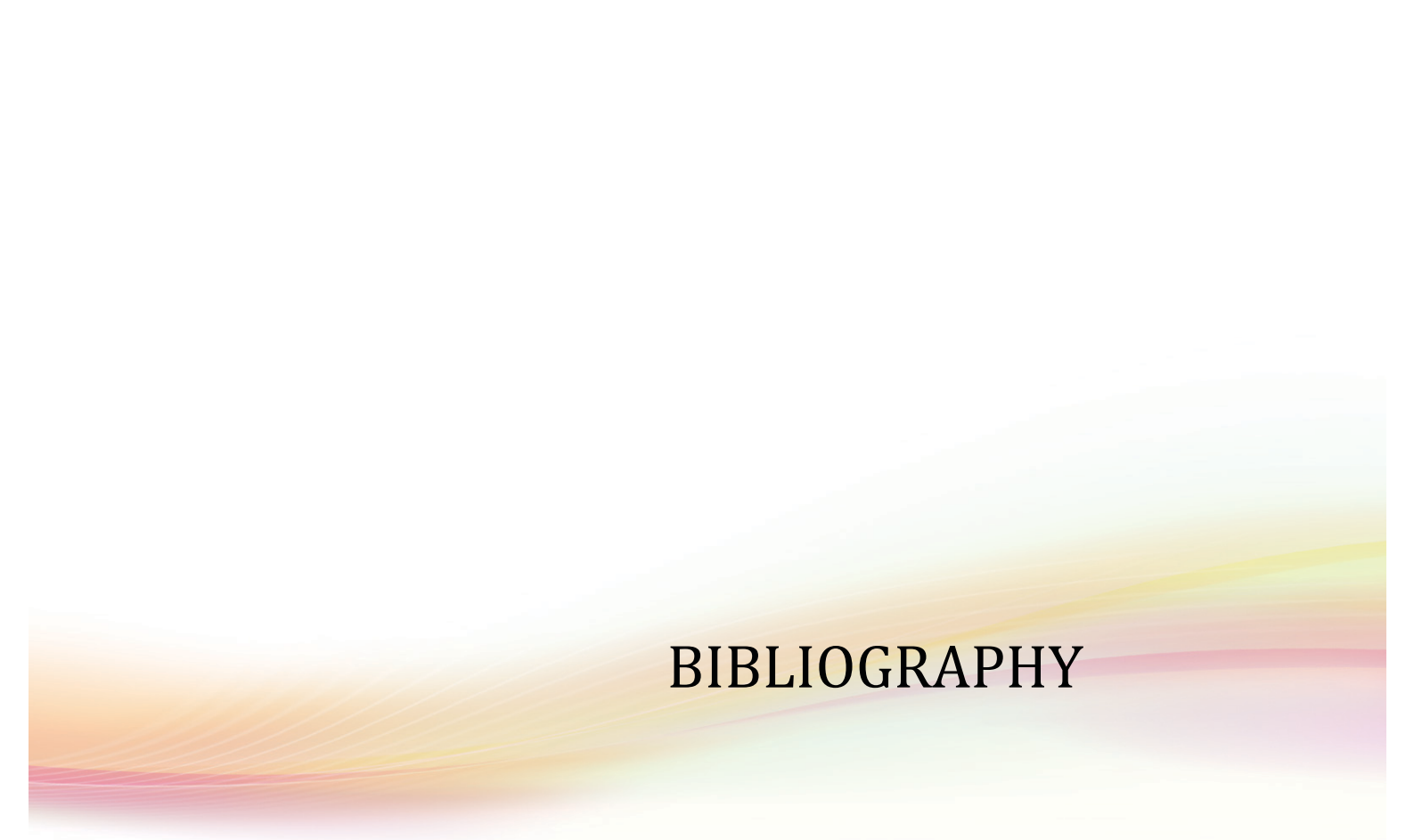
More generally, our study of the ciliopathy gene mutant *Rpgrip11/Ftm* calls for further examination of ciliary and ciliopathy genes in human neurodevelopmental diseases associated with SHH pathway defects.



CONCLUSION

CONCLUSION

Several functional studies of ciliopathy and other ciliary genes have shown the role of primary cilia in the formation of the central nervous system. Most of these studies focused on the spinal cord and on the cortex. Here we focused on two structures of the forebrain that had not been analysed in detail. We discovered an essential role of the *Ftm/Rpgrip11* ciliopathy gene in mouse forebrain and eye morphogenesis. We demonstrated that primary cilia and *Ftm* are required for the formation of specific regions of the forebrain through the high requirements of GliA to form the ventral diencephalon and hypothalamus, and the Th-R; and the high requirements of GliR for the retina formation. We also discovered that ZLI formation is independent of primary cilia and that *Ftm* mutants showed a differential prepatter of Hh target genes, *Ptch1* and *Gli1* expression in different diencephalic prosomeres. Morphological defects of the diencephalon and hypothalamus have rarely been studied in severe ciliopathies. However, OB and CC agenesis/hypoplasia have been often reported, as well as microphthalmia. Our results thus call for further examination of the diencephalon and hypothalamus in severe ciliopathies.



BIBLIOGRAPHY

BIBLIOGRAPHY

- Adly N, Alhashem A, Ammari A, Alkuraya FS. Ciliary genes TBC1D32/C6orf170 and SCLT1 are mutated in patients with OFD type IX. *Hum Mutat.* 2014 Jan;35(1):36-40. doi: 10.1002/humu.22477. Epub 2013 Nov 25.
- Ahdab-Barmada M, Claassen D. A distinctive triad of malformations of the central nervous system in the Meckel-Gruber syndrome. *J Neuropathol Exp Neurol* 1990;49:610-620.
- Alvarez-Bolado G, Paul FA, Blaess S. Sonic hedgehog lineage in the mouse hypothalamus: from progenitor domains to hypothalamic regions. *Neural Dev.* 2012 Jan 20;7:4. doi: 10.1186/1749-8104-7-4.
- Anselme I, Laclef C, Lanaud M, R  ther U, Schneider-Maunoury S. Defects in brain patterning and head morphogenesis in the mouse mutant Fused toes. *Dev Biol.* 2007 Apr 1;304(1):208-20. Epub 2006 Dec 15.
- Aoto K, Nishimura T, Eto K, Motoyama J. Mouse *GLI3* regulates *Fgf8* expression and apoptosis in the developing neural tube, face, and limb bud. *Dev Biol.* 2002 Nov 15;251(2):320-32.
- Aoto K, Shikata Y, Imai H, Matsumaru D, Tokunaga T, Shioda S, Yamada G, Motoyama J. Mouse *Shh* is required for prechordal plate maintenance during brain and craniofacial morphogenesis. *Dev Biol.* 2009 Mar 1;327(1):106-20. doi: 10.1016/j.ydbio.2008.11.022. Epub 2008 Dec 7.
- Arts HH, Doherty D, van Beersum SE, Parisi MA, Letteboer SJ, Gorden NT, Peters TA, M  rker T, Voesenek K, Kartono A, Ozyurek H, Farin FM, Kroes HY, Wolfrum U, Brunner HG, Cremers FP, Glass IA, Knoers NV, Roepman R. Mutations in the gene encoding the basal body protein RPKRIP1L, a nephrocystin-4 interactor, cause Joubert syndrome. *Nat Genet.* 2007 Jul;39(7):882-8. Epub 2007 Jun 10.
- Avidor-Reiss T, Ha A, Basiri ML. Transition Zone Migration: A Mechanism for Cytoplasmic Ciliogenesis and Postaxonemal Centriole Elongation. *Cold Spring Harb Perspect Biol.* 2017 Aug 1;9(8). pii: a028142. doi: 10.1101/cshperspect.a028142.
- Baas D, Meiniel A, Benadiba C, Bonnaf   E, Meiniel O, Reith W, Durand B. A deficiency in *RFX3* causes hydrocephalus associated with abnormal differentiation of ependymal cells. *Eur J Neurosci.* 2006 Aug;24(4):1020-30.
- Bai CB, Auerbach W, Lee JS, Stephen D, Joyner AL. *Gli2*, but not *Gli1*, is required for initial *Shh* signaling and ectopic activation of the *Shh* pathway. *Development.* 2002 Oct;129(20):4753-61.
- Bai CB, Stephen D, Joyner AL. All mouse ventral spinal cord patterning by hedgehog is *Gli* dependent and involves an activator function of *Gli3*. *Dev Cell.* 2004 Jan;6(1):103-15.
- Balaskas N, Ribeiro A, Panovska J, Dessaud E, Sasai N, Page KM, Briscoe J, Ribes V. Gene regulatory logic for reading the Sonic Hedgehog signaling gradient in the vertebrate neural tube. *Cell.* 2012 Jan 20;148(1-2):273-84. doi: 10.1016/j.cell.2011.10.047.
- Barkovich AJ, Quint DJ. Middle interhemispheric fusion: an unusual variant of holoprosencephaly. *Am J Neuroradiol* 1993;14:453-460.
- Barth KA, Wilson SW. Expression of zebrafish *nk2.2* is influenced by sonic hedgehog/vertebrate hedgehog-1 and demarcates a zone of neuronal differentiation in the embryonic forebrain. *Development.* 1995 Jun;121(6):1755-68.

- Benadiba C, Magnani D, Niquille M, Morlé L, Valloton D, Nawabi H, Ait-Lounis A, Otsmane B, Reith W, Theil T, Hornung JP, Lebrand C, Durand B. The ciliogenic transcription factor RFX3 regulates early midline distribution of guidepost neurons required for corpus callosum development. *PLoS Genet.* 2012;8(3):e1002606. doi: 10.1371/journal.pgen.1002606. Epub 2012 Mar 29.
- Berberi NF, Pasek RC, Malarkey EB, Yazdi SM, McNair AD, Lewis WR, Nagy TR, Kesterson RA, Yoder BK. Leptin resistance is a secondary consequence of the obesity in ciliopathy mutant mice. *Proc Natl Acad Sci USA* 2013;110:7796-7801.
- Besse L, Neti M, Anselme I, Gerhardt C, Rüther U, Laclef C, Schneider-Maunoury S. Primary cilia control telencephalic patterning and morphogenesis via Gli3 proteolytic processing. *Development.* 2011 May;138(10):2079-88. doi: 10.1242/dev.059808. Epub 2011 Apr 13.
- Blaess S, Szabó N, Haddad-Tóvölvi R, Zhou X, Álvarez-Bolado G. Sonic hedgehog signaling in the development of the mouse hypothalamus. *Front Neuroanat.* 2015 Jan 6;8:156. doi: 10.3389/fnana.2014.00156. eCollection 2014. Review.
- Bluske KK, Vue TY, Kawakami Y, Taketo MM, Yoshikawa K, Johnson JE, Nakagawa Y. β -Catenin signaling specifies progenitor cell identity in parallel with Shh signaling in the developing mammalian thalamus. *Development.* 2012 Aug;139(15):2692-702. doi: 10.1242/dev.072314. Epub 2012 Jun 28.
- Boehlke C, Bashkurov M, Buescher A, Krick T, John AK, Nitschke R, Walz G, Kuehn EW. Differential role of Rab proteins in ciliary trafficking: Rab23 regulates smoothed levels. *J Cell Sci.* 2010 May 1;123(Pt 9):1460-7. doi: 10.1242/jcs.058883. Epub 2010 Apr 7.
- Boehlke C, Kotsis F, Patel V, Braeg S, Voelker H, Brecht S, Beyer T, Janusch H, Hamann C, Gödel M, Müller K, Herbst M, Hornung M, Doerken M, Köttgen M, Nitschke R, Igarashi P, Walz G, Kuehn EW. Primary cilia regulate mTORC1 activity and cell size through Lkb1. *Nat Cell Biol.* 2010 Nov;12(11):1115-22. doi: 10.1038/ncb2117. Epub 2010 Oct 24.
- Böse J, Grotewold L, Rüther U. Pallister-Hall syndrome phenotype in mice mutant for Gli3. *Hum Mol Genet.* 2002 May 1;11(9):1129-35.
- Brancati F, Travaglini L, Zablocka D, Boltshauser E, Accorsi P, Montagna G, Silhavy JL, Barrano G, Bertini E, Emma F, Rigoli L; International JSRD Study Group, Dallapiccola B, Gleeson JG, Valente EM. RPGRIP1L mutations are mainly associated with the cerebello-renal phenotype of Joubert syndrome-related disorders. *Clin Genet.* 2008 Aug;74(2):164-70. doi: 10.1111/j.1399-0004.2008.01047.x. Epub 2008 Jun 28.
- Breslow DK, Koslover EF, Seydel F, Spakowitz AJ, Nachury MV. An in vitro assay for entry into cilia reveals unique properties of the soluble diffusion barrier. *J Cell Biol.* 2013 Oct 14;203(1):129-47. doi: 10.1083/jcb.201212024. Epub 2013 Oct 7.
- Briscoe J, Pierani A, Jessell TM, Ericson J. A homeodomain protein code specifies progenitor cell identity and neuronal fate in the ventral neural tube. *Cell.* 2000 May 12;101(4):435-45.
- Camerer E, Barker A, Duong DN, Ganesan R, Kataoka H, Cornelissen I, Darragh MR, Hussain A, Zheng YW, Srinivasan Y, Brown C, Xu SM, Regard JB, Lin CY, Craik CS, Kirchhofer D, Coughlin SR. Local protease signaling contributes to neural tube closure in the mouse embryo. *Dev Cell.* 2010 Jan 19;18(1):25-38. doi: 10.1016/j.devcel.2009.11.014.
- Caspary T, Larkins CE, Anderson KV. The graded response to Sonic Hedgehog depends on cilia architecture. *Dev Cell.* 2007 May;12(5):767-78.

- Chamberlain CE, Jeong J, Guo C, Allen BL, McMahon AP. Notochord-derived Shh concentrates in close association with the apically positioned basal body in neural target cells and forms a dynamic gradient during neural patterning. *Development*. 2008 Mar;135(6):1097-106. doi: 10.1242/dev.013086. Epub 2008 Feb 13.
- Chang JT, Lehtinen MK, Sive H. Zebrafish cerebrospinal fluid mediates cell survival through a retinoid signaling pathway. *Dev Neurobiol*. 2016 Jan;76(1):75-92. doi: 10.1002/dneu.22300. Epub 2015 Jun 8.
- Chen J, Laclef C, Moncayo A, Snedecor ER, Yang N, Li L, Takemaru KI, Paus R, Schneider-Maunoury S, Clark RA. The ciliopathy gene *Rpgrip11* is essential for hair follicle development. *J Invest Dermatol*. 2015 Mar;135(3):701-709. doi: 10.1038/jid.2014.483. Epub 2014 Nov 14.
- Chen X, Tukachinsky H, Huang CH, Jao C, Chu YR, Tang HY, Mueller B, Schulman S, Rapoport TA, Salic A. Processing and turnover of the Hedgehog protein in the endoplasmic reticulum. *J Cell Biol*. 2011 Mar 7;192(5):825-38. doi: 10.1083/jcb.201008090. Epub 2011 Feb 28.
- Cheng SY, Bishop JM. Suppressor of Fused represses Gli-mediated transcription by recruiting the SAP18-mSin3 corepressor complex. *Proc Natl Acad Sci U S A*. 2002 Apr 16;99(8):5442-7.
- Chiang C, Litingtung Y, Lee E, Young KE, Corden JL, Westphal H, Beachy PA. Cyclopia and defective axial patterning in mice lacking Sonic hedgehog gene function. *Nature*. 1996 Oct 3;383(6599):407-13.
- Coene KL, Roepman R, Doherty D, Afroze B, Kroes HY, Letteboer SJ, Ngu LH, Budny B, van Wijk E, Gordon NT, Azhimi M, Thauvin-Robinet C, Veltman JA, Boink M, Kleefstra T, Cremers FP, van Bokhoven H, de Brouwer AP. *OFD1* is mutated in X-linked Joubert syndrome and interacts with *LCA5*-encoded lebercilin. *Am J Hum Genet*. 2009 Oct;85(4):465-81. doi: 10.1016/j.ajhg.2009.09.002.
- Cole DG, Diener DR, Himelblau AL, Beech PL, Fuster JC, Rosenbaum JL. Chlamydomonas kinesin-II-dependent intraflagellar transport (IFT): IFT particles contain proteins required for ciliary assembly in *Caenorhabditis elegans* sensory neurons. *J Cell Biol*. 1998 May 18;141(4):993-1008.
- Conduit PT, Wainman A, Raff JW. Centrosome function and assembly in animal cells. *Nat Rev Mol Cell Biol*. 2015 Oct;16(10):611-24. doi: 10.1038/nrm4062. Epub 2015 Sep 16.
- Copp AJ, Greene ND, Murdoch JN. The genetic basis of mammalian neurulation. *Nat Rev Genet*. 2003 Oct;4(10):784-93. Review.
- Corbit KC, Aanstad P, Singla V, Norman AR, Stainier DY, Reiter JF. Vertebrate Smoothed functions at the primary cilium. *Nature*. 2005 Oct 13;437(7061):1018-21. Epub 2005 Aug 31.
- Corbit KC, Shyer AE, Dowdle WE, Gaulden J, Singla V, Chen MH, Chuang PT, Reiter JF. *Kif3a* constrains beta-catenin-dependent Wnt signalling through dual ciliary and non-ciliary mechanisms. *Nat Cell Biol*. 2008 Jan;10(1):70-6. Epub 2007 Dec 16.
- Coux O, Tanaka K, Goldberg AL. Structure and functions of the 20S and 26S proteasomes. *Annu Rev Biochem*. 1996;65:801-47.
- Crossley PH, Martin GR. The mouse *Fgf8* gene encodes a family of polypeptides and is expressed in regions that direct outgrowth and patterning in the developing embryo. *Development*. 1995 Feb;121(2):439-51.

- Crossley PH, Martinez S, Ohkubo Y, Rubenstein JL. Coordinate expression of *Fgf8*, *Otx2*, *Bmp4*, and *Shh* in the rostral prosencephalon during development of the telencephalic and optic vesicles. *Neuroscience*. 2001;108(2):183-206.
- Cruz C, Ribes V, Kutejova E, Cayuso J, Lawson V, Norris D, Stevens J, Davey M, Blight K, Bangs F, Mynett A, Hirst E, Chung R, Balaskas N, Brody SL, Marti E, Briscoe J. *Foxj1* regulates floor plate cilia architecture and modifies the response of cells to sonic hedgehog signalling. *Development*. 2010 Dec;137(24):4271-82. doi: 10.1242/dev.051714.
- Davey MG, Paton IR, Yin Y, Schmidt M, Bangs FK, Morrice DR, Smith TG, Buxton P, Stamataki D, Tanaka M, Münsterberg AE, Briscoe J, Tickle C, Burt DW. The chicken *talpid3* gene encodes a novel protein essential for Hedgehog signaling. *Genes Dev*. 2006 May 15;20(10):1365-77.
- Del Giudice E, Macca M, Imperati F, D'Amico A, Parent P, Pasquier L, Layet V, Lyonnet S, Stamboul-Darmency V, Thauvin-Robinet C, Franco B1; Oral-Facial-Digital Type I (OFD1) Collaborative Group. CNS involvement in OFD1 syndrome: a clinical, molecular, and neuroimaging study. *Orphanet J Rare Dis*. 2014 May 10;9:74. doi: 10.1186/1750-1172-9-74.
- Delogu A, Sellers K, Zagoraiou L, Bocianowska-Zbrog A, Mandal S, Guimera J, Rubenstein JL, Sugden D, Jessell T, Lumsden A. Subcortical visual shell nuclei targeted by ipRGCs develop from a *Sox14*⁺-GABAergic progenitor and require *Sox14* to regulate daily activity rhythms. *Neuron*. 2012 Aug 23;75(4):648-62. doi: 10.1016/j.neuron.2012.06.013.
- Delous M, Baala L, Salomon R, Laclef C, Vierkotten J, Tory K, Golzio C, Lacoste T, Besse L, Ozilou C, Moutkine I, Hellman NE, Anselme I, Silbermann F, Vesque C, Gerhardt C, Rattenberry E, Wolf MT, Gubler MC, Martinovic J, Encha-Razavi F, Boddaert N, Gonzales M, Macher MA, Nivet H, Champion G, Berthéléme JP, Niaudet P, McDonald F, Hildebrandt F, Johnson CA, Vekemans M, Antignac C, Rüther U, Schneider-Maunoury S, Attié-Bitach T, Saunier S. The ciliary gene *RPGRIP1L* is mutated in cerebello-oculo-renal syndrome (Joubert syndrome type B) and Meckel syndrome. *Nat Genet*. 2007 Jul;39(7):875-81. Epub 2007 Jun 10.
- Delous M, Hellman NE, Gaudé HM, Silbermann F, Le Bivic A, Salomon R, Antignac C, Saunier S. Nephrocystin-1 and nephrocystin-4 are required for epithelial morphogenesis and associate with PALS1/PATJ and Par6. *Hum Mol Genet*. 2009 Dec 15;18(24):4711-23. doi: 10.1093/hmg/ddp434. Epub 2009 Sep 14.
- Dessaud E, Yang LL, Hill K, Cox B, Ulloa F, Ribeiro A, Mynett A, Novitch BG, Briscoe J. Interpretation of the sonic hedgehog morphogen gradient by a temporal adaptation mechanism. *Nature*. 2007 Nov 29;450(7170):717-20.
- Dessaud E, McMahon AP, Briscoe J. Pattern formation in the vertebrate neural tube: a sonic hedgehog morphogen-regulated transcriptional network. *Development*. 2008 Aug;135(15):2489-503. doi: 10.1242/dev.009324.
- Dessaud E, Ribes V, Balaskas N, Yang LL, Pierani A, Kicheva A, Novitch BG, Briscoe J, Sasai N. Dynamic assignment and maintenance of positional identity in the ventral neural tube by the morphogen sonic hedgehog. *PLoS Biol*. 2010 Jun 1;8(6):e1000382. doi: 10.1371/journal.pbio.1000382.
- Díaz C, Morales-Delgado N, Puelles L. Ontogenesis of peptidergic neurons within the genoarchitectonic map of the mouse hypothalamus. *Front Neuroanat*. 2015 Jan 12;8:162. doi: 10.3389/fnana.2014.00162. eCollection 2014.

- Diaz LL, Grech KF, Prados MD. Hypothalamic hamartoma associated with Laurence-Moon-Biedl syndrome. Case report and review of the literature. *Pediatr Neurosurg.* 1991-1992;17(1):30-3.
- Ding Q, Motoyama J, Gasca S, Mo R, Sasaki H, Rossant J, Hui CC. Diminished Sonic hedgehog signaling and lack of floor plate differentiation in Gli2 mutant mice. *Development.* 1998 Jul;125(14):2533-43.
- Eichers ER, Abd-El-Barr MM, Paylor R, Lewis RA, Bi W, Meehan TP, Stockton DW, Wu SM, Lindsay E, Justice MJ, Beales PL, Katsanis N, Lupski JR. Phenotypic characterization of Bbs4 null mice reveals age-dependent penetrance and variable expressivity. *Hum Genet* 2006;120:211-226.
- Elliott KH, Brugmann SA. Sending mixed signals: Cilia-dependent signaling during development and disease. *Dev Biol.* 2018 Mar 13. pii: S0012-1606(17)30380-9. doi: 10.1016/j.ydbio.2018.03.007. [Epub ahead of print] Review.
- Elliott KH, Millington G, Brugmann SA. A novel role for cilia-dependent sonic hedgehog signaling during submandibular gland development. *Dev Dyn.* 2018 Jun;247(6):818-831. doi: 10.1002/dvdy.24627. Epub 2018 Apr 10.
- Elms P, Siggers P, Napper D, Greenfield A, Arkell R. Zic2 is required for neural crest formation and hindbrain patterning during mouse development. *Dev Biol.* 2003 Dec 15;264(2):391-406.
- Endoh-Yamagami S, Evangelista M, Wilson D, Wen X, Theunissen JW, Phamluong K, Davis M, Scales SJ, Solloway MJ, de Sauvage FJ, Peterson AS. The mammalian Cos2 homolog Kif7 plays an essential role in modulating Hh signal transduction during development. *Curr Biol.* 2009 Aug 11;19(15):1320-6. doi: 10.1016/j.cub.2009.06.046. Epub 2009 Jul 9.
- Engel BD, Ishikawa H, Wemmer KA, Geimer S, Wakabayashi K, Hirono M, Craige B, Pazour GJ, Witman GB, Kamiya R, Marshall WF. The role of retrograde intraflagellar transport in flagellar assembly, maintenance, and function. *J Cell Biol.* 2012 Oct 1;199(1):151-67. doi: 10.1083/jcb.201206068.
- Epstein DJ, Vekemans M, Gros P. Spotch (Sp2H), a mutation affecting development of the mouse neural tube, shows a deletion within the paired homeodomain of Pax-3. *Cell.* 1991 Nov 15;67(4):767-74.
- Epstein DJ. Regulation of thalamic development by sonic hedgehog. *Front Neurosci.* 2012 Apr 18;6:57. doi: 10.3389/fnins.2012.00057. eCollection 2012.
- Ericson J, Rashbass P, Schedl A, Brenner-Morton S, Kawakami A, van Heyningen V, Jessell TM, Briscoe J. Pax6 controls progenitor cell identity and neuronal fate in response to graded Shh signaling. *Cell.* 1997 Jul 11;90(1):169-80.
- Ezratty EJ, Stokes N, Chai S, Shah AS, Williams SE, Fuchs E. A role for the primary cilium in Notch signaling and epidermal differentiation during skin development. *Cell.* 2011 Jun 24;145(7):1129-41. doi: 10.1016/j.cell.2011.05.030.
- Failler M, Gee HY, Krug P, Joo K, Halbritter J, Belkacem L, Filhol E, Porath JD, Braun DA, Schueler M, Frigo A, Alibeu O, Masson C, Brochard K, Hurault de Ligny B, Novo R, Pietrement C, Kayserili H, Salomon R, Gubler MC, Otto EA, Antignac C, Kim J, Benmerah A, Hildebrandt F, Saunier S. Mutations of CEP83 cause infantile nephronophthisis and intellectual disability. *Am J Hum Genet.* 2014 Jun 5;94(6):905-14. doi: 10.1016/j.ajhg.2014.05.002. Epub 2014 May 29.
- Fernandes M, Hébert JM (2008) The ups and downs of holoprosencephaly: dorsal versus ventral patterning forces. *Clin Genet.* 73(5):413-23.
- Feuillan PP, Ng D, Han JC, Sapp JC, Wetsch K, Spaulding E, Zheng YC, Caruso RC, Brooks BP, Johnston JJ, Yanovski JA, Biesecker LG. Patients with Bardet-Biedl syndrome

- have hyperleptinemia suggestive of leptin resistance. *J Clin Endocrinol Metab* 2011;96:E528-E535.
- Foerster P, Daclin M, Asm S, Faucourt M, Boletta A, Genovesio A, Spassky N. mTORC1 signaling and primary cilia are required for brain ventricle morphogenesis. *Development*. 2017 Jan 15;144(2):201-210. doi: 10.1242/dev.138271. Epub 2016 Dec 19.
- Follit JA, Tuft RA, Fogarty KE, Pazour GJ. The intraflagellar transport protein IFT20 is associated with the Golgi complex and is required for cilia assembly. *Mol Biol Cell*. 2006 Sep;17(9):3781-92. Epub 2006 Jun 14.
- Friede RL, Boltshauser E. Uncommon syndromes of cerebellar vermis aplasia. I: Joubert syndrome. *Dev Med Child Neurol* 1978;20:758-763.
- Fuhrmann S. Eye morphogenesis and patterning of the optic vesicle. *Curr Top Dev Biol*. 2010;93:61-84. doi: 10.1016/B978-0-12-385044-7.00003-5. Review.
- Furimsky M, Wallace VA. Complementary Gli activity mediates early patterning of the mouse visual system. *Dev Dyn*. 2006 Mar;235(3):594-605.
- Galati DF, Mitchell BJ, Pearson CG. Subdistal Appendages Stabilize the Ups and Downs of Ciliary Life. *Dev Cell*. 2016 Nov 21;39(4):387-389. doi: 10.1016/j.devcel.2016.11.006.
- Garcia G, Raleigh DR, Reiter JF. How the Ciliary Membrane Is Organized Inside-Out to Communicate Outside-In. *Curr Biol*. 2018 Apr 23;28(8):R421-R434. doi: 10.1016/j.cub.2018.03.010.
- Garcia-Gonzalo FR, Corbit KC, Sirerol-Piquer MS, Ramaswami G, Otto EA, Noriega TR, Seol AD, Robinson JF, Bennett CL, Josifova DJ, García-Verdugo JM, Katsanis N, Hildebrandt F, Reiter JF. A transition zone complex regulates mammalian ciliogenesis and ciliary membrane composition. *Nat Genet*. 2011 Jul 3;43(8):776-84. doi: 10.1038/ng.891.
- Garda AL, Echevarría D, Martínez S. Neuroepithelial co-expression of Gbx2 and Otx2 precedes Fgf8 expression in the isthmic organizer. *Mech Dev*. 2001 Mar;101(1-2):111-8.
- Gazea M, Tasouri E, Tolve M, Bosch V, Kabanova A, Gojak C, Kurtulmus B, Novikov O, Spatz J, Pereira G, Hübner W, Brodski C, Tucker KL, Blaess S. Primary cilia are critical for Sonic hedgehog-mediated dopaminergic neurogenesis in the embryonic midbrain. *Dev Biol*. 2016 Jan 1;409(1):55-71. doi: 10.1016/j.ydbio.2015.10.033. Epub 2015 Nov 2.
- Gerdes JM, Katsanis N. Ciliary function and Wnt signal modulation. *Curr Top Dev Biol*. 2008;85:175-95. doi: 10.1016/S0070-2153(08)00807-7.
- Gerhardt C, Lier JM, Burmühl S, Struchtrup A, Deutschmann K, Vetter M, Leu T, Reeg S, Grune T, Rütter U. The transition zone protein Rpgrip1l regulates proteasomal activity at the primary cilium. *J Cell Biol*. 2015 Jul 6;210(1):115-33. doi: 10.1083/jcb.201408060.
- Gerhardt C, Wiegering A, Leu T, Rütter U. Control of Hedgehog Signalling by the Cilia-Regulated Proteasome. *J Dev Biol*. 2016 Sep 3;4(3). pii: E27. doi: 10.3390/jdb4030027. Review.
- Goetz JA, Singh S, Suber LM, Kull FJ, Robbins DJ. A highly conserved amino-terminal region of sonic hedgehog is required for the formation of its freely diffusible multimeric form. *J Biol Chem*. 2006 Feb 17;281(7):4087-93. Epub 2005 Dec 9.
- Gonçalves J, Pelletier L. The Ciliary Transition Zone: Finding the Pieces and Assembling the Gate. *Mol Cells*. 2017 Apr;40(4):243-253. doi: 10.14348/molcells.2017.0054. Epub 2017 Apr 12.

- Gorivodsky M, Mukhopadhyay M, Wilsch-Braeuninger M, Phillips M, Teufel A, Kim C, Malik N, Huttner W, Westphal H. Intraflagellar transport protein 172 is essential for primary cilia formation and plays a vital role in patterning the mammalian brain. *Dev Biol.* 2009 Jan 1;325(1):24-32. doi: 10.1016/j.ydbio.2008.09.019. Epub 2008 Sep 26.
- Götz K, Briscoe J, Rüter U. Homozygous Ft embryos are affected in floor plate maintenance and ventral neural tube patterning. *Dev Dyn.* 2005 Jun;233(2):623-30.
- Graw J. Eye development. *Curr Top Dev Biol.* 2010;90:343-86. doi: 10.1016/S0070-2153(10)90010-0.
- Habbig S, Bartram MP, Müller RU, Schwarz R, Andriopoulos N, Chen S, Sägmüller JG, Hoehne M, Burst V, Liebau MC, Reinhardt HC, Benzing T, Schermer B. NPHP4, a cilia-associated protein, negatively regulates the Hippo pathway. *J Cell Biol.* 2011 May 16;193(4):633-42. doi: 10.1083/jcb.201009069. Epub 2011 May 9.
- Haddad-Tóvulli R, Paul FA, Zhang Y, Zhou X, Theil T, Puelles L, Blaess S, Alvarez-Bolado G. Differential requirements for Gli2 and Gli3 in the regional specification of the mouse hypothalamus. *Front Neuroanat.* 2015 Mar 25;9:34. doi: 10.3389/fnana.2015.00034. eCollection 2015.
- Hagemann AI, Scholpp S. The Tale of the Three Brothers - Shh, Wnt, and Fgf during Development of the Thalamus. *Front Neurosci.* 2012 May 28;6:76. doi: 10.3389/fnins.2012.00076. eCollection 2012.
- Hahn JS, Barnes PD, Clegg NJ, Stashinko EE. Septopreoptic holoprosencephaly: a mild subtype associated with midline craniofacial anomalies. *Am J Neuroradiol* 2010;31:1596-1601.
- Hahn JS, Hahn SM, Kammann H, Barkovich AJ, Clegg NJ, Delgado ME, Levey E. Endocrine disorders associated with holoprosencephaly. *J Pediatr Endocrinol Metab* 2005;18:935-941.
- Han YG, Kim HJ, Dlugosz AA, Ellison DW, Gilbertson RJ, Alvarez-Buylla A. Dual and opposing roles of primary cilia in medulloblastoma development. *Nat Med.* 2009 Sep;15(9):1062-5. doi: 10.1038/nm.2020. Epub 2009 Aug 23.
- Hashimoto-Torii K, Motoyama J, Hui CC, Kuroiwa A, Nakafuku M, Shimamura K. Differential activities of Sonic hedgehog mediated by Gli transcription factors define distinct neuronal subtypes in the dorsal thalamus. *Mech Dev.* 2003 Oct;120(10):1097-111.
- Haycraft CJ, Banizs B, Aydin-Son Y, Zhang Q, Michaud EJ, Yoder BK. Gli2 and Gli3 localize to cilia and require the intraflagellar transport protein polaris for processing and function. *PLoS Genet.* 2005 Oct;1(4):e53. Epub 2005 Oct 28.
- Hébert JM, Fishell G. The genetics of early telencephalon patterning: some assembly required. *Nat Rev Neurosci.* 2008 Sep;9(9):678-85. doi: 10.1038/nrn2463. Review.
- Hirata T, Nakazawa M, Muraoka O, Nakayama R, Suda Y, Hibi M. Zinc-finger genes Fez and Fez-like function in the establishment of diencephalon subdivisions. *Development.* 2006 Oct;133(20):3993-4004. Epub 2006 Sep 13.
- Horani A, Ferkol TW, Dutcher SK, Brody SL. Genetics and biology of primary ciliary dyskinesia. *Paediatr Respir Rev.* 2016 Mar;18:18-24. doi: 10.1016/j.prrv.2015.09.001. Epub 2015 Sep 11. Review.
- Houde C, Dickinson RJ, Houtzager VM, Cullum R, Montpetit R, Metzler M, Simpson EM, Roy S, Hayden MR, Hoodless PA, Nicholson DW. Hippo is essential for node cilia

- assembly and Sonic hedgehog signaling. *Dev Biol.* 2006 Dec 15;300(2):523-33. Epub 2006 Sep 9.
- Huang L, Lipschutz JH. Cilia and polycystic kidney disease, kith and kin. *Birth Defects Res C Embryo Today.* 2014 Jun;102(2):174-85. doi: 10.1002/bdrc.21066. Epub 2014 Jun 5.
- Huangfu D, Anderson KV. Cilia and Hedgehog responsiveness in the mouse. *Proc Natl Acad Sci U S A.* 2005 Aug 9;102(32):11325-30. Epub 2005 Aug 1.
- Huangfu D, Liu A, Rakeman AS, Murcia NS, Niswander L, Anderson KV. Hedgehog signalling in the mouse requires intraflagellar transport proteins. *Nature.* 2003 Nov 6;426(6962):83-7.
- Hui CC, Joyner AL. A mouse model of greig cephalopolysyndactyly syndrome: the extra-toes mutation contains an intragenic deletion of the *Gli3* gene. *Nat Genet.* 1993 Mar;3(3):241-6. Erratum in: *Nat Genet* 1998 Aug;19(4):404.
- Humke EW, Dorn KV, Milenkovic L, Scott MP, Rohatgi R. The output of Hedgehog signaling is controlled by the dynamic association between Suppressor of Fused and the *Gli* proteins. *Genes Dev.* 2010 Apr 1;24(7):670-82. doi: 10.1101/gad.1902910.
- Hynes M, Stone DM, Dowd M, Pitts-Meek S, Goddard A, Gurney A, Rosenthal A. Control of cell pattern in the neural tube by the zinc finger transcription factor and oncogene *Gli-1*. *Neuron.* 1997 Jul;19(1):15-26.
- Ikegami K, Sato S, Nakamura K, Ostrowski LE, Setou M. Tubulin polyglutamylation is essential for airway ciliary function through the regulation of beating asymmetry. *Proc Natl Acad Sci U S A.* 2010 Jun 8;107(23):10490-5. doi: 10.1073/pnas.1002128107. Epub 2010 May 24.
- Inoko A, Matsuyama M, Goto H, Ohmuro-Matsuyama Y, Hayashi Y, Enomoto M, Ibi M, Urano T, Yonemura S, Kiyono T, Izawa I, Inagaki M. Trichoplein and Aurora A block aberrant primary cilia assembly in proliferating cells. *J Cell Biol.* 2012 Apr 30;197(3):391-405. doi: 10.1083/jcb.201106101. Epub 2012 Apr 23.
- Insinna C, Humby M, Sedmak T, Wolfrum U, Besharse JC. Different roles for KIF17 and kinesin II in photoreceptor development and maintenance. *Dev Dyn.* 2009 Sep;238(9):2211-22. doi: 10.1002/dvdy.21956.
- Iomini C, Li L, Esparza JM, Dutcher SK. Retrograde intraflagellar transport mutants identify complex A proteins with multiple genetic interactions in *Chlamydomonas reinhardtii*. *Genetics.* 2009 Nov;183(3):885-96. doi: 10.1534/genetics.109.101915. Epub 2009 Aug 31.
- Ishikawa H, Marshall WF. Ciliogenesis: building the cell's antenna. *Nat Rev Mol Cell Biol.* 2011 Apr;12(4):222-34. doi: 10.1038/nrm3085. Review.
- Ishikawa H, Marshall WF. Intraflagellar Transport and Ciliary Dynamics. *Cold Spring Harb Perspect Biol.* 2017 Mar 1;9(3). pii: a021998. doi: 10.1101/cshperspect.a021998. Review.
- Izraeli S, Lowe LA, Bertness VL, Good DJ, Dorward DW, Kirsch IR, Kuehn MR (1999) The *SIL* gene is required for mouse embryonic axial development and left-right specification. *Nature* 399(6737):691-4.
- Izraeli S, Lowe LA, Bertness VL, Campaner S, Hahn H, Kirsch IR, Kuehn MR. Genetic evidence that *Sil* is required for the Sonic Hedgehog response pathway. *Genesis.* 2001 Oct;31(2):72-7.
- Jensen VL, Li C, Bowie RV, Clarke L, Mohan S, Blacque OE, Leroux MR. Formation of the transition zone by *Mks5/Rpgrip1L* establishes a ciliary zone of exclusion (CIZE) that compartmentalises ciliary signalling proteins and controls PIP2 ciliary

- abundance. *EMBO J.* 2015 Oct 14;34(20):2537-56. doi: 10.15252/embj.201488044. Epub 2015 Sep 21.
- Jeong J, McMahon AP. Growth and pattern of the mammalian neural tube are governed by partially overlapping feedback activities of the hedgehog antagonists patched 1 and Hhip1. *Development.* 2005 Jan;132(1):143-54. Epub 2004 Dec 2.
- Jeong Y, Dolson DK, Waclaw RR, Matisse MP, Sussel L, Campbell K, Kaestner KH, Epstein DJ. Spatial and temporal requirements for sonic hedgehog in the regulation of thalamic interneuron identity. *Development.* 2011 Feb;138(3):531-41. doi: 10.1242/dev.058917.
- Jeong Y, Leskow FC, El-Jaick K, Roessler E, Muenke M, Yocum A, Dubourg C, Li X, Geng X, Oliver G, Epstein DJ (2008) Regulation of a remote Shh forebrain enhancer by the Six3 homeoprotein. *Nat Genet.* 40(11):1348-53.
- Jin H, White SR, Shida T, Schulz S, Aguiar M, Gygi SP, Bazan JF, Nachury MV. The conserved Bardet-Biedl syndrome proteins assemble a coat that traffics membrane proteins to cilia. *Cell.* 2010 Jun 25;141(7):1208-19. doi: 10.1016/j.cell.2010.05.015.
- Juric-Sekhar G, Adkins J, Doherty D, Hevner RF. Joubert syndrome: brain and spinal cord malformations in genotypes cases and implications for neurodevelopmental functions of primary cilia. *Acta Neuropathol* 2012;123:695-709.
- Kakar N, Ahmad J, Morris-Rosendahl DJ, Altmüller J, Friedrich K, Barbi G, Nürnberg P, Kubisch C, Dobyns WB, Borck G (2015) STIL mutation causes autosomal recessive microcephalic lobar holoprosencephaly. *Hum Genet.* 134(1):45-51.
- Kataoka A, Shimogori T. Fgf8 controls regional identity in the developing thalamus. *Development.* 2008 Sep;135(17):2873-81. doi: 10.1242/dev.021618. Epub 2008 Jul 24.
- Khanna H, Davis EE, Murga-Zamalloa CA, Estrada-Cuzcano A, Lopez I, den Hollander AI, Zonneveld MN, Othman MI, Waseem N, Chakarova CF, Maubaret C, Diaz-Font A, MacDonald I, Muzny DM, Wheeler DA, Morgan M, Lewis LR, Logan CV, Tan PL, Beer MA, Inglehearn CF, Lewis RA, Jacobson SG, Bergmann C, Beales PL, Attié-Bitach T, Johnson CA, Otto EA, Bhattacharya SS, Hildebrandt F, Gibbs RA, Koenekoop RK, Swaroop A, Katsanis N. A common allele in RPGRIP1L is a modifier of retinal degeneration in ciliopathies. *Nat Genet.* 2009 Jun;41(6):739-45. doi: 10.1038/ng.366. Epub 2009 May 10.
- Kiecker C, Lumsden A. Hedgehog signaling from the ZLI regulates diencephalic regional identity. *Nat Neurosci.* 2004 Nov;7(11):1242-9. Epub 2004 Oct 24.
- Kiecker C, Niehrs C. The role of prechordal mesendoderm in neural patterning. *Curr Opin Neurobiol.* 2001 Feb;11(1):27-33. Review.
- Kim S, Lee K, Choi JH, Ringstad N, Dynlacht BD. Nek2 activation of Kif24 ensures cilium disassembly during the cell cycle. *Nat Commun.* 2015 Aug 20;6:8087. doi: 10.1038/ncomms9087.
- Kinzel D, Boldt K, Davis EE, Burtscher I, Trümbach D, Diplas B, Attié-Bitach T, Wurst W, Katsanis N, Ueffing M, Lickert H. Pitchfork regulates primary cilia disassembly and left-right asymmetry. *Dev Cell.* 2010 Jul 20;19(1):66-77. doi: 10.1016/j.devcel.2010.06.005.
- Kobayashi D, Kobayashi M, Matsumoto K, Ogura T, Nakafuku M, Shimamura K. Early subdivisions in the neural plate define distinct competence for inductive signals. *Development.* 2002 Jan;129(1):83-93.

- Kozminski KG, Johnson KA, Forscher P, Rosenbaum JL. A motility in the eukaryotic flagellum unrelated to flagellar beating. *Proc Natl Acad Sci U S A*. 1993 Jun 15;90(12):5519-23.
- Laclef C, Anselme I, Besse L, Catala M, Palmyre A, Baas D, Paschaki M, Pedraza M, Métin C, Durand B, Schneider-Maunoury S. The role of primary cilia in corpus callosum formation is mediated by production of the Gli3 repressor. *Hum Mol Genet*. 2015 Sep 1;24(17):4997-5014. doi: 10.1093/hmg/ddv221. Epub 2015 Jun 12.
- Lancaster MA, Gopal DJ, Kim J, Saleem SN, Silhavy JL, Louie CM, Thacker BE, Williams Y, Zaki MS, Gleeson JG. Defective Wnt-dependent cerebellar midline fusion in a mouse model of Joubert syndrome. *Nat Med*. 2011 Jun;17(6):726-31. doi: 10.1038/nm.2380. Epub 2011 May 29.
- Lancaster MA, Louie CM, Silhavy JL, Sintasath L, Decambre M, Nigam SK, Willert K, Gleeson JG. Impaired Wnt-beta-catenin signaling disrupts adult renal homeostasis and leads to cystic kidney ciliopathy. *Nat Med*. 2009 Sep;15(9):1046-54. doi: 10.1038/nm.2010. Epub 2009 Aug 30.
- Lawo S, Hasegan M, Gupta GD, Pelletier L. Subdiffraction imaging of centrosomes reveals higher-order organizational features of pericentriolar material. *Nat Cell Biol*. 2012 Nov;14(11):1148-58. doi: 10.1038/ncb2591. Epub 2012 Oct 21.
- Lee J, Platt KA, Censullo P, Ruiz i Altaba A. Gli1 is a target of Sonic hedgehog that induces ventral neural tube development. *Development*. 1997 Jul;124(13):2537-52.
- Lee RT, Zhao Z, Ingham PW. Hedgehog signalling. *Development*. 2016 Feb 1;143(3):367-72. doi: 10.1242/dev.120154. Review.
- Lewis AJ, Simon EM, Barkovich AJ, Clegg NJ, Delgado MR, Levey E, Hahn JS. Middle interhemispheric variant of holoprosencephaly: a distinct cliniconoradiologic subtype. *Neurology* 2002;59:1860-1865).
- Li C, Jensen VL, Park K, Kennedy J, Garcia-Gonzalo FR, Romani M, De Mori R, Bruel AL, Gaillard D, Doray B, Lopez E, Rivière JB, Faivre L, Thauvin-Robinet C, Reiter JF, Blacque OE, Valente EM, Leroux MR. MKS5 and CEP290 Dependent Assembly Pathway of the Ciliary Transition Zone. *PLoS Biol*. 2016 Mar 16;14(3):e1002416. doi: 10.1371/journal.pbio.1002416. eCollection 2016 Mar.
- Liem KF Jr, He M, Ocbina PJ, Anderson KV. Mouse Kif7/Costal2 is a cilia-associated protein that regulates Sonic hedgehog signaling. *Proc Natl Acad Sci U S A*. 2009 Aug 11;106(32):13377-82. doi: 10.1073/pnas.0906944106. Epub 2009 Jul 29.
- Liu A, Wang B, Niswander LA. Mouse intraflagellar transport proteins regulate both the activator and repressor functions of Gli transcription factors. *Development*. 2005 Jul;132(13):3103-11. Epub 2005 Jun 1.
- Liu JP, Zeitlin SO. The long and the short of aberrant ciliogenesis in Huntington disease. *J Clin Invest*. 2011 Nov;121(11):4237-41. doi: 10.1172/JCI60243. Epub 2011 Oct 10.
- Loncarek J, Bettencourt-Dias M. Building the right centriole for each cell type. *J Cell Biol*. 2018 Mar 5;217(3):823-835. doi: 10.1083/jcb.201704093. Epub 2017 Dec 28.
- Lun MP, Monuki ES, Lehtinen MK. Development and functions of the choroid plexus-cerebrospinal fluid system. *Nat Rev Neurosci*. 2015 Aug;16(8):445-57. doi: 10.1038/nrn3921. Epub 2015 Jul 15.
- Mahuzier A, Gaudé HM, Grampa V, Anselme I, Silbermann F, Leroux-Berger M, Delacour D, Ezan J, Montcouquiol M, Saunier S, Schneider-Maunoury S, Vesque C. Dishevelled stabilization by the ciliopathy protein Rpgrip1l is essential for planar cell polarity. *J Cell Biol*. 2012 Sep 3;198(5):927-40. doi: 10.1083/jcb.201111009. Epub 2012 Aug 27.

- Mak LL. Ultrastructural studies of amphibian neural fold fusion. *Dev Biol.* 1978 Aug;65(2):435-46.
- Malicki J, Avidor-Reiss T. From the cytoplasm into the cilium: bon voyage. *Organogenesis.* 2014 Jan 1;10(1):138-57. doi: 10.4161/org.29055. Epub 2014 May 2.
- Malicki JJ, Johnson CA. The Cilium: Cellular Antenna and Central Processing Unit. *Trends Cell Biol.* 2017 Feb;27(2):126-140. doi: 10.1016/j.tcb.2016.08.002. Epub 2016 Sep 12. Review.
- Manning L, Ohyama K, Saeger B, Hatano O, Wilson SA, Logan M, Placzek M. Regional morphogenesis in the hypothalamus: a BMP-Tbx2 pathway coordinates fate and proliferation through Shh downregulation. *Dev Cell.* 2006 Dec;11(6):873-85.
- Marcorelles P, Laquerrière A. Neuropathology of holoprosencephaly. *Am J Med Genet (Part C)* 2010;154C:109-119.
- Martí E, Takada R, Bumcrot DA, Sasaki H, McMahon AP. Distribution of Sonic hedgehog peptides in the developing chick and mouse embryo. *Development.* 1995 Aug;121(8):2537-47.
- Martinez-Ferre A, Lloret-Quesada C, Prakash N, Wurst W, Rubenstein JL, Martinez S. Fgf15 regulates thalamic development by controlling the expression of proneural genes. *Brain Struct Funct.* 2016 Jul;221(6):3095-109. doi: 10.1007/s00429-015-1089-5. Epub 2015 Aug 27.
- Martinez-Ferre A, Martinez S. Molecular regionalization of the diencephalon. *Front Neurosci.* 2012 May 25;6:73. doi: 10.3389/fnins.2012.00073. eCollection 2012.
- Martinez-Ferre A, Navarro-Garberi M, Bueno C, Martinez S. Wnt signal specifies the intrathalamic limit and its organizer properties by regulating Shh induction in the alar plate. *J Neurosci.* 2013 Feb 27;33(9):3967-80. doi: 10.1523/JNEUROSCI.0726-12.2013.
- Mathieu J, Barth A, Rosa FM, Wilson SW, Peyriéras N. Distinct and cooperative roles for Nodal and Hedgehog signals during hypothalamic development. *Development.* 2002 Jul;129(13):3055-65.
- Matise MP, Joyner AL. Expression patterns of developmental control genes in normal and Engrailed-1 mutant mouse spinal cord reveal early diversity in developing interneurons. *J Neurosci.* 1997 Oct 15;17(20):7805-16.
- Matise MP, Epstein DJ, Park HL, Platt KA, Joyner AL. Gli2 is required for induction of floor plate and adjacent cells, but not most ventral neurons in the mouse central nervous system. *Development.* 1998 Aug;125(15):2759-70.
- May SR, Ashique AM, Karlen M, Wang B, Shen Y, Zarbalis K, Reiter J, Ericson J, Peterson AS. Loss of the retrograde motor for IFT disrupts localization of Smo to cilia and prevents the expression of both activator and repressor functions of Gli. *Dev Biol.* 2005 Nov 15;287(2):378-89. Epub 2005 Oct 17.
- McMahon AP, Bradley A. The Wnt-1 (int-1) proto-oncogene is required for development of a large region of the mouse brain. *Cell.* 1990 Sep 21;62(6):1073-85.
- McShane SG, Molè MA, Savery D, Greene ND, Tam PP, Copp AJ. Cellular basis of neuroepithelial bending during mouse spinal neural tube closure. *Dev Biol.* 2015 Aug 15;404(2):113-24. doi: 10.1016/j.ydbio.2015.06.003. Epub 2015 Jun 12.
- Mee L, Honkala H, Kopra O, Vesa J, Finnilä S, Visapää I, Sang TK, Jackson GR, Salonen R, Kestilä M, Peltonen L. Hydrolethalus syndrome is caused by a missense mutation in a novel gene HYLS1. *Hum Mol Genet.* 2005 Jun 1;14(11):1475-88. Epub 2005 Apr 20.

- Mennella V, Keszthelyi B, McDonald KL, Chhun B, Kan F, Rogers GC, Huang B, Agard DA. Subdiffraction-resolution fluorescence microscopy reveals a domain of the centrosome critical for pericentriolar material organization. *Nat Cell Biol.* 2012 Nov;14(11):1159-68. doi: 10.1038/ncb2597. Epub 2012 Oct 21.
- Mercier S, Dubourg C, Garcelon N, Campillo-Gimenez B, Gicquel I, Belleguic M, Ratié L, Pasquier L, Loget P, Bendavid C, Jaillard S, Rochard L, Quélin C, Dupé V, David V, Odent S (2011) New findings for phenotype-genotype correlations in a large European series of holoprosencephaly cases. *J Med Genet.* 48(11):752-60.
- Mirzadeh Z, Kusne Y, Duran-Moreno M, Cabrales E, Gil-Perotin S, Ortiz C, Chen B, Garcia-Verdugo JM, Sanai N, Alvarez-Buylla A. Bi- and unciliated ependymal cells define continuous floor-plate tanycytic territories. *Nat Commun* 2017;Jan 9;8:13759.
- Miyamoto T, Hosoba K, Ochiai H, Royba E, Izumi H, Sakuma T, Yamamoto T, Dynlacht BD4, Matsuura S5. The Microtubule-Depolymerizing Activity of a Mitotic Kinesin Protein KIF2A Drives Primary Cilia Disassembly Coupled with Cell Proliferation. *Cell Rep.* 2015 Feb 4. pii: S2211-1247(15)00004-2. doi: 10.1016/j.celrep.2015.01.003.
- Mohler J. Requirements for hedgehog, a segmental polarity gene, in patterning larval and adult cuticle of *Drosophila*. *Genetics.* 1988 Dec;120(4):1061-72.
- Morriss-Kay GM. Growth and development of pattern in the cranial neural epithelium of rat embryos during neurulation. *J Embryol Exp Morphol.* 1981 Oct;65 Suppl:225-41.
- Mouden C, de Tayrac M, Dubourg C, Rose S, Carré W, Hamdi-Rozé H, Babron MC, Akloul L, Héron-Longe B, Odent S, Dupé V, Giet R, David V (2015) Homozygous STIL mutation causes holoprosencephaly and microcephaly in two siblings. *PLoS One* 10(2):e0117418.
- Mouden C, Dubourg C, Carré W, Rose S, Quelin C, Akloul L, Hamdi-Rozé H, Viot G, Salhi H, Darnault P, Odent S, Dupé V, David V (2016) Complex mode of inheritance in holoprosencephaly revealed by whole exome sequencing. *Clin Genet.* 89(6):659-68.
- Mukhopadhyay S, Wen X, Ratti N, Loktev A, Rangell L, Scales SJ, Jackson PK. The ciliary G-protein-coupled receptor Gpr161 negatively regulates the Sonic hedgehog pathway via cAMP signaling. *Cell.* 2013 Jan 17;152(1-2):210-23. doi: 10.1016/j.cell.2012.12.026.
- Müller F, O'Rahilly R. Mediobasal prosencephalic defects, including holoprosencephaly and cyclopia, in relation to the development of the human forebrain. *Am J Anat* 1989;185:391-414.
- Nicastro D, Schwartz C, Pierson J, Gaudette R, Porter ME, McIntosh JR. The molecular architecture of axonemes revealed by cryoelectron tomography. *Science.* 2006 Aug 18;313(5789):944-8.
- Nikolopoulou E, Galea GL, Rolo A, Greene ND, Copp AJ. Neural tube closure: cellular, molecular and biomechanical mechanisms. *Development.* 2017 Feb 15;144(4):552-566. doi: 10.1242/dev.145904. Review.
- Nonaka S, Tanaka Y, Okada Y, Takeda S, Harada A, Kanai Y, Kido M, Hirokawa N. Randomization of left-right asymmetry due to loss of nodal cilia generating leftward flow of extraembryonic fluid in mice lacking KIF3B motor protein. *Cell.* 1998 Dec 11;95(6):829-37.
- Ocbina PJ, Anderson KV. Intraflagellar transport, cilia, and mammalian Hedgehog signaling: analysis in mouse embryonic fibroblasts. *Dev Dyn.* 2008 Aug;237(8):2030-8. doi: 10.1002/dvdy.21551.

- Ocbina PJ, Eggenschwiler JT, Moskowitz I, Anderson KV. Complex interactions between genes controlling trafficking in primary cilia. *Nat Genet.* 2011 Jun;43(6):547-53. doi: 10.1038/ng.832. Epub 2011 May 8.
- Oka M, Shimojima K, Yamamoto T, Hanaoka Y, Sato S, Yasuhara T, Yoshinaga H, Kobayashi K. A novel HYL51 homozygous mutation in living siblings with Joubert syndrome. *Clin Genet.* 2016 Jun;89(6):739-43. doi: 10.1111/cge.12752. Epub 2016 Mar 4.
- Paetau A, Honkala H, Salonen R, Ignatius J, Kestilä M, Herva R. Hydrolethalus syndrome: neuropathology of 21 cases confirmed by HYL51 gene mutation analysis. *J Neuropathol Exp Neurol* 2008;67:750-762.
- Paetau A, Salonen R, Haltia M. Brain pathology in the Meckel syndrome: a study of 59 cases. *Clin Neuropathol* 1985;4:56-62.
- Paetau A, Honkala H, Salonen R, Ignatius J, Kestilä M, Herva R. Hydrolethalus syndrome: neuropathology of 21 cases confirmed by HYL51 gene mutation analysis. *J Neuropathol Exp Neurol.* 2008 Aug;67(8):750-62. doi: 10.1097/NEN.0b013e318180ec2e.
- Pan J, Wang Q, Snell WJ. An aurora kinase is essential for flagellar disassembly in *Chlamydomonas*. *Dev Cell.* 2004 Mar;6(3):445-51.
- Pan Y, Bai CB, Joyner AL, Wang B. Sonic hedgehog signaling regulates Gli2 transcriptional activity by suppressing its processing and degradation. *Mol Cell Biol.* 2006 May;26(9):3365-77.
- Pan Y, Wang B. A novel protein-processing domain in Gli2 and Gli3 differentially blocks complete protein degradation by the proteasome. *J Biol Chem.* 2007 Apr 13;282(15):10846-52. Epub 2007 Feb 5.
- Pangilinan F, Molloy AM, Mills JL, Troendle JF, Parle-McDermott A, Signore C, O'Leary VB, Chines P, Seay JM, Geiler-Samerotte K, Mitchell A, VanderMeer JE, Krebs KM, Sanchez A, Cornman-Homonoff J, Stone N, Conley M, Kirke PN, Shane B, Scott JM, Brody LC. Evaluation of common genetic variants in 82 candidate genes as risk factors for neural tube defects. *BMC Med Genet.* 2012 Aug 2;13:62.
- Park HL, Bai C, Platt KA, Matise MP, Beeghly A, Hui CC, Nakashima M, Joyner AL. Mouse Gli1 mutants are viable but have defects in SHH signaling in combination with a Gli2 mutation. *Development.* 2000 Apr;127(8):1593-605.
- Patel V, Li L, Cobo-Stark P, Shao X, Somlo S, Lin F, Igarashi P. Acute kidney injury and aberrant planar cell polarity induce cyst formation in mice lacking renal cilia. *Hum Mol Genet.* 2008 Jun 1;17(11):1578-90. doi: 10.1093/hmg/ddn045. Epub 2008 Feb 9.
- Pazour GJ, Dickert BL, Vucica Y, Seeley ES, Rosenbaum JL, Witman GB, Cole DG. *Chlamydomonas* IFT88 and its mouse homologue, polycystic kidney disease gene *tg737*, are required for assembly of cilia and flagella. *J Cell Biol.* 2000 Oct 30;151(3):709-18.
- Persson M, Stamataki D, te Welscher P, Andersson E, Böse J, Rüter U, Ericson J, Briscoe J. Dorsal-ventral patterning of the spinal cord requires Gli3 transcriptional repressor activity. *Genes Dev.* 2002 Nov 15;16(22):2865-78.
- Peters T, Ausmeier K, Dildrop R, Rüter U. The mouse Fused toes (Ft) mutation is the result of a 1.6-Mb deletion including the entire Iroquois B gene cluster. *Mamm Genome.* 2002 Apr;13(4):186-8.
- Piperno G, Mead K. Transport of a novel complex in the cytoplasmic matrix of *Chlamydomonas* flagella. *Proc Natl Acad Sci U S A.* 1997 Apr 29;94(9):4457-62.

- Plotnikova OV, Nikonova AS, Loskutov YV, Kozyulina PY, Pugacheva EN, Golemis EA. Calmodulin activation of Aurora-A kinase (AURKA) is required during ciliary disassembly and in mitosis. *Mol Biol Cell*. 2012 Jul;23(14):2658-70. doi: 10.1091/mbc.E11-12-1056. Epub 2012 May 23.
- Poretti A, Huisman TA, Scheer I, Boltshauser E. Joubert syndrome and related disorders: spectrum of neuroimaging findings in 75 patients. *AJNR Am J Neuroradiol*. 2011 Sep;32(8):1459-63. doi: 10.3174/ajnr.A2517. Epub 2011 Jun 16.
- Poretti A, Snow J, Summers AC, Tekes A, Huisman TAGM, Aygun N, Carson KA, Doherty D, Parisi MA, Toro C, Yildirimli D, Vemulapalli M, Mullikin JC; NISC Comparative Sequencing Program, Cullinane AR, Vilboux T, Gahl WA, Gunay-Aygun M. Joubert syndrome: neuroimaging findings in 110 patients in correlation with cognitive function and genetic cause. *J Med Genet*. 2017 Aug;54(8):521-529. doi: 10.1136/jmedgenet-2016-104425. Epub 2017 Jan 13.
- Porter JA, Ekker SC, Park WJ, von Kessler DP, Young KE, Chen CH, Ma Y, Woods AS, Cotter RJ, Koonin EV, Beachy PA. Hedgehog patterning activity: role of a lipophilic modification mediated by the carboxy-terminal autoprocessing domain. *Cell*. 1996 Jul 12;86(1):21-34.
- Prévoit V, Dehouck B, Sharif A, Ciofi P, Giacobini P, Casadonte J. The versatile tanycyte: a hypothalamic integrator of reproduction and energy metabolism. *Endocr Rev* 2018;39:333-368.
- Puelles L, Harrison M, Paxinos G, Watson C. A developmental ontology for the mammalian brain based on the prosomeric model. *Trends Neurosci*. 2013 Oct;36(10):570-8. doi: 10.1016/j.tins.2013.06.004. Epub 2013 Jul 18. Review.
- Puelles L, Rubenstein JL. A new scenario of hypothalamic organization: rationale of new hypotheses introduced in the updated prosomeric model. *Front Neuroanat*. 2015 Mar 19;9:27. doi: 10.3389/fnana.2015.00027. eCollection 2015.
- Puelles L. Forebrain Development in Vertebrates : The Evolutionary Role of Secondary Organizers. *The Wiley Handbook of Evolutionary Neuroscience, First Edition*. Edited by Stephen V. Shepherd. © 2016 John Wiley & Sons, Ltd. Published 2016 by John Wiley & Sons, Ltd.
- Qin H, Wang Z, Diener D, Rosenbaum J. Intraflagellar transport protein 27 is a small G protein involved in cell-cycle control. *Curr Biol*. 2007 Feb 6;17(3):193-202.
- Rallu M, Machold R, Gaiano N, Corbin JG, McMahon AP, Fishell G. Dorsoventral patterning is established in the telencephalon of mutants lacking both Gli3 and Hedgehog signaling. *Development*. 2002 Nov;129(21):4963-74.
- Ramsbottom SA, Pownall ME. Regulation of Hedgehog Signalling Inside and Outside the Cell. *J Dev Biol*. 2016 Jul 20;4(3):23.
- Reiter JF, Leroux MR. Genes and molecular pathways underpinning ciliopathies. *Nat Rev Mol Cell Biol*. 2017 Sep;18(9):533-547. doi: 10.1038/nrm.2017.60. Epub 2017 Jul 12.
- Reiter JF, Skarnes WC. Tectonic, a novel regulator of the Hedgehog pathway required for both activation and inhibition. *Genes Dev*. 2006 Jan 1;20(1):22-7. Epub 2005 Dec 15.
- Reiter JF, Blacque OE, Leroux MR. The base of the cilium: roles for transition fibres and the transition zone in ciliary formation, maintenance and compartmentalization. *EMBO Rep*. 2012 Jun 29;13(7):608-18. doi: 10.1038/embor.2012.73.
- Rhamouni K, Fath MA, Seo S, Thedens DR, Berry CJ, Weiss R, Nishimura DY, Sheffield VC. Leptin resistance contributes to obesity and hypertension in mouse models of Bardet-Biedl syndrome. *J Clin Invest* 2008;118:1458-1467.

- Ribes V, Balaskas N, Sasai N, Cruz C, Dessaud E, Cayuso J, Tozer S, Yang LL, Novitch B, Marti E, Briscoe J. Distinct Sonic Hedgehog signaling dynamics specify floor plate and ventral neuronal progenitors in the vertebrate neural tube. *Genes Dev.* 2010 Jun 1;24(11):1186-200. doi: 10.1101/gad.559910.
- Ribes V, Briscoe J. Establishing and interpreting graded Sonic Hedgehog signaling during vertebrate neural tube patterning: the role of negative feedback. *Cold Spring Harb Perspect Biol.* 2009 Aug;1(2):a002014. doi: 10.1101/cshperspect.a002014. Review.
- Robert A, Margall-Ducos G, Guidotti JE, Br gerie O, Celati C, Br chet C, Desdouets C. The intraflagellar transport component IFT88/polaris is a centrosomal protein regulating G1-S transition in non-ciliated cells. *J Cell Sci.* 2007 Feb 15;120(Pt 4):628-37. Epub 2007 Jan 30.
- Robinson A, Escuin S, Doudney K, Vekemans M, Stevenson RE, Greene ND, Copp AJ, Stanier P. Mutations in the planar cell polarity genes CELSR1 and SCRIB are associated with the severe neural tube defect craniorachischisis. *Hum Mutat.* 2012 Feb;33(2):440-7. doi: 10.1002/humu.21662. Epub 2011 Dec 20.
- Roelink H, Porter JA, Chiang C, Tanabe Y, Chang DT, Beachy PA, Jessell TM. Floor plate and motor neuron induction by different concentrations of the amino-terminal cleavage product of sonic hedgehog autoproteolysis. *Cell.* 1995 May 5;81(3):445-55.
- Roepman R, Letteboer SJ, Arts HH, van Beersum SE, Lu X, Krieger E, Ferreira PA, Cremers FP. Interaction of nephrocystin-4 and RPGRIP1 is disrupted by nephronophthisis or Leber congenital amaurosis-associated mutations. *Proc Natl Acad Sci U S A.* 2005 Dec 20;102(51):18520-5. Epub 2005 Dec 9.
- Roume J, Genin E, Cormier-Daire V, Ma HW, Mehaye B, Attie T, Razavi-Encha F, Fallet-Bianco C, Buenerd A, Clerget-Darpoux F, Munnich A, Le Merrer M. A gene for Meckel syndrome maps to chromosome 11q13. *Am J Hum Genet.* 1998 Oct;63(4):1095-101.
- Roume J, Genin E, Cormier-Daire V, Ma HW, Mehaye B, Attie T, Razavi-Encha R, Fallet-Bianco C, Buenerd A, Clerget-Darpoux F, Munnich A, Le Merrer M. A gene for Meckel syndrome maps to chromosome 11q13. *Am J Hum Genet* 1998; 63: 1095-1101.
- Rubenstein JL, Martinez S, Shimamura K, Puelles L. The embryonic vertebrate forebrain: the prosomeric model. *Science.* 1994 Oct 28;266(5185):578-80. Review. No abstract available.
- S nchez I, Dynlacht BD. Cilium assembly and disassembly. *Nat Cell Biol.* 2016 Jun 28;18(7):711-7. doi: 10.1038/ncb3370. Review.
- Sang L, Miller JJ, Corbit KC, Giles RH, Brauer MJ, Otto EA, Baye LM, Wen X, Scales SJ, Kwong M, Huntzicker EG, Sfakianos MK, Sandoval W, Bazan JF, Kulkarni P, Garcia-Gonzalo FR, Seol AD, O'Toole JF, Held S, Reutter HM, Lane WS, Rafiq MA, Noor A, Ansar M, Devi AR, Sheffield VC, Slusarski DC, Vincent JB, Doherty DA, Hildebrandt F, Reiter JF, Jackson PK. Mapping the NPHP-JBTS-MKS protein network reveals ciliopathy disease genes and pathways. *Cell.* 2011 May 13;145(4):513-28. doi: 10.1016/j.cell.2011.04.019.
- Sasai N, Briscoe J. Primary cilia and graded Sonic Hedgehog signaling. *Wiley Interdiscip Rev Dev Biol.* 2012 Sep-Oct;1(5):753-72. doi: 10.1002/wdev.43. Epub 2012 Apr 4. Review.

- Sasaki H, Nishizaki Y, Hui C, Nakafuku M, Kondoh H. Regulation of Gli2 and Gli3 activities by an amino-terminal repression domain: implication of Gli2 and Gli3 as primary mediators of Shh signaling. *Development*. 1999 Sep;126(17):3915-24.
- Sawyer JM, Harrell JR, Shemer G, Sullivan-Brown J, Roh-Johnson M, Goldstein B. Apical constriction: a cell shape change that can drive morphogenesis. *Dev Biol*. 2010 May 1;341(1):5-19. doi: 10.1016/j.ydbio.2009.09.009. Epub 2009 Sep 12. Review.
- Schmidt KN, Kuhns S, Neuner A, Hub B, Zentgraf H, Pereira G. Cep164 mediates vesicular docking to the mother centriole during early steps of ciliogenesis. *J Cell Biol*. 2012 Dec 24;199(7):1083-101. doi: 10.1083/jcb.201202126. Epub 2012 Dec 17.
- Schneider L, Clement CA, Teilmann SC, Pazour GJ, Hoffmann EK, Satir P, Christensen ST. PDGFRalpha signaling is regulated through the primary cilium in fibroblasts. *Curr Biol*. 2005 Oct 25;15(20):1861-6.
- Schneider-Maunoury S, Gilardi-Hebenstreit P, Charnay P. How to build a vertebrate hindbrain. Lessons from genetics. *C R Acad Sci III*. 1998 Oct;321(10):819-34. Review.
- Scholpp S, Lumsden A. Building a bridal chamber: development of the thalamus. *Trends Neurosci*. 2010 Aug;33(8):373-80. doi: 10.1016/j.tins.2010.05.003. Epub 2010 Jun 11. Review.
- Scholpp S, Wolf O, Brand M, Lumsden A. Hedgehog signalling from the zona limitans intrathalamica orchestrates patterning of the zebrafish diencephalon. *Development*. 2006 Mar;133(5):855-64. Epub 2006 Feb 1.
- Schouteden C, Serwas D, Palfy M, Dammermann A. The ciliary transition zone functions in cell adhesion but is dispensable for axoneme assembly in *C. elegans*. *J Cell Biol*. 2015 Jul 6;210(1):35-44. doi: 10.1083/jcb.201501013. Epub 2015 Jun 29.
- Schrader EK, Harstad KG, Holmgren RA, Matouschek A. A three-part signal governs differential processing of Gli1 and Gli3 proteins by the proteasome. *J Biol Chem*. 2011 Nov 11;286(45):39051-8. doi: 10.1074/jbc.M111.274993. Epub 2011 Sep 15.
- Seo S, Guo DF, Bugge K, Morgan DA, Rhamouni K, Sheffield VC. Requirement of Bardet-Biedl syndrome proteins for leptin receptor signaling. *Hum Mol Genet* 2009;18:1323-1331.
- Shi X, Garcia G 3rd, Van De Weghe JC, McGorty R, Pazour GJ, Doherty D, Huang B, Reiter JF. Super-resolution microscopy reveals that disruption of ciliary transition-zone architecture causes Joubert syndrome. *Nat Cell Biol*. 2017 Oct;19(10):1178-1188. doi: 10.1038/ncb3599. Epub 2017 Aug 28. Erratum in: *Nat Cell Biol*. 2017
- Shimamura K, Hartigan DJ, Martinez S, Puelles L, Rubenstein JL. Longitudinal organization of the anterior neural plate and neural tube. *Development*. 1995 Dec;121(12):3923-33. Review.
- Shimamura K, Rubenstein JL. Inductive interactions direct early regionalization of the mouse forebrain. *Development*. 1997 Jul;124(14):2709-18.
- Shimogori T, Lee DA, Miranda-Angulo A, Yang Y, Wang H, Jiang L, Yoshida AC, Kataoka A, Mashiko H, Avetisyan M, Qi L, Qian J, Blackshaw S. A genomic atlas of mouse hypothalamic development. *Nat Neurosci*. 2010 Jun;13(6):767-75. doi: 10.1038/nn.2545. Epub 2010 May 2.
- Shum AS, Copp AJ. Regional differences in morphogenesis of the neuroepithelium suggest multiple mechanisms of spinal neurulation in the mouse. *Anat Embryol (Berl)*. 1996 Jul;194(1):65-73.

- Simon EM, Hevner RF, Pinter JD, Clegg NJ, Delgado M, Kinsman SL, Hahn JS, Barkovich AJ. The middle interhemispheric variant of holoprosencephaly. *Am J Neuroradiol* 2002;23:151-155.
- Singla V, Reiter JF. The primary cilium as the cell's antenna: signaling at a sensory organelle. *Science*. 2006 Aug 4;313(5787):629-33. Review.
- Snow JJ, Ou G, Gunnarson AL, Walker MR, Zhou HM, Brust-Mascher I, Scholey JM. Two anterograde intraflagellar transport motors cooperate to build sensory cilia on *C. elegans* neurons. *Nat Cell Biol*. 2004 Nov;6(11):1109-13. Epub 2004 Oct 17.
- Spassky N, Han YG, Aguilar A, Strehl L, Besse L, Laclef C, Ros MR, Garcia-Verdugo JM, Alvarez-Buylla A. Primary cilia are required for cerebellar development and Shh-dependent expansion of progenitor pool. *Dev Biol*. 2008 May 1;317(1):246-59. doi: 10.1016/j.ydbio.2008.02.026. Epub 2008 Mar 4.
- Spear PC, Erickson CA. Interkinetic nuclear migration: a mysterious process in search of a function. *Dev Growth Differ*. 2012 Apr;54(3):306-16. doi: 10.1111/j.1440-169X.2012.01342.x. Review.
- Spektor A, Tsang WY, Khoo D, Dynlacht BD. Cep97 and CP110 suppress a cilia assembly program. *Cell*. 2007 Aug 24;130(4):678-90.
- Stamatakis D, Ulloa F, Tsoni SV, Mynett A, Briscoe J. A gradient of Gli activity mediates graded Sonic Hedgehog signaling in the neural tube. *Genes Dev*. 2005 Mar 1;19(5):626-41.
- Stinchcombe JC, Randzavola LO, Angus KL, Mantell JM, Verkade P, Griffiths GM. Mother Centriole Distal Appendages Mediate Centrosome Docking at the Immunological Synapse and Reveal Mechanistic Parallels with Ciliogenesis. *Curr Biol*. 2015 Dec 21;25(24):3239-44. doi: 10.1016/j.cub.2015.10.028. Epub 2015 Dec 5.
- Stone DM, Hynes M, Armanini M, Swanson TA, Gu Q, Johnson RL, Scott MP, Pennica D, Goddard A, Phillips H, Noll M, Hooper JE, de Sauvage F, Rosenthal A. The tumour-suppressor gene patched encodes a candidate receptor for Sonic hedgehog. *Nature*. 1996 Nov 14;384(6605):129-34.
- Stottmann RW, Tran PV, Turbe-Doan A, Beier DR. Ttc21b is required to restrict sonic hedgehog activity in the developing mouse forebrain. *Dev Biol*. 2009 Nov 1;335(1):166-78. doi: 10.1016/j.ydbio.2009.08.023. Epub 2009 Sep 2.
- Struchtrup A, Wiegeling A, Stork B, Rütger U, Gerhardt C. The ciliary protein RPGRI1L governs autophagy independently of its proteasome-regulating function at the ciliary base in mouse embryonic fibroblasts. *Autophagy*. 2018;14(4):567-583. doi: 10.1080/15548627.2018.1429874. Epub 2018 Feb 21.
- Sui H, Downing KH. Molecular architecture of axonemal microtubule doublets revealed by cryo-electron tomography. *Nature*. 2006 Jul 27;442(7101):475-8. Epub 2006 May 31.
- Szabó NE, Zhao T, Cankaya M, Theil T, Zhou X, Alvarez-Bolado G. Role of neuroepithelial Sonic hedgehog in hypothalamic patterning. *J Neurosci*. 2009 May 27;29(21):6989-7002. doi: 10.1523/JNEUROSCI.1089-09.2009.
- Szabó NE, Zhao T, Zhou X, Alvarez-Bolado G. The role of Sonic hedgehog of neural origin in thalamic differentiation in the mouse. *J Neurosci*. 2009 Feb 25;29(8):2453-66. doi: 10.1523/JNEUROSCI.4524-08.2009.
- Taniguchi K, Anderson AE, Melhuish TA, Carlton AL, Manukyan A, Sutherland AE, Wotton D (2017) Genetic and Molecular Analyses indicate independent effects of TGIFs on Nodal and Gli3 in neural tube patterning. *Eur J Hum Genet*. 25(2):208-215.

- Taniguchi K, Anderson AE, Sutherland AE, Wotton D (2012) Loss of Tgif function causes holoprosencephaly by disrupting the SHH signaling pathway. *PLoS Genet.* 8(2):e1002524.
- Tanos BE, Yang HJ, Soni R, Wang WJ, Macaluso FP, Asara JM, Tsou MF. Centriole distal appendages promote membrane docking, leading to cilia initiation. *Genes Dev.* 2013 Jan 15;27(2):163-8. doi: 10.1101/gad.207043.112.
- Thazhath R, Jerka-Dziadosz M, Duan J, Wloga D, Gorovsky MA, Frankel J, Gaertig J. Cell context-specific effects of the beta-tubulin glycylation domain on assembly and size of microtubular organelles. *Mol Biol Cell.* 2004 Sep;15(9):4136-47. Epub 2004 Jul 14.
- Thibert C, Teillet MA, Lapointe F, Mazelin L, Le Douarin NM, Mehlen P. Inhibition of neuroepithelial patched-induced apoptosis by sonic hedgehog. *Science.* 2003 Aug 8;301(5634):843-6.
- Thomas S, Cantagrel V, Mariani L, Serre V, Lee JE, Elkhartoufi N, de Lonlay P, Desguerre I, Munnich A, Boddaert N, Lyonnet S, Vekemans M, Lisgo SN, Caspary T, Gleeson J, Attié-Bitach T. Identification of a novel ARL13B variant in a Joubert syndrome-affected patient with retinal impairment and obesity. *Eur J Hum Genet.* 2015 May;23(5):621-7. doi: 10.1038/ejhg.2014.156. Epub 2014 Aug 20.
- Tsao CC, Gorovsky MA. Tetrahymena IFT122A is not essential for cilia assembly but plays a role in returning IFT proteins from the ciliary tip to the cell body. *J Cell Sci.* 2008 Feb 15;121(Pt 4):428-36. doi: 10.1242/jcs.015826. Epub 2008 Jan 22.
- Tuson M, He M, Anderson KV. Protein kinase A acts at the basal body of the primary cilium to prevent Gli2 activation and ventralization of the mouse neural tube. *Development.* 2011 Nov;138(22):4921-30. doi: 10.1242/dev.070805. Epub 2011 Oct 17.
- Ulloa F, Martí E. Wnt won the war: antagonistic role of Wnt over Shh controls dorso-ventral patterning of the vertebrate neural tube. *Dev Dyn.* 2010 Jan;239(1):69-76. doi: 10.1002/dvdy.22058. Review.
- Vieira C, Garda AL, Shimamura K, Martinez S. Thalamic development induced by Shh in the chick embryo. *Dev Biol.* 2005 Aug 15;284(2):351-63.
- Vieira C, Martinez S. Sonic hedgehog from the basal plate and the zona limitans intrathalamica exhibits differential activity on diencephalic molecular regionalization and nuclear structure. *Neuroscience.* 2006 Nov 17;143(1):129-40. Epub 2006 Oct 10.
- Vieira C, Pombero A, García-Lopez R, Gimeno L, Echevarria D, Martínez S. Molecular mechanisms controlling brain development: an overview of neuroepithelial secondary organizers. *Int J Dev Biol.* 2010;54(1):7-20. doi: 10.1387/ijdb.092853cv. Review.
- Vierkotten J, Dildrop R, Peters T, Wang B, Rüther U. Ftm is a novel basal body protein of cilia involved in Shh signalling. *Development.* 2007 Jul;134(14):2569-77. Epub 2007 Jun 6.
- Vue TY, Aaker J, Taniguchi A, Kazemzadeh C, Skidmore JM, Martin DM, Martin JF, Treier M, Nakagawa Y. Characterization of progenitor domains in the developing mouse thalamus. *J Comp Neurol.* 2007 Nov 1;505(1):73-91.
- Vue TY, Bluske K, Alishahi A, Yang LL, Koyano-Nakagawa N, Novitsch B, Nakagawa Y. Sonic hedgehog signaling controls thalamic progenitor identity and nuclei specification in mice. *J Neurosci.* 2009 Apr 8;29(14):4484-97. doi: 10.1523/JNEUROSCI.0656-09.2009.

- Wallace VA. Proliferative and cell fate effects of Hedgehog signaling in the vertebrate retina. *Brain Res.* 2008 Feb 4;1192:61-75. Epub 2007 Jun 16. Review.
- Wallingford JB, Mitchell B. Strange as it may seem: the many links between Wnt signaling, planar cell polarity, and cilia. *Genes Dev.* 2011 Feb 1;25(3):201-13. doi: 10.1101/gad.2008011.
- Wang B, Fallon JF, Beachy PA. Hedgehog-regulated processing of Gli3 produces an anterior/posterior repressor gradient in the developing vertebrate limb. *Cell* 200, 100:423–434.
- Wang B, Zhang Y, Dong H, Gong S, Wei B, Luo M, Wang H, Wu X, Liu W, Xu X, Zheng Y, Sun M. Loss of Tctn3 causes neuronal apoptosis and neural tube defects in mice. *Cell Death Dis.* 2018 May 1;9(5):520. doi: 10.1038/s41419-018-0563-4.
- Wang W, Wu T, Kirschner MW. The master cell cycle regulator APC-Cdc20 regulates ciliary length and disassembly of the primary cilium. *Elife.* 2014 Aug 19;3:e03083. doi: 10.7554/eLife.03083.
- Ware M, Hamdi-Rozé H, Dupé V. Notch signaling and proneural genes work together to control the neural building blocks for the initial scaffold in the hypothalamus. *Front Neuroanat.* 2014 Dec 2;8:140. doi: 10.3389/fnana.2014.00140. eCollection 2014. Review.
- Warr N, Powles-Glover N, Chappell A, Robson J, Norris D, Arkell RM (2008) Zic2-associated holoprosencephaly is caused by a transient defect in the organizer region during gastrulation. *Hum Mol Genet* 17(19):2986-96.
- Waterman RE. Topographical changes along the neural fold associated with neurulation in the hamster and mouse. *Am J Anat.* 1976 Jun;146(2):151-71.
- Westlake CJ, Baye LM, Nachury MV, Wright KJ, Ervin KE, Phu L, Chalouni C, Beck JS, Kirkpatrick DS, Slusarski DC, Sheffield VC, Scheller RH, Jackson PK. Primary cilia membrane assembly is initiated by Rab11 and transport protein particle II (TRAPP II) complex-dependent trafficking of Rabin8 to the centrosome. *Proc Natl Acad Sci U S A.* 2011 Feb 15;108(7):2759-64. doi: 10.1073/pnas.1018823108. Epub 2011 Jan 27.
- Wheatley DN, Wang AM, Strugnell GE. Expression of primary cilia in mammalian cells. *Cell Biol Int.* 1996 Jan;20(1):73-81.
- Wiegering A, Dildrop R, Kalfhues L, Spsychala A, Kuschel S, Lier JM, Zobel T, Dahmen S, Leu T, Struchtrup A, Legendre F, Vesque C, Schneider-Maunoury S, Saunier S, Rüther U, Gerhardt C. Cell type-specific regulation of ciliary transition zone assembly in vertebrates. *EMBO J.* 2018 May 15;37(10). pii: e97791. doi: 10.15252/embj.201797791. Epub 2018 Apr 12.
- Wilde JJ, Petersen JR, Niswander L. Genetic, epigenetic, and environmental contributions to neural tube closure. *Annu Rev Genet.* 2014;48:583-611. doi: 10.1146/annurev-genet-120213-092208. Epub 2014 Oct 6. Review.
- Wiley Interdiscip Rev Dev Biol. 2017 Jan;6(1). doi: 10.1002/wdev.215. Epub 2016 Dec 1. Neuroembryology. Darnell D, Gilbert SF.
- Willaredt MA, Hasenpusch-Theil K, Gardner HA, Kitanovic I, Hirschfeld-Warneken VC, Gojak CP, Gorgas K, Bradford CL, Spatz J, Wölfl S, Theil T, Tucker KL. A crucial role for primary cilia in cortical morphogenesis. *J Neurosci.* 2008 Nov 26;28(48):12887-900. doi: 10.1523/JNEUROSCI.2084-08.2008.
- Williams CL, Li C, Kida K, Inglis PN, Mohan S, Semenc L, Bialas NJ, Stupay RM, Chen N, Blacque OE, Yoder BK, Leroux MR. MKS and NPHP modules cooperate to establish basal body/transition zone membrane associations and ciliary gate function

- during ciliogenesis. *J Cell Biol.* 2011 Mar 21;192(6):1023-41. doi: 10.1083/jcb.201012116.
- Williams M, Yen W, Lu X, Sutherland A. Distinct apical and basolateral mechanisms drive planar cell polarity-dependent convergent extension of the mouse neural plate. *Dev Cell.* 2014 Apr 14;29(1):34-46. doi: 10.1016/j.devcel.2014.02.007. Epub 2014 Apr 3.
- Xu Q1 Zhang Y, Wei Q, Huang Y, Hu J, Ling K. Phosphatidylinositol phosphate kinase PIPK1γ and phosphatase INPP5E coordinate initiation of ciliogenesis. *Nat Commun.* 2016 Feb 26;7:10777. doi: 10.1038/ncomms10777.
- Xuan S, Baptista CA, Balas G, Tao W, Soares VC, Lai E. Winged helix transcription factor BF-1 is essential for the development of the cerebral hemispheres. *Neuron.* 1995 Jun;14(6):1141-52.
- Yakovlev PI. Pathoarchitectonic studies of cerebral malformations. III. Arrhinencephalies (holotelencephalies). *J Neuropathol Exp Neurol.* 1959 Jan;18(1):22-55. No abstract available.
- Yamada S, Uwabe C, Fujii S, Shiota K. Phenotypic variability in human embryonic holoprosencephaly in the Kyoto Collection. *Birth Defects Res A Clin Mol Teratol.* 2004 Aug;70(8):495-508.
- Yang J, Gao J, Adamian M, Wen XH, Pawlyk B, Zhang L, Sanderson MJ, Zuo J, Makino CL, Li T. The ciliary rootlet maintains long-term stability of sensory cilia. *Mol Cell Biol.* 2005 May;25(10):4129-37.
- Yang J, Li T. Focus on molecules: rootletin. *Exp Eye Res.* 2006 Jul;83(1):1-2. Epub 2005 Nov 28.
- Yang TT, Su J, Wang WJ, Craige B, Witman GB, Tsou MF, Liao JC. Superresolution Pattern Recognition Reveals the Architectural Map of the Ciliary Transition Zone. *Sci Rep.* 2015 Sep 14;5:14096. doi: 10.1038/srep14096.
- Ybot-Gonzalez P, Copp AJ. Bending of the neural plate during mouse spinal neurulation is independent of actin microfilaments. *Dev Dyn.* 1999 Jul;215(3):273-83.
- Ye W, Shimamura K, Rubenstein JL, Hynes MA, Rosenthal A. FGF and Shh signals control dopaminergic and serotonergic cell fate in the anterior neural plate. *Cell.* 1998 May 29;93(5):755-66.
- Yee LE, Garcia-Gonzalo FR, Bowie RV, Li C, Kennedy JK, Ashrafi K, Blacque OE, Leroux MR, Reiter JF. Conserved Genetic Interactions between Ciliopathy Complexes Cooperatively Support Ciliogenesis and Ciliary Signaling. *PLoS Genet.* 2015 Nov 5;11(11):e1005627. doi: 10.1371/journal.pgen.1005627. eCollection 2015 Nov.
- Yoshimura S, Egerer J, Fuchs E, Haas AK, Barr FA. Functional dissection of Rab GTPases involved in primary cilium formation. *J Cell Biol.* 2007 Jul 30;178(3):363-9. Epub 2007 Jul 23.
- Zeltser LM, Larsen CW, Lumsden A. A new developmental compartment in the forebrain regulated by Lunatic fringe. *Nat Neurosci.* 2001 Jul;4(7):683-4. No abstract available.
- Zeltser LM. Shh-dependent formation of the ZLI is opposed by signals from the dorsal diencephalon. *Development.* 2005 May;132(9):2023-33. Epub 2005 Mar 23.
- Zhang Q, Seo S, Bugge K, Stone EM, Sheffield VC. BBS proteins interact genetically with the IFT pathway to influence SHH-related phenotypes. *Hum Mol Genet.* 2012 May 1;21(9):1945-53. doi: 10.1093/hmg/ddc004. Epub 2012 Jan 6.
- Zhang Y, Alvarez-Bolado G. Differential developmental strategies by Sonic hedgehog in thalamus and hypothalamus. *J Chem Neuroanat.* 2016 Sep;75(Pt A):20-7. doi: 10.1016/j.jchemneu.2015.11.008. Epub 2015 Dec 12. Review.

- Zhao C, Malicki J. Nephrocystins and MKS proteins interact with IFT particle and facilitate transport of selected ciliary cargos. *EMBO J.* 2011 May 20;30(13):2532-44. doi: 10.1038/emboj.2011.165.
- Zhao L, Zevallos SE, Rizzoti K, Jeong Y, Lovell-Badge R, Epstein DJ. Disruption of SoxB1-dependent Sonic hedgehog expression in the hypothalamus causes septo-optic dysplasia. *Dev Cell.* 2012 Mar 13;22(3):585-96. doi: 10.1016/j.devcel.2011.12.023.

RÉSUMÉ

Les cils primaires sont essentiels au développement du système nerveux central. Chez la souris, ils jouent un rôle essentiel dans l'organisation de la moelle épinière et du télencéphale via la régulation de la signalisation Hedgehog/Gli. Cependant, malgré la perturbation fréquente de cette voie de signalisation dans les malformations du cerveau antérieur chez l'homme, le rôle des cils primaires dans la morphogenèse du cerveau antérieur a été peu étudié en dehors du télencéphale. Pendant mon doctorat, j'ai étudié le développement du diencephale, de l'hypothalamus et des yeux chez des souris mutantes pour le gène de ciliopathie *Ftm/Rgrip11*. En fin de gestation, les fœtus *Ftm*^{-/-} présentent une anophtalmie, une réduction de l'hypothalamus ventral et une désorganisation du diencephale. Chez les embryons *Ftm*^{-/-}, l'expression de *Sonic hedgehog (Shh)* est perdue dans le cerveau antérieur ventral, mais maintenue dans la zona limitans intrathalamica (ZLI), l'organisateur diencephalique. Dans le diencephale, l'activité de Gli est atténuée dans les régions adjacentes à la ZLI, mais montre un niveau de base plus élevé dans les autres régions. Nos données révèlent un rôle complexe des cils dans le développement du diencephale, de l'hypothalamus et des yeux via le contrôle régional du ratio entre les formes activatrices et répressives des facteurs de transcription Gli. Ils sont en faveur d'un examen plus approfondi des anomalies du cerveau antérieur dans les ciliopathies sévères et de la recherche de gènes de ciliopathie comme modificateurs dans d'autres maladies humaines présentant des anomalies du cerveau antérieur.

ABSTRACT

Primary cilia are essential for central nervous system development. In the mouse, they play a critical role in patterning the spinal cord and telencephalon via the regulation of Hedgehog/Gli signaling. However, despite the frequent disruption of this signaling pathway in human forebrain malformations, the role of primary cilia in forebrain morphogenesis has been little investigated outside the telencephalon. Here we studied development of the diencephalon, hypothalamus and eyes in mutant mice in which the *Ftm/Rgrip11* ciliopathy gene is disrupted. At the end of gestation, *Ftm*^{-/-} fetuses displayed anophthalmia, a reduction of the ventral hypothalamus and a disorganization of diencephalic nuclei and axonal tracts. In *Ftm*^{-/-} embryos, we found that the ventral forebrain structures and the rostral thalamus were missing. Optic vesicles formed but lacked the optic cups. We analyzed the molecular causes of these defects. In *Ftm*^{-/-} embryos, *Sonic hedgehog (Shh)* expression was lost in the ventral forebrain but maintained in the zona limitans intrathalamica (ZLI), the mid-diencephalic organizer. In the diencephalon, Gli activity was dampened in regions adjacent to the *Shh*-expressing ZLI but displayed a higher Hh-independent ground level in the other regions. Our data uncover a complex role of cilia in development of the diencephalon, hypothalamus and eyes via the region-specific control of the ratio of activator and repressor forms of the Gli transcription factors. They call for a closer examination of forebrain defects in severe ciliopathies and for a search for ciliopathy genes as modifiers in other human conditions with forebrain defects.